

## **INFORMATION TO USERS**

This manuscript has been reproduced from the microfilm master. UMI films the text directly from the original or copy submitted. Thus, some thesis and dissertation copies are in typewriter face, while others may be from any type of computer printer.

The quality of this reproduction is dependent upon the quality of the copy submitted. Broken or indistinct print, colored or poor quality illustrations and photographs, print bleedthrough, substandard margins, and improper alignment can adversely affect reproduction.

In the unlikely event that the author did not send UMI a complete manuscript and there are missing pages, these will be noted. Also, if unauthorized copyright material had to be removed, a note will indicate the deletion.

Oversize materials (e.g., maps, drawings, charts) are reproduced by sectioning the original, beginning at the upper left-hand corner and continuing from left to right in equal sections with small overlaps.

Photographs included in the original manuscript have been reproduced xerographically in this copy. Higher quality 6" x 9" black and white photographic prints are available for any photographs or illustrations appearing in this copy for an additional charge. Contact UMI directly to order.

Bell & Howell Information and Learning  
300 North Zeeb Road, Ann Arbor, MI 48106-1346 USA  
800-521-0600

**UMI<sup>®</sup>**





## **ABSTRACT**

**Title of Dissertation:** TIDAL FRESHWATER MARSHES AS NUTRIENT SINKS: PARTICULATE NUTRIENT BURIAL AND DENITRIFICATION

**Jennifer Zelenke Merrill, Doctor of Philosophy, 1999**

**Dissertation directed by:** Associate Research Professor Jeffrey C. Cornwell  
Professor J. Court Stevenson  
Marine and Estuarine Environmental Science

Chesapeake Bay and Hudson River tidal freshwater marshes were examined to quantify their role in maintaining water quality through sedimentation, particulate nutrient burial and denitrification. Lead-210 analysis was used to measure sediment accretion at thirty-one sites. Sedimentation rates ranged from 1.1 to 22 mm  $y^{-1}$  and were higher in marshes of the Patuxent River subestuary. Burial of nitrogen and phosphorus was measured using sedimentation rates and particulate nutrient concentrations and ranged from 0.49 to 36 g N  $m^{-2} y^{-1}$  and 0.06 to 13 g TP  $m^{-2} y^{-1}$ . Denitrification was measured in each system using a recently-developed membrane-inlet mass spectrometric technique which measures  $N_{2(g)}$  concentrations. Sediment

cores were collected with minimal disturbance and sealed with overlying water to conduct flux experiments during three seasons. Denitrification rates were highest in the spring, with nitrogen fixation found in some summer and fall experiments. Maximum rates of denitrification were  $60 \mu\text{mol N}_2\text{-N m}^{-2} \text{ h}^{-1}$  in the Patuxent River and  $230 \mu\text{mol N}_2\text{-N m}^{-2} \text{ h}^{-1}$  in Hudson River marshes. Spring denitrification was closely related to sediment oxygen demand in the Hudson River marshes. During other seasons denitrification was most closely correlated to nitrate concentration in both systems. Nutrient removal by sediments of tidal freshwater marshes is a relatively large component in the nutrient budgets of surrounding estuaries when compared to measured and calculated nutrient inputs. While denitrification may be an important sink, the majority of nutrient removal occurs as particulate burial. Patuxent River tidal freshwater marshes retain 280,000 kg nitrogen and 60,000 kg phosphorus annually, 24 and 68% of the fall line loading of nitrogen and phosphorus. Annually, nutrient burial in the marshes of the Hudson River may remove as much as 10,500 and 2000 kg nitrogen and phosphorus, respectively, equivalent to the estimated nutrient input of wastewater treatment plants in that estuarine system. Tidal freshwater marshes are located at a critical land-water and freshwater-marine interface that enhances their value to the maintenance of estuarine water quality. Abundant suspended sediments, high nutrient concentrations and biological productivity in upper estuarine systems allows tidal freshwater marshes to greatly alter the nutrient dynamics of the surrounding estuarine ecosystem.



**TIDAL FRESHWATER MARSHES AS NUTRIENT SINKS:  
PARTICULATE NUTRIENT BURIAL AND DENITRIFICATION**

by

**Jennifer Zelenke Merrill**

**Dissertation submitted to the Faculty of the Graduate School of the  
University of Maryland, College Park in partial fulfillment  
Of the requirements for the degree of  
Doctor of Philosophy  
1999**

**Advisory Committee:**

Associate Research Professor Jeffrey C. Cornwell, Chair  
Professor Walter R. Boynton  
Associate Research Professor Russell Brinsfield  
Associate Professor Patrick C. Kangas  
Dr. Christopher J. Madden  
Professor J. Court Stevenson

**UMI Number: 9981789**

**Copyright 1999 by  
Merrill, Jennifer Zelenke**

**All rights reserved.**



---

**UMI Microform 9981789**

**Copyright 2000 by Bell & Howell Information and Learning Company.  
All rights reserved. This microform edition is protected against  
unauthorized copying under Title 17, United States Code.**

---

**Bell & Howell Information and Learning Company  
300 North Zeeb Road  
P.O. Box 1346  
Ann Arbor, MI 48106-1346**

©Copyright by

**Jennifer Zelenke Merrill**

**1999**

## **DEDICATION**

**Dedicated to the Loving Memory of  
Mildred E. Plantier  
(Grandma)**

## ACKNOWLEDGEMENTS

Work presented in this dissertation was funded by a variety of organizations, the National Oceanic and Atmospheric Administration, EPA's Multi-scale Experimental Ecosystem Research Center at HPL, the Hudson River Foundation and the Maryland National Estuarine Research Reserve System. These funding programs allowed me to follow the direction this work took me and I am grateful for the support.

Without the guidance and friendship of Jeff Cornwell this work would not have been possible. An advisor who is always supportive of and confident in his students is rare, and I consider myself incredibly lucky to have found such an advisor. My Committee made my time at HPL a positive experience. Chats with Court Stevenson on a wide variety of topics reminded me that life exists beyond graduate school, and kept me interested in learning new things. Russ Brinsfield and Walter Boynton both contributed to this work with their questions and suggestions and both always made time for me when I needed it. Chris Madden took the time to help my modeling effort and greatly improved the final document with his comments. Pat Kangas came to the rescue as an additional committee member at the last minute and still was able to provide positive, constructive feedback. All of my interactions with my Committee were positive and helpful and I thank them for their encouragement.

Without a fleet of help in the field and lab I would still be out in the marsh collecting sediment. Mike Owens supplied the answers to so many questions in the lab and elsewhere that I believe he must be almost out of replies- thank you! Thanks also go to Chuck Nieder and the staff of the Tivoli Bays Research Reserve for their assistance, access to the sites and sampling equipment. Chris Swarth and the staff of Jug Bay Wetlands Sanctuary were always welcoming and helpful.

I am indebted to my friends and family for their help and encouragement during the completion of this dissertation. Graduate student relationships can sometimes evolve from -or degrade into- a series of traded favors. Instead, I found true friends at Horn Point who never left me on my own- despite obvious risks to personal safety, whether from turtles, leeches, or long hours in cold chambers. Thank you Peter Hentschke, Kai Scheppe, Brian Sturgis, Lora Pride, Jeanna Bryner, Rick Bartleson, Judith Stribling, Erik Haberkern. Special thanks to the "Pit Crew" Teresa Coley, Amy Hentschke and Jackie Takacs for the support, physical (a place to crash at odd hours) and emotional (why are we doing this again?), that only close friends can provide. Mom and Dad, you guys really are the best- thank you for the encouragement and confidence. Dad- thanks for your help at Tivoli Bays- I do hereby officially acknowledge that you were the only one of three in the field to not fall on your duff in the mud- er, sediment. Robert Merrill, you are an inspiration and I thank you for keeping me at it when it may have been easier to just walk away. Thank You Love, I hope to return the favor.

## TABLE OF CONTENTS

List of Tables	viii
List of Figures	x
Chapter 1: Introduction to Sediment and Nutrient Retention Studies In a Variety of Tidal Freshwater Marshes with an Emphasis on Estuarine Nutrient Processing	1
Introduction	1
Tidal Freshwater Marshes	6
Goal	10
Chapter 2: Role of Tidal Marshes in the Nitrogen and Phosphorus Budgets of the Patuxent River, an urbanized Chesapeake Bay Tributary	16
Introduction	16
The Patuxent River	23
Methods	24
Results	30
Discussion	33
Summary	37
Chapter 3: Denitrification in Tidal Freshwater Marshes of the Patuxent River	57
Introduction	57
Denitrification	59
Site Description and Methods	63
Results	67
Spring 1997	67
Summer 1997	68
Autumn 1997	70
Spring 1998	70
Annual Observations	72
Discussion	73
Seasonal Nitrogen Cycling	75
Spring	75
Summer	76
Autumn	77
Spring 1998	78
Jug Bay Summary	78
Denitrification in Tidal Freshwater Marshes	79
Conclusions	81

<b>Chapter 4:</b>	<b>Tidal Freshwater Marshes of the Hudson River as Nutrient Sinks: Long Term Nutrient Retention and Denitrification</b>	104
Introduction		104
System Description		108
Methods		109
Sediment Accretion		112
Seasonal Estimates of Pore Water Concentration and Sediment-Water Fluxes		113
Results		116
Particulate Material and Sedimentation		116
Seasonal Sediment-Water Fluxes		119
Fall 1996		119
Spring 1997		121
Summer 1997		122
Discussion		124
Marsh Sediment Accretion and Long-term Nutrient Burial		124
Seasonal Activity and Site Variability		127
Ecosystem Calculations		131
Summary		134
<b>Chapter 5:</b>	<b>Preliminary Development and Calibration of a Simulation Model of Nitrogen Cycling and Macrophyte Growth in a Coastal Marsh</b>	156
Introduction		156
Model Description		157
Forcing Functions		158
State Variables		158
Model Structure		158
Macrophyte Sector		159
Aboveground Biomass		159
Belowground Biomass		161
Dissolved Inorganic Nitrogen Sector		162
Ammonium		162
Nitrate		164
Results and Calibration		165
Macrophyte Production		165
Dissolved Inorganic Nitrogen		166
Groundwater Scenarios		169
Discussion and Summary		170

## APPENDICES

Appendix A: The Effect of a Brackish Chesapeake Bay Marsh on the Nutrient Budget of a Rural Watershed	196
Appendix B: Sedimentation in Upper Estuarine Marshes of the Chesapeake Bay as Determined by $^{210}\text{Pb}$ Dating	227
Appendix C: Sediment Characteristics, Nutrients, Metals and $^{210}\text{Pb}$ in Five Coastal Wetlands	250
Bibliography	326

## LIST OF TABLES

1-1.	Matrix of marsh characteristics included in this study	13
2-1.	Patuxent River marsh sediment accretion and nutrient burial	39
2-2.	Nitrogen and phosphorus burial rates measured by various authors using radiotracers	40
2-3.	Calculation of nitrogen and phosphorus retention in the tidal freshwater and brackish marshes of the Patuxent River	41
3-1.	Sediment-water flux rates found in Jug Bay, Patuxent River, Maryland tidal freshwater marsh sediments in the spring of 1997	83
3-2.	Summer 1997 Jug Bay NERRS, Patuxent River sediment-water flux incubation experiment, conducted at 23°C	84
3-3.	Fall 1997 Jug Bay, Patuxent River sediment-water flux incubation experiment, conducted at 15°C	85
3-4.	Spring 1998 Jug Bay NERRS sediment-water fluxes measured during NO <sub>3</sub> <sup>-</sup> amendment experiments	86
4-1.	Sediment accretion and nutrient burial rates as determined by <sup>210</sup> Pb dating and particulate nutrient profiles	136
4-2.	Nutrient burial rates from a selection of other marsh studies	137
4-3.	Seasonal oxygen and nitrogen sediment-water flux rates in Tivoli Bays experimental cores	138
4-4.	Ambient ammonium concentrations in Tivoli Bays	139
4-5.	Ambient nitrate concentrations in Tivoli Bays	139
4-6.	Tivoli Bays marsh nutrient removal budget calculations	140
4-7.	Rates of aquatic denitrification from Seitzinger 1988	141
5-1.	Computer simulation model forcing functions	172
5-2.	Macrophyte aboveground carbon stocks and flows including shoot litter	173

5-3.	<b><i>Spartina alterniflora</i> carbon fixation calculations used in the simulation model</b>	176
5-4.	<b>Belowground macrophyte carbon stocks and flows including root litter</b>	178
5-5.	<b>Ammonium flows and factors in the nitrogen sector of the marsh simulation model</b>	180
5-6.	<b>Nitrate stock, flows and variables included in the marsh simulation model</b>	182
5-7.	<b>Groundwater nitrate supplies included in the marsh nitrogen computer simulation model</b>	184

## LIST OF FIGURES

1-1.	Chesapeake Bay sites included in this dissertation	14
1-2.	The New York state National Estuarine Research Reserve at Tivoli Bays	15
2-1.	Chesapeake Bay and the Patuxent River sampling sites	42
2-2.	Patuxent River marsh transect diagrams	43
2-3.	Constant input concentration (CIC) models using $^{210}\text{Pb}$ data from sediment cores from the Patuxent River marshes	44
2-4.	Sediment accretion rates by dominant vegetation community as determined by $^{210}\text{Pb}$ analysis and CIC model	48
2-5.	Profiles of particulate nitrogen in Transect C cores	49
2-6.	Profiles of particulate total and inorganic phosphorus in Patuxent River marsh sites	50
2-7.	Particulate nitrogen and phosphorus burial in Patuxent River tidal marshes	54
2-8.	Conceptual nitrogen and phosphorus budgets for the Patuxent River Estuary compiled by Boynton et al. (1995) and modified with the marsh data gathered in this study	55
3-1.	Location map for the Patuxent River marsh denitrification study	87
3-2.	Changes in dissolved oxygen and ammonium concentrations in individual Jug Bay cores over time during the spring 1997 incubation experiment	88
3-3.	Changes in gaseous $\text{N}_2$ in overlying water with time in individual cores during the spring 1997 incubation experiment	89
3-4.	Changes in dissolved oxygen, ammonium and nitrate concentrations with time during the summer 1997 experiment	90
3-5.	Changes in $\text{N}_{2(g)}$ concentration with time during the summer 1997 incubation experiment	91
3-6.	Changes in dissolved oxygen, ammonium and nitrate	

concentrations with time during the fall 1997 experiment	92
3-7. Change in N <sub>2(g)</sub> concentration with experimental incubation time on the x-axis during the fall 1997 experiment	93
3-8. Oxygen and nitrogen concentrations during the spring 1998 NO <sub>3</sub> <sup>-</sup> addition experiment	94
3-9. Spring 1998 N <sub>2(g)</sub> fluxes from Jug Bay, Patuxent River	95
3-10. Rates of nitrate uptake and denitrification in Jug Bay marsh cores during the spring 1998 experiment	96
3-11. Rates of marsh sediment oxygen demand measured throughout the study	97
3-12. Ammonium sediment-water fluxes measured in Jug Bay tidal freshwater marshes	98
3-13. Denitrification in the Jug Bay, Patuxent River tidal freshwater marshes under ambient nitrate concentrations across four seasons	99
3-14. Conceptual models of nitrogen cycling in the low and high marshes of Jug bay for spring, summer and fall	100
3-15. Denitrification as a function of sediment oxygen demand	102
3-16. Denitrification rates measured in Jug Bay, a Patuxent River tidal freshwater marsh	103
4-1. Site location of Tivoli Bays National Estuarine Research Reserve, Hudson River, New York	142
4-2. Physical characteristics of Tivoli Bays marsh sediment	143
4-3. Profiles of <sup>210</sup> Pb activity in Tivoli Bays marsh sediment	144
4-4. Tivoli Bays sediment particulate carbon and nitrogen profiles.	145
4-5. Vertical profiles of total and inorganic phosphorus in the Tivoli Bays marsh sediment	146
4-6. Oxygen fluxes measured in Tivoli Bays marsh and subtidal sediment	147

4-7.	Porewater nutrient profiles of duplicate cores collected from Tivoli Bays In the Fall of 1996	148
4-8.	Ammonium fluxes measured in Tivoli Bays marsh and subtidal sediments	152
4-9.	Net N <sub>2(g)</sub> exchange in Tivoli Bays marsh and subtidal sediments	153
4-10.	Ammonium and phosphate porewater profiles from the spring of 1997	154
4-11.	Spring denitrification and sediment oxygen consumption in Tivoli Bays	155
5-1.	Macrophyte aboveground biomass presented with calibration data.	185
5-2.	Net macrophyte primary production for one year following losses to respiration, grazing and mortality	186
5-3.	Model ammonium porewater concentration and supply rates	187
5-4.	Porewater ammonium losses in the marsh simulation model	189
5-5.	Nitrate pool and supply terms in the simulation model	191
5-6.	Nitrate losses included in the simulation model	193
5-7.	Denitrification rates from model output with calibration data	195

# **CHAPTER 1: INTRODUCTION TO SEDIMENT AND NUTRIENT RETENTION STUDIES IN A VARIETY OF TIDAL FRESHWATER MARSHES WITH AN EMPHASIS ON ESTUARINE NUTRIENT PROCESSING**

## **INTRODUCTION**

Water quality problems are evident in every major United States east coast estuary (Bricker and Stevenson 1996, Harding et al. 1986, Lipschultz et al. 1986, Valiela et al. 1992, Cornwell et al. 1996). Estuarine ecosystems such as the Chesapeake Bay have become nutrient enriched and undergo annual periods of bottom water anoxia (see Smith et al. 1992). Primary production is enhanced by nutrient enrichment, algal decomposition leads to high rates of oxygen consumption and eventual oxygen depletion in estuarine bottom waters, degrading habitat quality. While seasonal shifts in nitrogen or phosphorus limitation to estuarine primary production occur (Fisher et al. 1992), nitrogen generally limits algal production during periods of summer anoxia in Chesapeake Bay (Malone 1992). Others suggest recent controls on

phosphorus loading may be leading to P limitation in some areas (Magnien et al. 1992). Increasing our understanding of ecosystem nutrient cycling processes may help us to reduce the problem of eutrophication. Despite the widely-held belief that wetland systems are important nutrient sinks, surprisingly few studies have attempted to quantify their overall impact on estuarine ecosystems (Kahn and Brush 1994).

The long and sometimes passionate debate over the fate of U.S. wetlands is a continuing part of the environmental policy landscape. Federal and state governments are under pressure to allow development of small tracts of wetlands and the mitigation of larger wetlands. A clear direct relationship between population density and wetland loss (Gosselink and Baumann 1980) indicates that wetlands will continue to be under pressure in the future. Legislation such as the Emergency Wetlands Resources Act of 1986 is intended to protect wetland resources:

The Congress finds that wetlands play an integral role in maintaining the quality of life through material contributions to our national economy, food supply, *water supply and quality*, flood control, and fish, wildlife, and plant resources, and thus to the health, safety, recreation, and economic well-being of all citizens of the Nation.

However, the scientific literature relating improved water quality to wetlands is scattered and inconclusive. Two known mechanisms by which coastal wetlands may remove nutrients from estuarine water are (1) burial of nutrients as particulate matter in the sediments, and (2) the removal of dissolved nitrogen by conversion to nitrogen gas, a process known as denitrification. While these mechanisms are widely believed to occur in coastal marshes

(see Nixon 1980), the magnitude of their impact remains poorly characterized. Marsh retention of particulate nutrients is rarely reported (DeLaune et al. 1981, Craft and Richardson 1993) and only a few published studies of nutrient retention in tidal freshwater marshes exist (Odum 1988, Orson et al. 1990, Bowden et al. 1991, Kahn and Brush 1994). While denitrification has received much attention by the scientific community, it has only rarely been reported for marshes, and this review has been unable to locate any rate measurements made within a tidal freshwater marsh. A review of the scientific research relating wetlands to water quality (Nixon and Lee 1986) identified tidal freshwater marshes as perhaps the least understood of all the wetland classes.

The spatially and temporally dynamic nature of marshes can obscure findings and often lead to inconclusive results. One of the most popular approaches to determine estuarine-marsh interactions has been to measure tidal exchanges of nutrients. Numerous studies have attempted to draw inferences about marsh-estuarine interactions by measuring the nutrient concentrations of flooding and draining marsh water over tidal cycles (Heinle and Flemer 1976, Roberts and Pierce 1976, Stevenson et al. 1977, Woodwell et al. 1979, Jordan et al. 1983, Simpson et al. 1983, Dame et al. 1986, Childers et al. 1993). However, tidal exchange studies do not provide an adequate means for estimating marsh-estuary nutrient budgets. Uncertainty and imprecision in the hydrologic budget allows for calculation errors large enough to overwhelm small exchanges. Despite significant improvements to

the basic technique of tidal exchange, such as the flumes used by Wolaver et al. (1983), none of these studies has measured or even reasonably estimated groundwater inputs which may deliver large quantities of nitrogen directly to estuarine water (Staver and Brinsfield 1996). This additional input can overwhelm impacts the marsh may have on water quality. Tidal exchange studies also rely on the extrapolation of discrete time points to annual budgets. Major events such as storms and even irregular tides are generally not included, yet may be important to annual material processing (Baumann et al. 1984, Reed 1989, Orson et al. 1990, Murray and Spencer 1997). Intensive, long term (multi-year) automated sampling may be the only way to develop realistic estimates of tidal exchanges using this approach.

A more direct method of estimating sediment-water interactions in aquatic sediments is to run small-scale incubation chamber experiments (Kaplan et al. 1979, Boynton and Kemp 1985, Sundback et al. 1991, Chambers et al. 1992). Primarily used in subtidal sediments, this approach also requires detailed hydrologic data to allow its extrapolation to a marsh ecosystem. However, incubation chambers allow the researcher to control the environment, while directly measuring changes in solute concentrations and inferring fluxes over a known, constant surface. This approach is one of two used in this study to estimate the impact of marsh sediments on overlying water.

Marshes remove sediment from overlying water by decreasing water velocity allowing particulates to be deposited on the marsh surface (Frey and

Basan 1985). Nixon (1980) estimated Chesapeake Bay salt marshes are capable of retaining 15% of the annual sediment input to the Bay. Stevenson et al. (1988) revised this estimate, discounting the high salinity marshes as sediment sinks and estimating the tidal freshwater and brackish marshes are capable of retaining 5-11% of the incoming sediment load. Sediment retention used in the calculation was based on short-term flux studies, which may not reflect long term rates since storm activity has been connected to both sediment deposition (Reed et al. 1989, Orson et al. 1990) and erosion (Stevenson et al. 1988). Long-term integration of sediment cores may be the best approximation of sedimentation over long time scales (~100 years). Roberts and Pierce (1976) calculated a sediment budget for the Patuxent River which has undergone extensive sedimentation; colonial trading ports have become land-locked. Their report suggests a zone of high deposition in the upper portion of the river, which coincides with the extensive tidal freshwater marshes. Kahn and Brush (1994) have estimated sedimentation rates of up to  $8.9 \text{ mm y}^{-1}$  in a marsh within this region using pollen ratios as horizon markers. Yarbro et al. (1983) developed a sediment budget for the Choptank River, a low topographic relief Eastern Shore tributary, which compared watershed sediment loads with long-term sedimentation rates. Upper estuarine tidal freshwater and brackish marshes were shown to act as sediment traps, reducing high sediment loads resulting from large agricultural areas in the upper watershed. Orson et al. (1990) report high rates of sediment accretion in tidal freshwater marshes of the Delaware River (up to

$10.7 \text{ mm y}^{-1}$ ).

Particulate deposition and organic matter retention in marsh sediment is a sink for nitrogen and phosphorus. Sediments in marshes accrete vertically, incorporating organic and mineral matter, and retaining nutrients within this matrix. Reported rates of vertical accretion in coastal marshes range between 2 (Harrison and Bloom 1974) and  $13.5 \text{ mm y}^{-1}$  (DeLaune et al. 1981). Nixon (1980) estimates nutrient burial may range from 5 to  $20 \text{ g N m}^{-2} \text{ y}^{-1}$  and 0.05 to  $0.3 \text{ g P m}^{-2} \text{ y}^{-1}$ . The long term burial of nutrients is the second process studied to examine marsh impacts on estuarine nutrient dynamics.

## TIDAL FRESHWATER MARSHES

Tidal freshwater marshes occur in a region of high nutrient inputs and human development. Enhanced productivity from tidal energy subsidies and high nutrient concentrations is common, occurring without the restraints on diversity imposed by high salinities (Odum 1988). As a result the marshes are very diverse and highly productive. Rates of primary production are generally between 1 and  $3 \text{ kg biomass m}^{-2} \text{ y}^{-1}$  (Mitsch and Gosselink 1993). Human development is frequently concentrated near the fall line of riparian watersheds as a result of the high energy fall line and limit to oceanic shipping. High development density causes increased nutrient inputs, generally as point sources from industry and wastewater treatment plants. The proximity of tidal freshwater marshes to these developed areas may

increase their potential for interception of nutrient loads before they can impact the lower estuary. Tidal freshwater marshes are also located above the turbidity maxima of estuarine systems. These zones are caused by a combination of estuarine circulation patterns and a response to increased salinity. Flocculation of colloidal particles occurs and results in the increase in total suspended solids. These particulates are potential sediment for the tidal freshwater marshes along the banks of the estuary.

The Chesapeake Bay is bordered by approximately one million acres of marshes (Field et al. 1991) and yet the importance of these marshes as nutrient sinks within the estuary remains unknown. Marsh-estuarine nutrient studies in the Chesapeake have focused on creek flux studies (Heinle and Flemer 1976, Stevenson et al. 1977, Jordan et al. 1983) which have not lead to a synthesized picture of marshes within the Bay. Other studies such as Kahn and Brush (1994) incorporate long term data but have been spatially and temporally limited and cannot be applied to the Chesapeake as a whole. This study seeks to improve the current state of understanding of the importance of tidal freshwater marshes in the surrounding landscape by examining marshes within Chesapeake Bay tributaries and along the Hudson River. Marshes in this study have been categorized by salinity and watershed urbanization for the purposes of placing the study in a landscape context (Table 1-1). Agricultural systems consist of <5% urbanized land area and >20% in agricultural use. The urban systems in this study have a watershed which is >30% urbanized, and the mixed use system combines relatively

equal coverage of urban, forested and non-developed uses, although they are not equally distributed in the watershed.

Marshes of two major east coast estuarine systems are considered. Both the Patuxent and Hudson Rivers have endured many years of heavy nutrient loading (Limburg et al. 1986, Jaworski et al. 1992, Boynton et al. 1995). Costly management strategies have been implemented in both systems in an attempt to restore water quality. Both estuaries are bordered by marshes in their freshwater, tidally-influenced reaches. Determining the role these marshes play in maintaining and possibly improving water quality may be especially interesting in these heavily managed systems.

The Patuxent River, a tributary to the Chesapeake Bay, has large tracts of undisturbed tidal marshes (Flemer et al. 1970), covering 22.7 km<sup>2</sup>, 1% of the entire Patuxent River watershed (McCormick and Somes 1982). High suspended sediment loads have allowed the development of new marshes along the length of the river. Kahn and Brush (1994) completed a palynological study in these marshes and were able to show an increase in sedimentation rates over the period of European development. Their data suggest that marsh sediments are capable of trapping significant quantities of nutrients from the estuary, but their limited sampling (2 marsh and 2 subtidal cores) prevents a reliable extrapolation of their data to the entire estuary. High nutrient and suspended sediment loads, coupled with a large coverage of tidal freshwater marshes, make the Patuxent River estuary an ideal place to conduct this study.

The pattern of development is different in the Hudson River watershed (Figure 1-2). The upper watershed is less developed than that of the Patuxent. The headwaters are located in the pristine Adirondack Mountains. Lower in the watershed, in the region of the fall-line, a mixture of urban, industrial and agricultural uses impacts the River. Management efforts in the Hudson are generally more concerned with heavy metal and PCB pollution than nutrient pollution (i.e.: Bopp et al. 1982). The watershed is much larger ( $45,000 \text{ km}^2$ ) and contains a lower proportion of tidal marshes. The estuarine system contains  $130 \text{ km}^2$  of salt and freshwater marshes, or about 0.3% of the watershed surface area. The high turbidity of the estuary causes light limitation of primary production in the water column (Cole et al. 1992). As a result, the tidal fresh portion of the estuary is heterotrophic, relying on external inputs of fixed carbon to supply energy for the system (Findlay et al. 1991, Howarth et al. 1992). This stretch of the river has been the focus of a series of investigations (Findlay et al. 1991, Cole et al. 1992, Bianchi et al. 1993), but the role of local marshes has not yet been determined and is not included in the existing carbon and conceptual models (Howarth 1996b).

Additional subestuaries of the Chesapeake Bay are also included in this project. Maryland's Choptank River is included as a representative of an agriculturally-dominated tidal freshwater marsh. Total suspended solids and nutrient loads were high (Staver et al. 1996) over a six year study period from 1986-1991. Much of the nitrogen enters the tidal River as nitrate-contaminated groundwater (Staver et al. 1996). Otter Point Creek is a tidal

freshwater marsh included in the Maryland National Estuarine Research Reserve (NERR) located at the northern end of Chesapeake Bay, at the mouth of the Bush River. Sediment loading at this site is high and the watershed is heavily developed. Monie Bay is the third system included in Maryland NERR, and is surrounded by a brackish marsh located on the eastern shore of Maryland. The surrounding watershed is dominated by agricultural inputs. The sediments are organic and moderate to high concentrations of sulfide have been measured in the porewaters (Stribling 1994).

## GOAL

The goal of this dissertation is to determine if the tidal marshes in the upper reaches of an estuary are quantitatively important to the nutrient budgets of the lower estuaries. Two nutrient removal mechanisms in upper estuarine marshes were investigated using the Patuxent River subestuary and the Hudson River estuary as examples of east coast tidal freshwater marshes in order to provide independent measurements from systems of similar characteristics to allow for a generalization to tidal freshwater marshes. Accretion rates within the marsh systems were measured as well as the nutrient concentration of the sediments as an estimate of nutrient burial rates. The average burial rate of all sites was extrapolated to the surface area of the marsh to approximate nutrient burial in the tidal marshes.

Removal of nitrogen via denitrification was also measured through the use of flux experiments in the Patuxent and Hudson River marshes. Nitrogen gas emitted from intact cores was measured seasonally and annual estimates of gaseous nitrogen were made. Estimates of nutrient removal were compared to a Patuxent River conceptual model compiled by Boynton et al. (1995) to relate nutrient retention to nutrient inputs to the river. A computer simulation model was developed from the measured seasonal fluxes to further constrain annual estimates of nitrogen removal.

The chapters in this dissertation answer the following questions:

**Chapter 2: Does particulate-bound nitrogen and phosphorus in this sediment matrix provide a large nutrient sink for the surrounding estuary?**

Particulate nutrient concentrations were measured in  $^{210}\text{Pb}$ -dated marsh sediment cores from the Patuxent River. Sites were located in all major tidal freshwater vegetation communities and nutrient burial rates were extrapolated to an ecosystem scale using reported vegetation coverage for the River.

**Chapter 3: Is denitrification in tidal freshwater marshes a potentially large removal mechanism for nitrogen? Seasonal core incubation experiments were conducted on sediment cores collected from the marshes of Jug Bay, Patuxent River.**

**Chapter 4: Are rates of sedimentation, nutrient burial and denitrification similar between comparable tidal freshwater marshes in different estuaries? Nutrient burial and denitrification were measured in a tidal freshwater marsh**

system of the Hudson River for a comparison of results with those from the Patuxent River.

Chapter 5: Can a computer simulation model reasonably describe seasonal denitrification patterns using measured values for calibration and validation?

Appendix A: How does nutrient retention in a submerged upland, brackish marsh of Chesapeake Bay compare to idealized inputs to the system from a rural agricultural watershed? Nutrient burial was measured using  $^{210}\text{Pb}$  cores taken from Monie Bay. Inputs to the system from the surrounding watershed were calculated using land coverage and published nutrient loading coefficients. Inputs to the system and nutrient burial within the marshes is compared.

Appendix B: How much sediment can tidal freshwater marshes retain annually? Are tidal freshwater marshes important to the sediment budget of Chesapeake Bay? Long sediment cores were collected from three tidal freshwater marshes of the Chesapeake Bay and sedimentation rates were measured using  $^{210}\text{Pb}$ .

Table 1-1. Matrix of marsh types included in the study. For the purposes of the study agricultural landscapes consisted of <5% urban and >20% agricultural land use. Urban landscapes were defined by a watershed which is described as >30% developed.

Agricultural	Mixed Use	Urban	
Tidal Fresh	Choptank River <sup>1</sup>	Hudson River <sup>2</sup>	Patuxent River <sup>4</sup>
Brackish	Monie Bay <sup>5</sup>	Otter Creek <sup>3</sup>	
		<sup>1</sup> Lomax and Stevenson 1982	
		<sup>2</sup> Howarth et al. 1992	
		<sup>3</sup> Pasternack and Brush 1998	
		<sup>4</sup> Boynton et al. 1995	
		<sup>5</sup> Merrill, included as Appendix A	

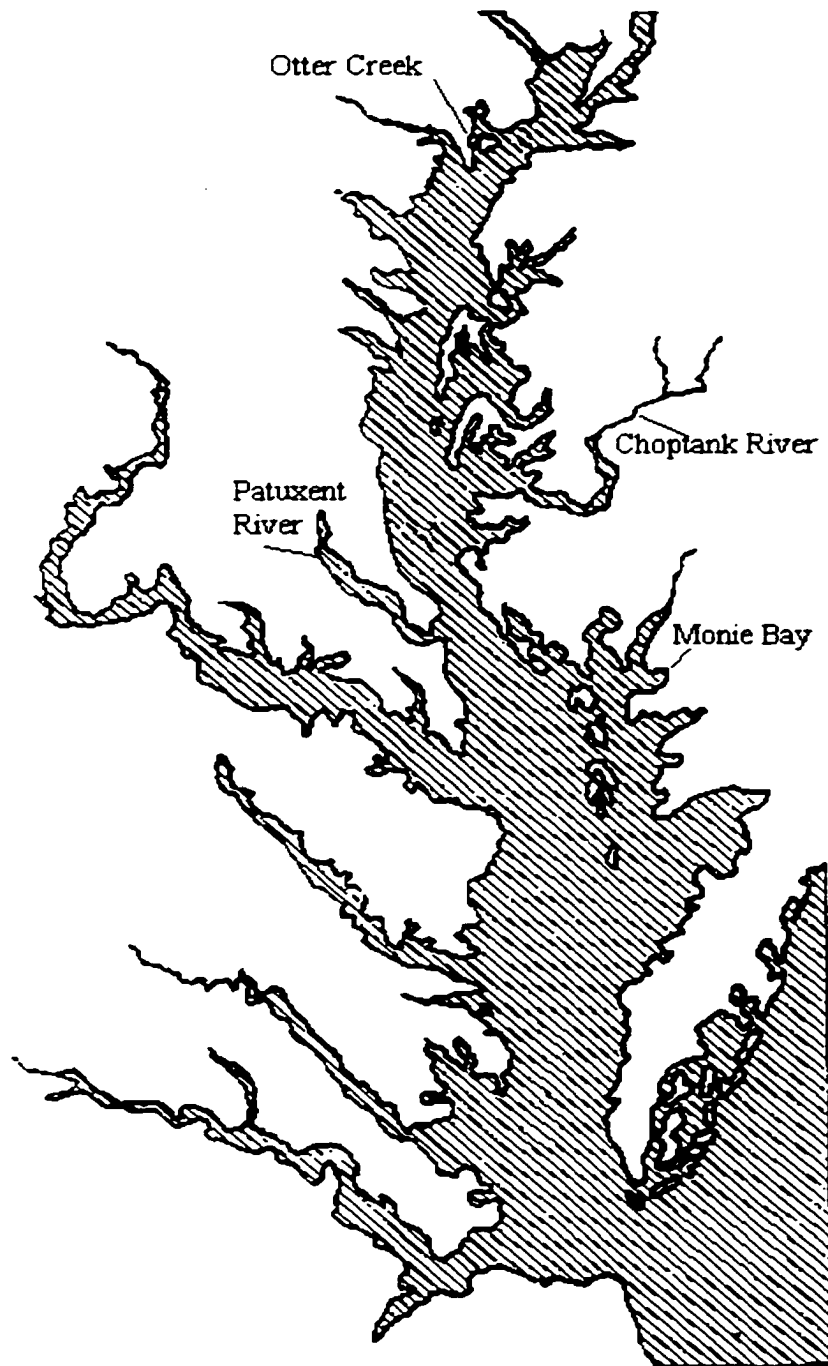


**Figure 1-1. Chesapeake Bay study sites included in this dissertation. All sites were located in tidal freshwater regions, with the exception of work completed in Monie Bay, a brackish eastern shore subestuary.**

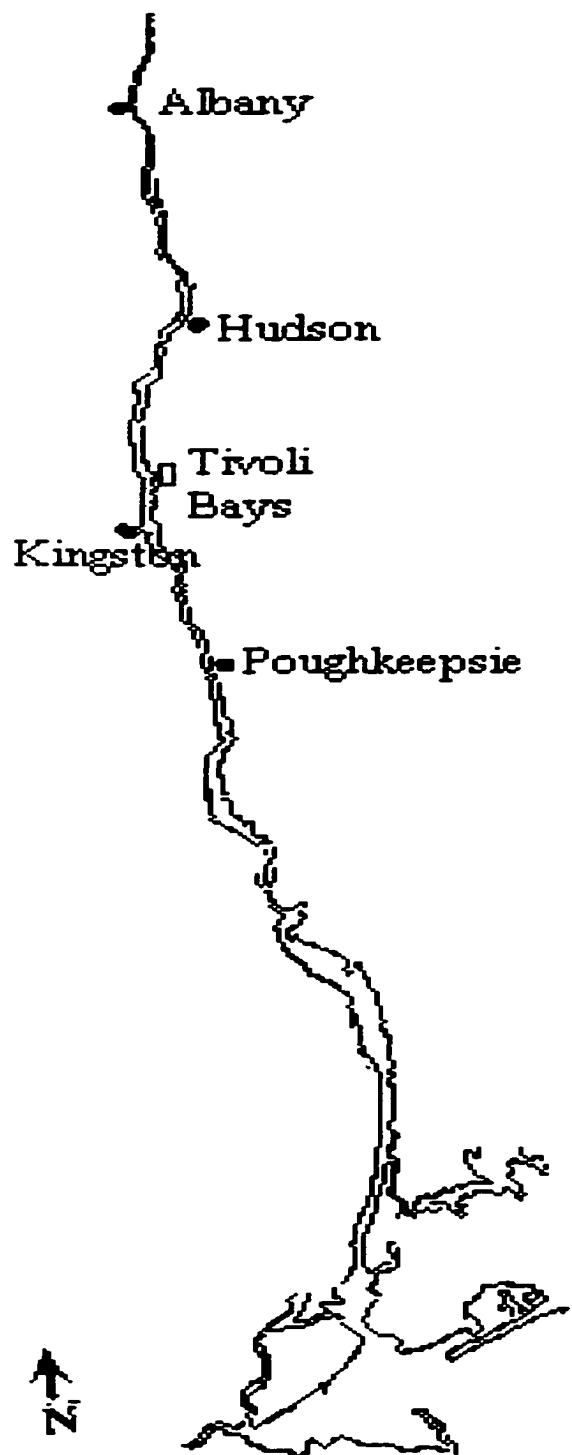


Figure 1-2. The New York state National Estuarine Research Reserve at Tivoli Bays on the Hudson River was included in this study. Work is presented in Chapter 4.

## **CHAPTER 2: ROLE OF TIDAL MARSHES IN THE NITROGEN AND PHOSPHORUS BUDGETS OF THE PATUXENT RIVER, AN URBANIZED CHESAPEAKE BAY TRIBUTARY**

### **INTRODUCTION**

Despite over thirty years of research, many questions about the role of coastal marshes in maintaining water quality remain unanswered. A thorough, critical review of wetland research by Nixon (1980) emphasized the need for definitive studies relating wetlands to water quality. Perhaps the most commonly espoused attribute of coastal marshes is the ability to trap or remove harmful nutrients from estuarine waters (Emergency Wetlands Resources Act 1986, Howarth et al. 1996). Data supporting this assertion are uncommon in coastal marshes (DeLaune et al. 1981), and almost nonexistent for upper estuarine, tidal freshwater wetlands (Kahn and Brush 1994).

Two basic approaches have been used to examine nutrient removal or retention by wetlands. Tidal flux studies attempt to characterize a marsh system by measuring nutrient concentrations on flood and ebb tides in tidal creeks. When fitted to a hydrologic budget, net nutrient exchanges can be estimated. This is the most common approach used by researchers when investigating estuarine-marsh interactions (Heinle and Flemer 1976, Stevenson et al. 1977, Woodwell et al. 1979, Jordan et al. 1983, Simpson et al. 1983, Dame et al. 1986). The technique was modified by the use of flumes to constrain horizontal hydrologic variability associated with the marsh surface (Wolaver et al. 1983, Whiting and Childers 1989, Childers et al. 1993). Labor-intensive tidal flux studies are fraught with uncertainty due to variability across the surface of the marsh and unknown parameters such as groundwater flow and contributions of nutrients. External supplies of nutrients can create the appearance of nutrient export by the marsh when in fact the marsh may be filtering unmeasured upland runoff. Annual estimates of nutrient exchanges require long term sampling and extrapolation of discrete time points to annual time scales may not be adequate due to effects of major events such as storms and irregular tides (Murray and Spencer 1997).

A second approach to determine the extent to which marshes can filter nutrients from estuarine waters uses the sedimentary record to estimate permanent sequestration of particulate material. Burial of nutrients in marsh sediments occurs as the marsh accretes on mineral inputs in systems with high particulate loads, and/or organic matter produced within the marsh (e.g.

Bricker-Urso et al. 1989, Craft et al. 1993). By measuring the vertical accretion rate and nutrient concentrations in the sediments, net burial (following deposition and diagenesis) can be estimated (DeLaune 1981, Johnston et al. 1984, Johnston 1991, Craft & Richardson 1993).

A variety of tools have been used to measure vertical accretion in marshes. Artificial markers such as brick dust have been used effectively (Richard 1978), but the method requires years of deposition to reliably estimate long-term burial. Atmospheric nuclear testing in the 1960's released <sup>137</sup>Cs which effectively labeled atmospheric particles with the radioactive isotope. Cesium-137 has been used successfully in many locations to measure sedimentation where a well-defined peak in concentration occurs in vertical profiles of sediment (DeLaune et al. 1981, Nyman et al. 1993). However, <sup>137</sup>Cs can be mobilized during organic matter decomposition (Davis et al. 1984), potentially limiting its application as a sediment accretion marker in the organic-rich sediments of coastal marshes. Pollen analysis of invading plant species has also been used to estimate deposition (Kahn and Brush 1994). The method correlates relative concentrations of pollen grains from invasive species such as ragweed to years of intensive land clearing by European settlers. Once the peak ratio of ragweed:oak pollen grains is determined, local historic records must be used to determine time periods of European colonization. Clearly the method has limited temporal resolution and is very labor intensive.

Atmospherically-derived  $^{210}\text{Pb}$  has been used to successfully determine vertical accretion in many marsh systems (Armentano and Woodwell 1975, Sharma et al. 1987, Bricker-Urso et al. 1989), although bioturbation and potential mobility with transition metals (Carpenter et al. 1981) can affect the  $^{210}\text{Pb}$  profiles. Lead-210 undergoes natural, alpha particle emitting radioactive decay, resulting in exponential decreases in concentration with time, represented by depth in the sediments. At natural levels  $^{210}\text{Pb}$  extraction and analysis techniques detect the presence of atmospherically-derived  $^{210}\text{Pb}$  until decay has proceeded for five half-lives. Detection, therefore, is possible for the most recent 100 years, since the half-life of  $^{210}\text{Pb}$  is 22.3 years. Naturally-occurring  $^{210}\text{Pb}$  is an appropriate tracer for an approximately 100 year time period. This study used  $^{210}\text{Pb}$  to measure rates of sedimentation in Patuxent River marshes to estimate nutrient burial in the sediments over the previous century.

Large scale sedimentation patterns have been reported for coastal marshes. DeLaune et al. (1981) and Bricker-Urso et al. (1989) found declines in marsh sediment accretion with distance from the estuarine shore. Vegetation associations also exhibit spatial patterns within marsh ecosystems, largely controlled by flooding regime (Simpson et al. 1983, Odum et al. 1984). The interdependence of flooding regime and vegetation was used as a cue for sedimentation in this study. Vertical accretion was measured in a variety of vegetation communities and extrapolated to the

Patuxent River marsh ecosystem using vegetation coverage estimates of each plant community (McCormick and Somes 1982).

Nutrient pollution in Chesapeake Bay has led to a decline in water quality (see Smith et al. 1992). While estuarine subtidal sediments are recognized as major sinks for nitrogen and phosphorus (Boynton et al. 1995, Cornwell et al. 1996), deposition of particulate material and associated nutrients within the tidal marshes of the Chesapeake remains largely unknown. An estimated one million acres ( $4050 \text{ km}^2$ ) of wetlands fringe the Chesapeake Bay, representing 61% of the estuarine surface area of the Bay and major tributaries (Cronin and Pritchard 1975, Field et al. 1991), yet the importance of this potentially large nutrient sink remains unexamined in the context of a larger, estuarine water quality perspective.

Examples of nitrogen and phosphorus burial studies are found in North American estuarine marshes, including Chesapeake Bay, but results are site specific without any attempt to extrapolate the data to an entire wetland system or the estuarine system of which they are a part. Louisiana marshes bury large amounts of nitrogen and phosphorus, as well as a large portion of the carbon fixed by photosynthesis within the marsh (DeLaune et al. 1981, Hatton et al. 1982). However, the long-term potential for nutrient retention remains unclear if these marshes cannot keep pace with rapid rates of sea level rise on the Mississippi Delta. Bricker-Urso et al. (1989) conducted a large sedimentation study in the salt marshes of Narragansett Bay, examining contributions of organic and inorganic material to vertical accretion, but

measurements of nutrients were not made. Kahn and Brush (1994) have used pollen analysis to estimate nutrient burial rates at two sites in Jug Bay on the Patuxent River. High and low marsh sediment profiles were compared. Higher nutrient accumulation rates in the high marsh were attributed to a slower rate of decomposition and more efficient retention of plant material than in the low marsh. A review in non-tidal freshwater marshes by Johnston (1991) showed retention rates of 0.9 to 52.4 g N m<sup>-2</sup> y<sup>-1</sup> and 0.04 to 8.2 g P m<sup>-2</sup> y<sup>-1</sup>, for nitrogen and phosphorus respectively, clearly demonstrating that freshwater marshes can retain large amounts of particulate nutrients.

Perhaps the most extensive study of tidal freshwater marshes to date was completed in the upper estuarine portion of Delaware Bay (Simpson et al. 1983). A brief (5 day) tidal flux study was coupled with measurements of vegetation and litter crops and measurements of soil nutrient content. Seasonal patterns in soil nutrient content were not apparent, while directional fluxes of nutrients and metals on the tides suggest that nitrogen and phosphorus exhibited seasonal variability. The authors concluded these marshes may not be able to retain nutrients permanently. However, their data suggest the marshes damp the effects of nutrient loading by temporarily sequestering dissolved nutrients during periods of high concentration, and releasing them later in the year when they may not be as harmful to the estuarine system. Again, variability in the calculations of the hydrologic budget and the exchange of dissolved nutrients between the tidal creek and

marsh can be high and some reported fluxes are at or below 20% of the measured inflows and outflows. Presumably tidal exchanges are not within the precision of the tidal flux method. Tidal flux data were collected on only five days of the year which may not adequately represent marsh processing.

Questions addressed by this chapter: (1) Are the marshes of the upper Patuxent River capable of retaining notable quantities of nutrients in their sediment matrix; and (2) How do these burial estimates compare to nutrient loading to the system from largely anthropogenic sources in the watershed? The approach relied on the estimation of sediment accretion rates at numerous locations within the marsh. Solid-phase nitrogen and phosphorus concentrations were measured and burial rates determined at each sampling location. Results were categorized by their dominant vegetation community and estimates of marsh coverage made by McCormick and Somes (1982) were used to extrapolate data to the marsh system. Final estimates were then compared to nutrient input data reported by Magnien et al. (1992). A mass balance model of nitrogen and phosphorus loading and removal processes by Boynton et al. (1995) was modified with the marsh burial data to further examine the relative impact of nutrient burial in the marshes to estuarine water quality.

## THE PATUXENT RIVER

The Patuxent River drains a 2,230 km<sup>2</sup> watershed and is the 6th largest tributary of the Chesapeake Bay. Located on the western side of the Bay, the Patuxent River crosses the fall line as it divides the Washington, D.C. and Baltimore, Maryland regions. Two dams in the River's upper reaches create reservoirs to supply drinking water for the metropolitan area. This study includes samples from the upstream tidal limit, south to a maximum salinity of approximately 10 ppt. (Figure 2-1).

Despite the rapid loss of tidal marshes surrounding the Chesapeake Bay to development and in some areas submergence, Patuxent River marshes have remained virtually intact (Fleming et al. 1970). Tidal marshes in the Patuxent River watershed cover 22.7 km<sup>2</sup> (McCormick & Somes 1982), and are located below the majority of point source inputs to the River. Non-tidal wetlands cover an additional 20 km<sup>2</sup> (Water Resources Administration 1980). The wetland:watershed area ratio for the Patuxent is 1%, close to the 0.8% for the Chesapeake Bay as a whole (derived from Field et al. 1991 and Chesapeake Bay Program data 1995). The combination of large acreage and location in the high turbidity, high nutrient part of the River, provides the potential for tidal marshes to greatly impact the nutrient budget of the Patuxent River subestuary.

In the past, attention has focused on Chesapeake Bay marsh loss associated with sea level rise (Stevenson et al. 1986, Kearney and Stevenson

1991, Kearney et al. 1994). While marsh loss may be a problem within submerged upland and estuarine marshes, riparian marshes appear to capture large loads of sediment, which enable them to maintain elevation in the face of rising sea level. Erosion in the Patuxent River watershed has deposited enough sediment in the upper estuary to severely restrict navigation into one-time trading ports for ocean-going vessels.

The Patuxent River receives high loads of nutrients and particulate material, making it an ideal system for this study. Particulate concentrations up to  $46 \text{ mg L}^{-1}$  have been measured (Roberts and Pierce 1976). Nutrient inputs to the system are from a variety of sources, including agricultural drainage, industrial wastes, and 43 million gallons daily of effluent from eight major sewage treatment plants, most of which are located above the fall line. While nitrogen inputs from the treatment plants have increased almost ten-fold between 1963 and 1989 (Magnien et al. 1992), the removal of phosphorus from effluent, coupled with the 1986 phosphate ban, has reduced current effluent phosphorus contributions to one-third that of the early 1980's.

## METHODS

A McAuley corer (Bricker 1989) was used for collection of marsh sediment samples during the summers of 1993 and 1994. The corer limits compaction and retrieves an intact core. Twenty-seven cores were collected from the Patuxent River tidal marshes, at varying distances from the river and

in a variety of vegetation communities (Figure 2-1). Included were three lateral transects of four cores each, collected to address sedimentation variability with distance from the river. Cores were taken from the river bank to 50, 60 or 90 m inland (Figure 2-2). Three cores were also taken from the walkway of the Jug Bay Wetland Sanctuary, one at the edge of a tidal creek, one bordering the upland plant community, and a third core mid-way between the two, approximately 40 m from the tidal creek. All cores were immediately divided into 3, 5 or 10 cm sections, sealed in vials, and stored on ice until they were returned to the laboratory and weighed. Sample volume was determined by water displacement. After weighing, samples were dried at 60°C and pulverized using a mortar and pestle.

Sedimentation rates were determined using  $^{210}\text{Pb}$  dating. The technique required the assumption of secular equilibrium between  $^{210}\text{Pb}$  and its daughter isotope,  $^{210}\text{Po}$ . Due to the slower decay of  $^{210}\text{Pb}$  than its daughter isotope  $^{210}\text{Po}$  (22.3 years and 138 days, respectively) the decay of  $^{210}\text{Pb}$  was considered to be rate limiting. Therefore,  $^{210}\text{Pb}$  decay was estimated by the measurement of  $^{210}\text{Po}$  decay. Polonium-210 decays by emitting an easily-detectable alpha particle, while  $^{210}\text{Pb}$  emits beta particles.

Sediments were analyzed from one half of the samples collected per core, distributed over all depths. A known amount of activity, as NIST standard  $^{208}\text{Po}$  or  $^{209}\text{Po}$ , was added to sediment samples taken from different depths in the cores. Activity of  $^{210}\text{Po}$ , which allows the determination of sediment age, was measured relative to the known tracer activity. Polonium-

<sup>210</sup>Po was extracted from the sediment using an acid digestion with concentrated HNO<sub>3</sub> and HCl at 80-90°C (Sugai 1990). Centrifugation removed particulate material from the solution, which was repeatedly evaporated and diluted with 6 N HCl to replace nitrates which interfere with plating. A weak acid solution (0.10 N HCl) was used to increase the volume and create the plating solution. Iron interference was reduced by the addition of ascorbic acid. Both polonium isotopes were plated on silver and counted on an alpha counting system. Uncertainty associated with the counting system was always less than  $\pm 10\%$ , based on instrument specifications and the length of observation. Measured <sup>209</sup>Po activity was used to calculate <sup>210</sup>Po activity originating from the sediment sample by comparison of integrated peak values.

To understand the mathematical models which are used to interpret <sup>210</sup>Pb the cycle of <sup>210</sup>Pb in the environment must be understood. Lead-210 is an eventual daughter isotope of <sup>238</sup>U, however <sup>226</sup>Ra is the closest predecessor of <sup>210</sup>Pb with a half-life on the order of years (1600 years) and so discussion will be limited to decay beginning with <sup>226</sup>Ra. While there are five intermediate isotopes between <sup>226</sup>Ra and <sup>210</sup>Pb the most critical to geochronological dating is <sup>222</sup>Rn, a gas. This gaseous daughter of <sup>226</sup>Ra diffuses from the earth's crust into the atmosphere, where it decays rapidly with a half-life of 3.8 days. Radon-222 decays to <sup>210</sup>Pb, which is readily bound to particulate matter and falls to the earth's surface either as dryfall or during precipitation events. Once deposited on the surface, a portion of these

particles make their way to the surface of aquatic sediments. Some fall directly to the water surface and are deposited after falling through the water column and some are deposited in the watershed and must be transported to the estuary. The two most commonly applied mathematical models rely on assumptions relating to the movement of these  $^{210}\text{Pb}$ -laden particles through the environment.

The Constant Input Concentration (CIC) model (Robbins 1978) is the simplest model commonly applied to calculate sediment age from  $^{210}\text{Pb}$  data. The CIC model assumes supply of  $^{210}\text{Pb}$  to the sediment was constant (Robbins 1978). The implication is cycling of  $^{210}\text{Pb}$  through the environment is at steady-state. The CIC model assumes  $^{222}\text{Rn}$  release has remained constant, as well as watershed supply of particles. As a result, the CIC model calculates one sedimentation rate and assumes the rate has remained constant over the preceding 100 years.

The Constant Rate of Supply (CRS) model is also commonly used in geochronology. Unlike the CIC model, the CRS model does not assume  $^{210}\text{Pb}$  supply to the sediment is the result of steady-state environmental cycling. The CRS model calculates sedimentation rates for individual data points, or depths in the sediment core, allowing for a variable sedimentation rate. The major assumption of the model is  $^{222}\text{Rn}$  is being released at a constant rate. Changes in watershed particle retention, for example, is accounted for in the calculations. The drawback of this model is the need for a large number of  $^{210}\text{Pb}$  analyses per core. Due to the extensive landscape

coverage in this study, it was not feasible to analyze all fifteen sections of every core which was collected. The CIC model was chosen in order to increase the coverage of the study with limited resources.

Calculations using the CIC model began with the separation of supported and unsupported activity. Because  $^{226}\text{Ra}$  is present in sediments, the quantity of  $^{210}\text{Pb}$  derived from the atmosphere was first separated from that which was present as a result of the *in situ* decay of  $^{226}\text{Ra}$ . Profiles of total  $^{210}\text{Pb}$  activity with depth in the sediment revealed an asymptote of activity. This "baseline" activity is referred to as "supported activity" and results from the decay of  $^{226}\text{Ra}$  in the sediment. Surface sediments have a higher  $^{210}\text{Pb}$  activity and generally show an exponential decrease to the asymptote. This surface increase in activity was the result of atmospherically-derived  $^{210}\text{Pb}$  and is referred to as unsupported activity. Unsupported activity data were natural log-transformed to simplify calculations. Sedimentation rate in depth per year was calculated by performing a linear regression on the transformed data with section depth. Using cumulative mass in the regressions generated sedimentation rates in terms of annual mass burial per unit area. Linear regressions of the data were accepted for calculation of sedimentation rate if the value of  $r^2$  was greater than 0.90.

Phosphorus (total and inorganic) was analyzed from 1 N HCl extractions of ashed and unashed samples (Aspila et al. 1976) using the molybdenum blue technique of Parsons et al. (1984). Organic P was calculated as the difference between total and inorganic P. Repeated

measurements were within  $\pm 5\%$ . Nitrogen analysis was carried out using a Control Instruments CHN analyzer with a precision better than 5% for both elements. Nutrient concentrations are expressed in mg per gram sediment on a dry weight basis.

Independent burial rates were calculated for each of the twenty-five sites for which accretion was estimated. Burial rates for nitrogen were calculated using the average concentrations to 100 cm following DeLaune et al. (1981), allowing calculations to reflect the variability found throughout each core. Phosphorus burial was estimated using average total phosphorus concentrations found between 20 and 100 cm depth to avoid inflated estimates due to high phosphorus concentrations resulting from post-diagenetic mobility. Chambers and Odum (1990) described coupling of iron redox reactions and phosphorus sorption. As insoluble Fe(III) oxides are buried in an anoxic environment such as would follow prolonged submergence due to tidal flooding soluble Fe(II) is produced. As sediments become reoxygenated, perhaps due to tidal recession, Fe(II) is oxidized to insoluble Fe(III) which has an affinity for phosphorus. As a result, this cycling of iron can trap large amounts of phosphorus bound to iron oxides in surface sediments. The Patuxent River receives high loads of mineral sediment which may enhance the potential for this inflated phosphorus concentration in surface sediments. To ensure a conservative estimate of phosphorus burial this study did not include phosphorus measured in the surface sediments. Nutrient concentrations were multiplied by mass accretion ( $\text{g m}^{-2} \text{y}^{-1}$ ) of

sediment, as determined by a linear regression of the  $^{210}\text{Pb}$  data on the cumulative bulk density at each site which accounts for compaction to the depth of the limit of the  $^{210}\text{Pb}$  detection (generally 40 cm).

Data were extrapolated to the entire Patuxent River tidal marsh network using vegetation as an indicator of sedimentary environment. Sediment accretion varies with distance from the estuarine water source (Bricker-Urso et al. 1989, DeLaune et al. 1981). In this study, sediment cores were collected from a variety of vegetation associations and communities identified by dominant plant (referred to as "associations"). Sedimentation and nutrient burial rates were grouped by these associations and acreage estimates of each vegetation type were used to extrapolate the data to Patuxent River tidal freshwater, oligohaline and brackish marshes. Vegetation coverage used estimates from McCormick and Somes (1982). Sampled communities accounted for 79% of the reported vegetation coverage. For the remaining unexamined 21% association types overall average burial rates were used to represent retention.

## RESULTS

At 25 of 27 sites the expected exponential decay of  $^{210}\text{Pb}$  with depth was observed (Figure 2-3). Sedimentation rates were higher than observed in other Chesapeake Bay marsh studies (Stevenson et al. 1985, Finkelstein and Hardaway 1988, Kearney and Ward 1986, Kahn and Brush 1994). While

no distinct pattern of sedimentation was found along the length of the River, rates did appear to change with distance from the edge of the River (Table 2-1). Rates of sediment deposition ranged from 1.1 to 22 mm  $y^{-1}$ , or 0.1 to 9.3 kg  $m^{-2} y^{-1}$ . Vertical sediment accretion rates were variable within each vegetation type, and did not appear to be statistically distinct (Figure 2-4). Cores from the *Scirpus* locations showed the least variability. Relative contributions of organic material increased with distance from the River, as observed in three of the four series of cores collected in transects to the interior of the marsh (Table 2-1). Average sedimentation in the marsh was 8.5 mm  $y^{-1}$  ( $sd = 5.01$ ), or an annual retention of 3.4 kg of material per square meter of marsh surface ( $sd = 2.07$ ).

Vertical profiles of total nitrogen exhibited expected variability with depth (Figure 2-5). Trends in nitrogen content with distance from the River were apparent in the data. Average nitrogen concentrations ranged from 3.5 to 21 mg  $g^{-1}$  sediment. Average ( $n=17$ ) nitrogen burial was 17 g  $m^{-2}$  marsh  $y^{-1}$  ( $sd=9.86$ ) and ranged between 0.5 and 36 g  $m^{-2} y^{-1}$ . These rates cover the range reported by other researchers in marsh systems (Table 2-2) and reached rates which were higher than those reported for other marshes.

No trend in phosphorus concentration was observed along the axis of the Patuxent River, but transects show shifts with distance from the River (Table 2-1). Total phosphorus concentrations are higher near the River. The proportion of organic phosphorus contributions to total phosphorus are generally small and constant with depth, becoming more important at the

interior sites where inorganic contributions decline (Figure 2-6). In most cases, the phosphorus profiles showed a surface maximum concentration, with the largest enhancement observed at the riverbank site. Total phosphorus concentrations (20 to 100 cm deep) ranged from 0.54 to 1.9 mg g<sup>-1</sup> sediment (Table 2-1). Calculated burial rates ranged from 0.06 to 13 g m<sup>-2</sup> y<sup>-1</sup>, with an average of 4.3 g TP m<sup>-2</sup> y<sup>-1</sup> (n=25, sd=3.13), higher than reported for other marsh systems (Table 2-2).

Annual estimates of nutrient burial were made for individual plant associations by pooling all cores from each specific vegetation type after McCormick and Somes (1982). Nitrogen burial did not appear to be related to vegetation type, with the exception of the low rates found in *Scirpus*- or *Zizania*- dominated sampling sites (Figure 2-7). Phosphorus burial rates in the *Nuphar*-dominated marsh areas were much higher than in other sites, while phosphorus retention in the *Scirpus*-dominated marsh was almost negligible.

A system-wide calculation was completed to estimate total particulate nitrogen and phosphorus removed by the Patuxent River marshes (Table 2-3). Tidal fresh *Typha*-dominated areas were the largest single contributors to coverage and to phosphorus burial. Nitrogen burial was dominated by the contributions of *Spartina cynosuroides*, with *Typha* marsh contributions ranking second. The high rates of phosphorus burial in the *Nuphar*-dominated portions of the marsh contributed almost 10% of the annual budget, despite the limited coverage (2%).

A comparison of annual nutrient burial in the marshes to estimates of nutrient inputs to the tidal freshwater portion of the River (Magnien et al. 1992) clearly indicates the potential contribution of the marshes to Patuxent River water quality. The marshes retain an estimated 24% of the total nitrogen load to this upper estuarine system, and 68% of the estimated phosphorus load.

## DISCUSSION

These study results clearly indicate the importance of marshes in the nutrient budgets of surrounding estuaries. Other researchers have found similar burial rates, which suggests that nutrient burial in upper estuarine wetlands may be an important sink which is not currently included in estuarine nutrient models (Table 2-2). The quantity and form of nutrients supplied to the Patuxent River must be considered when examining this type of conceptual model. Particulates compose only 7% of the head of the estuary load of nitrogen, while phosphorus is delivered in a much higher proportion of particulate forms (39-52%) (Magnien et al. 1992). Ninety percent of wastewater treatment plant (WWTP) phosphorus enters the estuary as phosphate. Kemp and Boynton (1984) estimate that about half of the dissolved phosphate is removed from the water column by flocculation with a combination of iron, dissolved and particulate organic matter and clay particles, leading to enriched sediments. The marshes are clearly an

important sink for much of this particulate-bound phosphorus. The researchers also found approximately the same conversion between dissolved and particulate forms for total nitrogen. Ammonium releases from the waste water treatment plants, after being converted to particulate forms, are available for burial in marsh and subtidal sediments.

Studies of marsh tidal fluxes and porewater have generally shown marshes to act as nutrient transformers, importing inorganic forms and exporting organic nutrients (Heinle and Flemer 1976, Stevenson et al. 1977, Jordan et al. 1983, Gehrels and Mulamoottil 1989, Whiting et al. 1989, Chambers et al. 1992, Phillips et al. 1993). This study focused only on the chemistry and magnitude of particulate burial, which are typically much higher than net dissolved exchanges. For example, Stevenson et al. (1977) reported an export of  $4.14 \text{ g N m}^{-2} \text{ y}^{-1}$  from a Patuxent River marsh, about 1/4 of nitrogen burial estimated in this study. Exchanges of dissolved nutrients between the marsh and estuary are discussed in Chapter 3 of this dissertation.

Nitrogen and phosphorus marsh burial rates can account for 24% and 39% of total estimated nitrogen and phosphorus inputs to the entire Patuxent River ecosystem (as reported by Magnien et al. 1992). Reported nutrient loads include monitored river inputs, unmonitored non-point inputs, atmospheric and point sources to the upper and lower watershed. Non-point inputs were estimated with land use (Beulac and Reckow 1982) and watershed coverage (Maryland Automated Geographic Information System).

The majority of marshes in the Patuxent River are located in the upper reaches, in close proximity to the majority of nutrient sources, estimated at 60% for both nitrogen and phosphorus in the Patuxent. Tidal freshwater marshes reduce nutrient loading to lower estuarine systems by virtue of their location in regions which receive high nutrient and sediment loads.

A mass balance approach was used by Boynton et al. (1995) to determine the direction and approximate magnitude of nutrient exchange between the Patuxent River and Chesapeake Bay. Inputs were presented as above and below fall line, and sources include point, non-point, and atmospheric deposition. Total inputs for the Boynton et al. (1995) and Magnien et al. (1992) studies are similar (TN: 1.73 and  $1.98 \times 10^6$  kg  $y^{-1}$ , TP: 0.28 and  $0.15 \times 10^6$  kg  $y^{-1}$ ). Nutrient sinks include subtidal burial and denitrification, and removal by fisheries. Boynton et al. (1995) calculate an export from the Patuxent River to the Chesapeake Bay of 210,000 kg N and 24,000 kg TP annually. When marsh nutrient burial is included in the calculations the final results are greatly altered (Figure 2-8). The additional loss term provided by the marshes is sufficient to account for the calculated exports of nitrogen and phosphorus to the Chesapeake Bay. This suggests the Patuxent River may be a nutrient sink for the Bay, importing 70,000 kg TN, and 36,000 kg TP annually. Including marshes as a part of the estuarine system appears to be critical when applying large scale conceptual models to urbanized estuarine systems.

These large-scale estimates should be used with caution. Error may be introduced with extrapolation of average burial rates to marsh vegetation coverage. Depositional processes vary with distance from the river (Stevenson et al. 1986, Hatton et al. 1983, Bricker-Urso et al. 1989) which may effect our burial rates. This artifact should have been reduced by the application of vegetation, and therefore, elevation-specific sedimentation rates. Only phosphorus deposition appeared to vary greatly between vegetation communities. Marsh areas dominated by *Scirpus* were located behind natural levees which was reflected in their lower rates of accretion and nutrient burial. This reduction in burial should be reflected in the final calculations by the use of the vegetation mapping for data extrapolation. A larger sampling pool for each individual vegetation type may help constrain the estimates, although normal environmental variability in sedimentation, and presumably nutrient burial, is generally very large. *Spartina cynosuroides* was the most heavily sampled vegetation association in this study ( $n=13$ ) and resulted in the largest variability.

Non-tidal marshes of the Patuxent River watershed have not been included. Maryland Water Resources Administration (1980) reports 20 km<sup>2</sup> of non-tidal wetlands along the Patuxent River. Typical freshwater marsh retention values are half of that found in this study (Table 2-2), possibly due to their relative distance from important nutrient sources, such as waste water treatment plants. However, because of the extensive land area, non-tidal marshes have the potential to impact the nutrient budget of the River as much

as the tidal marshes by intercepting watershed runoff before it enters the tidal portion of the Patuxent River.

Phosphorus reduction strategies have decreased phosphorus fluxes in the Patuxent River, dropping phosphorus inputs from a high of 420,000 kg TP yr<sup>-1</sup> to 166,000 kg TP y<sup>-1</sup> in 1989 (Magnien et al. 1992). Nitrogen inputs from wastewater treatment plants increased approximately ten fold between 1963 and 1989. As a result, the TN:TP ratio of inputs has increased from 8 in 1978, to 32 in 1989. It has been suggested that this change will cause a functional shift in the estuary from nitrogen to phosphorus limitation of phytoplankton productivity in the River (Magnien et al. 1992). Potential consequences of this in the marshes is unknown. Tidal marshes can lower the N:P ratios of flooding tidal and watershed-derived waters (Dame et al. 1991, Correll et al. 1992), which may effect the nutrient limitation status of the River even further.

## SUMMARY

Tidal marshes of the Patuxent River play an important role in the maintenance of water quality by retaining a large portion of nutrients entering the system. Burial in the marshes can account for as much as 24% of the nitrogen and 68% of the phosphorus entering the upper portion of this Chesapeake Bay subestuary. The marshes are located near the high turbidity zone and below the primary point sources, making them perfectly

situated to act as nutrient filters. Interpretation of Patuxent River nutrient budgets should include the effect of the extensive marshes on water quality. The percent of watershed as wetland in the entire Chesapeake Bay (0.8%) is similar to that of the Patuxent River (1.0%). Consequently, if Patuxent River marshes are representative of removal processes for the entire Chesapeake Bay the current ecosystem nutrient balance models need to be revised to include large-scale marsh-estuary interactions such as nitrogen and phosphorus burial.

**Table 2-1. Patuxent River marsh sediment accretion and nutrient burial.**  
 Sites correspond to Figure 2-1 and distances in the first column refer to proximity to riverbank. Lead-210 data was analyzed using the constant input concentration model presented by Robbins (1978). Average nutrient concentrations to 100 cm are reported and used in the nutrient burial calculations. Nitrogen data are not available for Transects A and B.

	Vertical Accretion mm y <sup>-1</sup>	Accretion kg m <sup>-2</sup> y <sup>-1</sup>	Total P mg g <sup>-1</sup> sediment	TP Burial g m <sup>-2</sup> y <sup>-1</sup>	Nitrogen mg g <sup>-1</sup> sediment	N Burial g m <sup>-2</sup> y <sup>-1</sup>
<b>Transect A</b>						
11 m	12.6	5.1	1.41	7.30		
30 m	17.0	8.5	1.32	11.3		
50 m	18.1	6.3	1.21	7.68		
50 m	16.3	4.9	1.31	6.41		
<b>Transect B</b>						
2 m	15.9	9.3	1.27	11.8		
11 m	3.1	1.1	1.04	1.17		
30 m	5.5	2.0	1.24	2.51		
60 m	4.1	1.1	1.06	1.16		
<b>Transect C</b>						
0 m	6.4	3.4	1.10	3.74	9.22	31.4
30 m	1.1	0.1	0.64	0.06	4.89	0.49
60 m	2.0	0.3	0.98	0.29	13.3	4.00
90 m	2.1	0.3	0.80	0.24	17.0	5.09
<b>Jug Bay</b>						
1 m	21.9	5.2	2.42	12.6	4.15	21.6
Upland Border	5.4	1.6	0.78	1.24	11.7	18.7
<b>Patuxent River</b>						
1	7.6	5.1	0.54	2.73	3.64	18.6
2	2.3	1.4	1.02	1.43	3.94	5.51
3	6.6	4.0	1.24	4.98	3.52	14.1
4	1.6	0.7	1.45	1.00	3.64	2.6
5	11.1	3.9	0.98	3.82	6.41	25.0
6	13.4	4.2	0.77	3.24	8.43	35.4
7	7.8	3.7	1.18	4.33	9.81	36.1
8	12.8	6.9	1.46	10.0	4.67	32.2
9	2.40	0.4	0.51	0.18	21.0	7.56
10	--	--	1.94	--	4.89	--
11	7.8	3.7	1.42	5.25	3.59	13.3
12	7.7	3.2	0.61	1.96	4.90	15.7
Average of all sites	8.5 ± 5.01	3.4 ± 2.07		4.26 ± 3.13	16.9 ± 9.86	

Table 2-2. Nitrogen and phosphorus burial rates measured by various authors using radiotracers.

Location	Tracer	N burial g m <sup>-2</sup> y <sup>-1</sup>	P burial g m <sup>-2</sup> y <sup>-1</sup>	Author(s)
<i>Brackish</i>				
Louisiana	<sup>137</sup> Cs	21	--	DeLaune et al. 1981
Choptank River, MD	<sup>210</sup> Pb	23.0	2.03	Merrill, Appendix B
Monie Bay, MD	<sup>210</sup> Pb	11.1	0.32	Merrill, Appendix A
<i>Tidal Freshwater</i>				
Patuxent River, MD	<sup>210</sup> Pb	21.4	3.76	this study
Otter Creek, MD	<sup>210</sup> Pb	8.78	1.16	Merrill, Appendix B
<i>Freshwater</i>				
Wisconsin	<sup>137</sup> Cs	12.8	2.6	Johnston et al. 1984
Average organic soils	various	14.6	1.46	Johnston 1991
Average inorganic soils	various	1.6	0.26	Johnston 1991
Florida everglades	<sup>210</sup> Pb	14.1	0.66	Craft & Richardson 1993
Florida everglades	<sup>137</sup> Cs	--	0.54-1.14	Reddy et al. 1993

Table 2-3. Calculation of nitrogen and phosphorus retention in the tidal freshwater and brackish marshes of the Patuxent River.

Plant Community	Vegetation Coverage <sup>1</sup> (km <sup>2</sup> )	Vertical Accretion (mm y <sup>-1</sup> )	N burial		P burial	
			(g N m <sup>-2</sup> y <sup>-1</sup> )	(kg N y <sup>-1</sup> )	(g P m <sup>-2</sup> y <sup>-1</sup> )	(kg P y <sup>-1</sup> )
<i>Hibiscus</i>	0.27	5.4	18.7	5,049	1.24	335
<i>Polygonum</i>	0.52	7.6	18.6	9,672	2.73	1,420
<i>Nuphar</i>	0.53	17	21.6	11,534	12.6	6,728
<i>Scirpus</i>	1.8	3.4	4.55	7,999	0.27	466
<i>Spartina cynosuroides</i>	4.0	12	27.5	109,570	4.62	18,440
<i>Zizania</i>	4.6	3.2	5.46	24,898	2.17	9,895
<i>Typha</i>	6.3	5.8	23.3	146,345	2.55	15,993
Unknown	4.8	9.3	21.4	102,720	3.76	18,048
			TOTAL	417,787		71,325
			Inputs <sup>2</sup>	1,182,000		88,000
			Percent Retention	35.4		81.0

<sup>1</sup>Dominant vegetation coverage from McCormick and Somes (1982) listed by Genus name.

<sup>2</sup>Estimated total inputs of nitrogen and phosphorus to the tidal fresh portion of the Patuxent River (Magnien et al. 1992).

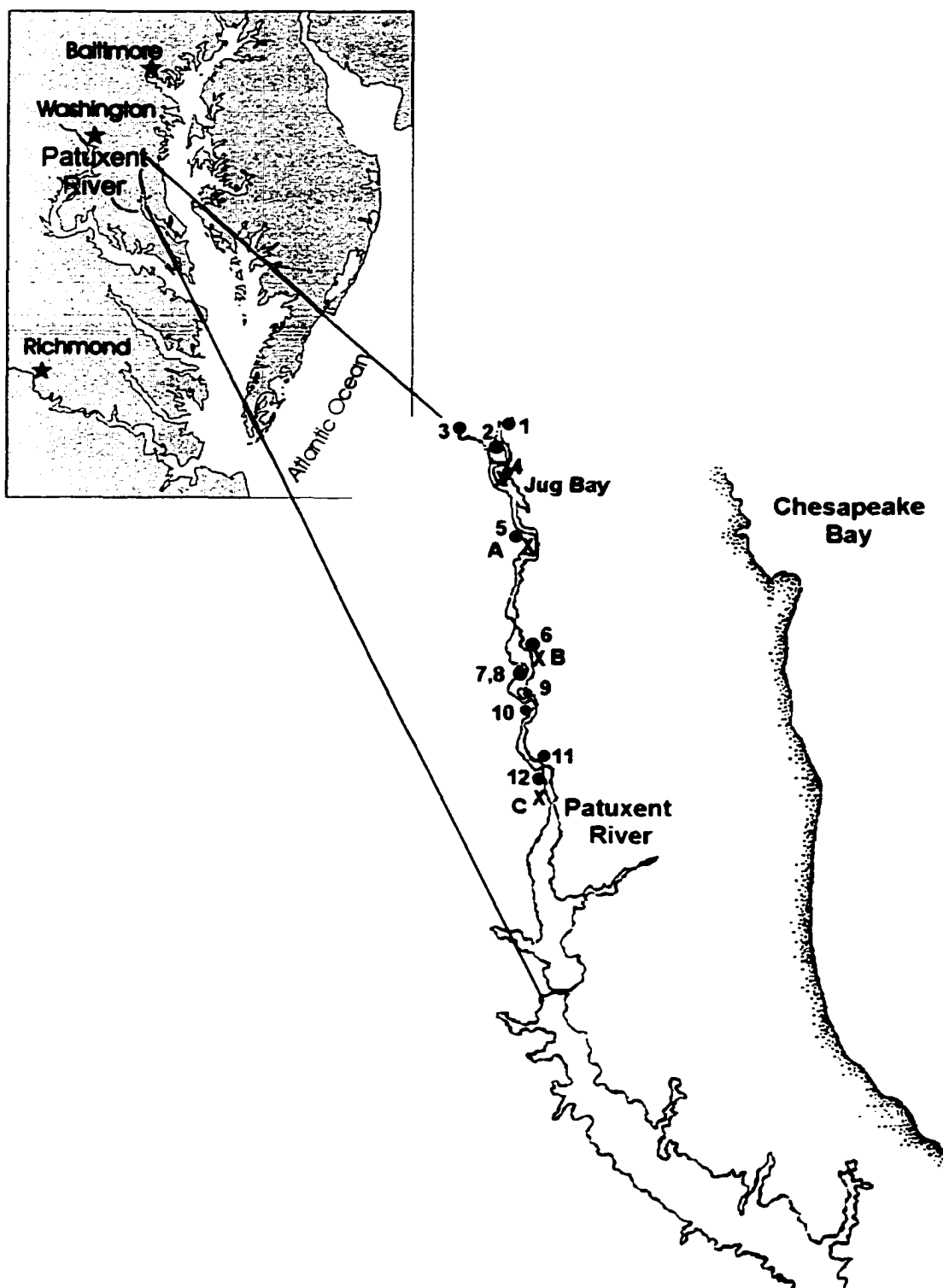
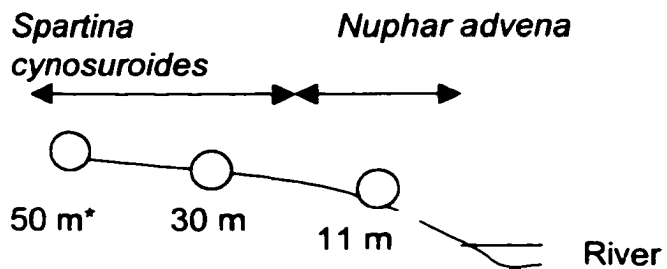
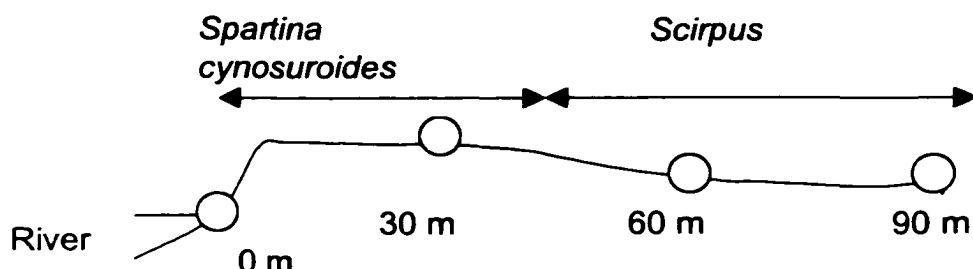


Figure 2-1. Chesapeake Bay and the Patuxent River sampling sites. Transect locations are indicated with an 'X'.

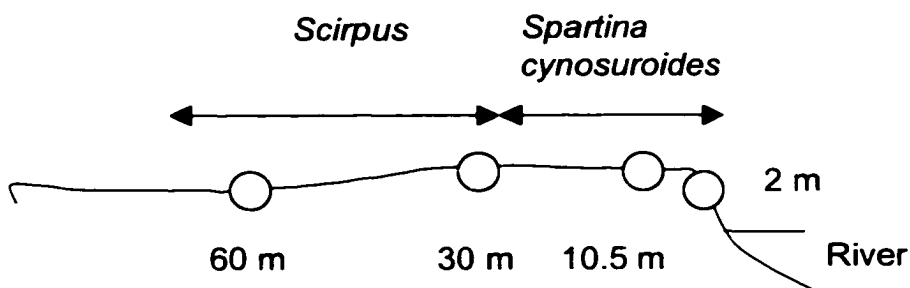
Transect A  
38.44'819" N by 76.41'882" W



Transect B  
38.42'260" N by 76.41'843" W



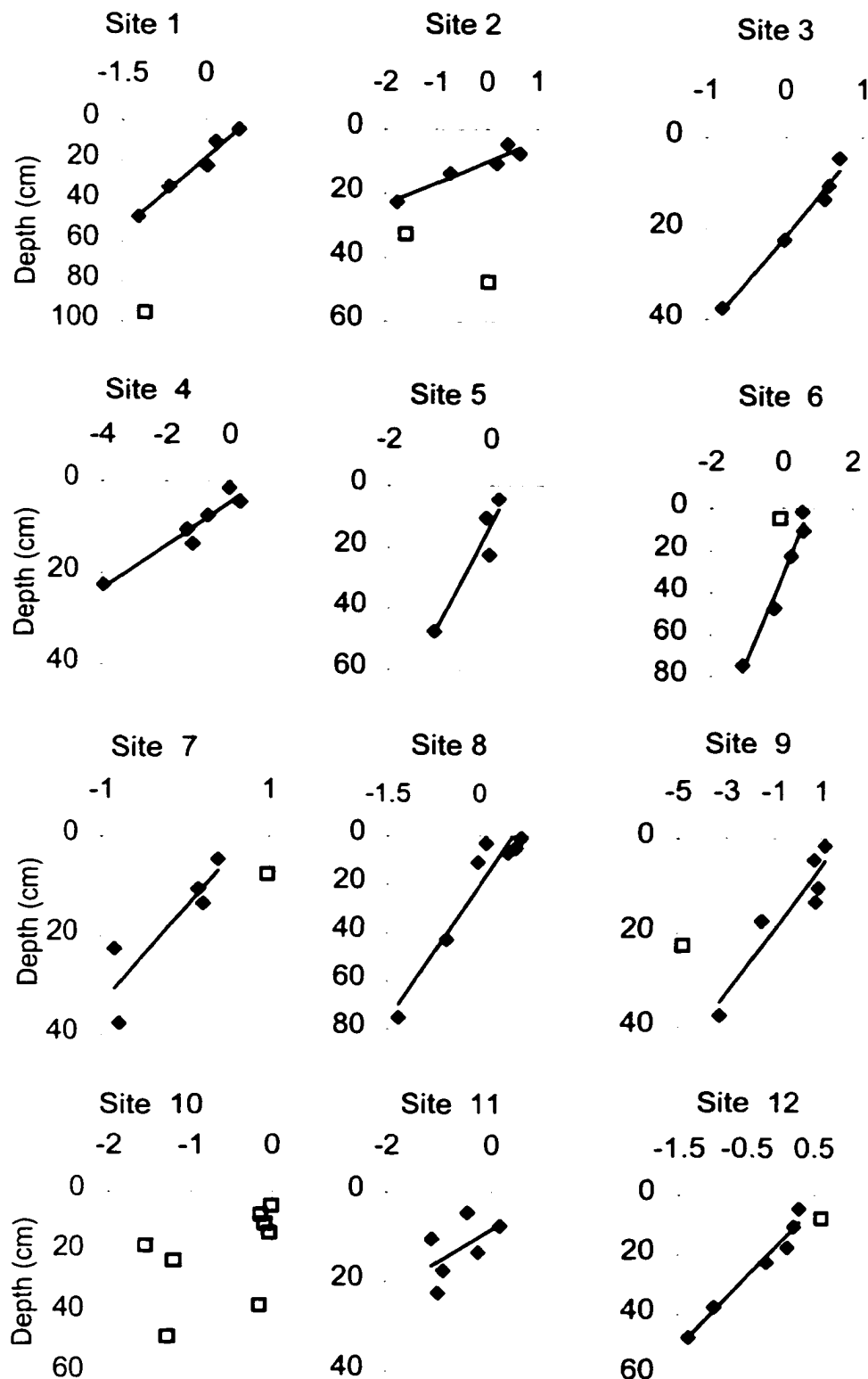
Transect C



1 cm = 10 m

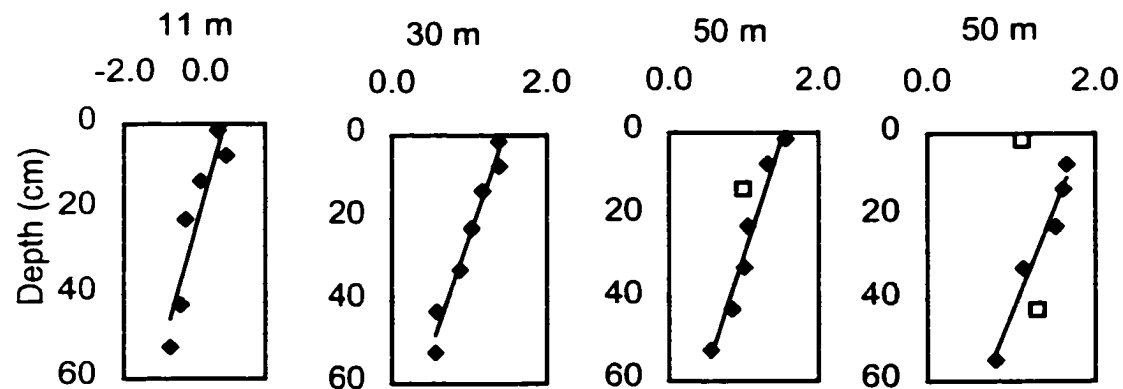
Figure 2-2. Patuxent River marsh transect diagrams. Transects A and C were collected on the western riverbank, while Transect B was collected on the east bank. Vegetation associations are identified by the dominant plant. The vertical scale is exaggerated.

Figure 2-3. Constant input concentration (CIC) models using  $^{210}\text{Pb}$  data from sediment cores from the Patuxent River marshes. Site numbers correspond to Figure 2-1. The x-axis represents natural log-converted data and the y-axis depth in the sediment (cm). The line represents Constant Input Concentration (CIC) model output. Open symbols represent data which were not included in regressions. Sediment cores collected along the axis of the Patuxent River are shown in (a). Cores collected in transects are given in (b), while data presented in (c ) were collected from Jug Bay National Estuarine Research Reserve. Distance to river shoreline is given for each core.

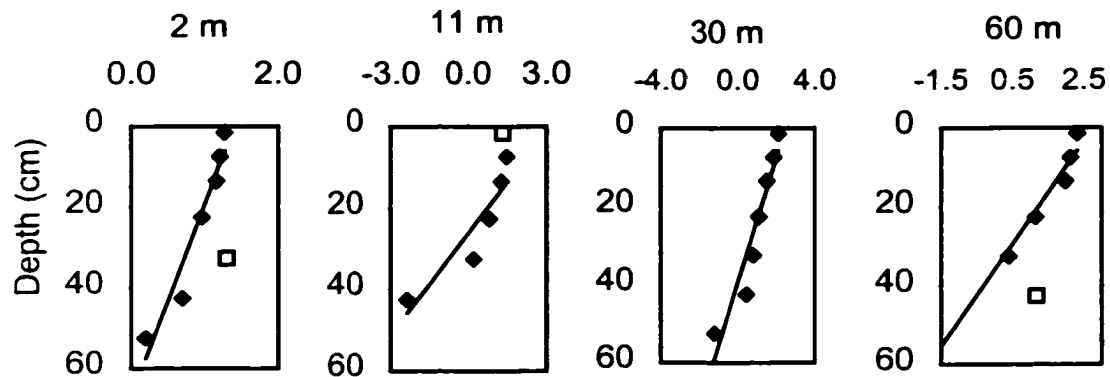


(b)

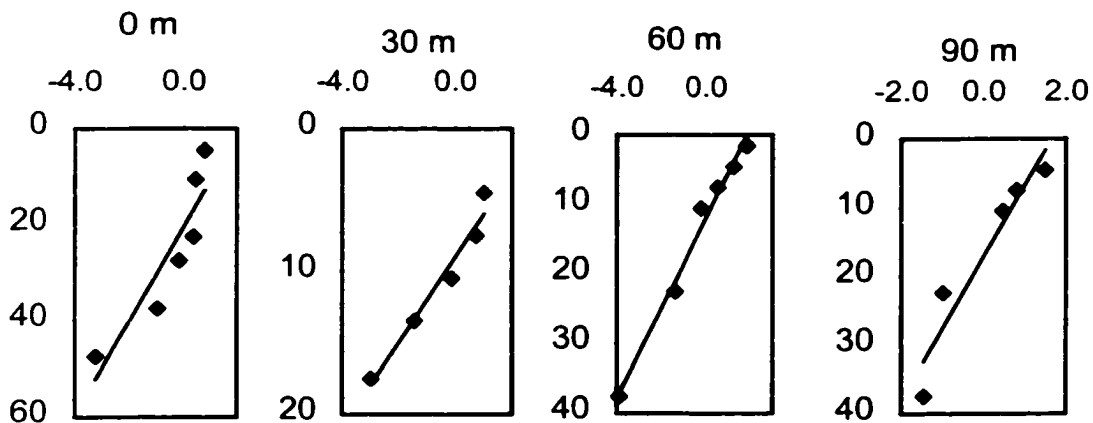
Transect A



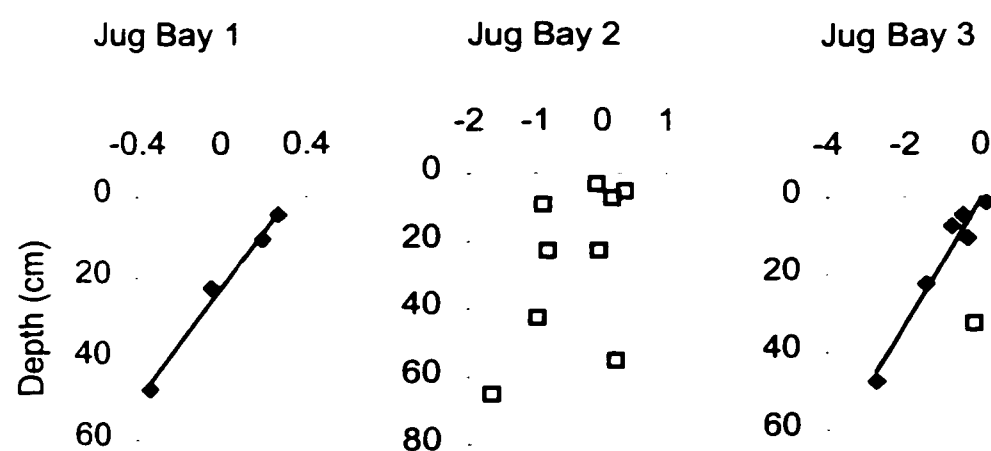
Transect B



Transect C



( c )



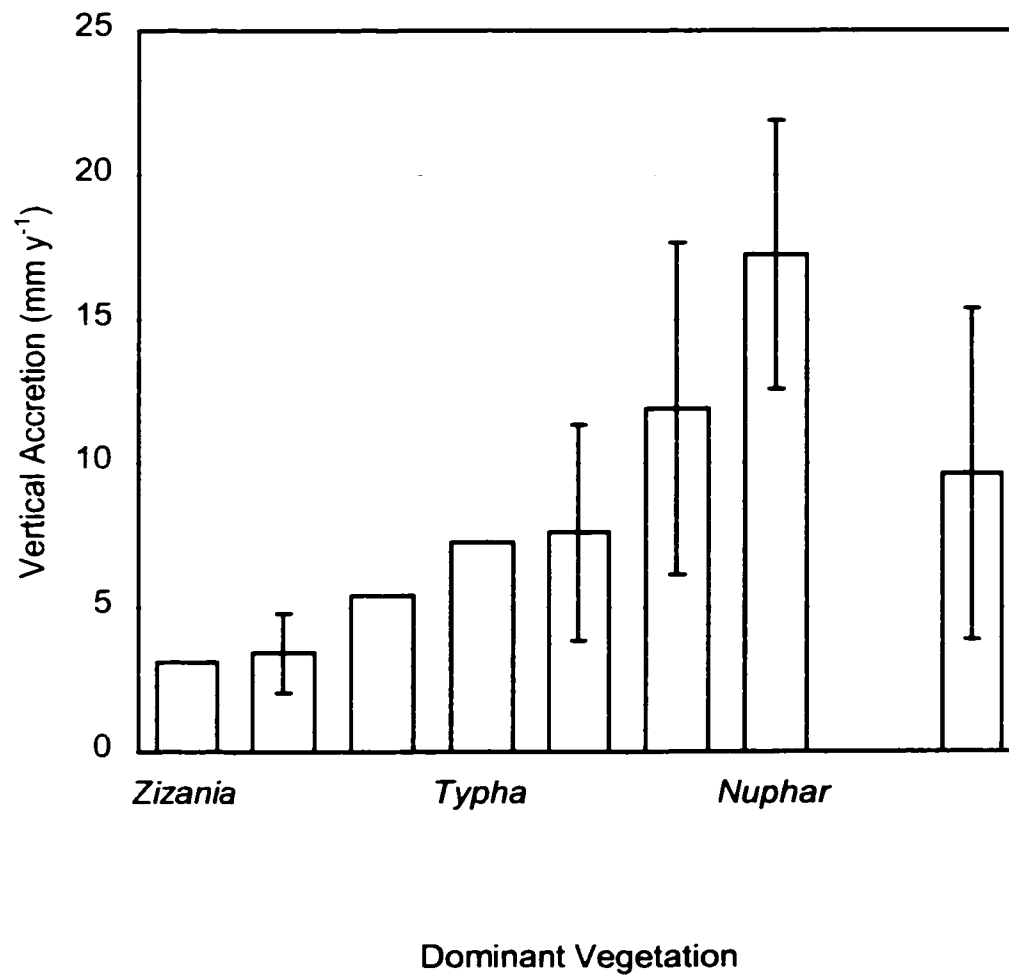
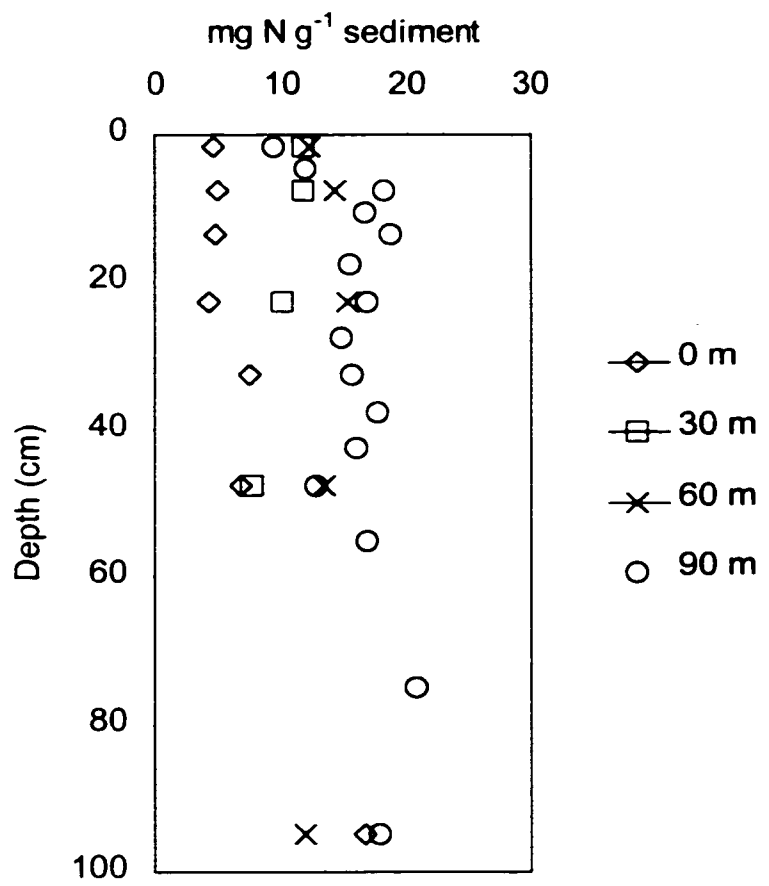
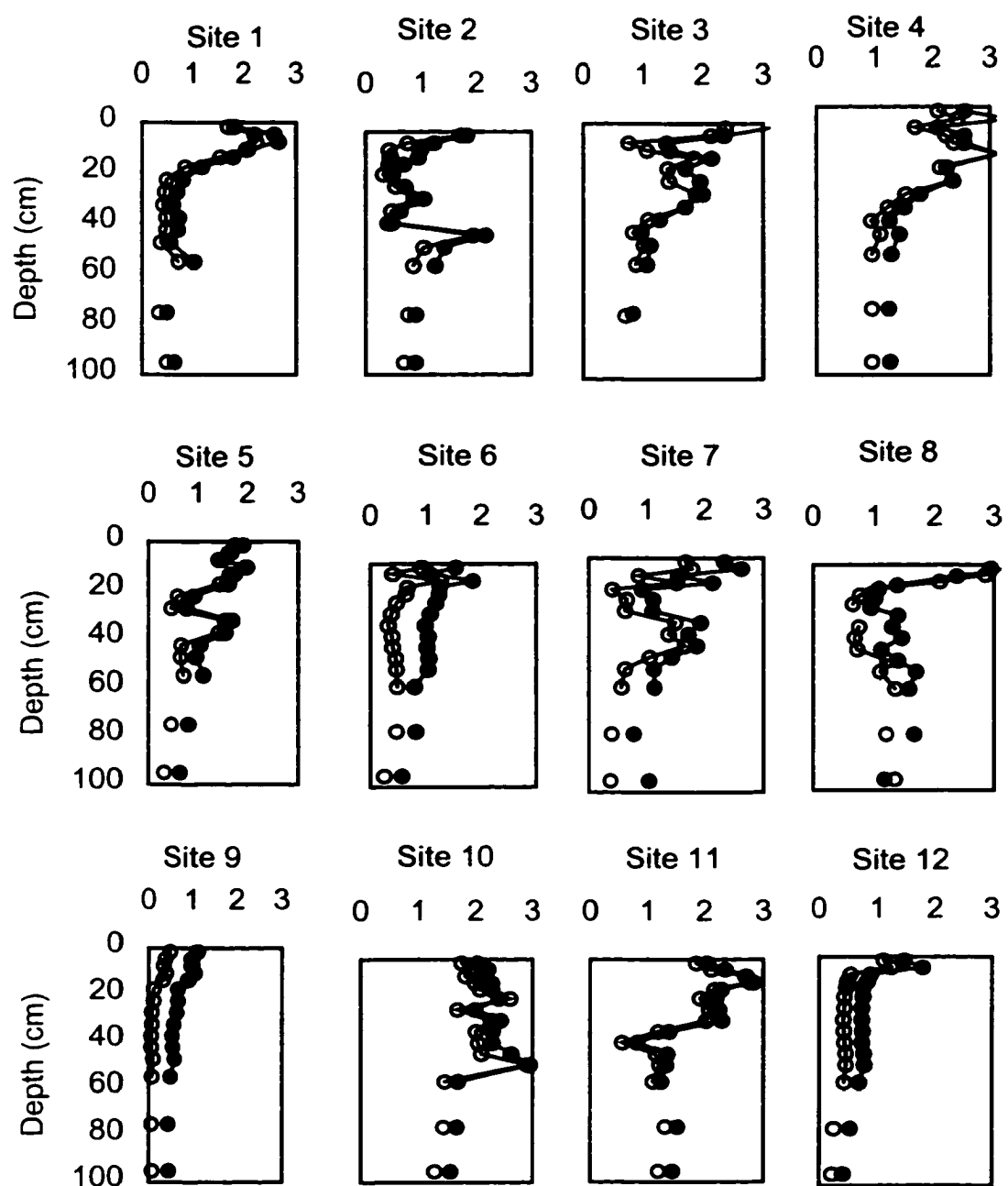


Figure 2-4. Sediment accretion rates by dominant vegetation community as determined by  $^{210}\text{Pb}$  analysis and constant input concentration model. Standard errors are presented where more than one core was successfully dated.



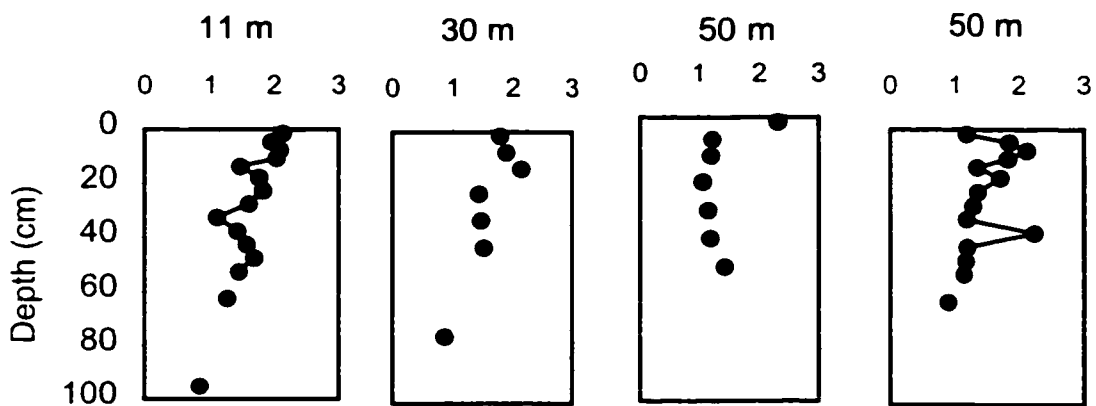
**Figure 2-6.** Profiles of particulate total (closed circle) and inorganic (open circle) phosphorus in Patuxent River marsh sites. The x-axis represents phosphorus in mg P per gram sediment. Sites locations are given in Figure 2-1. Average TP concentration from 20 to 100 cm was used for burial calculations. Cores collected along the axis of the river are shown in (a). Transect (b) and Jug Bay NERR cores (c) are presented with distance from river shoreline.

(a)

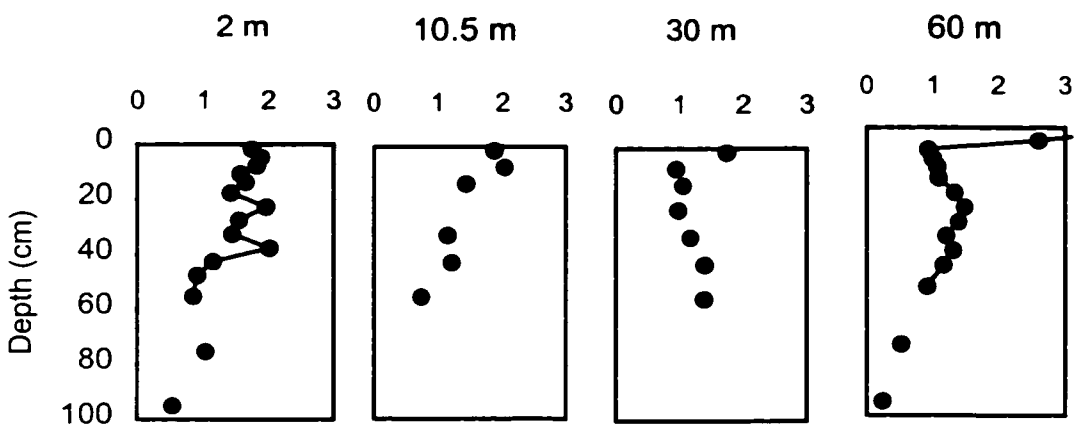


(b)

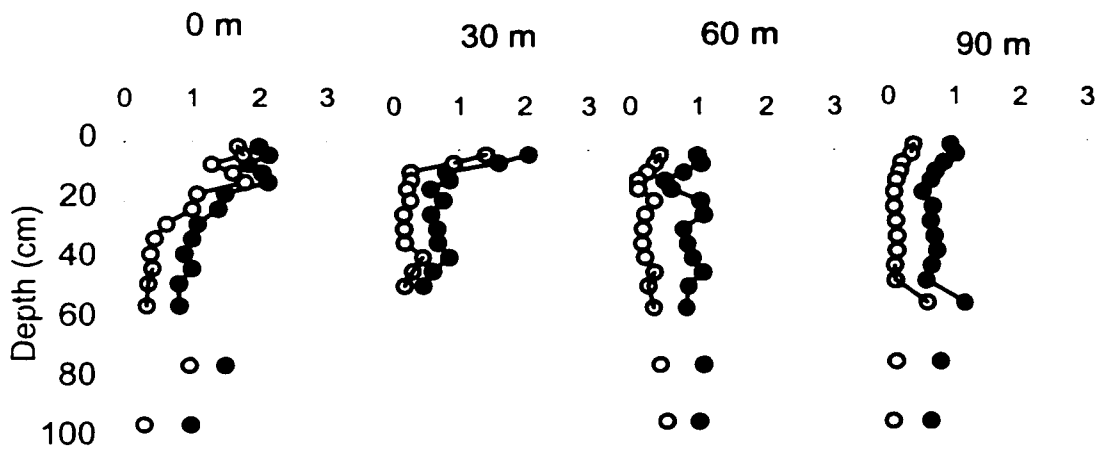
Transect A



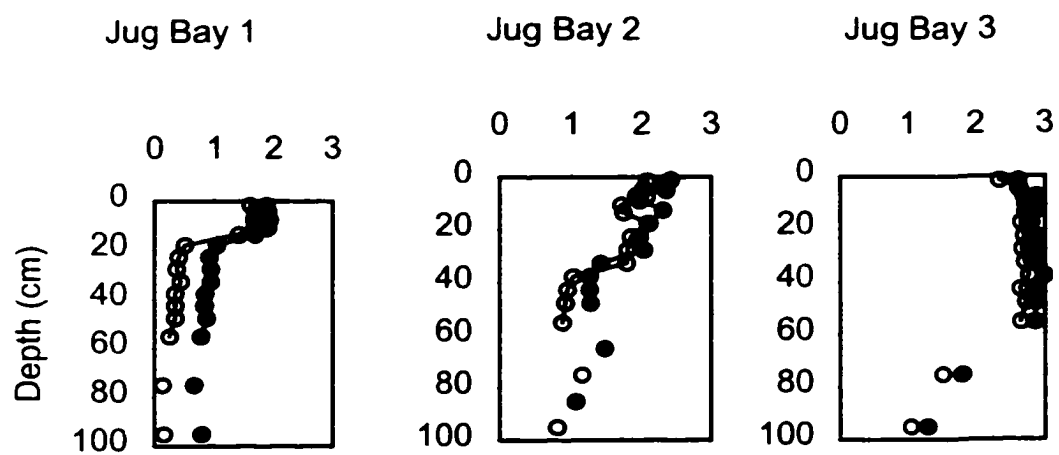
Transect B



Transect C



(c)



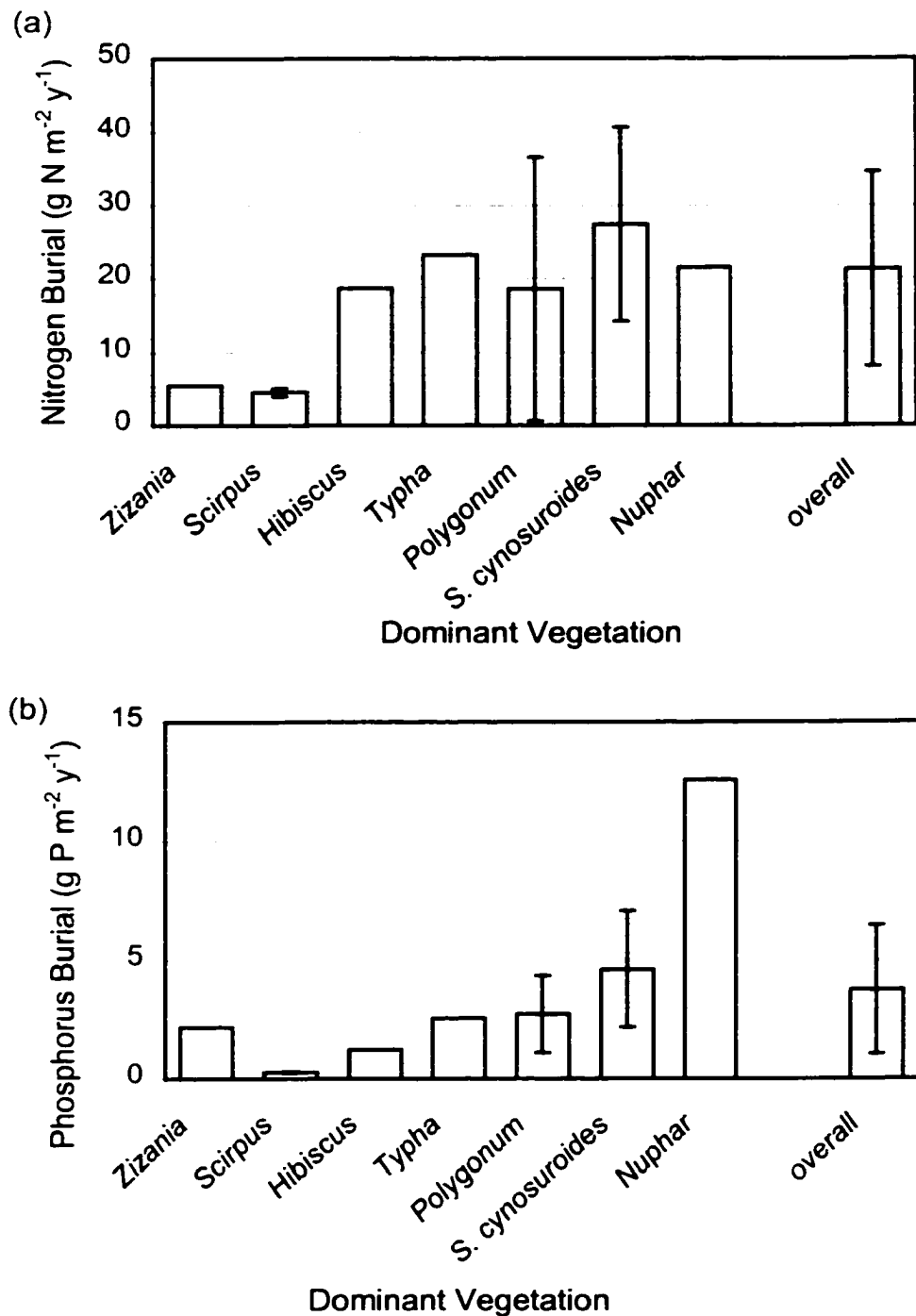
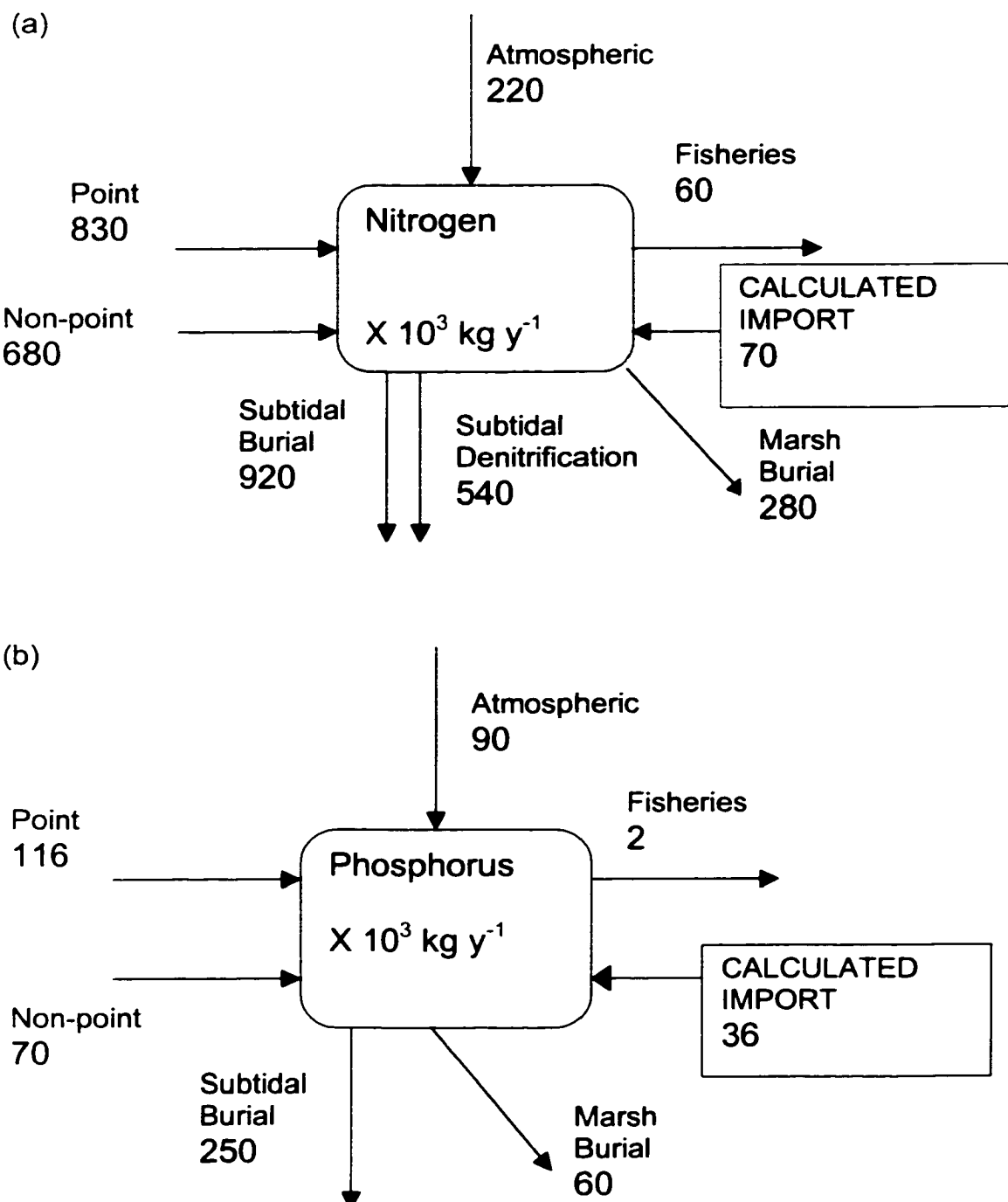


**Figure 2-7. Particulate (a) nitrogen and (b) phosphorus burial in Patuxent River tidal marshes. Rates are presented by dominant vegetation community and standard errors are presented when more than one core was successfully dated.**

Figure 2-8. Conceptual (a) nitrogen and (b) phosphorus budgets for the Patuxent River Estuary compiled by Boynton et al. (1995) and modified with the marsh data generated by this study. Arrows indicate sources (top and left of diagram) and sinks (bottom and right) of nitrogen and phosphorus to and in the Patuxent River Estuary. Point source loads were reported for all major nutrient contributors as listed by the Environmental Protection Agency. Non-point loads were estimated from calculations of River flow and measured nutrient concentration. Atmospheric deposition data reflects nutrient concentrations in wet deposition during many significant rainfall events. Removal by fisheries was calculated using estimates of nutrient concentration and annual reports of commercial and recreational harvests. Subtidal burial was calculated based on limited sediment coring and geochronological techniques. Denitrification was estimated from rates measured earlier within Patuxent Estuary sediments. See Boynton et al. (1995) for more detail. Marsh burial was calculated using sediment accretion and nutrient concentration. Final Import/Export numbers are simple sums resulting from the estimated inputs and removals of both nitrogen and phosphorus. All estimates are presented in  $10^3 \text{ kg y}^{-1}$ .



# **CHAPTER 3: DENITRIFICATION IN TIDAL FRESHWATER MARSHES OF THE PATUXENT RIVER**

## **INTRODUCTION**

For more than twenty-five years, researchers have sought to determine patterns for making broad-based generalizations relating marsh characteristics to estuarine water quality. Numerous investigations have produced a spectrum of results, showing tidal marshes acting as nutrient sinks (Dame et al. 1991), transformers (Correll et al. 1992) and exporters (i.e. Stevenson et al. 1977, Whiting et al. 1989). Clearly the relationship of marshes and their surrounding ecosystems is related to the nutrient loading the marsh receives (Dame et al. 1991). Characteristics such as hydrology (Bowden 1987) and geologic age (Childers et al. 1993, Childers and Day 1990) appear to influence the direction and magnitude of nutrient exchange between marshes and estuaries. The vast majority of coastal marsh studies focus on salt marshes (Armentano and Woodwell 1975, Kaplan et al. 1979,

Howarth and Giblin 1983, Schubauer and Hopkinson 1984, Howes et al. 1985, Howes et al. 1986, Sharma et al. 1987, Bricker-Urso et al. 1989, DeLaune et al. 1989, Sullivan and Moncreiff 1990, Thompson et al. 1995), with fewer studies reported for brackish marshes (Jordan et al. 1983, Cahoon and Stevenson 1986, Stribling 1994, Nyman and DeLaune 1991) and for tidal freshwater marshes (Odum 1988, Simpson et al. 1983, Bowden 1986, Findlay et al. 1990, Orson et al. 1990, Pasternack and Brush 1998). Odum's (1988) review is a comprehensive comparison of tidal freshwater marshes and salt marshes.

Denitrification has been measured in marine (Barnes et al. 1975, Jahnke et al. 1982, Devol 1991, Lohse et al. 1996), coastal (Jenkins and Kemp 1984, Jorgensen 1989, Ogilvie et al. 1997) and freshwater (Christensen et al. 1990, Blackburn et al. 1994, Groffman 1994) aquatic systems in great detail. Denitrification studies have also been conducted in salt marshes (Kaplan et al. 1979, Thompson et al. 1995). Aspects of nitrogen cycling in tidal freshwater marshes have been investigated by Bowden (1986) but denitrification was not measured. This study presents the first directly measured rates of denitrification in a tidal freshwater marsh.

Denitrification is a natural microbial process which removes potentially eutrophying concentrations of nitrate from aquatic systems and releases it as dinitrogen gas. Seitzinger (1988) has shown that denitrification can account for as much as 60% of nitrogen inputs in coastal and freshwater aquatic ecosystems. Tidal freshwater marshes embody a set of characteristics which

may maximize denitrification rates. Mass balance calculations indicate that the fresh areas of upper estuaries may be nitrogen sinks (Howarth et al. 1996). The contribution of bordering marshes has not been addressed. This study is the first attempt to measure rates and describe spatial and temporal variability of denitrification within a fresh marsh. The approach presented here is to observe small nitrogen concentration changes in overlying water in sediment cores infer rates of  $N_{2(g)}$  flux. This method offers advantages over attempts to measure nutrients entering and leaving the marsh (Heinle and Flemer 1976, Stevenson et al. 1977, Whiting et al. 1989), because measurements are direct and experimental conditions can be controlled to remove much of the natural heterogeneity which occurs in the marsh.

## Denitrification

Sediment organic matter is degraded by sediment-dwelling microbial communities in a series of energy-liberating reactions. A sequence of terminal electron acceptors ( $O_2$ ,  $NO_3^-$ , Fe(III),  $SO_4^{2-}$ ) is coupled with the oxidation of organic matter (Santschi et al. 1990) which allows decomposition to occur in a variety of redox regimes. After oxygen is depleted, microbial communities convert  $NO_3^-$  to  $N_2$ , a process known as denitrification, which results in a loss of fixed nitrogen from the system. When nitrate supply becomes limiting iron and sulfate reduction dominate, and finally

methanogenesis is the last of the energy-liberating reactions in the sequence of organic matter oxidation. Microbial communities capable of denitrification are believed to be ubiquitous and require (1) hypoxic or anoxic conditions, (2) labile organic matter as a substrate, and (3) nitrate to accept the electrons from the oxidation reaction. Hypoxic and anoxic conditions are common in marsh sediments, which undergo periods of flooding, limiting the supply of oxygen to the sediment. Organic matter supply can limit denitrification (Caffrey et al. 1993) but its abundance in marsh sediment (>12% versus <4% in most subtidal sediments) generally should provide a more than adequate supply. Nitrate can be supplied from overlying water when water column concentrations are high, which is common in upper estuarine systems near areas of tidal freshwater marshes (Swarth and Peters 1993). Microbial conversion of ammonium to nitrate (nitrification) is another source of nitrate and can be closely linked to overall rates of denitrification (Jenkins and Kemp 1984, Rysgaard et al. 1993, Kana et al. 1998). Referred to as "coupled nitrification-denitrification," readily available ammonium in marsh sediments may provide abundant fuel for nitrification. Nitrification, which requires oxygen, increases in the presence of active plant roots (Reddy et al. 1989, Caffrey and Kemp 1992).

Nitrate may be the limiting factor to salt marsh denitrification since this species is in short supply in lower estuaries (Smart and Barko 1980). Furthermore, Joye and Hollibaugh (1995) found that sulfide inhibits nitrification, suggesting that in salt marshes, sulfide may de-couple

nitrification and denitrification. The relative importance of coupled versus uncoupled denitrification may be dependent on external nitrate supply and the salinity of the marsh. Low sulfide concentrations in tidal freshwater marshes may remove this inhibition of nitrification, allowing a higher overall rate of  $N_{2(g)}$  loss.

Traditional techniques for measuring denitrification in aquatic systems are difficult and error-prone, and depend on inhibiting nitrogen cycle transformations (Seitzinger et al. 1993). The acetylene block technique has been used frequently (Sorensen 1978, Sloth et al. 1992, Thompson et al. 1995), but may underestimate denitrification since nitrification, a potential source of nitrate supply, is inhibited (Knowles 1990). Denitrification can be traced by the addition of the stable isotope  $^{15}NO_3^-$  (Bowden 1986), and nitrification can be traced using additions of  $^{15}NH_4^+$  (Blackburn 1979, Nishio et al 1982, Jenkins and Kemp 1984), but uneven labeling of the nitrogen pools and fertilization of natural rates can occur (Middleburg et al 1996). Direct measurements of  $N_{2(g)}$  production have been made by sufficiently reducing the background concentration of  $N_{2(g)}$  in air space over sealed cores to measure small concentration changes (Seitzinger et al. 1993). However, even with purging of background gases, long incubation times (weeks) are necessary to measure such small changes relative to the large concentration of  $N_{2(g)}$ . Degradation of large fractions of the most labile organic matter during the pre-experiment incubation period likely effects the rate of denitrification and results do not reflect natural conditions at the sediment surface.

Recently, a membrane-inlet mass spectrometric technique was developed to measure small changes in large pools of dissolved nitrogen in water samples (Kana et al. 1994). This technique measures the end-product of denitrification ( $N_{2(g)}$ ) directly, and experimental incubation times of less than 18 hours appear sufficient. Water samples may be drawn from intact cores with minimal sediment disruption, nutrient pools and other factors regulating denitrification are not enhanced or depleted, all of which allows a close approximation of natural conditions.

The approach requires a simplification of the natural system: experimental sediment cores are constantly flooded to remove error associated with gas-water phase equilibrium and eliminate redox shifts. A variable redox regime may increase the number of microsites in the sediment where nitrate is present in an otherwise anaerobic environment (Jenkins and Kemp 1984) thereby enhancing overall denitrification. While the variable redox conditions could not be replicated in the lab with simulated tides experimental artifacts were significantly reduced by approximating a tidal cycle (6 to 12.5 hours) in experimental incubation periods. In subtidal sediments, Risgaard-Petersen et al. (1994), showed a clear response of denitrification to diurnal cycles- the result of benthic algal oxygen production promoting more rapid rates of nitrification. Dark incubations were conducted to minimize variability associated with shifting sediment oxygen consumption and production rates by benthic algae.

This study measured denitrification during four seasons in a tidal freshwater marsh on the Patuxent River, Maryland using the mass spectrometric technique to address the following questions: (1) is denitrification occurring in these marshes; (2) are rates comparable to those measured in other aquatic systems; (3) do increased nitrate concentrations lead to higher rates of denitrification; and (4) are tidal fresh marshes a significant sink for nitrogen?

## SITE DESCRIPTION AND METHODS

The tidal freshwater marshes of Jug Bay, on the Patuxent River, Maryland were sampled in the spring, summer and fall of 1997 and the spring of 1998 (Figure 3-1). Three locations in the marsh were chosen to describe variability across different flooding regimes in the marsh and are described throughout this chapter as low, middle, and high marsh. The low marsh site was located approximately one meter from the edge of a tidal creek in Jug Bay and the vegetative cover consisted of widely spaced *Nuphar advena*. The sediment here contained less organic matter than other marsh sites. Surface sediments appeared oxidized when the cores were collected at low tide. A mix of *Nuphar* and *Peltandra* covered the mid-marsh site, and sediments had higher organic matter concentrations than at the low marsh site. Vegetation at the high marsh site consisted of a dense mixture of *Typha*

spp. and *Peltandra*. Sediment at the high marsh site contained large fragments of decaying plant detritus. A fourth tidal creek-bottom site was included for comparison to the marsh sites and is referred to as the subtidal site.

Thirty centimeter long PVC cores (10 cm inner-diameter) were used to collect sediment cores 15 cm in height. Cores were collected at low tide with minimal sediment disturbance. The sediment was transported to Horn Point Laboratory on ice and stored in a dark environmental chamber. The environmental chamber was kept at temperatures measured in the tidal creek water, 14°C, 23°C, and 15°C, spring, summer and autumn, respectively. Cores were equilibrated at this temperature for more than 18 hours before experiments were begun. Time course experiments were conducted without light. Overlying water was drained and the cores were refilled with river water from the site. Blanks consisting of PVC core tubes filled with river water with a rubber bottom at 15 cm were incubated alongside experimental cores. Cores were sealed with 15 cm of overlying water and no airspace. Gas bubbles were gently forced out of the polycarbonate flux lid which was fitted with a sample port, fill port and a magnetic stir bar which was turned via an external motor-driven magnetic carousel. Core chambers which showed any indication of leakage were removed from the experiment. For the spring 1998 experiment six cores were collected from both the low and high marsh sites and three from each site were supplemented with 220 µM NO<sub>3</sub>. The

cores were conditioned for 3 days with tidal cycles simulated by filling and draining the cores with treatment water (natural or NO<sub>3</sub>-supplemented) every 8 hours. Prior to the experiment cores were drained and refilled as in other experiments.

Time course incubations were terminated when oxygen concentrations measured in overlying water dropped to approximately 5 mg O<sub>2</sub> L<sup>-1</sup>. Such maintenance of high oxygen concentrations avoids stoichiometric complications due to non-aerobic metabolic pathways of organic matter degradation (Santschi et al. 1990). Oxygen and gaseous nitrogen concentrations were determined simultaneously on duplicate samples collected in glass tubes with ground glass stoppers. Samples were submerged in water at the experimental temperature and analyzed on a dissolved gas analyzer (DGA) within three hours of collection. Details of the instrumentation can be found in Kana et al. (1994). Briefly, whole water samples were pumped through a gas permeable membrane which was kept at a constant temperature and under high vacuum (mTorr). The membrane allows the passage of gas molecules from the water into the attached mass spectrophotometer (Balzers Prisma with a Varian Turbo V70 vacuum pump). Oxygen, nitrogen and argon concentrations were reported calibrated relative to an equilibrated standard of similar salinity. Oxygen and nitrogen concentrations were measured relative to a conservative gas, argon. All samples were run in duplicate and average concentrations are reported. Data were corrected for instrument drift.

Ammonium and phosphate concentrations were also measured during the time course experiment. Twenty milliliters of water were collected, syringe filtered, and immediately frozen for ammonium and nitrate analysis. Ammonium concentrations were analyzed following the Parsons et al. (1984) alternative method with phenol, nitroprusside and oxidizing reagents. Nitrate samples were analyzed on a Dionex ion chromatograph.

Concentration changes over time were modeled using a linear regression to determine sediment-water exchange rates. Results yielding an  $r^2 < 0.80$  are reported as no flux. In experiments where the blank concentration changes were linear and significantly different from zero (ANOVA  $\alpha=0.05$ ) the blank flux was subtracted from experimental core flux rates. Average rates are reported for sites when >50% of the experimental cores indicate a nutrient flux.

Molar ratios of solid phase carbon, nitrogen and phosphorus are included from an earlier study (Merrill Chapter 2). Sediment was collected from the low and high marsh sites during the summer of 1994 using a McAuley corer and sectioning the one meter long cores in the field. The top 3 cm was homogenized and total phosphorus was measured on ashed ( $550^{\circ}\text{C}$  2.5 hours) samples following a 1 N HCl extraction and a molybdenum blue assay (Parsons et al. 1984). Carbon and nitrogen were measured on a CHN Control Equipment analyzer ( $\pm 5\%$ ).

Incubation cores were manipulated in the spring 1998 experiment to determine any potential fertilization effects with increased  $\text{NO}_3^-$  concentrations in the tidal freshwater systems. Nitrate concentrations were increased approximately three and one-half times over ambient concentrations using a solution of sodium nitrate added to overlying water.

## RESULTS

### Spring 1997

Water column oxygen concentrations declined in all cores indicating sediment oxygen uptake (Figure 3-2). Dissolved oxygen flux rates were calculated and ranged from 1240 to 2300  $\mu\text{mol O}_2 \text{ m}^{-2} \text{ h}^{-1}$  (Table 3-1).

Sediment uptake of oxygen in the subtidal cores was not as rapid as cores collected from the marsh. Oxygen was consumed more rapidly sites with higher elevations (Table 3-1). Despite an apparent increase in oxygen consumption with location, only the high marsh site was distinct from the other sites due to variability among replicate cores.

Ammonium concentration in the blank core remained constant at 45  $\mu\text{mol NH}_4^+ \text{ L}^{-1}$ , indicating no net flux of ammonium due to resident water column microbes or phytoplankton (Figure 3-2). Sediment collected from the subtidal site released ammonium, increasing the water column concentration

to approximately  $60 \mu\text{mol NH}_4^+ \text{ L}^{-1}$  before remaining constant. Both low and middle elevation sediment cores reduced ammonium in the water column to a concentration of  $37\text{--}40 \mu\text{mol NH}_4^+ \text{ L}^{-1}$ . High marsh sediment effected no net change on the water column concentration of ammonium. Decreases in ammonium concentrations in low marsh cores were non-linear, therefore low marsh sediment effects on ammonium in this experiment are reported as not different from zero (Table 3-1). Ammonium exchange at the high marsh site also was not different from zero. Nitrate exchange rates are not available for the spring experiment.

Gaseous nitrogen concentrations increased in the overlying water of all marsh cores (Figure 3-3). Flux rates based on these increases were calculated as 24 to  $59 \mu\text{mol N}_2\text{-N m}^{-2} \text{ h}^{-1}$  after correcting for  $\text{N}_2\text{-Ar}$  drift in the Patuxent River water blank. Rates of  $\text{N}_{2(g)}$  release appeared to increase with marsh elevation, but due to the high variability the increase was not statistically significant (Table 3-1). By contrast, only one of the two subtidal cores exhibited  $\text{N}_{2(g)}$  exchange and  $\text{N}_{2(g)}$  concentration declined, indicating a flux of  $\text{N}_{2(g)}$  into the sediment at a rate of  $28.4 \mu\text{mol N m}^{-2} \text{ h}^{-1}$ .

## Summer 1997

In the summer experiment oxygen fluxes were all directed into the sediment of marsh cores (Figure 3-4). Uptake rates were calculated at 853 to

2180  $\mu\text{mol O}_2 \text{ m}^{-2} \text{ h}^{-1}$ . High variability in oxygen consumption between replicate cores at each site prevented distinguishing clear trends in oxygen consumption with location in the marsh (Table 3-2).

All ammonium fluxes were directed out of the sediments (Figure 3-4). Release of ammonium from the subtidal cores the highest at  $320 \pm 5.0 \mu\text{mol N m}^{-2} \text{ h}^{-1}$ , but not distinguishable from the low marsh. Release of  $\text{NH}_4^+$  from marsh cores ranged from 150 to  $320 \mu\text{mol N m}^{-2} \text{ h}^{-1}$ , but rates were not statistically different from each other. Rates of ammonium release in summer were the highest measured in this study. Ambient nitrate concentrations were low ( $18 \mu\text{M NO}_3^-$ ) yet all fluxes were from the water column into the sediments (Figure 3-4). Subtidal and low marsh cores took nitrate up at very similar rates, 102 and  $90 \mu\text{mol NO}_3^- \text{ m}^{-2} \text{ h}^{-1}$ , respectively. No nitrate flux rates are reported for the mid marsh site since only one of three cores exhibited a net exchange (Table 3-2).

Gaseous nitrogen concentrations showed no linear trend in the subtidal and high marsh cores (Figure 3-5). While concentration changes in  $\text{N}_{2(\text{g})}$  were linear in cores collected from the middle marsh, the fluxes inferred were not significantly different from zero (ANOVA  $\alpha=0.05$ ). As a result, net denitrification was found only in two low marsh cores and the average release was calculated at  $33.3 \mu\text{mol N m}^{-2} \text{ h}^{-1}$ .

## Autumn 1997

Subtidal cores were not collected due to sampling problems. Oxygen uptake was observed in all cores (Figure 3-6) and rates were not statistically different between the marsh sites, ranging from 1250 to 1800  $\mu\text{mol O}_2 \text{ m}^{-2} \text{ h}^{-1}$  (Table 3-3).

Nitrogen fluxes during this experiment were very small in all cases. Ambient ammonium concentrations were low, less than 1.0  $\mu\text{M NH}_4^+$ . No regular increase in concentration was found during the incubations (Figure 3-6). Nitrate concentrations were low, 21  $\mu\text{M NO}_3^-$ , and linear changes in concentration were not observed in any of the cores.

Experimental core flux rates presented have been corrected for drift in  $\text{N}_{2(\text{g})}$  in the river water blank (Figure 3-7). The calculations result in a net uptake of  $\text{N}_{2(\text{g})}$  by the sediment in all marsh cores. The fluxes are small but show significant nitrogen fixation on the surface of the marsh. Nitrogen uptake by the low marsh was not different from zero (standard deviation = 41.8).

## Spring 1998

The spring 1998 experiment investigated the response of marsh sediment to increases in nitrate supply. Control cores were incubated in

ambient river water and experimental cores were incubated in  $\text{NO}_3^-$ -supplemented river water (64 and 220  $\mu\text{M}$   $\text{NO}_3^-$ , respectively). High and low marsh sites were sampled and incubations were conducted at 16°C. Oxygen uptake rates in the high marsh were greater in both cases, at 2690 and 2240  $\mu\text{mol O}_2 \text{ m}^{-2} \text{ h}^{-1}$  in control and  $\text{NO}_3^-$ -amended cores, respectively (Table 3-4). High and low marsh cores responded differently to an increased supply of nitrate (Figure 3-8). Oxygen uptake decreased with the addition of  $\text{NO}_3^-$  in the high marsh cores, while the oxygen uptake rate increased with added  $\text{NO}_3^-$ , from 1620 to 1920  $\mu\text{mol O}_2 \text{ m}^{-2} \text{ h}^{-1}$ .

Dissolved nitrogen fluxes increased in response to enhanced nitrate supply. Ammonium was released from the sediment in all treatments and cores. The lowest release of  $\text{NH}_4^+$ -N was in the low marsh, ambient  $\text{NO}_3^-$  cores. Nitrate additions increased ammonium release in the low marsh, but did not appear to effect the high marsh sediment. All sediment cores took up  $\text{NO}_3^-$  from the water column (Figure 3-8), with rates increasing in response to increased  $\text{NO}_3^-$  in the overlying water. Control cores from both low and high marshes removed  $\text{NO}_3^-$  at a rate of 126 ( $\pm 8.23$ ) and 225 ( $\pm 4.12$ )  $\mu\text{mol N m}^{-2} \text{ h}^{-1}$ . The rates increased to 692 ( $\pm 181$ ) and 788 ( $\pm 263$ )  $\mu\text{mol N m}^{-2} \text{ h}^{-1}$ , respectively, with  $\text{NO}_3^-$  amendments.

Gaseous nitrogen exchanges were directed out of the sediment to the water column and the rates increased with  $\text{NO}_3^-$  amendments. Only two of five control cores released  $\text{N}_{2(\text{g})}$  (Figure 3-9). No net denitrification occurred in

control cores since the majority of cores showed no flux. Releases of N<sub>2(g)</sub> were measured in four of five NO<sub>3</sub>-amended cores. Nitrogen release was 311 µmol N m<sup>-2</sup> h<sup>-1</sup> in the low marsh and 398 µmol N m<sup>-2</sup> h<sup>-1</sup> in the high marsh (Table 3-4). Denitrification rates were higher than any measured in this study under ambient, low nitrate conditions. Additional nitrate supply to the sediment appeared to allow denitrification to occur consistently in the marsh cores (Figure 3-10).

### Annual Observations

Relatively little variability in sediment oxygen demand was observed throughout the year (Figure 3-11). Oxygen demand in sediments of the high marsh were consistently higher than at other sites, with the exception of subtidal cores in the summer of 1997. Overall the sediment oxygen demand observed in this study was similar to that reported by Seitzinger (1994) for a variety of riparian wetlands. Temperature variability did not appear to influence the rates of sediment oxygen demand. The summer experiment was conducted at 23°C, 9 to 11 degrees higher than any of the other seasonal experiments. Temperature was clearly not an important factor in determining sediment oxygen demand.

Seasonal ammonium fluxes were highly variable, indicating shifting patterns of nitrogen cycling within the marsh throughout the year (Figure 3-

12). Ammonium release from the sediment was greatest in the summer, coinciding with a period of no net denitrification. Generally, rates of ammonium exchange were within the range reported by Bowden (1986) and release from the subtidal sediments was only slightly higher than release from marsh sediments.

Denitrification was clearly a seasonal phenomenon in the tidal freshwater marsh (Figure 3-13). Spring rates peaked at  $60 \mu\text{mol N m}^{-2} \text{ h}^{-1}$  in the high marsh. The low marsh, despite the lower rates of denitrification, may contribute more to the total marsh denitrification since the site appears to support net denitrification over a greater portion of the year. Spring rates were comparable to those reviewed by Seitzinger (1988) for rivers, lakes, and coastal marine systems. Rates measured in the Patuxent River marshes were very similar to denitrification rates measured in the Patuxent River subtidal sediments (Jenkins and Kemp 1984) at  $77-89 \mu\text{mol N m}^{-2} \text{ h}^{-1}$  using  $^{15}\text{N}$  to trace nitrogen cycling.

## DISCUSSION

This first series of measurements of denitrification in tidal freshwater marsh sediments met with mixed success. Spatial coverage within the marsh was emphasized in this study and revealed significant differences. Data from the high marsh alone, for instance, would result in a very different estimates

of system denitrification than the low marsh. Variability between seasons would likely result in similar errors. This series of experiments produced a variable data set with few statistically significant patterns, but implied spatial and seasonal trends in marsh nitrogen cycling.

Prediction of  $N_{2(g)}$  flux based on stoichiometric relationships of oxygen consumption, organic matter nutrient concentrations were not reliable. From work presented in Chapter 2, the solid phase molar C:N ratios of low and high marsh sediments were 11.6 and 14.7, respectively. These ratios were used to calculate expected dissolved nitrogen availability per mole of oxygen taken up by the sediments, a common approach in benthic studies. A mass balance for inorganic nitrogen is calculated from all fluxes, including nitrate and ammonium and nitrogen available as oxygen is consumed and organic matter mineralized. The remaining dissolved nitrogen is theoretically available for denitrification in the absence of vegetative uptake. Predictions based on stoichiometric calculations did not accurately reflect measured rates of denitrification in this study. For example, sediment oxygen uptake rates in the low marsh summer 1997 cores (Table 3-2) suggest  $102 \mu\text{mol N m}^{-2} \text{ h}^{-1}$  are available as a result of organic matter degradation. An additional  $90 \mu\text{mol N m}^{-2} \text{ h}^{-1}$  are available due to nitrate uptake. Ammonium released from the sediment at a rate of  $267 \mu\text{mol N m}^{-2} \text{ h}^{-1}$ , leaving a balance of  $75 \mu\text{mol N m}^{-2} \text{ h}^{-1}$  needed by the sediments to balance the ammonium release. Gaseous nitrogen flux due to net denitrification was calculated as  $33 \mu\text{mol N m}^{-2} \text{ h}^{-1}$ ,

leaving a deficit of over 100  $\mu\text{mol N m}^{-2} \text{ h}^{-1}$ . Similar calculations were completed for other seasons and nitrogen exchanges were not well-balanced. Intermediate products of the denitrification reaction (e.g.  $\text{N}_2\text{O}$ ) were not measured during this experiment but are likely to account for less than 1% of the gaseous nitrogen released (Seitzinger 1988). Macrophyte-derived organic matter exhibits an increase in nitrogen concentration as it begins to decompose. A combination of microbial incorporation of nitrogen and abiotic adsorption (Rice 1982, Findlay et al. 1990) on decaying organic matter may be responsible for the nitrogen which was not accounted for during these seasons. Estimates of denitrification calculated by difference in tidal freshwater marsh systems should be applied with caution.

## Seasonal Nitrogen Cycling

### SPRING

During the spring of 1997 the Jug Bay marsh sediment was a sink for ammonium which was likely nitrified and then denitrified in the experimental cores (Figure 3-14) (Seitzinger 1994). Excess ammonium consumed by the sediment likely supported microbial growth, since macrophytes were not included in the flux chambers. Uptake of ammonium by macrophytes should be a competing uptake process during the spring, when growth rates are highest (Simpson et al. 1983). Nitrate data are not available, but there likely

was an uptake of nitrate from the overlying water, contributing to the rates of denitrification. In the field, the microbial populations will compete with macrophytic vegetation for these supplies of nitrogen.

## SUMMER

Ammonium was released from all sites due to the mineralization of organic matter and ammonification of nitrate taken up by the sediments under anoxic conditions (Figure 3-14). Subtidal sediments sampled during this experiment were on a creek bottom, with moderate to fast channel flow, while high marshes sediments are shaded by dense vegetation. A high C:N:P ratio of 182:12:1 in the high marsh sediment prevented rapid turnover of organic material. Net denitrification occurred only in the low marsh cores, where labile organic material is most readily available (C:N:P 69:5.9:1), a site characterized by broad-leaf, widely-spaced macrophytes.

While nitrate reduction to ammonium may seasonally be a major pathway for nitrogen in marine sediments (Jorgensen 1989), rates are low in tidal freshwater marsh sediments (Bowden et al. 1991). This may be due to the larger exchangeable ammonium "buffer" in freshwater sediments as compared to more saline systems (Seitzinger et al. 1991). In the current study dissimilatory nitrate reduction to ammonium appears to be a significant pathway only during the summer.

## AUTUMN

During autumn measurements, nitrate at a concentration of  $21 \mu\text{mol NO}_3 \text{ L}^{-1}$ , was not removed by the marsh sediment, nor was ammonium released to the water column (Figure 3-14). Organic matter decomposition occurred, as evidenced by the uptake of oxygen, and it appears that the associated ammonium was incorporated in the microbial biomass as described by Bowden (1986). A decrease in water column  $\text{N}_{2(\text{g})}$  was detected indicating nitrogen fixation, resulting in diffusion of  $\text{N}_{2(\text{g})}$  into the sediments. Nitrogen fixation occurring in the high marsh provided additional nitrogen for the microbial breakdown of high C:N organic matter present as a result of the dense, nitrogen-poor marsh vegetation. While nitrogen fixation has been measured in salt marshes (Currin and Paerl 1998a, b), microbes are also capable of supporting energy requirements by reducing sulfate (Nedwell and Aziz 1980) which is not present in large quantities in tidal freshwater marshes. I have not found any previous estimates of nitrogen fixation in tidal freshwater marshes for a comparison, but rates are as high as  $3600 \mu\text{mol N m}^{-2} \text{ d}^{-1}$  in salt marshes (Currin and Paerl 1998b). The low marsh exchange of  $\text{N}_2$  was not distinguishable from zero and may be the result of the lower C:N of the broad-leaved vegetation and deposited phytoplankton. *Nuphar* has been shown to decay more rapidly than high marsh species such as *Typha*.

(Findlay et al. 1990) most likely due to its lower C:N ratio, suggesting little, if any need for external nitrogen for microbial decay of the material.

## SPRING 1998

During the spring of 1998 the marsh sediment removed nitrate from the overlying water column and released ammonium at moderate rates. Denitrification was not detected at ambient nitrate concentrations, as predicted by stoichiometric calculations, and was limited by nitrate supply. Denitrification rates increased from negligible to 300 and 400  $\mu\text{mol N m}^{-2} \text{ h}^{-1}$  in the low and high marshes, respectively, when nitrate was increased 3.4-fold. Measured nitrogen fluxes were not balanced in the nitrate amendment experiments. Ammonium release was increased in the low marsh and unchanged in the high marsh, again suggesting the incorporation of nitrogen into high C:N organic material in the high marsh sediments.

## Jug Bay Summary

Denitrification in tidal freshwater systems is dependent upon organic matter cycling and nitrogen supply. Under ambient conditions denitrification was limited, possibly due to the limited rates of nitrification in the anoxic sediments. The ambient water used during these experiments had somewhat lower concentrations than were expected if the water had been

collected during high tide (Swarth and Peters 1993), leading to a potential underestimate of net system denitrification. Organic matter on the surface of the marsh may have moderated nitrogen fluxes, a result noted by Bowden (1986) in a Massachusetts tidal freshwater marsh. Odum et al. (1984) hypothesized that the lower contributions of organic matter to the sediments of low tidal freshwater marshes were the result of high rates of organic matter turnover and export, an idea supported by Findlay et al. (1990). This is not inconsistent with the results of this study which show low marsh rates of sediment metabolism to be similar to that of other marsh locations but which appears to have a different seasonal pattern of nitrogen cycling.

## Denitrification in Tidal Freshwater Marshes

Denitrification rates have been measured directly using the MIMS technology in two tidal freshwater marsh systems. A summary of data from Jug Bay and Tivoli Bays, a tidal freshwater marsh system located on the Hudson River, New York (Merrill Chapter 4) will be used to examine similarities between tidal fresh marshes. All reported site averages are included for all seasons. Sediment oxygen consumption was not clearly related to denitrification in Jug Bay marshes, but showed a good relationship within the marshes of Tivoli Bays (Figure 3-15). Pooling data from the two tidal freshwater marsh systems shows a relationship between nitrate

concentration and denitrification (Figure 3-16). Denitrification increases with nitrate supply following a linear relation. Maximum rates were approximately 350  $\mu\text{mol N m}^{-2} \text{h}^{-1}$ , and occurred when the sediment received highest concentrations of nitrate. Nitrogen fixation was indicated when nitrate concentrations fell below 14  $\mu\text{M NO}_3^-$ .

Coastal marshes are discharge environments for watershed-derived groundwater. The nitrate addition experiments completed in the spring of 1998 reflected the denitrification rates which would occur in the natural marsh if the surface sediments were exposed to a moderately high concentration of nitrate, such as might be found in a watershed with agricultural activity. Nitrate supplements (220  $\mu\text{M NO}_3^-$ ) were meant to reflect moderately high nitrate concentrations found in groundwater although Jug Bay marshes likely receive the majority of their external nitrate supply from the Patuxent River, rather than groundwater (Swarth and Peters 1993). This nitrate supplement was modest; Staver and Brinsfield (1996) report agricultural groundwater nitrate concentrations as high as 1570  $\mu\text{M NO}_3^-$ . The data suggest tidal freshwater marshes receiving high loads of nitrate are capable of higher rates of denitrification, but these rates will not be sufficient to remove all of the added nitrate.

Nitrate concentrations reach as high as 125  $\mu\text{M NO}_3^-$  (Magnien et al. 1992) during the spring in the upper Patuxent River. Denitrification rates of approximately 240  $\mu\text{mol N}_2\text{-N m}^{-2} \text{h}^{-1}$  should be found in these upper

estuarine marshes. Annual tidal freshwater marsh denitrification was estimated assuming the marshes are flooded 12 hours per day, and denitrification occurs at a rate of  $240 \mu\text{mol N}_2\text{-N m}^{-2} \text{ h}^{-1}$  for 3 months per year, and at  $120 \mu\text{mol N}_2\text{-N m}^{-2} \text{ h}^{-1}$  six months of the year. As a first order estimate the marshes remove  $390 \text{ mmol N}_2\text{-N m}^{-2} \text{ y}^{-1}$ . Using a marsh area of  $20 \times 10^6 \text{ m}^2$  (McCormick and Somes 1982), these marshes remove approximately  $7.8 \times 10^6 \text{ mol N}_2\text{-N y}^{-1}$  ( $109,200 \text{ kg N}_2\text{-N y}^{-1}$ ).

Tidal freshwater marshes support rates of net denitrification within the range of coastal marine systems. The MIMS technique for measuring denitrification relies on the net  $\text{N}_2$  balance, and may provide conservative estimates during periods of nitrogen fixation by the surface of the marsh. Denitrification appears to be related to ambient nitrate concentration in both the Patuxent River and Hudson River tidal freshwater marshes.

## CONCLUSIONS

In response to the questions posed at the opening of this chapter:

1. The marshes of Jug Bay, Patuxent River support net denitrification during portions of the year.
2. Rates of denitrification in the marsh sediment (to  $60 \mu\text{mol N m}^{-2} \text{ h}^{-1}$ ) are comparable to those reported for Patuxent River subtidal sediment (77-90

$\mu\text{mol N m}^{-2} \text{ h}^{-1}$ , Jenkins and Kemp 1984), also measured in the spring.

The rates measured during this study were within the range of rates summarized for coastal marine sediments (0 to 1067  $\mu\text{mol N m}^{-2} \text{ h}^{-1}$ ) by Seitzinger (1988).

3. Nitrate appears to limit denitrification during the spring, even when ambient concentrations are moderate and high, likely due to the competition for nitrogen by microbial, algal and macrophytic primary production.
4. The tidal freshwater marshes of the Patuxent River may remove 109,000 kg nitrogen as  $\text{N}_{2(\text{g})}$  each year. This is equivalent to approximately 10% of the total nitrogen loading to the Patuxent River estuary from sources above the fall line (Boynton et al. 1995), making them valuable sinks for nitrogen in the estuarine ecosystem.

Table 3-1. Sediment-water flux rates found in Jug Bay, Patuxent River, Maryland tidal freshwater marsh sediments in the Spring of 1997. Field temperature and incubations were 14°C. Fluxes are indicated where linear fit ( $r^2 > 0.80$ ) described time course changes in concentration and negative fluxes are directed into the sediment. Non-linear changes are indicated with -. Averages are presented for individual sites where >50% of the cores exhibited a flux. Non-linear results were not included in the averages.

	Oxygen μmol O <sub>2</sub> m <sup>-2</sup> h <sup>-1</sup>	Ammonium μmol NH <sub>4</sub> -N m <sup>-2</sup> h <sup>-1</sup>	N <sub>2(g)</sub> μmol N <sub>2</sub> -N m <sup>-2</sup> h <sup>-1</sup>
Subtidal	-1311	101	-
Subtidal	-1258	147	-28.4
Average ± S.E.	-1284 ± 26.8	124 ± 23.0	
Low Marsh	-1577	-105	19.1
Low Marsh	-1237	--	50.2
Low Marsh	-1547	--	1.69
Average ± S.E.	-1453 ± 144		23.6 ± 17.7
Mid Marsh	-1706	--	19.4
Mid Marsh	-1800	-120	40.7
Mid Marsh	-1288	-119	32.5
Average ± S.E.	-1598 ± 206	-120 ± 0.36	30.8 ± 7.64
High Marsh	-2270	50.5	39.0
High Marsh	-2306	--	94.4
High Marsh	-1804	-18.1	44.4
Average ± S.E.	-2127 ± 215	16.2 ± 34.4	59.2 ± 23.4

Table 3-2. Summer 1997 Jug Bay NERRS, Patuxent River sediment-water flux incubation experiment, conducted at 23°C. Details as in Table 1.

	Oxygen μmol O <sub>2</sub> m <sup>-2</sup> h <sup>-1</sup>	Ammonium μmol NH <sub>4</sub> -N m <sup>-2</sup> h <sup>-1</sup>	Nitrate μmol NO <sub>3</sub> -N m <sup>-2</sup> h <sup>-1</sup>	N <sub>2(g)</sub> μmol N <sub>2</sub> -N m <sup>-2</sup> h <sup>-1</sup>
Subtidal	-1228	328	—	—
Subtidal	-2160	316	-108	—
Subtidal	-2182	317	-96.0	—
Average ± S.E.	-1856 ± 419	320 ± 5.05	-102 ± 5.93	
Low Marsh	-1463	213	-92.0	—
Low Marsh	-1248	321	-88.1	47.9
Low Marsh	-853	--	--	18.8
Average ± S.E.	-1188 ± 223	267 ± 53.9	-90.0 ± 1.94	33.3 ± 14.6
Mid Marsh	-1197	157	--	--
Mid Marsh	-1359	194	-40.4	--
Mid Marsh	-1356	150	--	--
Average ± S.E.	-1304 ± 71.2	167 ± 17.9		
High Marsh	-2079	157	-61.8	--
High Marsh	—	--	--	--
High Marsh	-1377	--	-52.6	--
Average ± S.E.	-1728 ± 351		-57.2 ± 4.60	

Table 3-3. Fall 1997 Jug Bay, Patuxent River flux incubation experiments, conducted at 15°C. All nitrate fluxes were non-linear. Details as in Table 3-1.

	Oxygen μmol O <sub>2</sub> m <sup>-2</sup> h <sup>-1</sup>	Ammonium μmol NH <sub>4</sub> -N m <sup>-2</sup> h <sup>-1</sup>	N <sub>2(g)</sub> μmol N <sub>2</sub> -N m <sup>-2</sup> h <sup>-1</sup>
Low Marsh	-1786	--	-58.7
Low Marsh	-1558	--	-37.9
Low Marsh	-1251	--	42.2
Average ± S.E.	<b>-1614 ± 144</b>		<b>-8.86 ± 41.8</b>
Mid Marsh	-1391	--	-11.4
Mid Marsh	-1375	14.5	-52.1
Mid Marsh	-1263	--	-39.5
Average ± S.E.	<b>-1343 ± 53.4</b>		<b>-27.4 ± 15.1</b>
High Marsh	-1806	--	-41.1
High Marsh	-1638	--	-46.2
High Marsh	-1400	--	-3.39
Average ± S.E.	<b>-1614 ± 144</b>		<b>-22.7 ± 12.3</b>

Table 3-4. Spring 1998 Jug Bay NERRS sediment-water fluxes measured during  $\text{NO}_3^-$  amendment experiments. Control cores were run with ambient nitrate ( $64 \mu\text{mol NO}_3^- \text{ L}^{-1}$ ) and amended cores were incubated in  $500 \mu\text{mol NO}_3^- \text{ L}^{-1}$  water.

### Control Cores

	Oxygen $\mu\text{mol O}_2 \text{ m}^{-2} \text{ h}^{-1}$	Ammonium $\mu\text{mol NH}_4\text{-N m}^{-2} \text{ h}^{-1}$	Nitrate $\mu\text{mol NO}_3\text{-N m}^{-2} \text{ h}^{-1}$	$\text{N}_{2(\text{g})}$ $\mu\text{mol N}_2\text{-N m}^{-2} \text{ h}^{-1}$
Low Marsh	-1658	80.2	-120	--
Low Marsh	-1318	92.9	-120	--
Low Marsh	-1880	112	-138	283
Average $\pm$ S.E.	$-1618 \pm 201$	$95.2 \pm 11.5$	$-126 \pm 8.23$	
High Marsh	-2856	128	-221	327
High Marsh	-2533	138	-230	--
Average $\pm$ S.E.	$-2694 \pm 161$	$133 \pm 4.85$	$-225 \pm 4.13$	

### $\text{NO}_3^-$ Amended Cores

	Oxygen $\mu\text{mol O}_2 \text{ m}^{-2} \text{ h}^{-1}$	Ammonium $\mu\text{mol NH}_4\text{-N m}^{-2} \text{ h}^{-1}$	Nitrate $\mu\text{mol NO}_3\text{-N m}^{-2} \text{ h}^{-1}$	$\text{N}_{2(\text{g})}$ $\mu\text{mol N}_2\text{-N m}^{-2} \text{ h}^{-1}$
Low Marsh	-1772	140	-441	322
Low Marsh	-2098	195	-963	--
Low Marsh	-1903	172	-671	301
Average $\pm$ S.E.	$-1924 \pm 116$	$169 \pm 19.4$	$-692 \pm 181$	$311 \pm 10.9$
High Marsh	-2117	--	-1050	344
High Marsh	-2361	122	-525	451
Average $\pm$ S.E.	$-2239 \pm 122$		$-788 \pm 263$	$398 \pm 53.5$

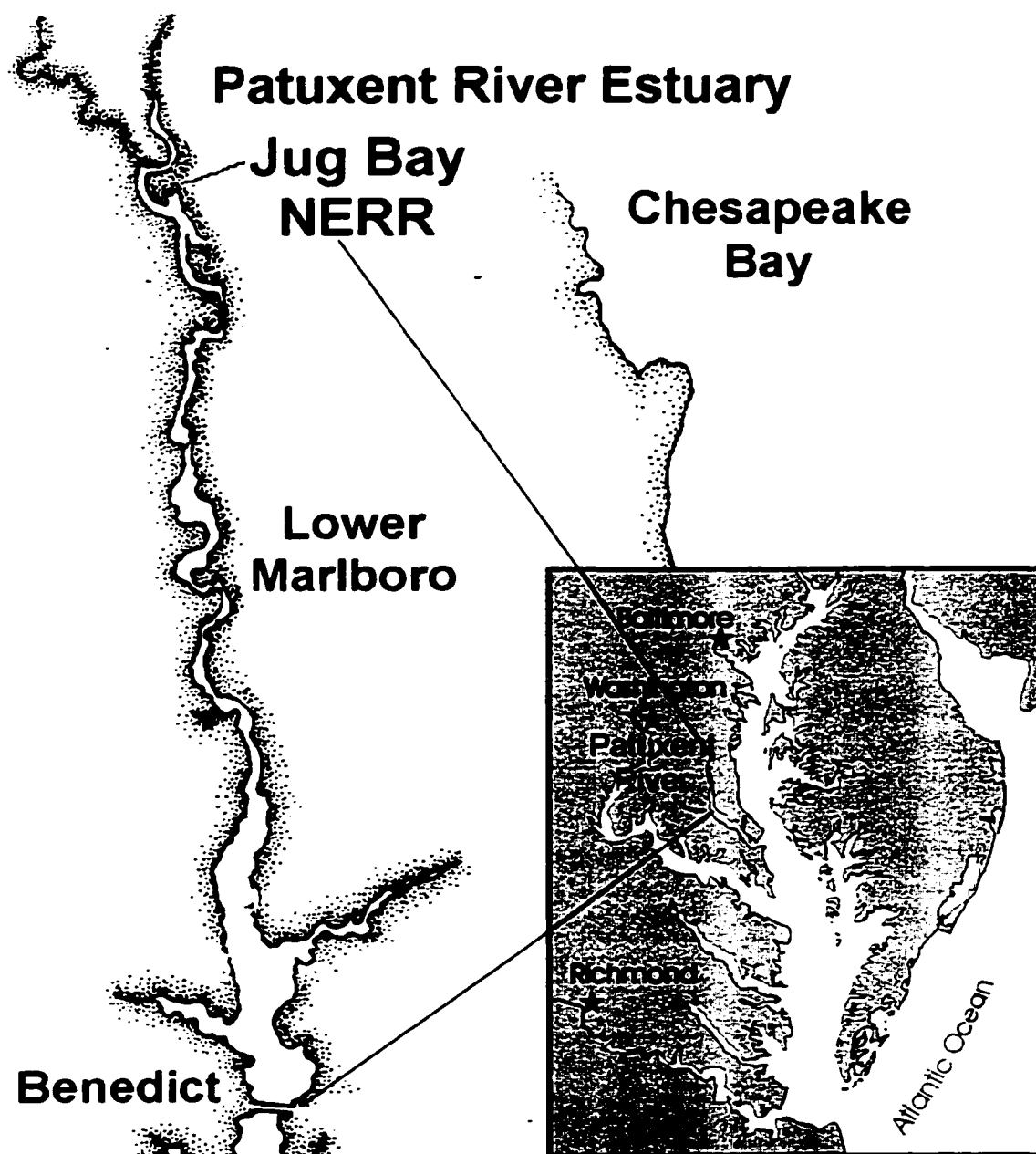


Figure 3-1. Location map for the Patuxent River marsh denitrification study. Cores were collected from the marsh bordering the north side of Jug Bay, in the Maryland National Estuarine Research Reserve.

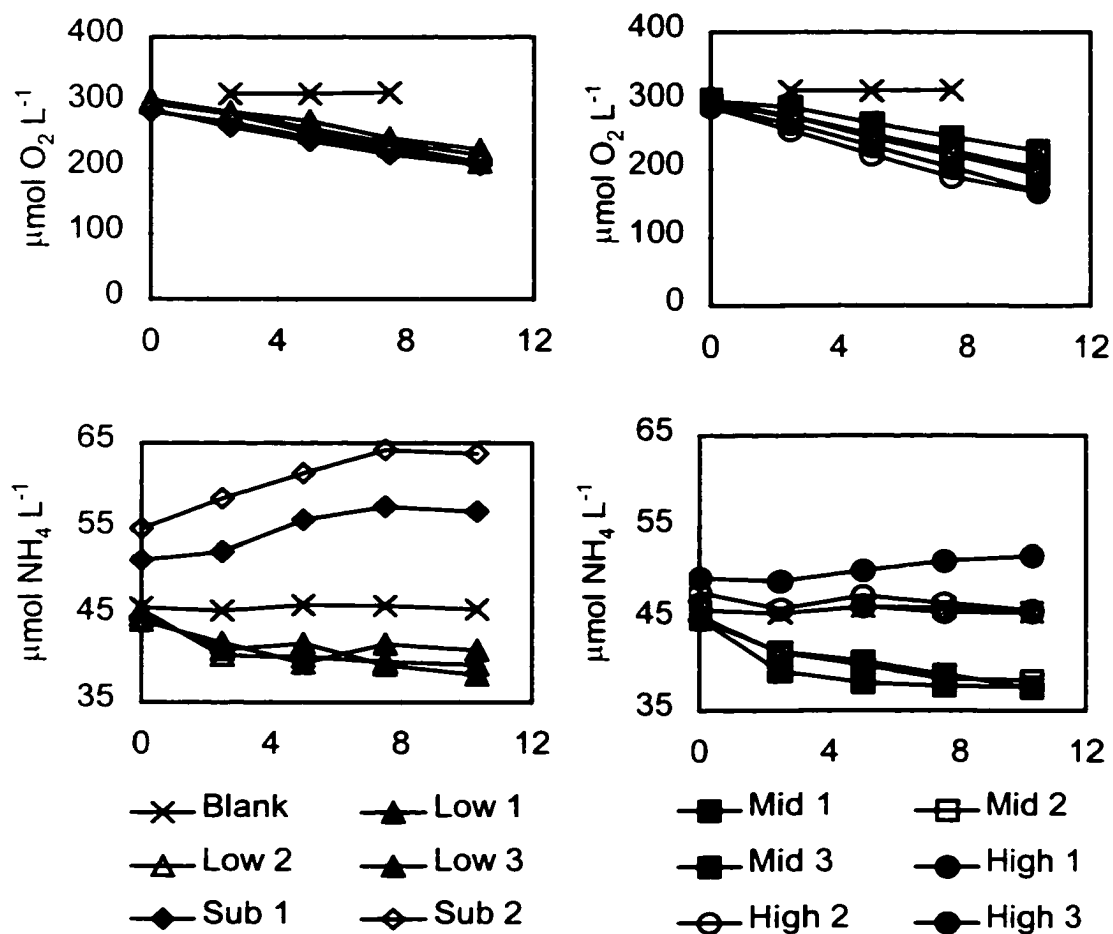


Figure 3-2. Changes in dissolved oxygen and ammonium concentrations in individual Jug Bay, Patuxent River cores over time during the spring 1997 incubation. The experiment was conducted in the dark at 14°C. The x-axis represents experiment time (hours) in all cases. The Blank represents the same core in all charts and is shown for comparison to experimental data. Subtidal cores were collected below mean low water, the low marsh was dominated by *Nuphar advena*, the mid-marsh vegetation consisted of a mix of broadleaf macrophytes such as *Peltandra* spp., and the high marsh was dominated by *Typha angustifolia*. Triplicate cores from each site are shown.

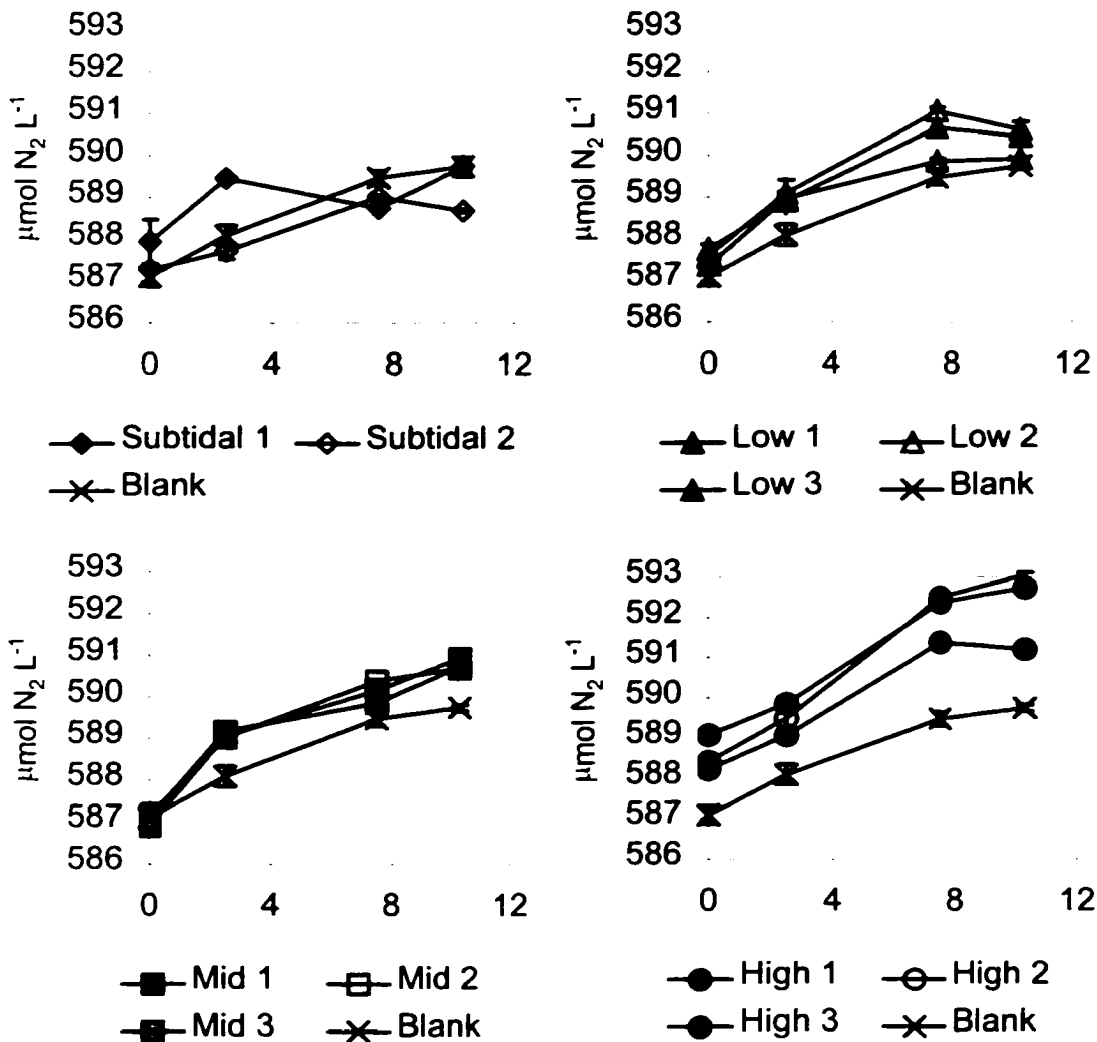


Figure 3-3. Changes in gaseous  $\text{N}_2$  in overlying water with time in individual cores during spring 1997 incubation experiment. Graphs are grouped by location in the marsh and the x-axis represents time (hours) in all cases. Standard error of two samples is shown for all data points. Denitrification fluxes were calculated from data collected from time zero to the 7.5 hour time point.

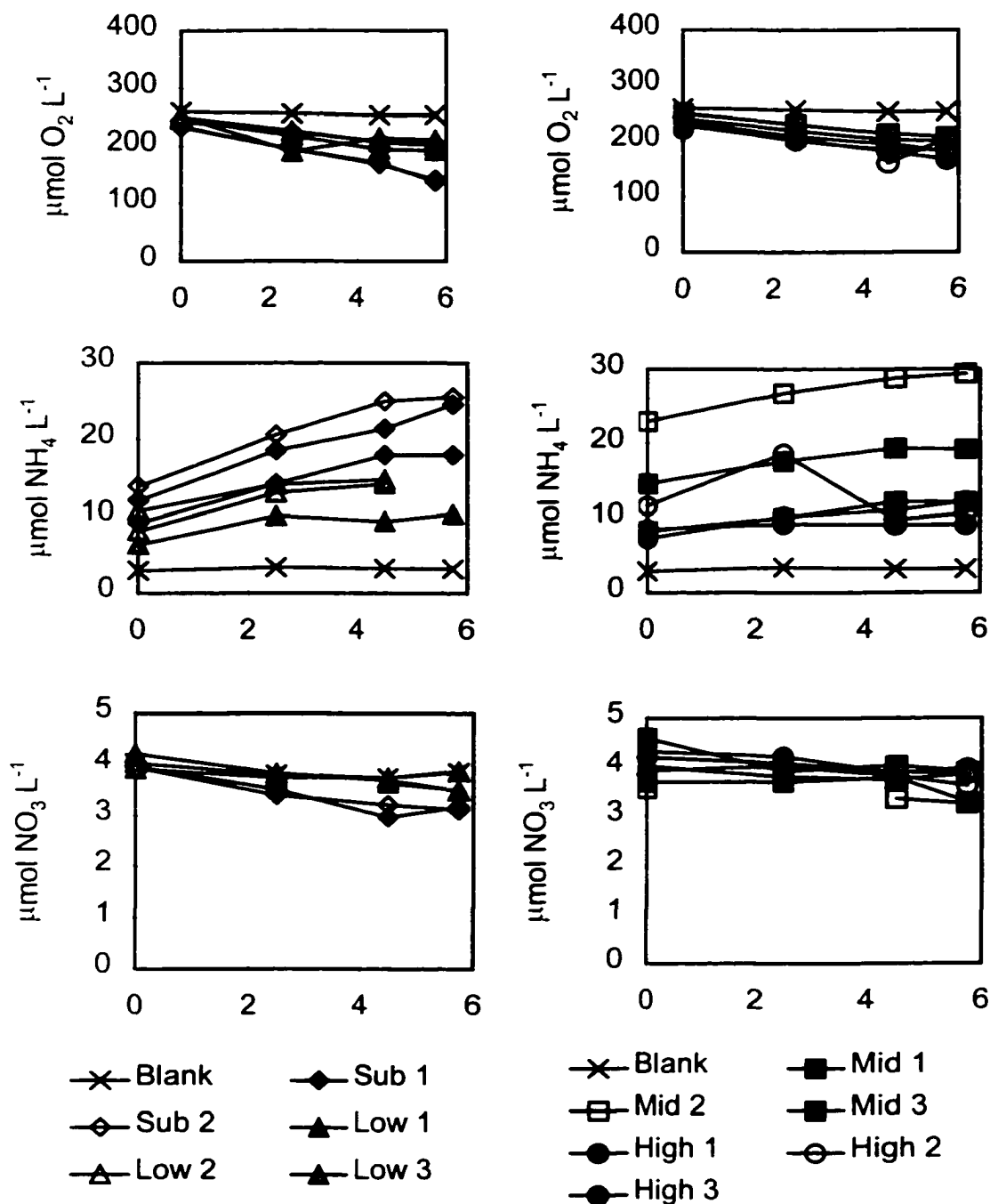


Figure 3-4. Changes in dissolved oxygen, ammonium and nitrate concentrations with time during the summer 1997 experiment (23°C). The x-axis represents experiment time (hours). Sites correspond to those described in Figure 3-2 and triplicate cores are shown.

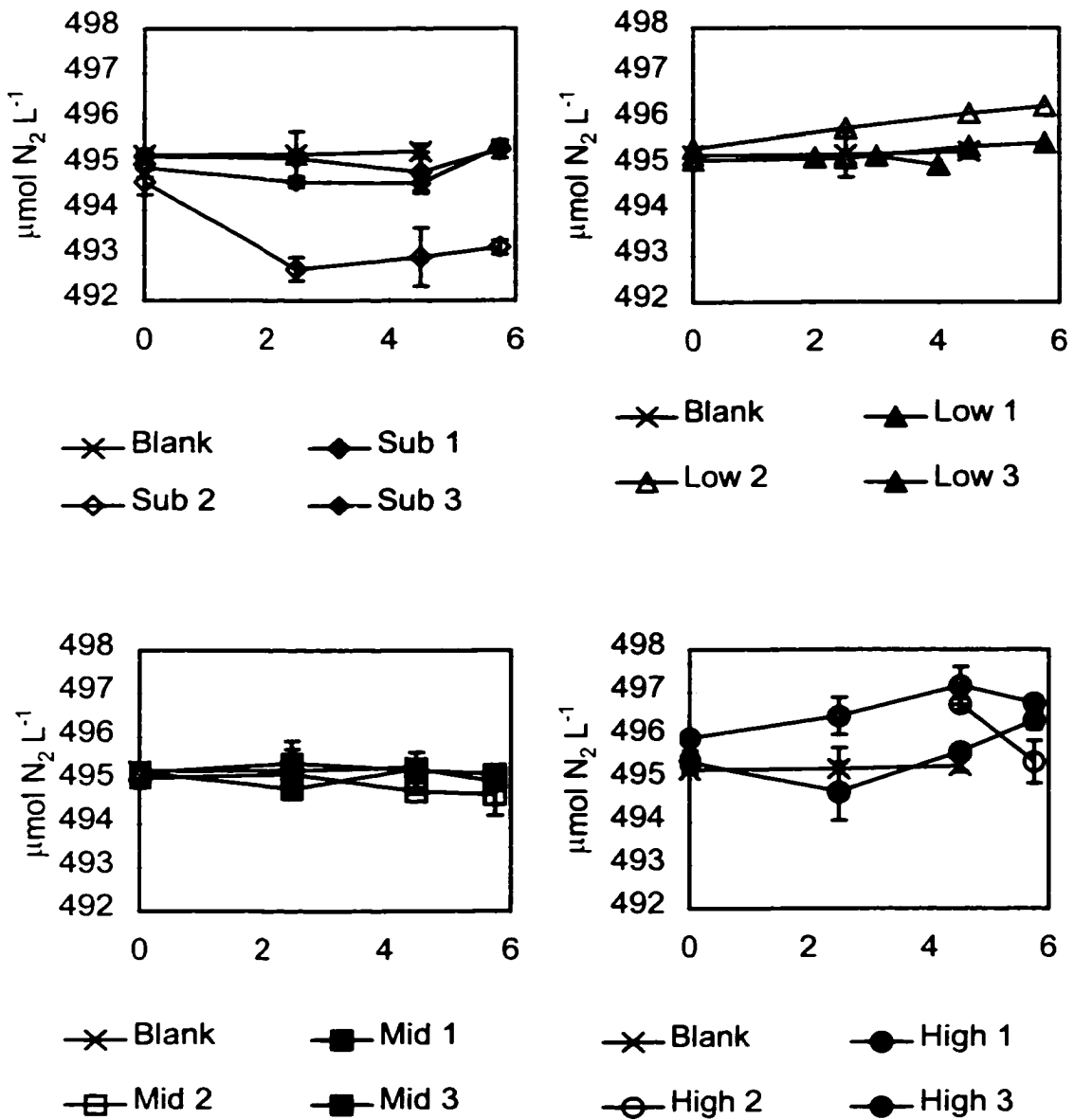


Figure 3-5. Changes in  $\text{N}_{2(\text{g})}$  concentration with time (hours, x-axis) during the summer 1997 incubation experiment. Standard error of 3 samples is shown in all cases.

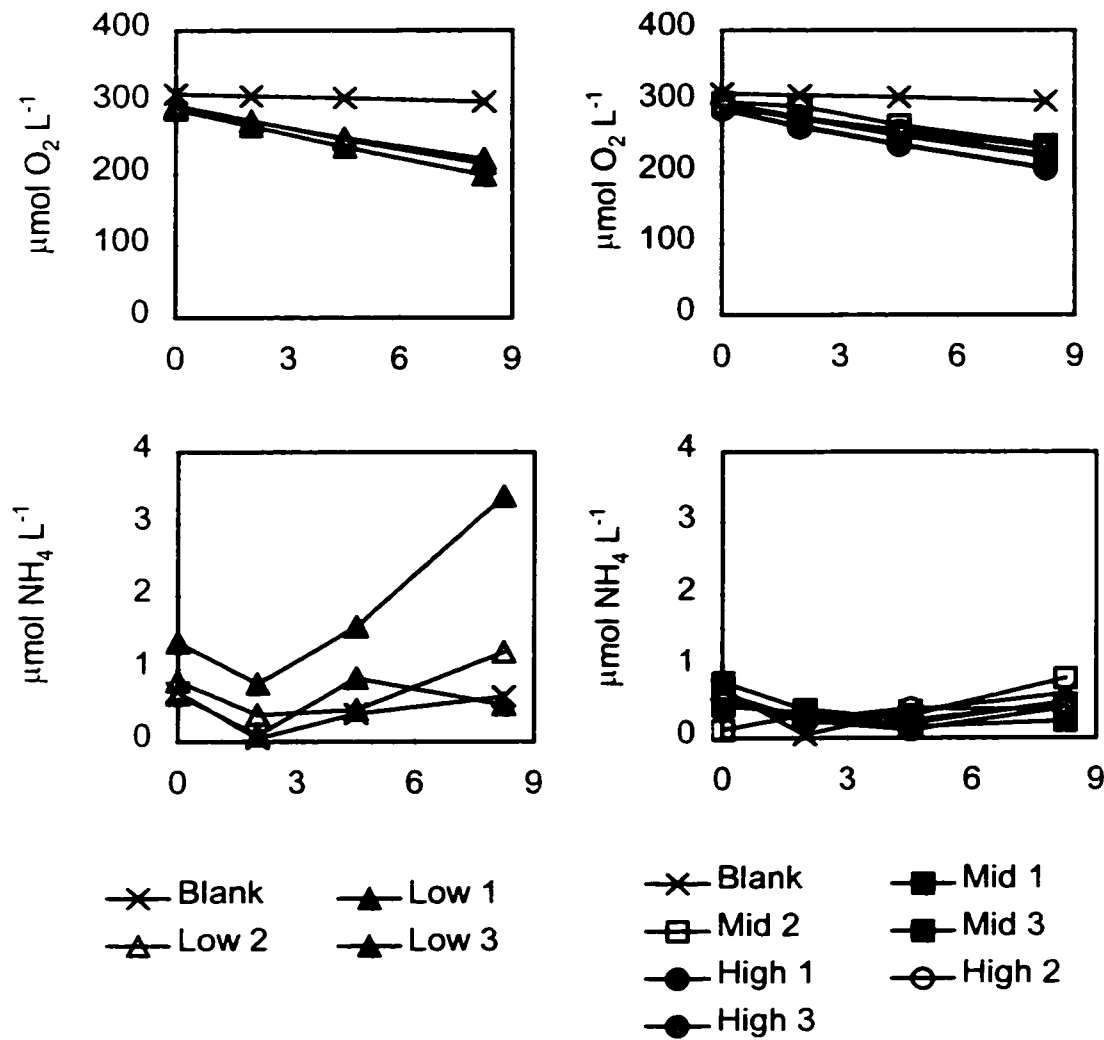


Figure 3-6. Changes in dissolved oxygen, ammonium and nitrate concentrations with time during the fall 1997 experiment (15°C). The x-axis represents experiment time (hours). Sites correspond to those described in Figure 3-2 and triplicate cores are shown.

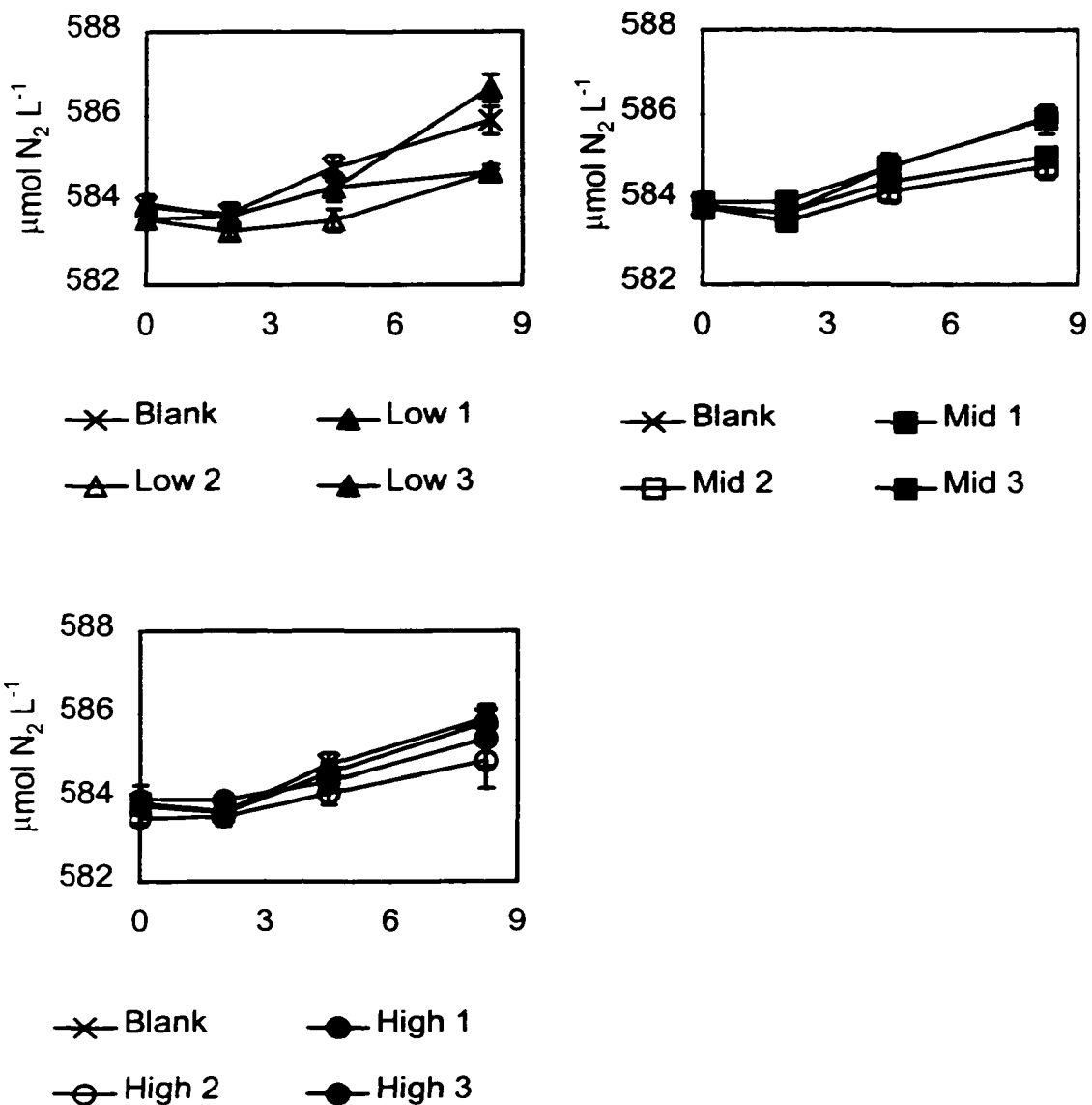


Figure 3-7. Change in  $\text{N}_{2(\text{g})}$  concentration with experimental incubation time on the x-axis (hours) during the fall 1997 experiment. Detailed site descriptions are listed in the text an Figure 3-2. Nitrogen gas was measured using membrane-inlet mass spectrometry (MIMS). The standard error of two samples is shown for each data point.

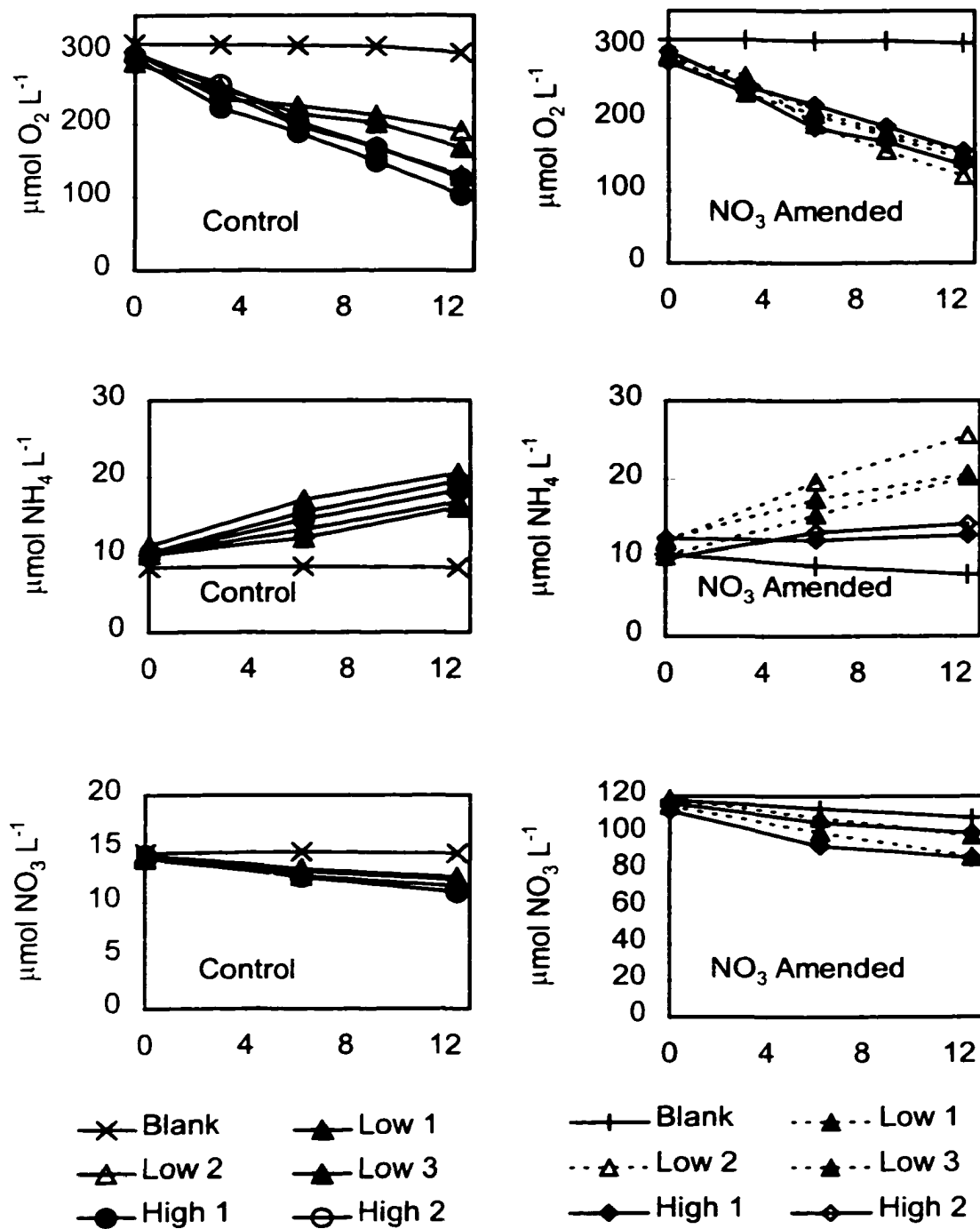


Figure 3-8. Oxygen and nitrogen concentrations during the spring 1998 NO<sub>3</sub> addition experiment. Replicate cores are shown, on the left the control cores, on the right the cores which were supplemented to 220  $\mu\text{mol NO}_3 \text{ L}^{-1}$ .

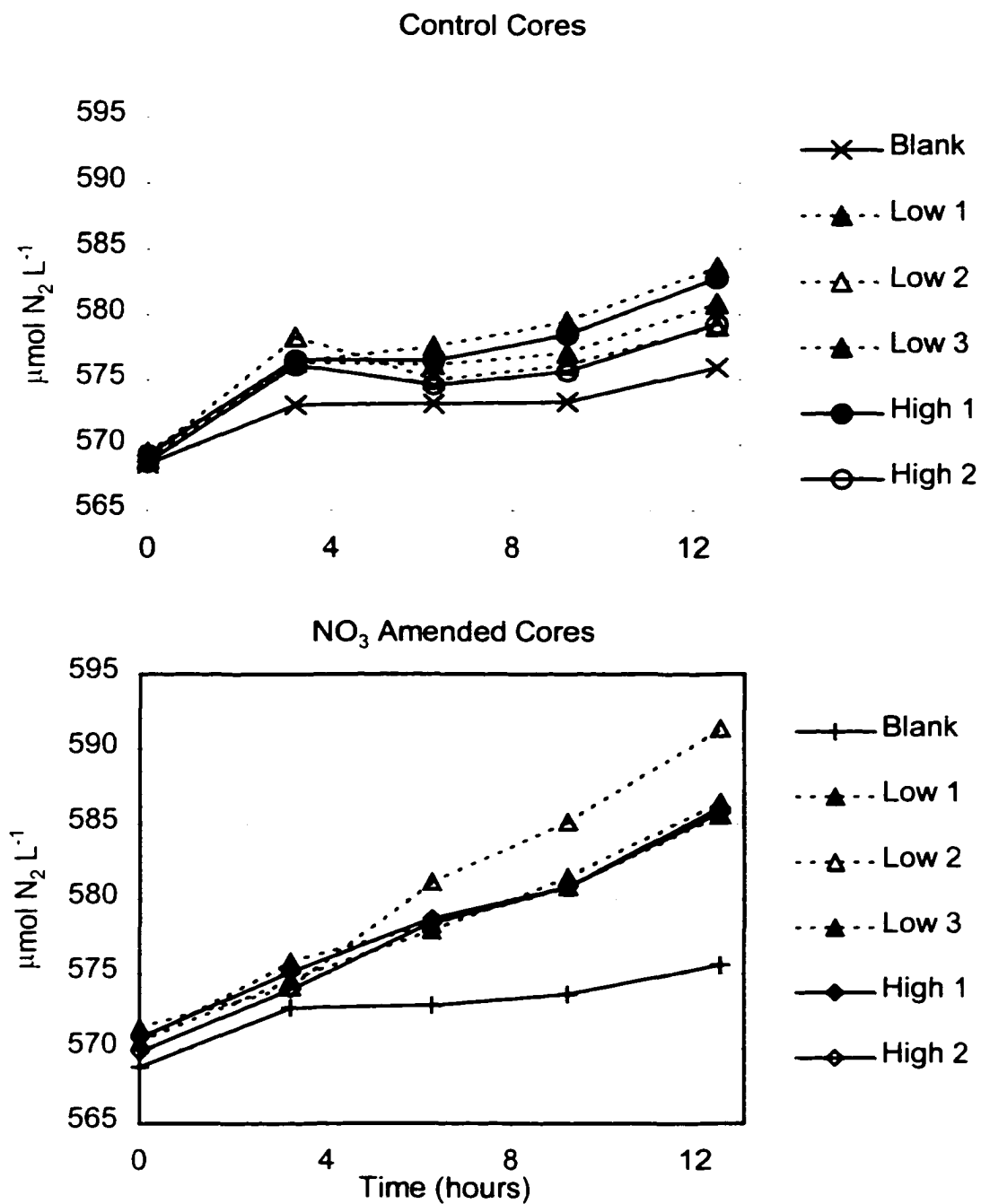


Figure 3-9. Spring 1998  $\text{N}_{2(\text{g})}$  fluxes from Jug Bay, Patuxent River. Sites correspond to those described in Figure 3-2. Control cores were not amended with nitrate, experimental cores were amended to  $220 \mu\text{mol } \text{NO}_3 \text{ L}^{-1}$ .

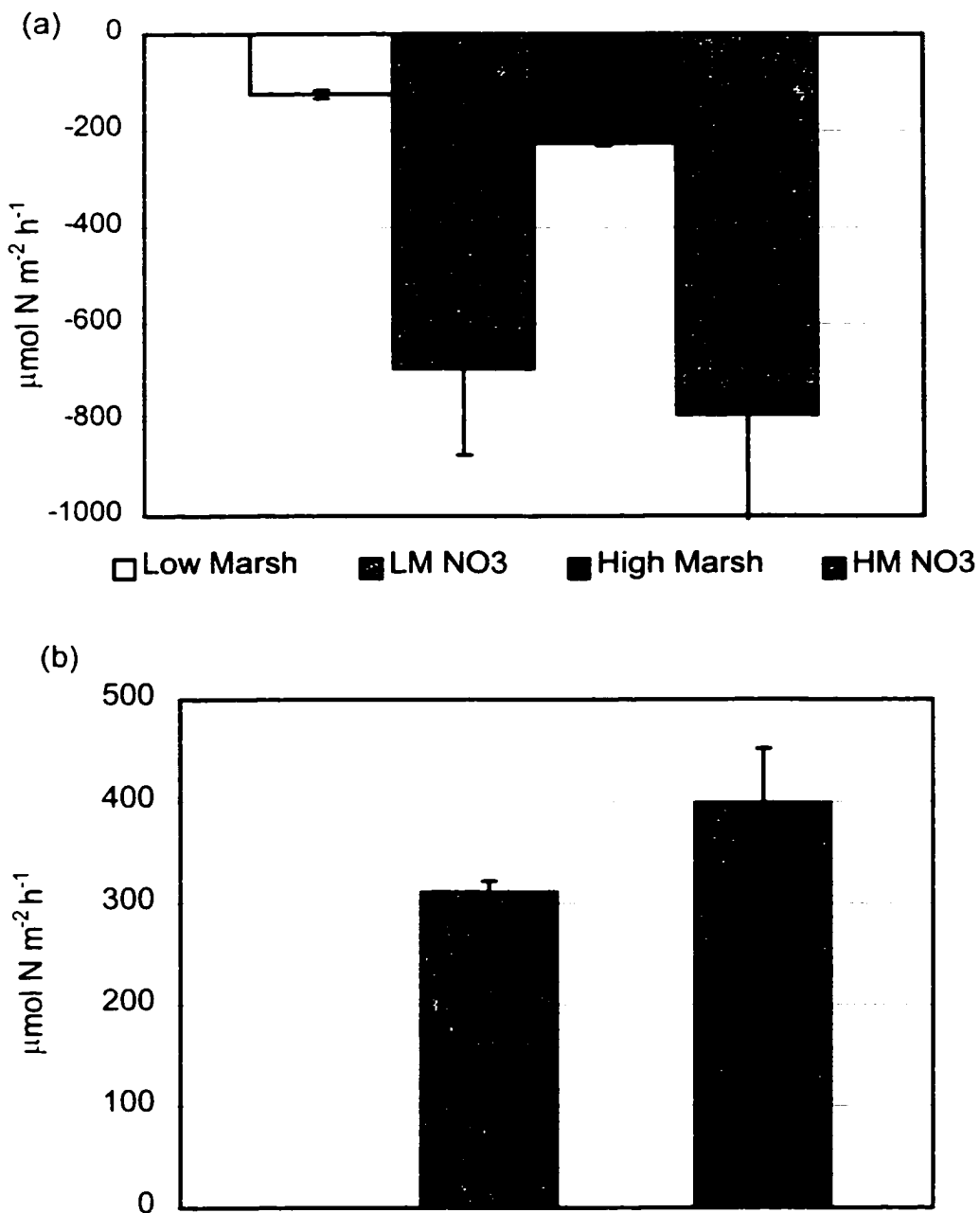


Figure 3-10. Rates of (a) nitrate uptake and (b) denitrification in Jug Bay, Patuxent River marsh cores during the spring 1998 experiment. Striped bars represent cores which were amended to  $220 \mu\text{mol L}^{-1}$  nitrate as described in the text. Error bars represent the standard error of duplicate or triplicate cores from the same location. Negative fluxes are into the sediment.

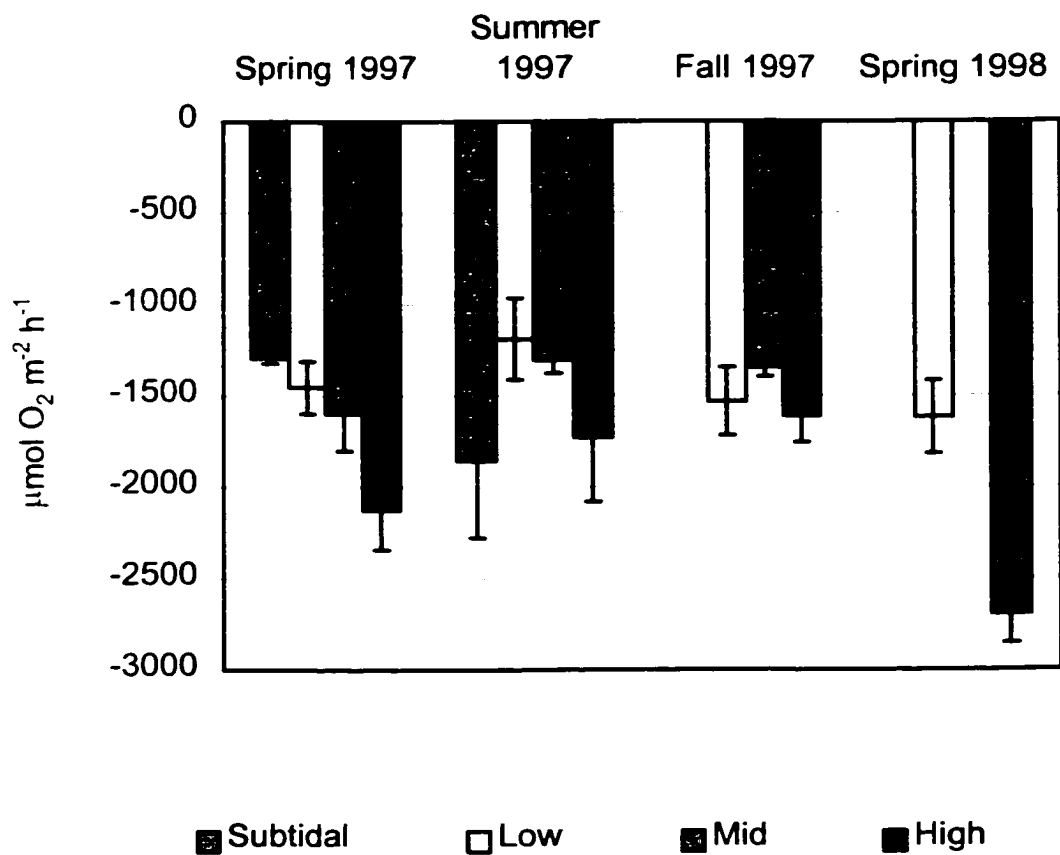


Figure 3-11. Rates of marsh sediment oxygen demand measured throughout the course of this study. Error bars represent standard error of two to three cores.

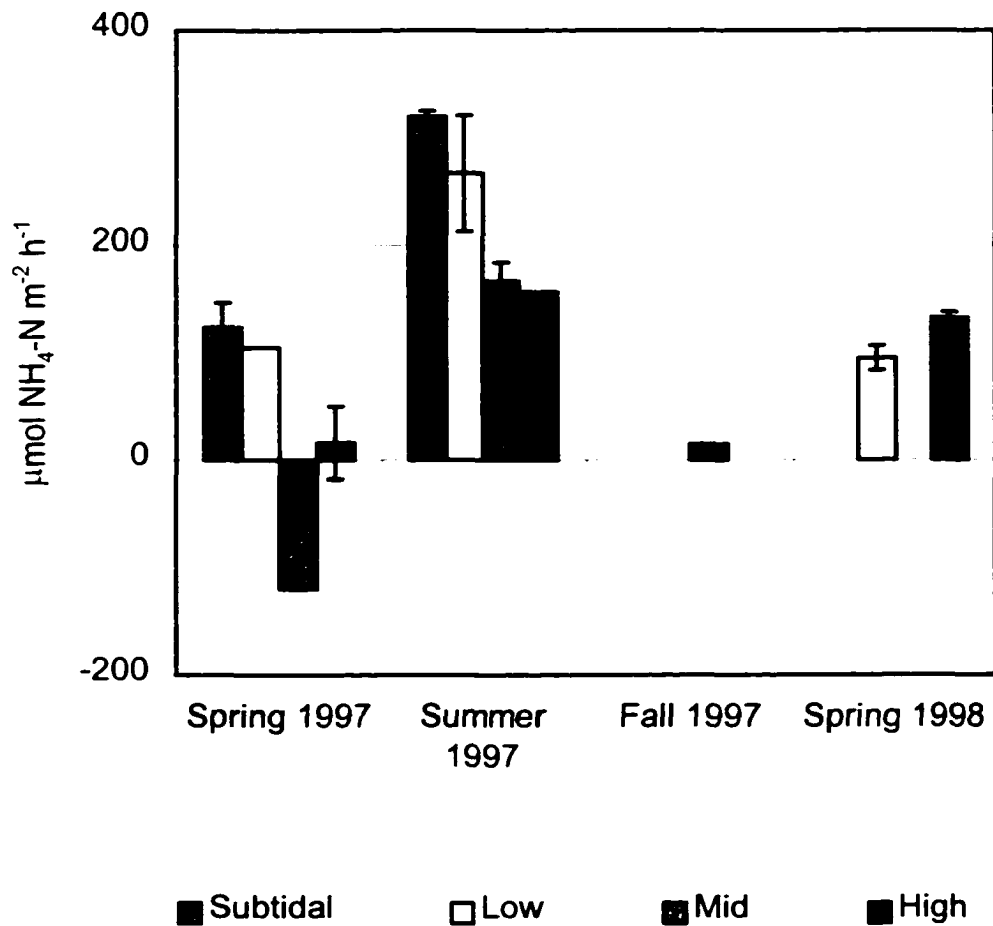
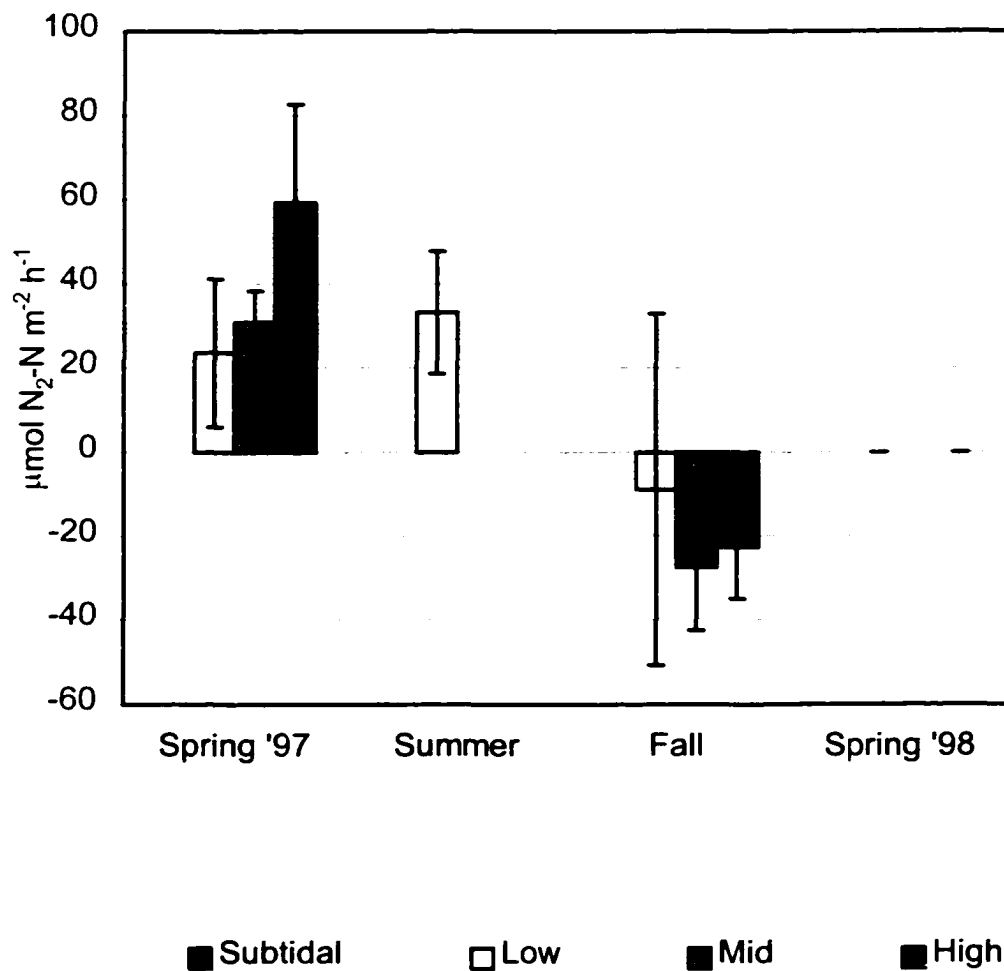
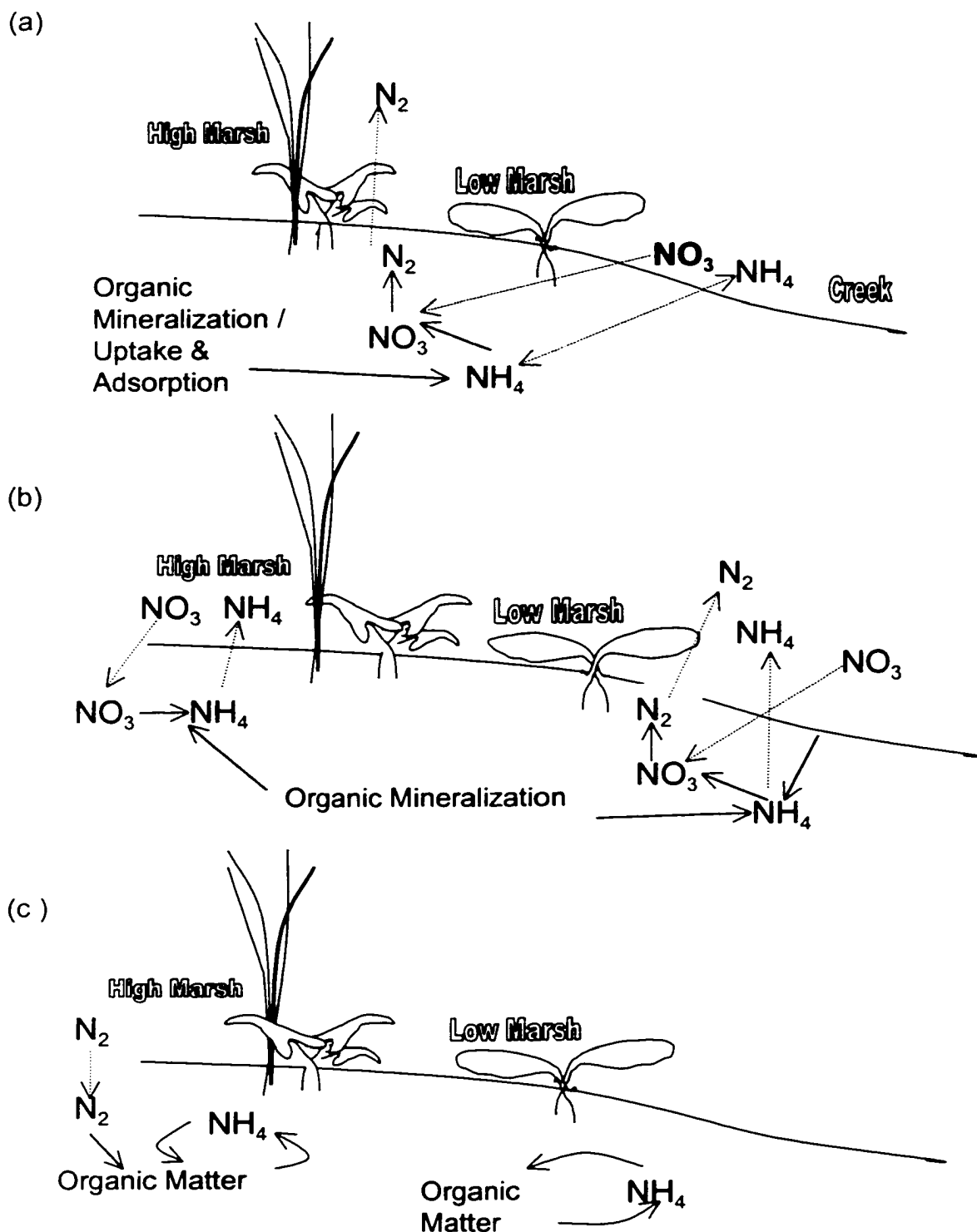


Figure 3-12. Ammonium sediment-water fluxes measured in Jug Bay, Patuxent River tidal freshwater marshes. Errors presented are the standard error of three cores, no error bar indicated one core of three exhibited a flux different from zero. Positive fluxes are out of the sediment.



**Figure 3-13. Denitrification in the Jug Bay, Patuxent River tidal freshwater marshes under ambient nitrate concentrations across four seasons. Standard error of three replicate cores is shown. All denitrification rates were measured directly using MIMS technology.**

**Figure 3-14. Conceptual models of nitrogen cycling in the low and high marshes of Jug Bay, Patuxent River, Maryland for (a) spring, (b) summer, and (c ) fall. Solid lines indicate physical transfer and dashed lines indicate chemical reaction.**



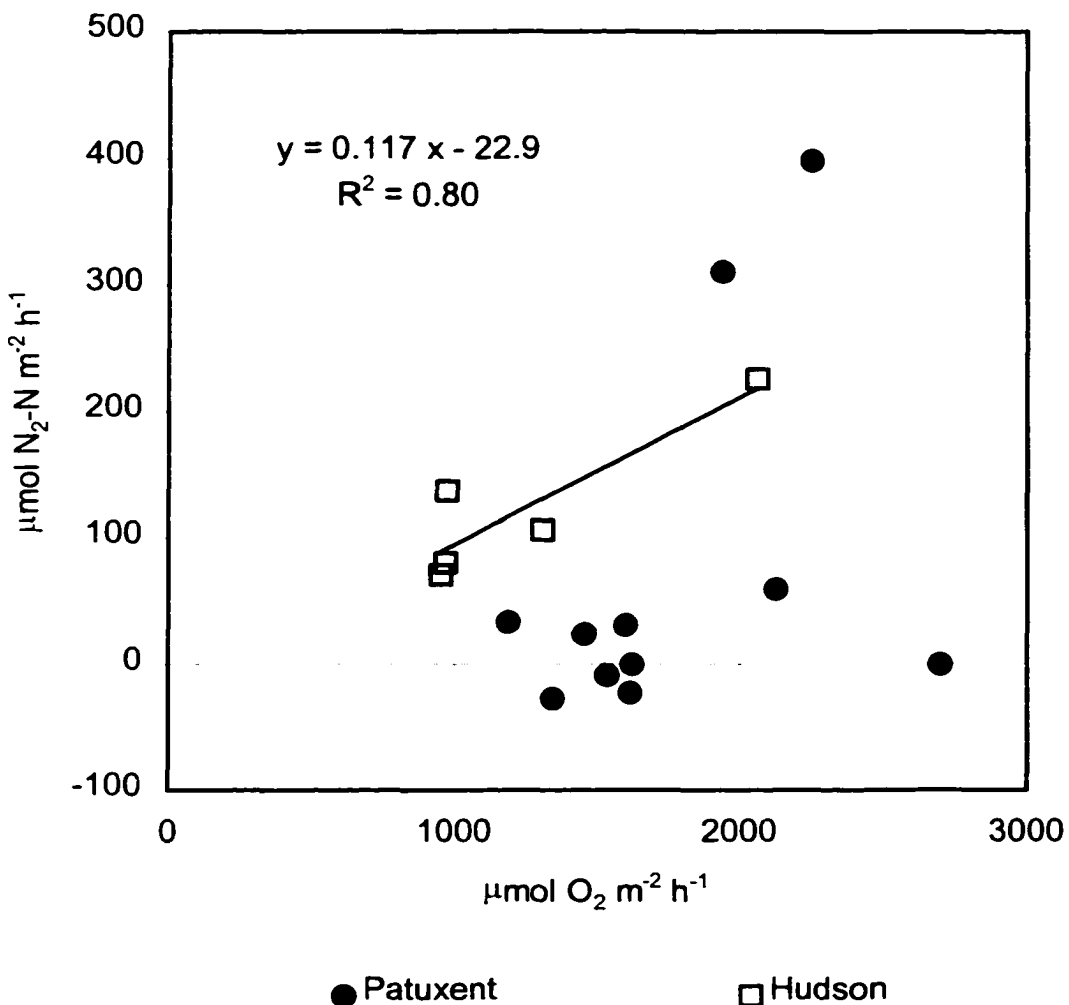


Figure 3-15. Denitrification as a function of sediment oxygen demand. All denitrification rates have been measured using MIMS technology. Data are pooled from all seasons and all sites sampled. The Patuxent and Hudson River data are from tidal freshwater marshes. Best fit linear regressions are given for Hudson River data. Patuxent River data resulted in a very low  $R^2$  (0.20).

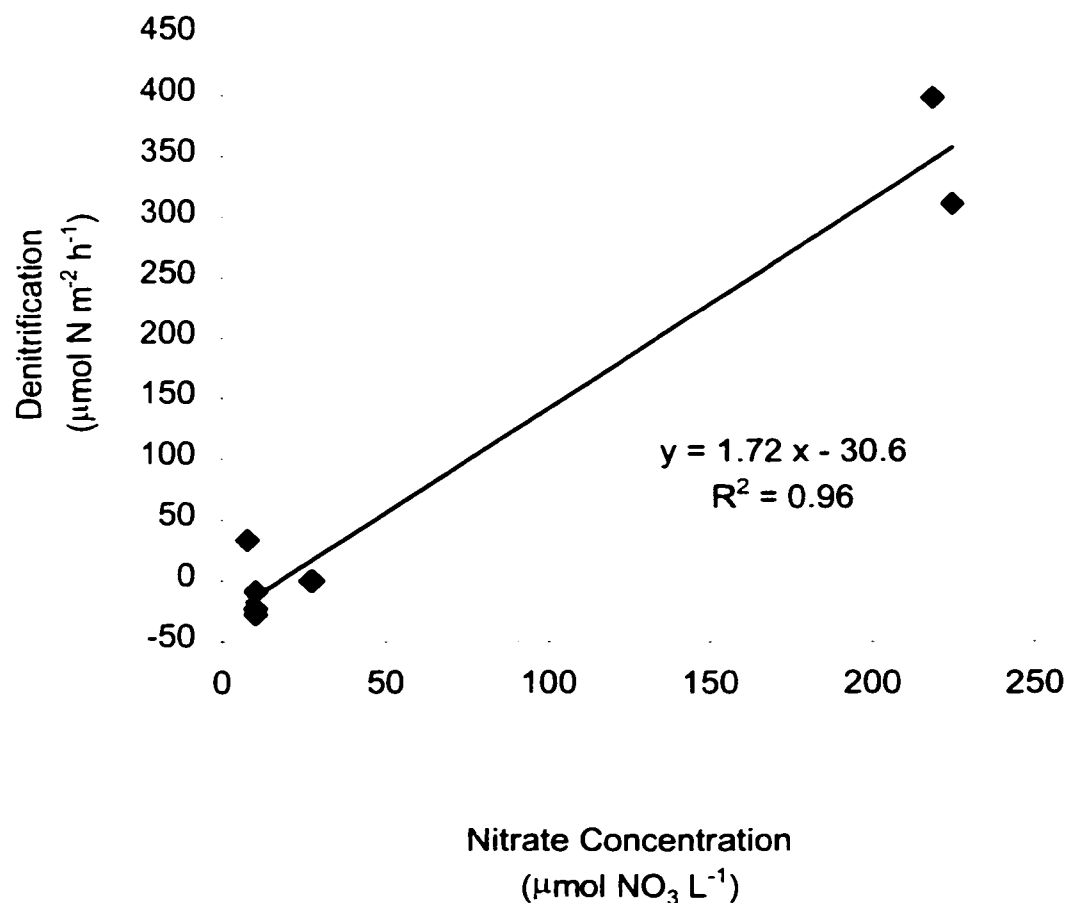


Figure 3-16. Denitrification rates measured in Jug Bay, a Patuxent River tidal freshwater marsh. All measurements used MIMS technology and are shown with ambient nitrate concentration in overlying water.

# **CHAPTER 4: TIDAL FRESHWATER MARSHES OF THE HUDSON RIVER AS NUTRIENT SINKS: LONG TERM NUTRIENT RETENTION AND DENITRIFICATION**

## **INTRODUCTION**

The role of tidal wetlands in the maintenance, and even enhancement, of water quality remains equivocal. Despite over thirty years of research, the question has still not been adequately answered. Although a variety of studies have examined short term tidal fluxes of organic matter, nutrients and sediments (i.e.: Stevenson et al. 1977, Simpson et al. 1983), or long-term sediment accretion (Armentano and Woodwell 1975), few attempts have been made to estimate nutrient burial (DeLaune et al. 1981) and no ecosystem nutrient or sediment budgets have been developed.

The goal of this project is to determine if the tidal freshwater marshes of the Hudson River can have a significant impact on the nutrient budget of the River ecosystem. Poor water quality has been linked to excess nutrient

supply in estuarine systems (Bricker-Urso and Stevenson 1996). Marshes may remove enough of this nutrient supply to actually maintain and improve water quality (Nixon 1980). Coastal marshes must produce or trap and retain sufficient material to build the sediment vertically, if they are to maintain themselves in the face of rising sea level. This sediment building is one long-term process that may be responsible for trapping large amounts of nutrients.

In this study, retention of nutrients on long time scales (5 half-lives or ~100 years) was examined by determining rates of  $^{210}\text{Pb}$ -derived sediment accretion and associated sediment nutrient concentrations. Average nutrient concentrations below the active plant root zone were combined with sedimentation data to estimate the quantity of nutrients retained over time.

Krishnaswamy et al. (1971) introduced a technique for estimating sediment age using naturally occurring  $^{210}\text{Pb}$ . Once sediment age is known, accretion can be calculated by observing the change in age over sediment depth. Lead-210 is a distant daughter in the  $^{238}\text{U}$  decay series. Radium-226 is an intermediate ( $t_{1/2}=1620$  years) which decays to radon gas ( $^{222}\text{Rn}$ ). This decay to a gaseous product is key to the  $^{210}\text{Pb}$  dating technique. Radon-222 is either trapped within the earth's crust, or is released to the atmosphere over its 3.82 day half-life. Through a series of four rapidly decaying daughters (each  $t_{1/2}<0.5$  hour),  $^{222}\text{Rn}$  decays to  $^{210}\text{Pb}$ . Lead-210 produced as a result of  $^{222}\text{Rn}$  decay within the earth's crust is referred to as background, or supported,  $^{210}\text{Pb}$  activity. Atmospheric  $^{222}\text{Rn}$  decay produces  $^{210}\text{Pb}$ , which is scavenged by particulate matter in the atmosphere and falls back to earth.

This additional  $^{210}\text{Pb}$  is deposited on waters and watersheds and eventually makes its way to the sediment surface. While the supply and decay are constant, this atmospherically-derived, or unsupported,  $^{210}\text{Pb}$  declines with sediment depth, since the only supply is to the sediment surface. The exponential decay observed with depth in sediments is used to calculate sediment age, which is estimated over depth in the sediment to determine the rate of sediment accretion. One complicating factor is that  $^{210}\text{Pb}$  decay, a  $\beta$ -emitting process, is difficult to measure. Lead-210 has a long half-life in laboratory terms, 22.3 years. The first decay product is  $^{210}\text{Bi}$  ( $t_{1/2}$  5 days), which after emitting another beta particle, becomes  $^{210}\text{Po}$ . Polonium-210, although the half-life is 138 days, emits relatively easy to measure alpha particles. Since the half-life of  $^{210}\text{Pb}$  is much longer than that of both  $^{210}\text{Bi}$  and  $^{210}\text{Po}$ , we may assume that the decay of  $^{210}\text{Pb}$  is rate-limiting. Known as secular equilibrium, this assumption allows the measurement of  $^{210}\text{Po}$  as a direct indicator of  $^{210}\text{Pb}$  decay. Effectively, a measurement of polonium-210 decay is a measurement of lead-210 decay.

Sediment deposition and marsh accretion are the processes responsible for maintaining the physical integrity of the marsh. Dynamic processes occur with each tide, the impacts of which are superimposed upon the long-term nutrient exchange. Nutrient uptake and release over much shorter time periods (hours) was estimated using flux incubation experiments (e.g. Boynton and Kemp 1985). Earlier approaches examined the impact of

marshes on estuarine water quality by relying on a larger-scale, more integrated approach. Dissolved nutrients measured on flood and ebb tides were extrapolated using a hydrologic budget to determine the impact of marshes on water quality in adjacent tidal creeks (Stevenson et al. 1977, Whiting et al. 1989). Results were often obscured by large variability and error associated with the contrived hydrologic budget. Flux incubation experiments narrowed examination to the exchange of nutrients between sediment and water and allowed the measurement of small changes in nutrient concentrations over short time periods. The tighter experimental control of this study eliminated the influence of nitrate-laden groundwater on the findings, a trade-off for reducing variability in the results. Exchanges of ammonium and nitrate, as well as some of the first measurements of dissolved dinitrogen gas, were estimated using state of the art technology which allows for the rapid, high precision measurement of N<sub>2(g)</sub> (Kana et al. 1994). Both burial and denitrification processes were measured at a variety of marsh elevations, and results of each ecotype were extrapolated to the appropriate surface area within the marsh. This large-scale budget is the first attempt to determine the overall importance of tidal freshwater marshes to the nutrient budget of the surrounding Hudson River Estuary.

The chapter addresses the following questions: (1) Do marshes of Tivoli Bays, Hudson River trap large quantities of nutrients in the sediment over long time scales? (2) Does denitrification in the marsh sediment provide a seasonal nitrogen sink for the River?

## SYSTEM DESCRIPTION

The study was completed within Tivoli Bays National Estuarine Research Reserve Site (NERR) which is composed of two distinct marsh systems (Figure 4-1). The marshes lie along the eastern bank of the Hudson River, approximately 160 river km north of Battery Park and are separated from the River by a railroad causeway. Both are tidally flooded (semi-diurnal) through constricted channels under the railroad tracks. North Bay has two connections to the River, and South Bay has three. The tidal range has been measured as high as 1.8 meters. Low tide water levels remain consistent over the lunar cycle, but fluctuations in high tide water levels can be as much as 0.9 meters (Marchesi and Barten 1992). Groundwater flows remain unknown, but may be low due to the low hydraulic conductivity of the soils which is limited by a large proportion of clay (Lickus and Barten 1991).

The northern bay is a tidal freshwater emergent marsh covering 1.56 km<sup>2</sup> (Lickus and Barten 1991). The plant communities range from peltate-dominated (ie: *Nuphar*, *Pontederia*, *Peltandra*) to cattail- and shrub-dominated. A basic surface water hydrologic budget has been prepared (Lickus and Barten 1991) which demonstrates that 90% of the surface water inputs to the system originate from the two channels that connect it to the Hudson River under a railroad bed. Stony Creek is the second largest source of water to the system, and is also the recipient of effluent from the sewage treatment plant of the town of Tivoli (Chuck Nieder, personal communication).

South Bay is dominated by water chestnut (*Trapa natans*), an exotic floating-leaf macrophyte, and the majority of the marsh surface area is subtidal. Decomposition of water chestnut in South Bay is not rapid enough to account for the disappearance of plant material, and yet very little organic matter remains on the marsh surface (Findlay et al. 1990). Subtidal, low and high marsh sediment-water fluxes of oxygen, ammonium, nitrate and dinitrogen gas have been estimated in each bay.

Differences in the physical and biological characteristics have been investigated, and work by Lickus and Barten (1991) suggested the two bays maintain very different ecosystems as the result of differences in hydrologic characteristics. The slower turnover within North Bay allowed for higher sedimentation rates and quicker plant establishment than South Bay. They suggest North Bay has reached a hydrological-biogeochemical equilibrium which will maintain the marsh. The rapid turnover of water in South Bay prevents equilibrium establishment.

## METHODS

Sampling of the Tivoli Bays National Estuarine Research Reserve was carried out in three seasons. Sediment cores were collected during the fall 1996 trip for nutrient burial analysis using a McAuley corer, which limits compaction during core collection (Bricker-Urso et al. 1989). Four cores were

collected from North Bay for  $^{210}\text{Pb}$  analysis, and three were collected from South Bay (Figure 4-1). Two cores were collected from within the low, *Nuphar advena*-dominated marsh of North Bay. These sites were located 36 meters apart to estimate the spatial variability of accretion within a given marsh elevation. Cores from South Bay were collected from (1) an unvegetated subtidal site, (2) a *Trapa natans*-dominated site and (3) a high, scrub-shrub fringe marsh site. The cores were sectioned into 2, 3, 5, and 10 cm segments in the field. Samples were sealed in plastic vials, placed on ice, and returned to Horn Point Laboratory (HPL) for processing.

TriPLICATE cores for nitrogen fluxes, as well as smaller porewater cores, were collected at each site in the fall of 1996, and in the spring and summer of 1997. North Bay samples were collected along a 100 m transect which began with a high marsh site, dominated by *Typha* spp., and traversed a low marsh site dominated by *Nuphar luteum*. The transect ended with an unvegetated subtidal site. In South Bay an unvegetated subtidal site and a site located within a stand of water chestnut (*Trapa natans*) were sampled. Subtidal cores from South Bay could not be collected during the summer trip due to logistical problems. Unexpected field conditions resulted in two sampling trips in the fall of 1996. North Bay was sampled in September (21°C) and South Bay was sampled in October (12°C).

Core tubes (30 cm tall, 10 cm inner-diameter) were pushed into the substrate to collect cores of sediment between 13 and 17 cm long. If cores from a specific sampling site were collected during a period of inundation, the

core tubes were filled to the top with ambient water to stabilize the sediment during transport. Cores which were not flooded during collection were transported without additional water. All cores were tightly sealed with PVC lids and transported on ice to HPL. Duplicate 18 cm-long cores were collected in smaller tubes (7.6 cm inner-diameter) for porewater analysis. Cores were tightly sealed at both ends, placed on ice and returned to HPL. Approximately forty liters of water was collected from each bay to be used as replacement water in the flux experiments.

Sediment samples from the McAuley corer were weighed, volumes were measured by water displacement and samples were dried. After a dry weight ( $W_{dry}$ ) was taken, the samples were ground with a mortar and pestle. Percent water was calculated as:  $W_{wet} - W_{dry} / W_{wet} * 100$ . Bulk density was calculated as:  $W_{dry}/Volume$  and is reported as g cm<sup>-3</sup>.

Particulate phosphorus was analyzed on a 1 N HCl extract using a molybdenum-blue colorimetric technique (Parsons et al. 1984). Analysis of total phosphorus proceeded on samples that were ashed at 550°C for 2 hours. Organic content of the sediment was approximated using % loss on ignition (( $W_{dry} - W_{ash}$ )/ $W_{dry} * 100$ ). Inorganic phosphorus was analyzed on unashed sediment acid extracts.

## Sediment Accretion

Sediment accretion was determined using a  $^{210}\text{Pb}$  technique originally described by Krishnaswamy et al. (1971). Polonium-210, a proxy for  $^{210}\text{Pb}$  as previously described, was analyzed by adding a known quantity of a separate alpha-emitting radioactive tracer to a known mass of sediment. Relative activities were used to calculate the quantity of  $^{210}\text{Po}$  in the original sample. Sediment samples were weighed and an aliquot of  $^{209}\text{Po}$  added. Samples were digested with  $\text{HNO}_3$  and  $\text{HCl}$  and centrifuged to remove the sediment, which was now stripped of the  $^{210}\text{Po}$ . The acid mixture was gently heated and dried and the  $^{210}\text{Po}$  and  $^{209}\text{Po}$  material was resuspended in a weak acid solution. Ascorbic acid was added to reduce the interference of iron; the  $^{210}\text{Po}$  and  $^{209}\text{Po}$  were plated on silver and were counted in a four channel Alpha spectrometer system at HPL (Tennelec and Ortec detectors; Sugai 1990).

Sedimentation rates were generated by using a mathematical model known as the constant initial concentration (CIC) model (Robbins 1978) which assumes sedimentation rates have remained constant. Excess or unsupported, atmospherically-derived  $^{210}\text{Pb}$  activity (A) was used to derive the sedimentation rate (r) by the following equation:

$$A = A_0 e^{-\lambda z/r}$$

where  $A_0$  was the unsupported activity of the surface sediment,  $\lambda$  was the reciprocal half-life of  $^{210}\text{Pb}$ , and 'z' was depth in the sediment. Unsupported

$^{210}\text{Pb}$  activity was estimated by subtracting the steady-state, supported  $^{210}\text{Pb}$  value from the total activity. The unsupported activity was converted to a natural log and linear regression performed. In limited cases (a total of four measurements)  $^{210}\text{Pb}$  measurements were left out of the linear regression equations and were attributed to limited physical mixing of the sediment. Cumulative sediment mass at each  $^{210}\text{Pb}$  data point was used to generate sedimentation rates in terms of annual mass burial per unit area. Linear regressions of the data were accepted for calculation of sedimentation rate if the value of  $r^2$  was greater than 0.80 (approximately 90% confidence interval).

### Seasonal Estimates of Pore Water Concentration and Sediment-Water Fluxes

Pore water cores were returned to the lab and sectioned (0.5, 1, and 2 cm) in a nitrogen-purged glove bag. Sections were sealed and centrifuged, and the supernatant was withdrawn and syringe-filtered. Samples were immediately frozen for analysis of  $\text{NH}_4^+$  and  $\text{NO}_3^-$ .

Flux cores for batch incubations were returned to HPL and placed in a dark chamber at ambient water temperature. Replacement water was bubbled with air to maintain dissolved gas concentrations. Cores were opened and allowed to equilibrate with the incubation temperature overnight. Overlying water was gently siphoned off, and replaced with water collected

from the appropriate bay. Disturbance to the surface of the core was minimized at each step. Cores were sealed with an acrylic lid fitted with a suspended magnetic stir bar, sample port and inflow port. Air bubbles were removed by gently pressurizing the sample port, and each core was connected to the water supply. Blanks consisted of a core tube filled with water from either bay. Cores were placed around a motorized magnet carousel which rotated the stir bars at a rate of 42 rpm, at a distance approximately 10 cm above the sediment-water interface. Samples for dissolved oxygen, dissolved gas analysis (DGA-for N<sub>2</sub>:Ar), ammonium and nitrate were collected at five time points per experiment. Dissolved oxygen levels were used to determine appropriate sampling intervals. Oxygen measurements were made within fifteen minutes of collection in ground glass-stoppered volumetric flasks on a Strath-Kelvin Model 781 ( $\pm 0.02 \text{ mg L}^{-1}$ ) during the fall and spring experiments. During the summer experiment oxygen and N<sub>2(g)</sub> concentrations were determined simultaneously by the membrane-inlet mass spectrometer for dissolved gas analysis (DGA). DGA samples were collected in 5 ml test tubes with ground glass stoppers and placed in water of the same temperature. Nutrient samples were collected in syringes, filtered, and immediately frozen until analysis.

Analysis of NH<sub>4</sub> followed Parsons et al. (1984) and nitrate was analyzed on a DIONEX Ion Chromatograph. Analysis for N<sub>2(g)</sub> concentrations was completed on the DGA. Briefly, whole water samples are pumped through a gas permeable membrane which is kept at a constant temperature

and under high vacuum. The membrane allows the passage of gas molecules from the water into the attached mass spectrophotometer (Balzers Prisma with a Varian Turbo V70 vacuum pump). Oxygen, nitrogen and argon concentrations are reported and calibrated to an equilibrated standard with similar salinity. The standard was equilibrated for more than 48 hours in a sealed, stirred and temperature-regulated container to allow dissolved nitrogen, oxygen and argon to reach a stable equilibrium at the experimental temperature for correction of the water samples to standard conditions. Argon concentrations were used for the corrections. Oxygen and nitrogen were measured relative to argon, assumed to be a conservative gas, and fluxes were estimated. All samples were run in duplicate and average concentrations are reported; data have been corrected for instrument drift. Dissolved N<sub>2(g)</sub> concentrations as determined by the DGA are available for the spring and summer experiments, but fall data is not available due to instrument instability.

Linear regressions of time versus dissolved oxygen, nutrient, or N<sub>2(g)</sub> were performed to measure fluxes. Fluxes were reported if the changes in concentration were linear ( $r^2 > 0.80$ , approximately 90% confidence interval,  $\alpha=0.05$ ). The change in concentration (dC/dt) was corrected for the volume of the experimental core by multiplying by water column height, resulting in an expression of flux rates on a per unit area basis. Flux rates were grouped by site and averaged, and this average was tested for difference from zero

(student's t-test,  $\alpha=0.05$ ). Site averages were reported only when >50% of the cores indicated a flux.

## RESULTS

### Particulate Material and Sedimentation

Physical properties of the sediments showed little variability between the North and South Tivoli Bay systems. Subtidal sediments in both systems ranged from 50-70% water, and dry bulk density ranged from 0.40 to 1.00 g cm<sup>-3</sup> (Figure 4-2). Low marsh sites in North Bay (*Nuphar* 1 and 2) had percent water and dry bulk density values similar to the subtidal sediments and exhibited good replication of physical properties. Sediments of the North Bay high marsh (*Typha angustifolia*) had the lowest bulk density of the North Bay cores, 0.30 to 0.60 g cm<sup>-3</sup> and physical properties did not change with depth, as in the low marsh and subtidal cores. Sediments of the fringing marsh in South Bay were the most distinct found in the study. Composed primarily of organic matter, the core exhibited constant depth profiles of percent water (approximately 80%) and dry bulk density (0.20-0.35 g cm<sup>-3</sup>), which was approximately half the dry density of the subtidal core.

Profiles of <sup>210</sup>Pb in the sediment displayed the expected exponential decreases (Figure 4-3), with total <sup>210</sup>Pb activities as high as 6 dpm g<sup>-1</sup> sediment. Both North and South Bay cores had asymptotic, <sup>226</sup>Ra-supported,

$^{210}\text{Pb}$  activities of 1 dpm g $^{-1}$ . Some limited surface mixing was apparent in the second North Bay low marsh core and the surface samples were eliminated from the regression. High  $^{210}\text{Pb}$  activities found in the subtidal North Bay site were included in the long-term sedimentation calculations, but were likely caused by a single, large deposition event.

Sedimentation in North Bay ranged from 1.3 to 6.8 mm y $^{-1}$  (Table 4-1). Two cores collected 36 meters apart within the low *Nuphar*-dominated marsh zone accounted for most of this variability. South Bay sites exhibited uniform sedimentation (3.3-3.7 mm y $^{-1}$ ). All marsh sedimentation rates were well above the relative sea level rise of approximately 2.4 mm y $^{-1}$  (Lyles et al. 1988).

Carbon concentrations in the fringe marsh of South Bay were the highest found (Figure 4-4) at approximately 15% carbon, reflecting the large contribution of organic matter to the sediment. Both South Bay cores showed relatively constant carbon concentrations with depth, while the North Bay sites all showed a decrease in carbon content. There appeared to be a direct relationship between marsh elevation and carbon content in North Bay, but scatter in the data prevent this from being a statistically significant finding.

In both bays the subtidal, unvegetated cores showed no apparent trend in nitrogen content with depth (Figure 4-4b). Declines in nitrogen with depth were found in all North Bay marsh cores, with the high marsh exhibiting the highest concentration in North Bay. In contrast, the fringe marsh of South Bay showed a 50% increase in nitrogen concentration with depth to reach the

highest nitrogen concentrations found in this data set, 1.7% nitrogen.

Surface sediment (0 to 3 cm) from the marshes of North Bay had an average C:N:P of 141:9.3:1 which has been used in later stoichiometric calculations of seasonal fluxes.

Total phosphorus profiles showed little variability either in depth or between sites (Figure 4-5). Despite constant concentrations of total phosphorus throughout the North Bay transect, the proportion of organic phosphorus changed. Phosphorus retained in the subtidal cores of both North and South Bay is predominantly inorganic, while in the high marsh, the organic phosphorus contribution becomes more substantial, accounting for approximately half of the phosphorus at all depths. Phosphorus profiles in South Bay are more variable through depth.

Nutrient burial in the Tivoli Bay marshes was similar to that found within other tidal marsh systems (Table 4-2). Nitrogen burial in the high marsh of North Bay was moderate, as was total phosphorus burial (9.35 and 2.10 g m<sup>-2</sup> y<sup>-1</sup>, respectively) (Table 4-1). The two low marsh cores of North Bay exhibited a large range in values. Nitrogen burial was estimated at 8.0 and 13 g TN m<sup>-2</sup> y<sup>-1</sup>, and phosphorus 2.5 to 3.6 g TP m<sup>-2</sup> y<sup>-1</sup>. Subtidal deposition in North Bay accounted for 2.3 g TN m<sup>-2</sup> y<sup>-1</sup> and 0.7 g TP m<sup>-2</sup> y<sup>-1</sup>. South Bay nitrogen deposition in the fringe marsh was high, 15.9 g TN m<sup>-2</sup> y<sup>-1</sup>, driven primarily by the high nitrogen content of the organic sediment. Deposition of phosphorus was closer to the other values at 1.1 g TP m<sup>-2</sup> y<sup>-1</sup>. Nitrogen deposition in the subtidal zone was only one-third that of the fringe

marsh, a combination of the lower nitrogen concentration of the buried mineral material and deposition rate, despite the high bulk density.

## Seasonal Sediment-Water Fluxes

FALL 1996

Incubations of the North Bay flux cores proceeded until oxygen concentrations in some of the cores reached  $5.0 \text{ mg L}^{-1}$  (9.5 hours).

Dissolved oxygen changes in the blank were not significantly different from zero ( $\alpha=0.05$ ), therefore flux measurements in experimental cores were not adjusted. All oxygen fluxes were directed into the sediment and were significantly different from zero (Figure 4-6). The maximum rate of oxygen consumption was found in the cores collected from the high marsh. The average flux rate of the three cores was  $2060 \mu\text{mol O}_2 \text{ m}^{-2} \text{ hour}^{-1}$ , subtidal cores consumed  $1310 \mu\text{mol O}_2 \text{ m}^{-2} \text{ h}^{-1}$ , and the low marsh, *Nuphar* site cores consumed only  $950 \mu\text{mol O}_2 \text{ m}^{-2} \text{ h}^{-1}$  (Table 4-3).

During the time course experiment ammonium fluxes were found in subtidal cores from North Bay at  $70.2 \mu\text{mol NH}_4 \text{ m}^{-2} \text{ h}^{-1}$  (Table 4-3). Changes in ammonium concentration in the majority of cores collected from each of the other sites were non-linear resulting in no measurable flux.

North Bay incubations used water with a nitrate concentration of  $49 \mu\text{M}$   $\text{NO}_3^-$ , collected at low tide. Time course fluxes were not significantly different

from zero ( $\alpha=0.05$ ) in any of the cores from North Bay during the Fall 1996 experiment.

All fluxes from South Bay were run at 12°C, nine degrees colder than the cores from North Bay. Dissolved oxygen uptake was not different between the water chestnut and unvegetated subtidal sites (Figure 4-6). Only one core exhibited a flux of ammonium (Table 4-3). Ambient nitrate concentrations were higher than in North Bay, at 59  $\mu\text{M}$   $\text{NO}_3$  but time course concentrations are not available.

Porewater ammonium profiles showed the subtidal sediments of North Bay to have the highest concentrations, with an asymptotic value of 1400  $\mu\text{M}$   $\text{NH}_4$  (Figure 4-7). Lower concentrations were found in the low marsh among the *Nuphar advenum*, and still lower concentrations (max. of 50  $\mu\text{M}$   $\text{NH}_4$ ) in the high marsh among the *Typha angustifolia*. South Bay porewater ammonium concentrations were higher in the vegetated than the unvegetated site. In all cores a drop in ammonium concentration at the sediment surface suggests that ammonium should be released from the sediment to the water column.

Fall nitrate porewater profiles show similar concentrations between the North Bay low and high marsh sites, fluctuating around 143  $\mu\text{M}$   $\text{NO}_3$ . South Bay concentrations were slightly lower, at 107  $\mu\text{M}$   $\text{NO}_3$ .

SPRING 1997

All spring time course incubation experiments were run at 16°C for 10.5 hours. Oxygen fluxes were greatest in North Bay high marsh cores ( $1800 \mu\text{mol O}_2 \text{ m}^{-2} \text{ h}^{-1}$ ) (Figure 4-6). Low marsh and subtidal cores from North Bay were similar, consuming oxygen at a rate of  $900 \mu\text{mol O}_2 \text{ m}^{-2} \text{ h}^{-1}$ . Both sites in South Bay were comparable at  $1000 \mu\text{mol O}_2 \text{ m}^{-2} \text{ h}^{-1}$ .

In North Bay, ammonium release from the sediments was observed in only one of three high marsh cores and so is not considered significant (Figure 4-8). Both South Bay sites exhibited a small  $\text{NH}_4^+$  uptake (Table 4-3). Uptake in the subtidal site was slightly greater at  $36 \mu\text{mol NH}_4^+ \text{ m}^{-2} \text{ h}^{-1}$ , compared to  $30 \mu\text{mol NH}_4^+ \text{ m}^{-2} \text{ h}^{-1}$  in the vegetated, low marsh cores.

Ambient nitrate concentrations were  $40$  and  $49 \mu\text{M NO}_3^-$  in North and South Bays, respectively. Linear fluxes in nitrate concentrations were not observed in any of the North Bay cores during the experiment. Subtidal sediments from the South Bay removed nitrate from the water column at  $37 \mu\text{mol NO}_3^- \text{ m}^{-2} \text{ h}^{-1}$ .

Increases in dissolved  $\text{N}_{2(g)}$  concentrations indicated net denitrification was occurring (Figure 4-9). Rates were significantly different between sites, with the North Bay high marsh releasing the greatest amount of gaseous nitrogen,  $230 \mu\text{mol N m}^{-2} \text{ h}^{-1}$  (Table 4-3). Rates in the *Nuphar*-dominated marsh were the lowest measured ( $71 \mu\text{mol N m}^{-2} \text{ h}^{-1}$ ) and denitrification in the North Bay subtidal sediment was moderate ( $106 \mu\text{mol N m}^{-2} \text{ h}^{-1}$ ). Average

rates of net denitrification in South Bay were 137 and 80  $\mu\text{mol N m}^{-2} \text{ h}^{-1}$ , but were not significantly different due to the high variability (Figure 4-9).

Porewater cores were analyzed for ammonium and phosphate. The highest ammonium concentrations were found in the subtidal site in North Bay (Figure 4-10). The maximum concentrations were 400  $\mu\text{M NH}_4$ . The low marsh site in North Bay reached only 40  $\mu\text{M}$ . South Bay subtidal sediments were also low in porewater ammonium, with concentrations ranging from 17 to 35  $\mu\text{M}$ . The *Trapa*-dominated site in South Bay exhibited an increase in concentration with depth, ranging from 40 to 100  $\mu\text{M NH}_4$ .

## SUMMER 1997

The summer time course incubation experiment was run at 21.5°C for 6.5 hours. Due to high rates of oxygen depletion, the experimental results beyond 2.5 hours will not be considered. The low oxygen concentrations complicate the analysis of the data, and make necessary stoichiometric assumptions invalid. Oxygen consumption occurred in all cores (Figure 4-6), but decreases were only linear in North Bay low marsh and subtidal cores. A decline in oxygen was also found in the blank from both bays, and this decline was subtracted from the consumption rates found in experimental cores to account for water column heterotrophic respiration. Oxygen was consumed at a rate of 3400  $\mu\text{mol O}_2 \text{ m}^{-2} \text{ h}^{-1}$  in the North Bay low marsh site, and at a rate of 6000  $\mu\text{mol O}_2 \text{ m}^{-2} \text{ h}^{-1}$  in the subtidal site (Table 4-3). Oxygen

consumption in the South Bay vegetated site was not significantly different from that of the blank, and so is reported as insignificant. Oxygen concentrations in all experimental cores were lower than the blanks at the initial time point, most likely due to the time necessary to assemble tubing and connectors after the experimental cores are sealed. Oxygen depletion rates were rapid enough to cause this shift in the 30 minutes required to finish the experimental assembly.

Nitrogen fluxes did not resemble those of other seasons. Ammonium concentrations in both Bays were higher than in other seasons (Table 4-4), and ammonium fluxes were found only at the North Bay subtidal and South Bay vegetated sites (Figure 4-8). Ambient nitrate concentrations were 77 and 44  $\mu\text{mol NO}_3$  in North and South Bay, respectively (Table 4-5). Fluxes in the experimental cores were not different from zero. In all experimental cores, a decline in dissolved gaseous nitrogen was observed, clearly indicating nitrogen fixation (Figure 4-9).

Summer porewater cores showed an increasing concentration of ammonium with depth (Figure 4-11). Ammonium concentrations in the North Bay subtidal sediments were the highest, reaching concentrations of 600  $\mu\text{M NH}_4$ . Ammonium profiles at the other North Bay sites were fairly constant with depth. Concentrations reached 300  $\mu\text{M NH}_4$  in the South Bay low marsh core.

## DISCUSSION

### Marsh Sediment Accretion and Long-term Nutrient Burial

Physical sediment properties varied steadily along the topographic gradient from subtidal to marsh sediments, with clear trends seen in the profiles of percent water and bulk density. Increasing organic matter towards the interior of the marsh is indicated by the increasing water content and declining bulk density. Relative contributions of organic forms of phosphorus to the total phosphorus pool also increase with distance from the bays. The origin of marsh sedimentary material changes from deposited fluvial inputs in subtidal and low marsh sites to macrophytic organic matter at higher marsh elevations. The fringing marshes of South Bay are an extreme example of the end of this gradient. The shrubby marsh habitat is supported by a true peat, characterized by a very low bulk density, high organic matter content and high percent water (Brady 1990). Similar sedimentation patterns have been noted previously in Rhode Island salt marshes by Bricker-Urso et al. (1989) who suggest that the vertical accretion of tidal marshes is dependent upon organic matter production. More recently, Pasternack and Brush (1998) were able to show a clear trend of increasing organic matter with distance from the tidal creek in a Chesapeake tidal freshwater marsh. Seasonal variability in accretion was, in part, dependent upon inputs of terrigenous organic material to marshes at higher elevations.

Clearly, the marshes of Tivoli Bays are keeping pace with the local relative sea level rise of approximately  $2.4 \text{ mm y}^{-1}$  (Lyles et al. 1988). Accretion rates were higher in North Bay than in South Bay, which agrees with the overall habitat shift seen between the two. In both North and South Bays subtidal deposition was lower than within the marsh. This trend in accretion rates conflicts with the findings of Jordan et al. (1986), who suggest that deposition in a Chesapeake brackish marsh system is dependent upon the time of submergence. It appears that in tidal freshwater marshes accretion is as much due to production, deposition and retention of organic matter as it is to tidal supply of particulate material. Again, this echoes work in Rhode Island by Bricker-Urso et al. (1989).

The large variability in accretion rates,  $6.8$  and  $3.7 \text{ mm y}^{-1}$ , found in two cores located only 36 meters from each other and within the same “zone”, highlights the spatial variability of the marsh. The cores showed little variability in sediment properties such as density and organic content, and the only observed difference between the cores was the low concentrations of  $^{210}\text{Pb}$  found in the first core. Maximum  $^{210}\text{Pb}$  activity reached only  $2.5 \text{ dpm g}^{-1}$  in the core, as opposed to a maximum of  $4.0 \text{ dpm g}^{-1}$  in the second. This is most likely due to a dilution of activity by the deposition of old sediment, moved from another part of the system. The high rate of  $6.8 \text{ mm y}^{-1}$  accretion then, is the result of sediment focusing at the site. Sediment focusing within this low marsh zone can accounts for large disparities in sediment deposition rates.

Previous estimates of sedimentation have been made for these marshes. Rates of sedimentation found in this study are higher than that reported by Peller and Bopp (1986) who used  $^{137}\text{Cs}$  to estimate accretion in the South Bay of the marsh. They report rates of sedimentation at  $1 \text{ mm y}^{-1}$ , approximately one-third the magnitude of the rates found in this study. Comparisons of the two sediment dating techniques show that  $^{137}\text{Cs}$  can lead to both over and underestimates of sedimentation. Post-depositional mobility, coupled with watershed release can spread the sharp signal needed to identify the peak input (Davis et al. 1984). Wang and Benoit (1992) used  $^{210}\text{Pb}$  dating, and report sedimentation rates in South Bay between 1 and 3  $\text{cm y}^{-1}$  in Tivoli Bays. My results are lower, suggesting that the estimates of nutrient burial presented in this report are relatively conservative. Variability due to site selection and mathematical model analysis may contribute to the disparity.

Nitrogen and phosphorus burial rates in Tivoli Bays are similar to those found in other tidal freshwater and brackish marshes (Table 4-2). It appears that oligohaline marshes are well-situated for nutrient removal through organic matter preservation and particulate deposition, retaining between 2 and 23  $\text{g TN m}^{-2} \text{ y}^{-1}$ , and 0.5 to 4  $\text{g TP m}^{-2} \text{ y}^{-1}$ .

The nutrient burial rates were extrapolated to the surface area of the marsh. By combining the burial rates, listed in Table 4-1, with vegetation coverage as reported by Nieder (personal communication) I estimated the burial of nutrients over the entire marsh surface (Table 4-6). Vegetation was

used as a cue for marsh elevation (DeVries and DeWitt 1987), which may be a major determinant of the rates of sediment deposition.

## Seasonal Activity and Site Variability

Seasonal shifts in the marsh's nitrogen metabolism are apparent from the seasonal flux studies. Denitrification was strongly suggested by the fall data and directly measured in the spring. Spring denitrification rates were relatively high in the Tivoli Bays marshes ( $70$  to  $230 \mu\text{mol N m}^{-2} \text{ h}^{-1}$ ) compared to those reported by Seitzinger (1988) for coastal marine systems (Table 4-7).

Stoichiometric calculations have been used to estimate denitrification rates by difference in previous research. By converting oxygen uptake into potential nitrogen release based on the C:N ratio of the organic matter, one can estimate  $\text{N}_{2(g)}$  release after accounting for exchanges of  $\text{NH}_4$  and  $\text{NO}_3$  (Seitzinger 1988). Organic matter decomposition, estimated from the uptake of oxygen from the water column, released one mole of nitrogen for every 15.2 moles of  $\text{O}_2$  consumed (measured C:N 15.2:1). No fluxes of dissolved inorganic nitrogen were measured in the North Bay cores, except for the release of  $\text{N}_{2(g)}$ . In all these cores it appears that coupled nitrification-denitrification removed all of the mineralized nitrogen from the organic matter and released it as  $\text{N}_{2(g)}$ . Reduced dissolved nitrogen ( $\text{NH}_4$ ) underwent nitrification and was converted to nitrate which was subsequently denitrified.

Coupled nitrification-denitrification has been found to be the predominant pathway through which denitrification occurs in some estuarine sediments (Jenkins and Kemp 1984, Rysgaard et al. 1994, 1995). Denitrification rates are higher than predicted by oxygen consumption (171% in the North Bay subtidal sediment) and may be due to variability in the C:N ratio of the organic material or to supplemental nitrogen provided by the porewater.

Porewater concentrations are high deep in the sediments (400  $\mu\text{M}$   $\text{NH}_4$ ) and decrease towards the surface, indicating an efflux of dissolved ammonium from the deep porewaters to the sediment-water interface. Since no ammonium release was measured it appears that porewater ammonium is supplementing the nitrification-denitrification pathway measured by the release of nitrogen gas. A similar but less extreme situation is apparent in the low marsh, North Bay cores during the spring, with  $\text{N}_{2(\text{g})}$  efflux measured at 124% of that predicted by  $\text{O}_2$  consumption and porewater  $\text{NH}_4$  concentrations reaching only 40  $\mu\text{M}$ . Porewater data are not available for the high marsh core, but again rates of denitrification were 188% of that predicted by oxygen consumption and may be supplemented by ammonium supply from the porewater.

Spring cores collected from South Tivoli Bay provided good examples of stoichiometric balances. Removing 970  $\mu\text{mol O}_2 \text{ m}^{-2} \text{ h}^{-1}$  releases 60  $\mu\text{mol N m}^{-2} \text{ h}^{-1}$ . Adding 30  $\mu\text{mol}$  of N from the  $\text{NH}_4$  uptake and nothing for nitrate exchange, the sediment should release 90  $\mu\text{mol N m}^{-2} \text{ h}^{-1}$  as  $\text{N}_{2(\text{g})}$ . Measured

denitrification released  $80 \mu\text{mol N m}^{-2} \text{ h}^{-1}$ , only a 12% difference from the calculated estimate. Nitrate uptake was an added source of nitrogen for denitrification in the subtidal cores resulting in an increase in the rate of denitrification consistent with the calculated estimates (13% difference, calculated vs. measured).

The summer experiment suggests nitrogen fixation is occurring in North Bay. Since the DGA technique measures net  $\text{N}_{2(\text{g})}$  exchange, a decline in the overlying water indicates net gaseous nitrogen fixation. The marsh may be nitrogen-deficient resulting in the need to fix nitrogen at the surface, supplying sediment microbial communities with nitrogen required for the decomposition of organic material. The low marsh of North Bay appeared to have the largest demand for nitrogen, a total of  $1020 \mu\text{mol N m}^{-2} \text{ h}^{-1}$  from estimated nitrogen remineralization and surficial nitrogen fixation. Nitrogen fixation has been reported previously during the summer in a brackish Chesapeake Bay marsh. Lipschultz (1978) reports a summer maximum nitrogen fixation rate  $30 \mu\text{mol N m}^{-2} \text{ h}^{-1}$ . A review by Nixon and Lee (1986) suggest an average nitrogen fixation rate of  $1\text{-}5 \text{ g N m}^{-2} \text{ y}^{-1}$  for mid-Atlantic marshes.

Competition for nitrogen may exist between the sediment microbial population and the local plant communities (Thompson et al 1995). This study examined cores collected between plants, and did not include any active nitrogen uptake by vegetation. As a result, the data suggests

denitrification can occur when plants are not actively incorporating sediment dissolved inorganic nitrogen. In the marsh, the plants are expected to remove between 5 and 35 g N m<sup>-2</sup> y<sup>-1</sup> (as estimated by Bowden 1987) which may limit denitrification.

The seasonal fluxes included in this study were intended to provide an annual estimate of nitrogen lost via denitrification under natural conditions within marsh sediments. Cores were incubated at field temperature, and with organic matter found at each site. Fall incubations of North and South Bay cores were conducted at different temperatures (21 and 12°C, respectively) and so direct comparisons of fall data are not possible. Seasonal differences in organic matter supply at the surface of the sediment were also not separated. Since denitrification is linked with organic matter content (Caffrey et al. 1993), it is expected that the highest rate of denitrification should coincide with the period of highest fresh organic matter supply to the sediment. Seitzinger (1994) also reports a strong correlation between sediment oxygen consumption and denitrification in freshwater wetland sediments.

The use of flux core incubations is not without uncertainty. Experiments were conducted in the dark, to eliminate variable light conditions on the surface of the cores. Light has been shown to enhance denitrification in estuarine sediments by stimulating microphytobenthos to produce oxygen, increasing rates of nitrification and consequent denitrification (Risgaard-Petersen et al. 1994). Rates of denitrification presented here may be

conservative estimates without this photo-stimulation. Shifting redox regimes in marsh sediments may also enhance denitrification, by allowing microzones of nitrification and denitrification to occur in the same position over time.

Work by Staver and Brinsfield (1996) clearly showed the discharge of high quantities of nitrate from groundwater into an estuarine system.

Groundwater contributions, shown to be much larger than previously estimated, cannot be included in the current experimental design.

Groundwater discharge is likely a large contributor of nitrate to coastal systems which undergoes dynamic variations in flow with tides and changes in hydraulic head. It remains unclear how and if tidal freshwater marshes can intercept a portion of this nitrate before it is introduced to the estuary.

## Ecosystem Calculations

The marshes of Tivoli Bays are burying large amounts of nutrients within their sediments. Approximately 10,000 kg nitrogen and 2,000 kg particulate phosphorus are retained each year in the marsh sediments of the bays. Subtidal sediments also retain large amounts of potentially harmful nutrients.

The goal of this study was to attempt an ecosystem budget for the marshes of the Hudson River in the estuarine nutrient budget. Field et al. (1991) reports  $5.95 \times 10^7 \text{ m}^2$  of Hudson River fresh marsh (tidal and non-

tidal), to which the average nutrient burial rates of the Tivoli Bays marshes were applied ( $11.6 \text{ g TN m}^{-2} \text{ y}^{-1}$  and  $2.33 \text{ g TP m}^{-2} \text{ y}^{-1}$ ). The calculation provided an estimate of what the watershed marshes may be capable of retaining,  $6.9 \times 10^5 \text{ kg TN y}^{-1}$  and  $1.4 \times 10^5 \text{ kg TP y}^{-1}$ . Limburg et al. (1986) compiled data on nitrogen and phosphorus loading to the upper Hudson River. They report  $3.98 \times 10^5 \text{ kg TN}$  and  $1.83 \times 10^5 \text{ kg TP}$  being added as sewage to the upper river annually. A comparison of the numbers suggests that freshwater marshes of the Hudson River may be able to retain the nutrients added by sewage effluent. This is presented as a first approximation of nutrient removal and includes freshwater marshes not connected to the River directly. Applying these burial numbers to freshwater marshes removed from the direct influence of the River may not be feasible. Despite these assumptions, the exercise is useful to begin to frame the importance of these marshes in the surrounding estuary.

Estimating removal of dissolved nitrogen by the marshes is a much more difficult task. Large variations in nitrogen processing with season were found in this study. In the spring, the marshes acted as moderate sinks for nitrogen, while in the summer they do not appear to remove significant quantities of fixed nitrogen. Spring experiments showed a good agreement between measured denitrification and stoichiometric predictions based on the measurement of oxygen, nitrate and ammonium. Results support the findings of Seitzinger (1994), showing denitrification directly related to sediment oxygen demand (Figure 4-12). In the summer, stoichiometric

calculations could not predict denitrification due to the microbial metabolic requirement of additional nitrogen, resulting in net fixation of  $N_{2(g)}$ . During the spring the marshes cycle nitrogen similar to a subtidal estuarine sediment, with excess nitrogen available in the high marsh where detritus layers can often be up to 15 cm thick (personal observation), supplied from organic matter mineralization and porewater efflux. During the summer the marsh requires more nitrogen to support high rates of organic matter decomposition, resulting in the net fixation of nitrogen. It is unclear why nitrate and ammonium were not utilized by these communities when both nitrogen forms were available ( $NO_3$  at 80 and 40  $\mu M$ , North and South Bays, respectively). Bowden (1991) has provided an annual nitrogen cycling hypothesis which suggests a small uptake of nitrogen by the marsh to support macrophyte growth in the spring, nitrogen release in the summer, and adsorption of reduced nitrogen to plant litter in the fall for release the following spring. Nitrogen cycling in this tidal freshwater marsh appears to be more open, relying on exchanges of nitrogen gas to provide an annual balance of nitrogen to the plant and microbial communities.

Marsh sediments in Tivoli Bays do not appear to be a large sink for nitrogen via denitrification on an annual cycle. Nitrogen fixation during the summer essentially balances nitrogen lost during the spring to denitrification. Subtidal sediments in the Bays appear to be net denitrifiers and may remove as much as 2.5 and 1.9  $mmol\ N\ m^{-2}\ d^{-1}$  as  $N_{2(g)}$ .

## SUMMARY

- Rates sedimentation are between 3.6 and 6.9 mm  $y^{-1}$  in the marshes and lower in the subtidal sediments where supplemental organic matter from macrophytes is not deposited.
- Burial of nitrogen and phosphorus range from 8 to 19 g N  $m^{-2} y^{-1}$  and 1.1 to 3.6 g P  $m^{-2} y^{-1}$  in the marsh sediments and are related to the origin of the sedimentary material. Higher organic matter content is responsible for more efficient retention of nitrogen relative to phosphorus.
- Denitrification is moderate to high in the spring and relies on the nitrification of reduced nitrogen forms, rather than uptake of nitrate from the water column. Porewater supply of ammonium appears to supplement rates of denitrification.
- The marshes of the North Bay fix nitrogen in the summer, ostensibly to support the rapid decomposition of organic matter.
- During the spring, sediment oxygen demand is a good predictor of denitrification, but during other seasons organic matter production and decomposition complicate the nitrogen cycle, making stoichiometric calculations often used in subtidal geochemical research invalid.
- The marshes of Tivoli Bays may remove 10,500 kg particulate nitrogen and 2000 kg particulate phosphorus annually. Removal of fixed nitrogen from the water column by the sediment is insignificant. Contributions of

reduced nitrogen to the water column are small since remineralized nitrogen is nitrified and denitrified.

**Table 4-1. Sediment accretion and nutrient burial rates as determined by  $^{210}\text{Pb}$  dating and particulate nutrient profiles.**

	Accretion (mm $\text{y}^{-1}$ )	Deposition (kg $\text{m}^{-2} \text{y}^{-1}$ )	$r^2$ of linear regression	Total N Burial (g TN $\text{m}^{-2} \text{y}^{-1}$ )	Total P Burial (g TP $\text{m}^{-2} \text{y}^{-1}$ )
N. High	4.56	2.33	0.90	9.35	2.10
N. Low 1	6.85	3.04	0.90	8.01	2.50
N. Low 2	3.70	4.99	0.84	13.3	3.61
N. Subtidal	1.30	0.845	0.85	2.30	0.69
S. Fringe	3.74	1.15	0.89	15.9	1.12
S. Low	3.59	-	0.90	-	-
S. Subtidal	3.34	1.91	0.92	5.23	1.25

Table 4-2. Nutrient burial rates from a selection of other marsh studies.

	Tracer	N burial g m <sup>-2</sup> y <sup>-1</sup>	P burial g m <sup>-2</sup> y <sup>-1</sup>	Author(s)
<i>Salt</i>				
North Carolina	<sup>137</sup> Cs	1.3-4.1	-	Craft et al. 1993
<i>Brackish</i>				
Louisiana	<sup>137</sup> Cs	21	-	DeLaune et al. 1981
North Carolina	<sup>137</sup> Cs	6.9-10.3	-	Craft et al. 1993
Choptank River, MD	<sup>210</sup> Pb	19.2-27.1	0.18-1.96	Merrill and Cornwell <i>in preparation</i>
Monie Bay, MD	<sup>210</sup> Pb	13.6	0.01-1.30	Merrill Appendix A
<i>Tidal Freshwater</i>				
Patuxent River, MD	<sup>210</sup> Pb	21.4	3.76	Merrill Chapter 2
Tivoli Bays, NY	<sup>210</sup> Pb	2.30-15.9	0.69-3.61	Merrill this study
<i>Nontidal Freshwater</i>				
Wisconsin	<sup>137</sup> Cs	12.8	2.6	Johnston et al. 1984
Average organic soils	various	14.6	1.46	Johnston 1991
Average inorganic soils	various	1.6	0.26	Johnston 1991
Florida everglades	<sup>210</sup> Pb	14.1	0.66	Craft and Richardson 1993

Table 4-3. Seasonal oxygen and nitrogen sediment-water flux rates in Tivoli Bays experimental cores. Standard errors of triplicate cores are given. Negative fluxes are directed into the sediments and all nitrogen fluxes are expressed as  $\mu\text{mol N m}^{-2} \text{ h}^{-1}$ . Experimental temperatures were adjusted to field temperatures (Fall 21.0 °C North, 12.0 °C South, Spring 16.0 °C, Summer 21.5 °C). No core was collected from the subtidal South Bay site during the summer 1997 experiment, -- indicates non-linear concentration changes resulting in no flux.

	NORTH BAY			SOUTH BAY	
	High	Low	Subtidal	Vegetated	Subtidal
<b>Fall '96</b>					
O <sub>2</sub>	-2100 ± 240	-950 ± 60	-1300 ± 200	-1100 ± 240	-950 ± 50
NH <sub>4</sub>	--	--	70.2 ± 40.1	--	--
<b>Spring '97</b>					
O <sub>2</sub>	-1830 ± 120	-870 ± 10	-940 ± 100	-970 ± 150	-970 ± 180
NH <sub>4</sub>	--	--	--	-30.0 ± 1.87	-36.1 ± 0.04
NO <sub>3</sub>	--	--	--	--	-23.6 ± 1.01
N <sub>(g)</sub>	226 ± 34.6	71.0 ± 10.6	106 ± 10.4	80.3 ± 13.5	137 ± 52.4
<b>Summer 97</b>					
O <sub>2</sub>	--	-3400 ± 160	-6000 ± 920	--	n.d.
NH <sub>4</sub>	--	--	38 ± 44.7	153 ± 28.4	n.d.
N <sub>(g)</sub>	-113 ± 109	-797 ± 140	--	--	n.d.

O<sub>2</sub> in  $\mu\text{mol O}_2 \text{ m}^{-2} \text{ h}^{-1}$ , NH<sub>4</sub>, NO<sub>3</sub> and N<sub>(g)</sub> in  $\mu\text{mol N m}^{-2} \text{ h}^{-1}$   
 Nitrate fluxes during the Fall 1996 and Summer 1997 experiments were all nonlinear.

Table 4-4. Ambient NH<sub>4</sub> concentrations in Tivoli Bays ( $\mu\text{mol NH}_4\text{-N L}^{-1}$ ).

	Fall 1996	Spring 1997	Summer 1997
North	2.8	4.0	5.1
South	3.2	3.1	4.0

Table 4-5. Ambient nitrate concentrations in Tivoli Bays ( $\mu\text{mol NO}_3\text{-L}^{-1}$ ).

	Fall 1996	Spring 1997	Summer 1997
North	49	40	77
South	59	49	44

Table 4-6. Tivoli Bays marsh nutrient removal budget calculations.

Nitrogen Burial

	Areal Coverage (m <sup>2</sup> )	N Burial Rate (g TN m <sup>-2</sup> y <sup>-1</sup> )	Total N Retention (kg TN y <sup>-1</sup> )
South Fringe	3.04 x 10 <sup>5</sup>	15.9	4836
Marsh			
North Low	3.57 x 10 <sup>5</sup>	10.6	3784
Marsh			
North High	8.14 x 10 <sup>5</sup>	2.30	1872
Marsh			
		TOTAL	10,492

Phosphorus Burial

	Areal Coverage (m <sup>2</sup> )	P Burial Rate (g TP m <sup>-2</sup> y <sup>-1</sup> )	Total P Retention (kg TP y <sup>-1</sup> )
South Fringe	3.04 x 10 <sup>5</sup>	1.12	340
Marsh			
North Low	3.57 x 10 <sup>5</sup>	3.05	1089
Marsh			
North High	8.14 x 10 <sup>5</sup>	0.69	562
Marsh			
		TOTAL	1991

Table 4-7. Rates of aquatic denitrification from Seitzinger 1988.

	Rate ( $\mu\text{mol N m}^{-2} \text{ h}^{-1}$ )	Reference
<b>Rivers/Streams</b>		
Potomac River, MD	210-235	Seitzinger et al. 1987
San Francisquito Creek, CA	54	Duff et al. 1984
<b>Lakes</b>		
Michigan, MI	12-51	Gardner et al. 1987
Okeechobee, FL	2-25	Messer and Brezonik 1983
<b>Coastal Marine</b>		
Patuxent River, MD	77-89	Jenkins and Kemp 1984
Narragansett Bay, RI	39-109	Seitzinger et al. 1984
Tivoli Bays, NY	71-226	

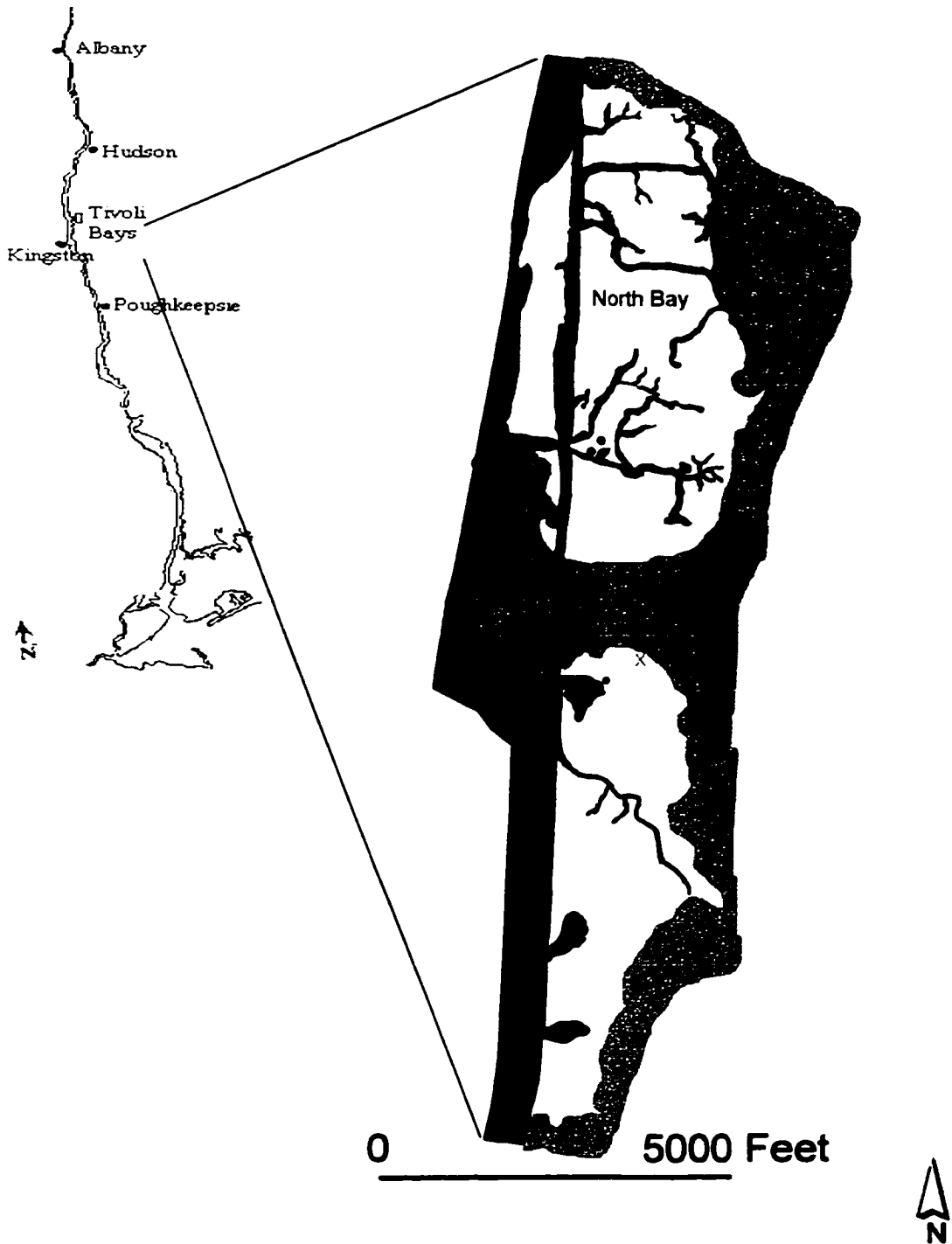
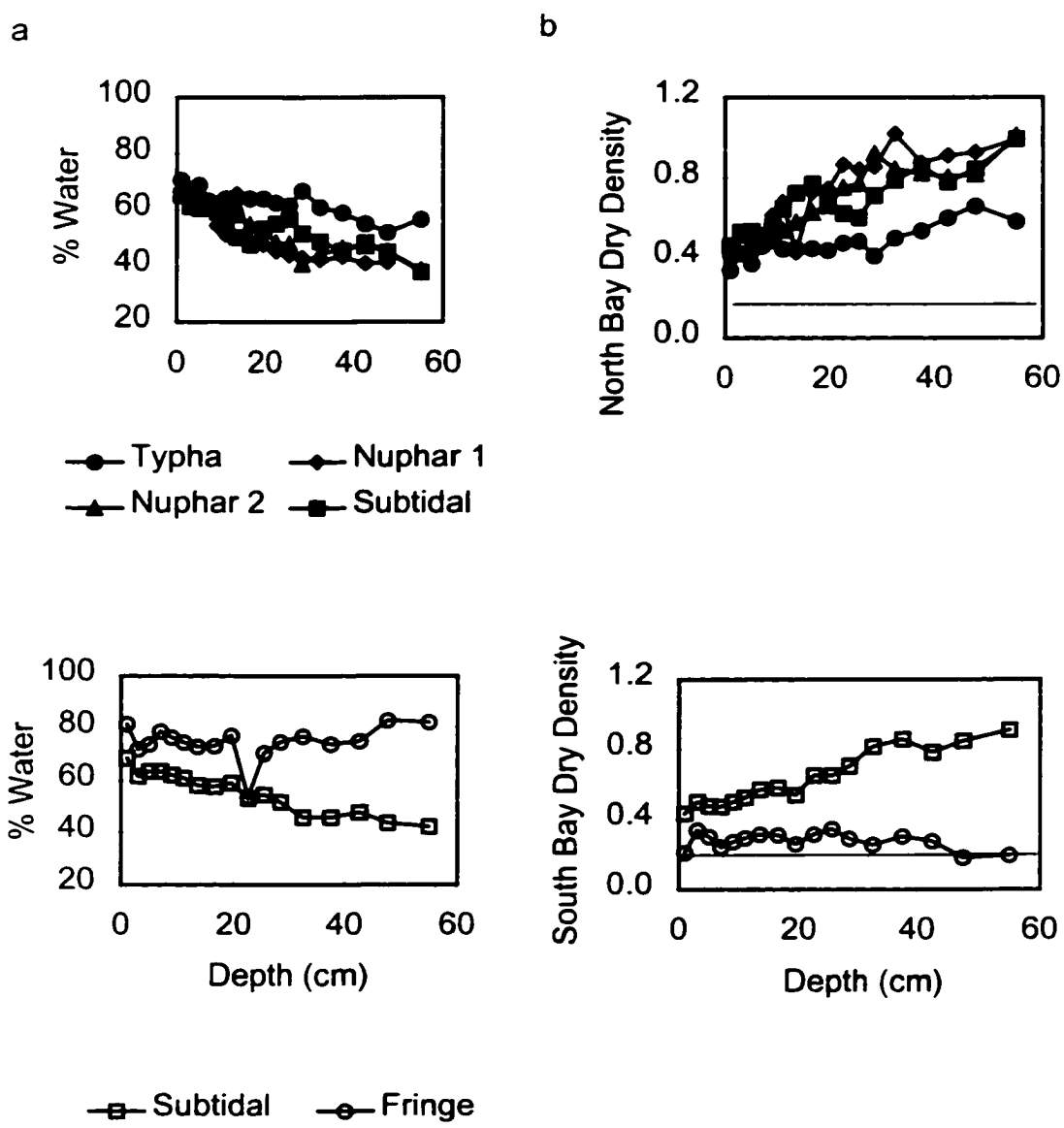
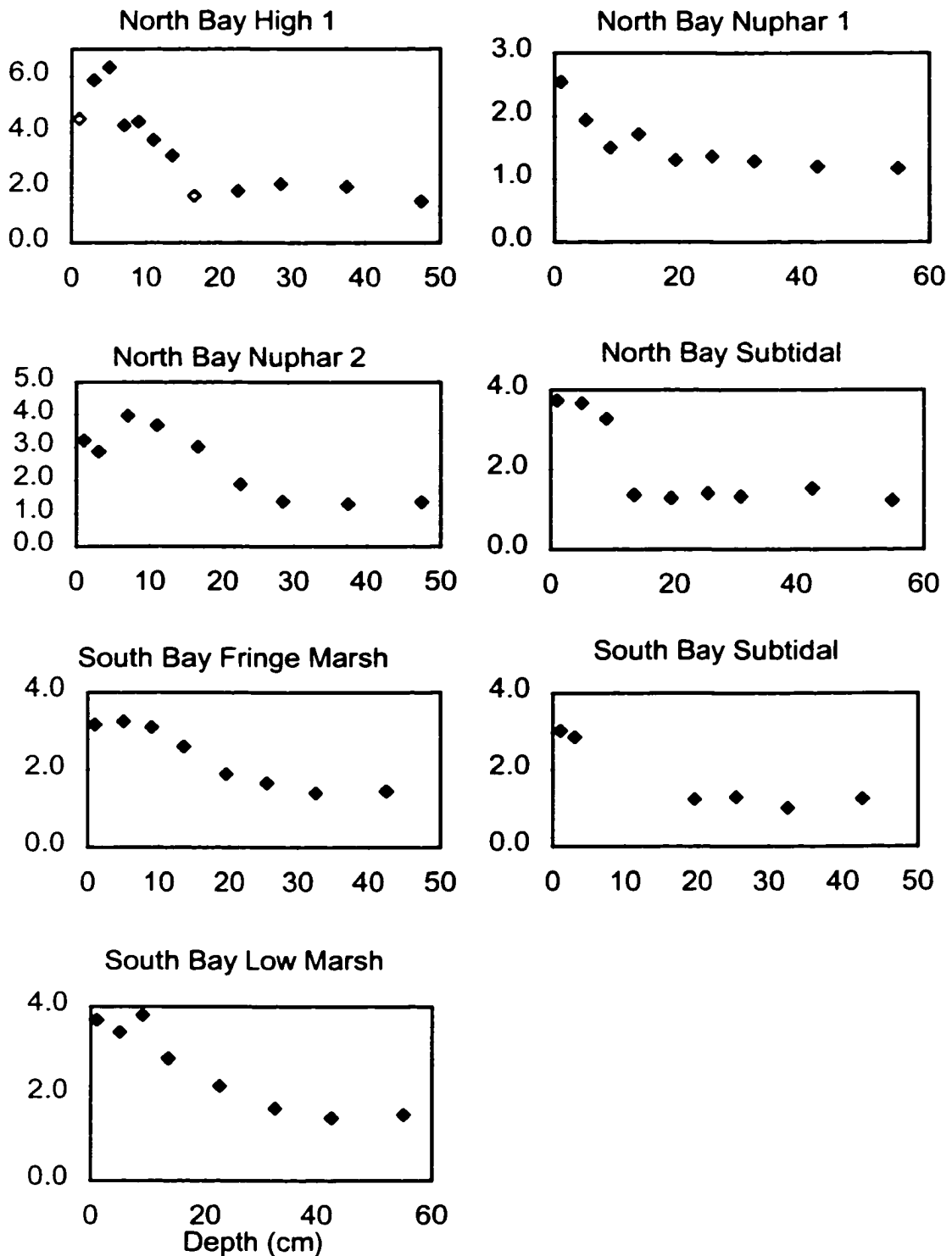


Figure 4-1. Tivoli Bay National Estuarine Research Reserve on the Hudson River in New York State. Sites of  $^{210}\text{Pb}$  and flux sampling are indicated with a circle. The "X" indicates where only a long,  $^{210}\text{Pb}$  core was collected.



**Figure 4-2.** Physical characteristics of Tivoli Bays Marsh sediment, top: North Bay, bottom: South Bay. (a) percent water, (b) dry bulk density,  $\text{g cm}^{-3}$ . The horizontal line indicates the bulk density of a saprist peat,  $0.2 \text{ g cm}^{-3}$  (Brady 1990).



**Figure 4-3. Profiles of total  $^{210}\text{Pb}$  activity (dpm g $^{-1}$  sediment) in Tivoli Bays marsh sediments. Data omitted from regressions are indicated with an open symbol.**

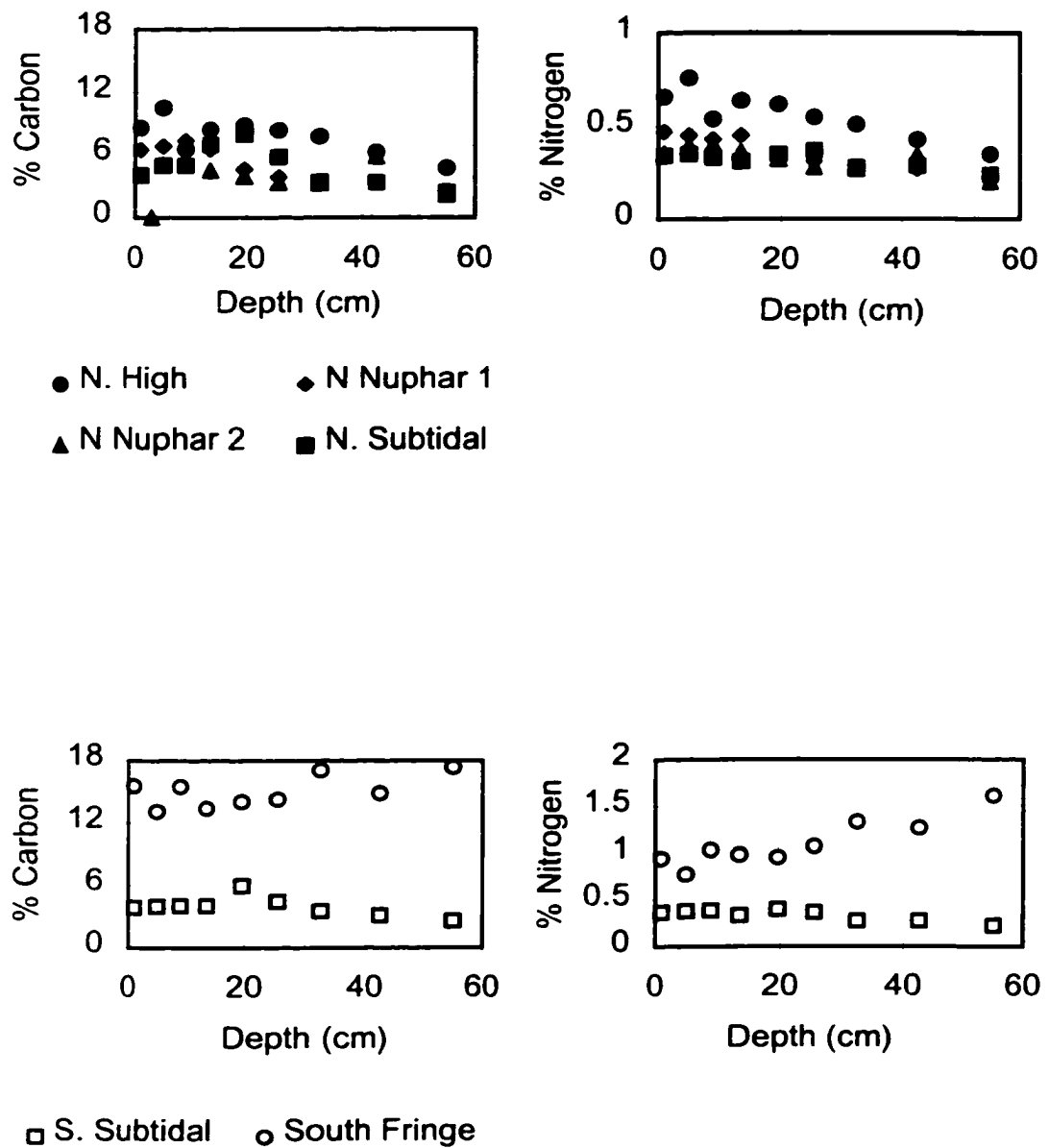


Figure 4-4. Tivoli Bays sediment particulate carbon and nitrogen profiles. Note change in scale.

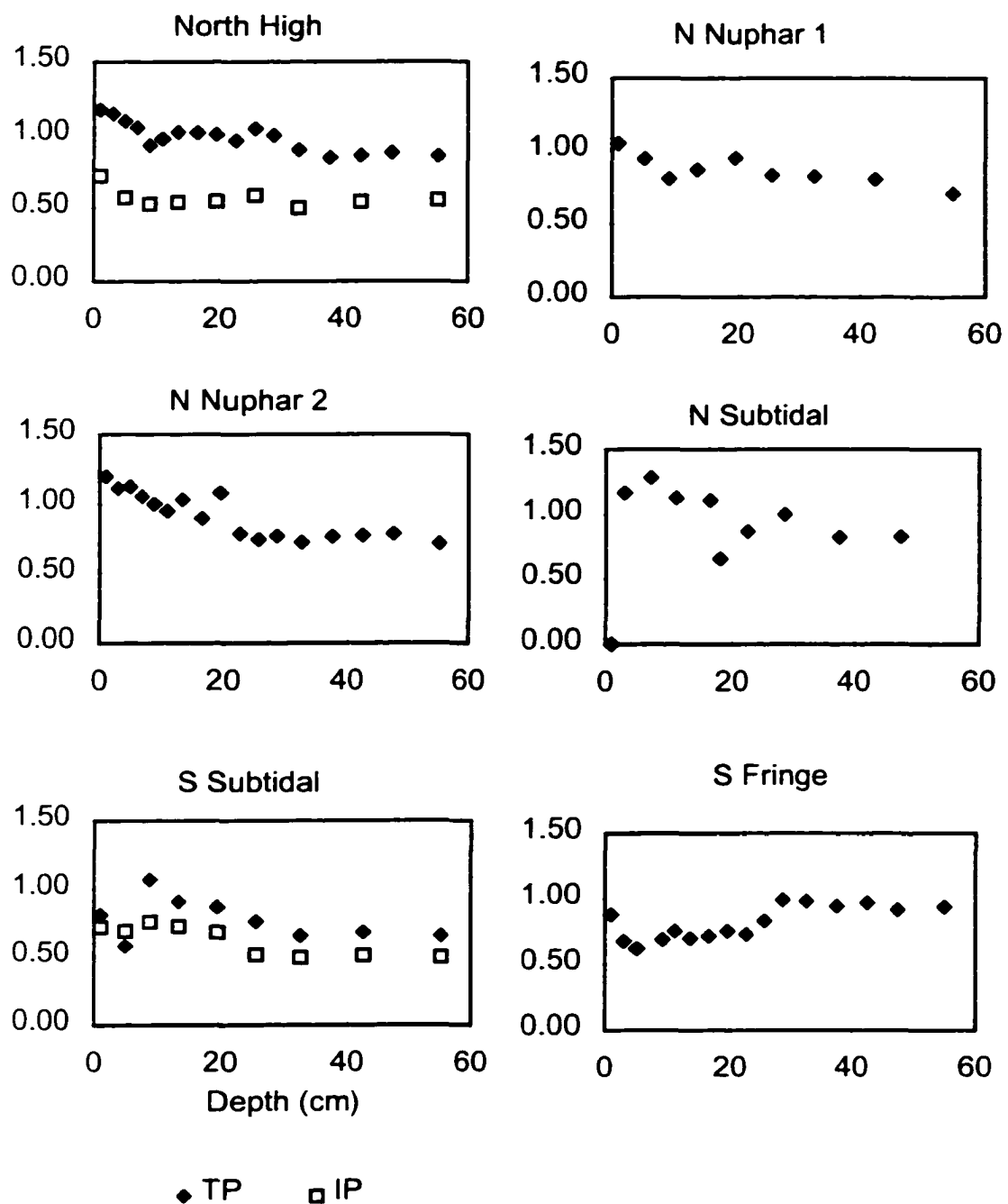


Figure 4-5. Vertical profiles of total (TP) and inorganic (IP) phosphorus in the Tivoli Bays marsh sediment. All values are given as mg P per gram of sediment.

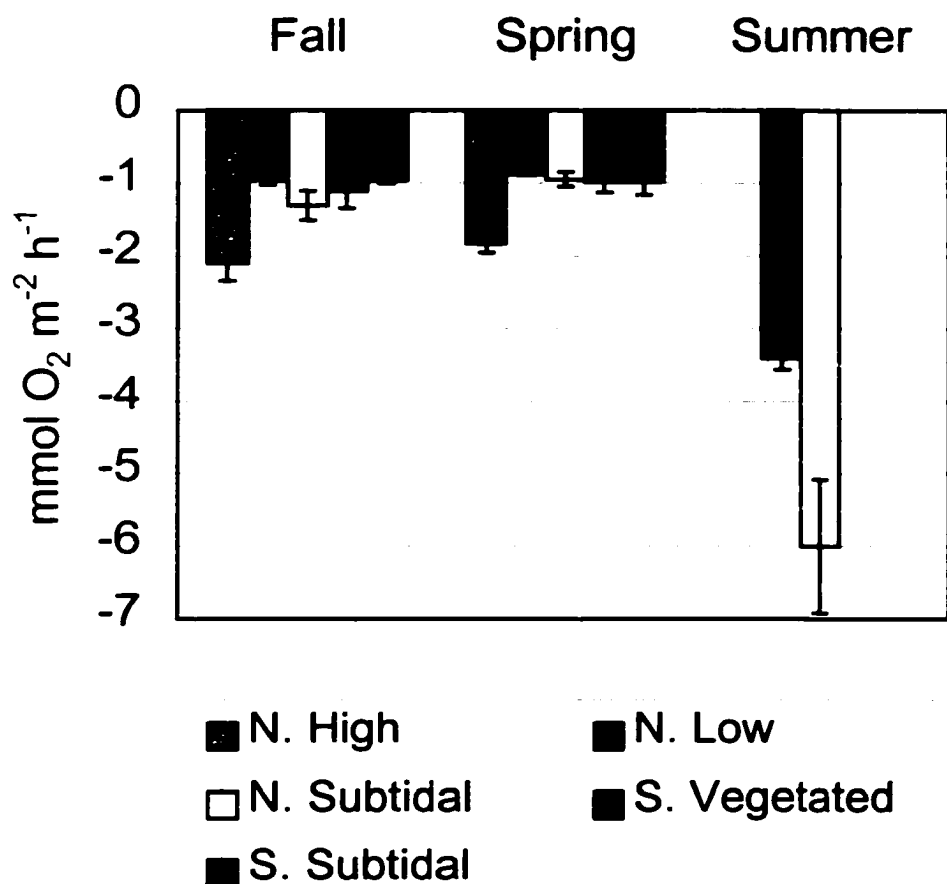
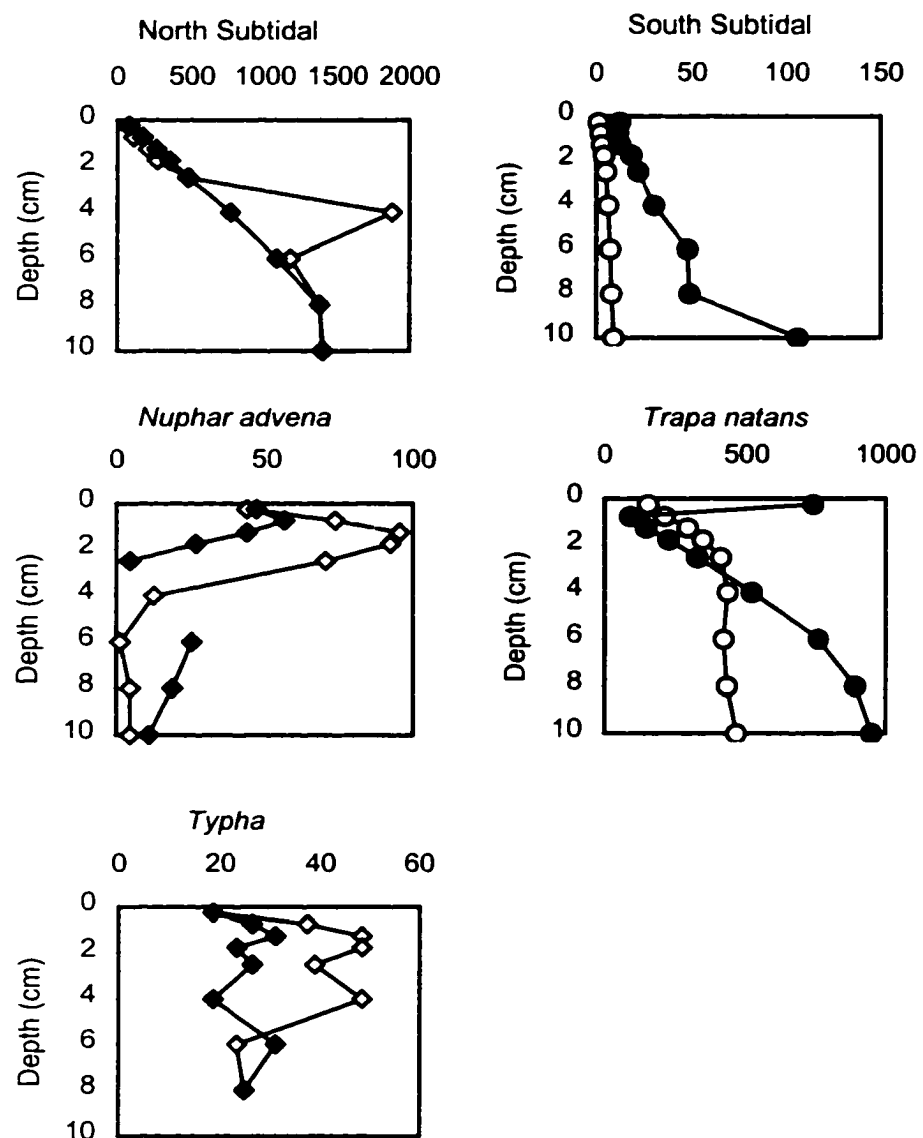


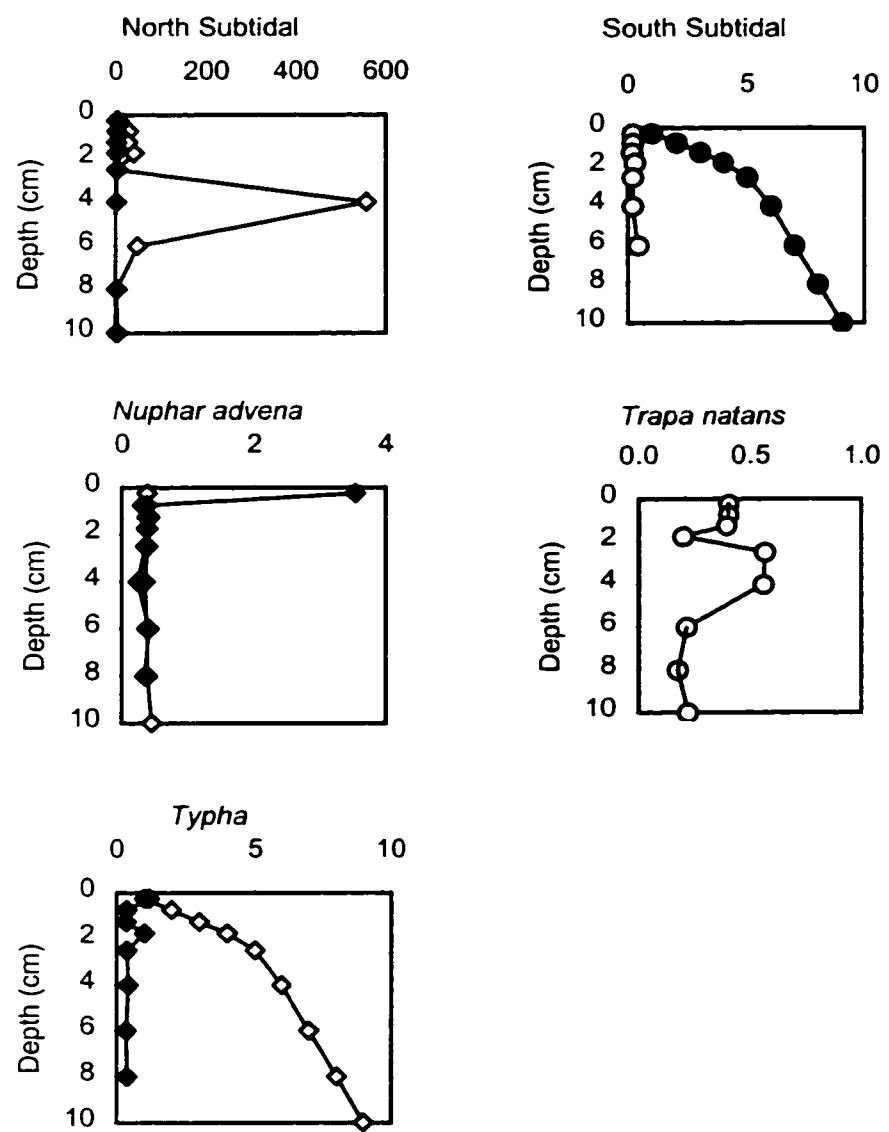
Figure 4-6. Oxygen fluxes measured in Tivoli Bays marsh and subtidal sediments. Negative fluxes are into the sediment; standard errors of two to three cores are shown.

**Figure 4-7.** Porewater profiles of duplicate cores collected from Tivoli Bays in the Fall of 1996. Duplicate cores are shown on the same graph, North Bay sites are on the left. Ammonium (a) is shown as  $\mu\text{mol NH}_4 \text{ L}^{-1}$ , (b) shows nitrate as  $\mu\text{mol NO}_3 \text{ L}^{-1}$ , and (c ) shows phosphate as  $\mu\text{mol PO}_4 \text{ L}^{-1}$ . Note changing magnitude of y axis. Phosphate concentrations in the South Bay subtidal core were below detection.

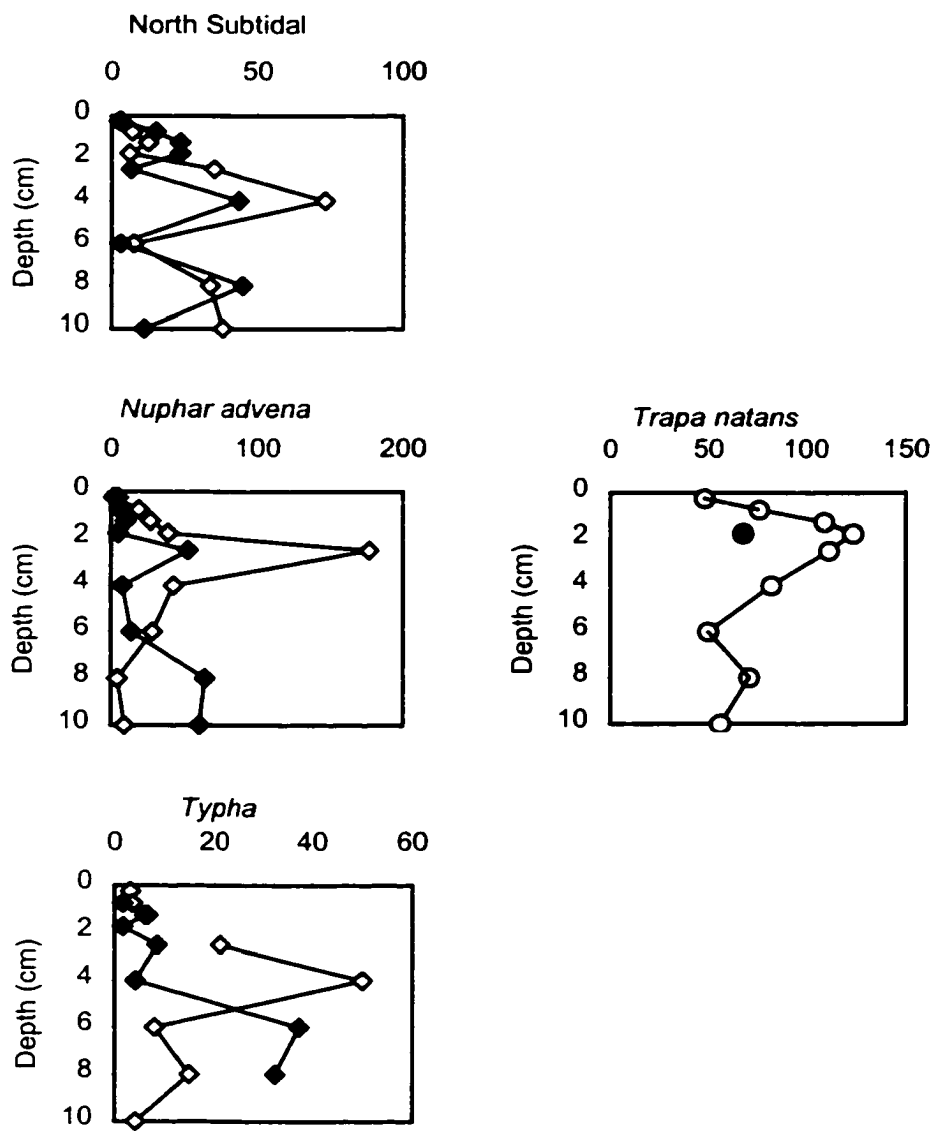
(a) Ammonium ( $\mu\text{mol NH}_4 \text{ L}^{-1}$ )



(b) Nitrate ( $\mu\text{mol NO}_3 \text{ L}^{-1}$ )



(c) Phosphate ( $\mu\text{mol PO}_4 \text{ L}^{-1}$ )



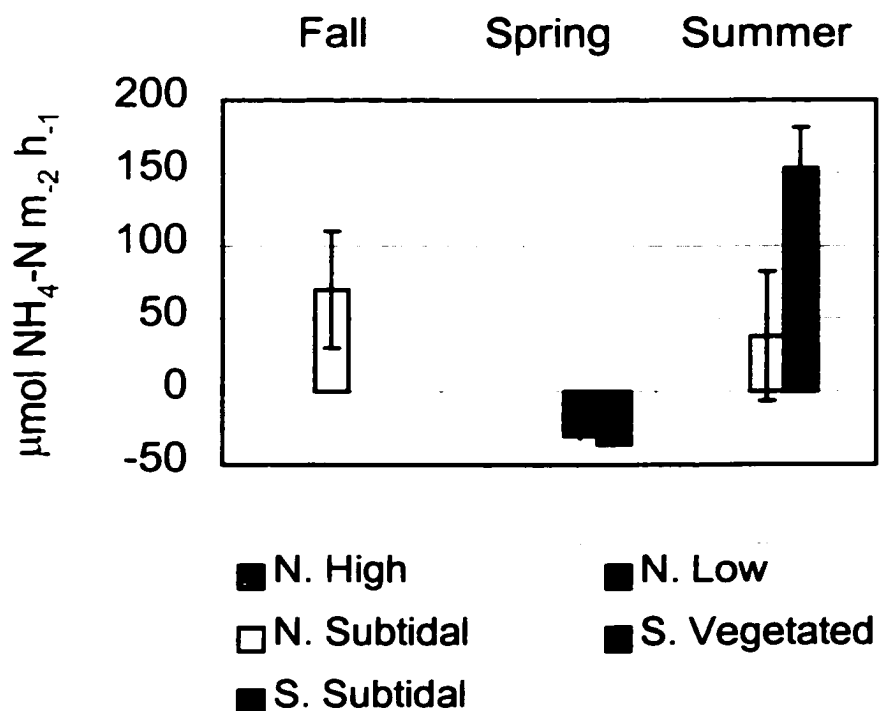


Figure 4-8. Ammonium fluxes measured in Tivoli Bays marsh and subtidal sediments. Negative fluxes are directed into the sediments. Standard errors of 2 to 3 cores are presented. No data were collected from the subtidal site in the summer experiment. All other sites showed no linear concentration changes of ammonium over time.

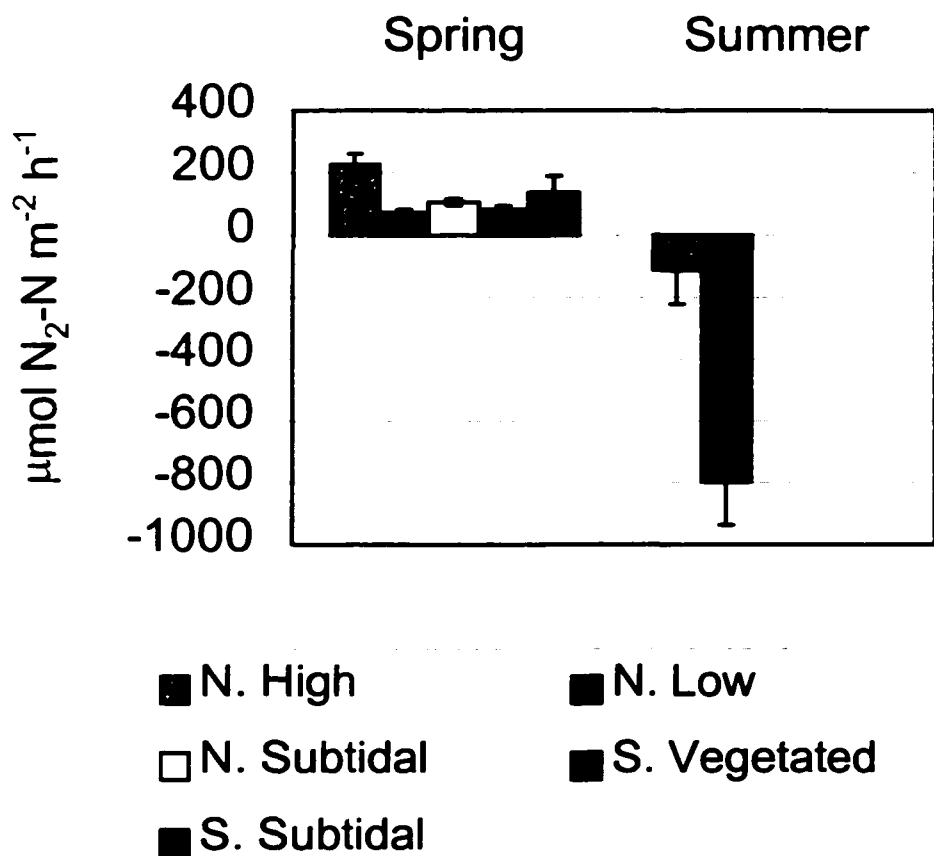


Figure 4-9. Net  $\text{N}_{2(\text{g})}$  exchange in Tivoli Bays marsh and subtidal sediments directly measured using a membrane inlet mass spectrometer. Standard error of three cores is given for each site. Fall data were not collected. Positive fluxes are out of the sediment, indicating net denitrification, negative fluxes are into the sediment and indicate net nitrogen fixation.

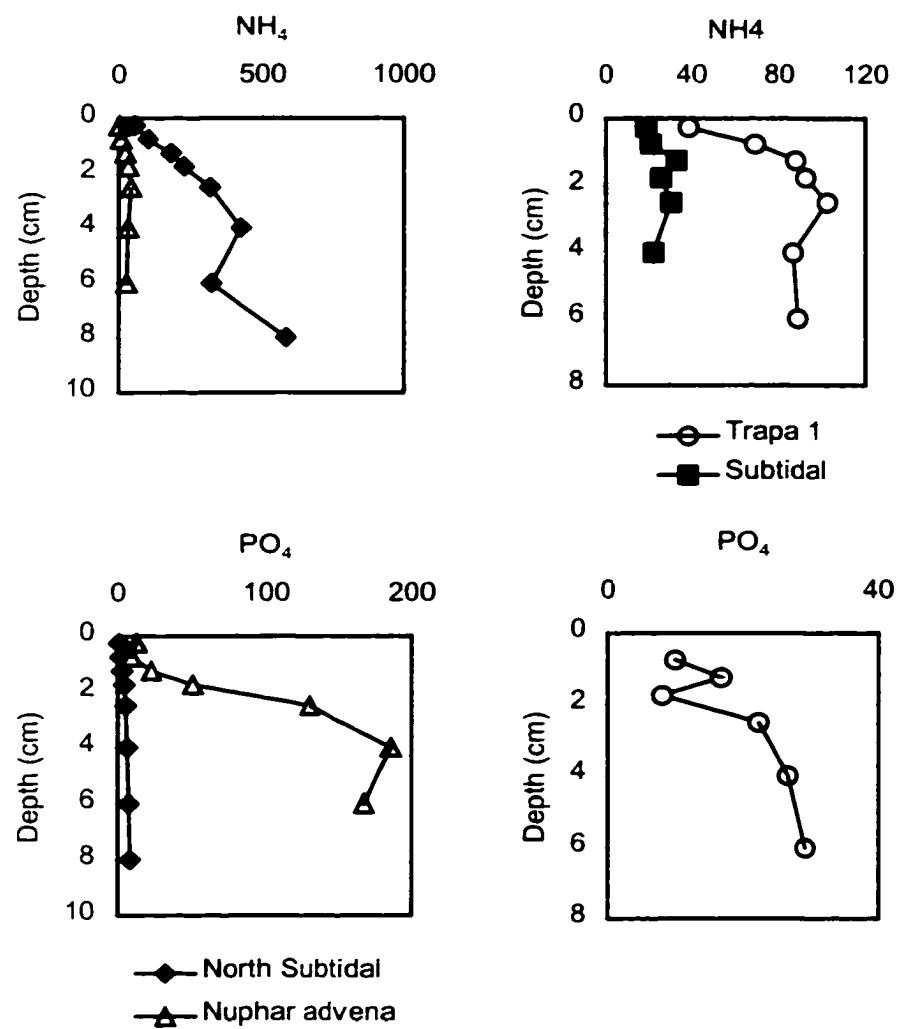


Figure 4-10. Ammonium and phosphate porewater profiles from the spring of 1997. All concentrations are in  $\mu\text{mol L}^{-1}$  and single cores are shown.

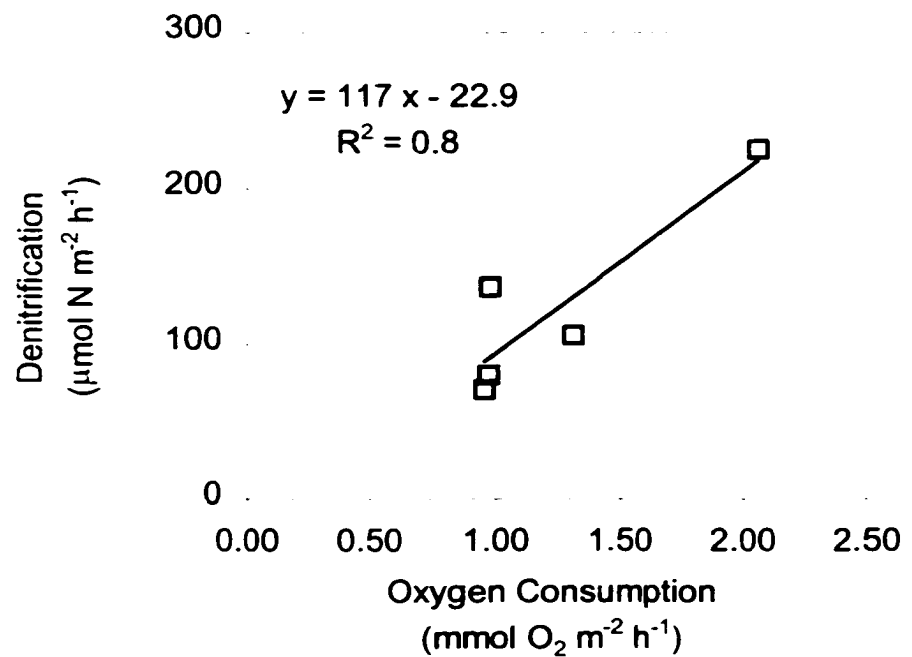


Figure 4-11. Spring denitrification and sediment oxygen consumption in Tivoli Bays. Denitrification was determined using membrane inlet mass spectrometry.

# **CHAPTER 5: PRELIMINARY DEVELOPMENT AND CALIBRATION OF A SIMULATION MODEL OF NITROGEN CYCLING AND MACROPHYTE GROWTH IN A COASTAL MARSH**

## **INTRODUCTION**

Computer simulation modeling has been used to extrapolate experimental results to complex natural ecosystems (Morris and Bowden 1986, Howarth et al. 1991, Mitsch and Reeder 1991, Marchetti and Verna 1992, Costanza et al. 1993, Blackburn et al. 1994). While such models are often used to predict system response to perturbations, they may be most useful in elucidating complex interactions between various processes and components of a system.

Use of spatially and temporally dynamic, mechanistic models of systems such as tidal freshwater marshes requires the use of detailed computer

simulation models. Critical factors which can influence nitrogen cycling in the sediment, such as nitrate concentration, sediment oxygen demand and temperature, often change rapidly over a tidal cycle. Sediment temperature can fluctuate significantly over the course of a tidal cycle, heating to 35°C during low tides in the summer as the sun heats the marsh surface (personal observation). Effects of groundwater on marsh nitrogen processing are especially difficult to measure, and use of a computer model may assist in understanding the dynamic interactions of varying groundwater nitrate concentrations and flows throughout the course of a year. Simulation modeling is a viable method for predicting the effect of environmental conditions on biogeochemical processes in the marsh.

Data from measurements of the Patuxent River and Hudson River was used to develop a computer simulation model of a tidal freshwater marsh. The goal of the modeling exercise was to determine the effect of variable environmental conditions on denitrification rates in marsh sediments.

## Model Description

The time unit for the model is one day, and the model runs using a dt of 0.25 day. A sub-daily time step allows tidal variations to influence the rate of flow of groundwater through the system. Simulations are run for one and several years.

## Forcing Functions

Temperature, sunlight, tidal cycle, groundwater nitrate supply, atmospheric nitrogen deposition and primary production by macrophytes were included to develop a prediction of annual denitrification (Table 5-1).

## State Variables

The model simulates vegetation and inorganic nitrogen in a square meter of marsh within the low, *Nuphar*-dominated marsh of Jug Bay on the Patuxent River. Porewater dissolved inorganic nitrogen was modeled as ammonium and nitrate. Concentrations were converted to mass per square meter using a depth of 5 cm in the sediment. Mass of each nitrogen variable were corrected for the quantity of sediment particles in the unit using a constant for porosity. When possible, data from empirical measurements was used for model development. Due to a lack of data on freshwater marsh plant processes, data from the salt marsh plant, *Spartina alterniflora*, was used in the model.

## Model Structure

The model simulates carbon and nitrogen dynamics for two state variables of interest: a marsh macrophyte, *S. alterniflora* and dissolved

inorganic sediment nitrogen. Total biomass is represented as two state variables: aboveground photosynthetic, or shoot, biomass and belowground, or root, biomass. Both stocks are represented as grams carbon per square meter of marsh. Each of the state variables maintains an outflow to a "litter" state variable. Shoot and root litter state variables receive carbon according to a mortality flow from live biomass. Litter state variables provide a mechanism for nitrogen release during decomposition.

Sediment nitrogen is tracked as two forms: nitrate and ammonium (Figure 5-2). Both are modeled as grams nitrogen per square meter of marsh. A constant porosity of 0.72 (Liebert 1996) was used in the calculation of sediment pools to ensure concentrations reflect only the pore spaces between sediment particles. The estimate of porosity was taken from data gathered on a sediment similar to that found at the low marsh, Jug Bay site. Nitrogen release as a result of macrophyte decomposition is converted from carbon units to nitrogen units as it flowed into, or out of, the nitrogen sector using a constant molar C:N ratio for *S. alterniflora* (White and Howes 1994).

## Macrophyte Sector

### Aboveground Biomass

Macrophyte biomass has an initial standing stock of  $33 \text{ g C m}^{-2}$  corresponding to published data for January biomass is similar wetlands

(Houghton 1985). Shoot material is produced through two mechanisms: net photosynthesis and seasonal translocation of carbon from roots (Table 5-2). Net production is calculated by applying a series of potentially limiting factors to an estimate of the maximum theoretical rate of potential production (Wiegert and Wetzel 1979). Possible limitations are nitrogen, light availability and temperature (Table 5-3). A density limit is included to reflect spatial constraints on production, such as self-shading. The density limit of  $220 \text{ g C m}^{-2}$  served to prevent production from exceeding observed field conditions. All potentially growth limiting variables were compared, and the most limiting is used to reduce maximum potential primary production to calculate net primary productivity.

Partitioning macrophyte material into above and belowground biomass requires the translocation of fixed carbon. Seasonal translocation from roots to shoots allows plants to initiate growth in the spring when no photosynthetic material yet exists. The upward translocation of carbon reserves is seasonal, occurring as a pulse in the spring. Downward translocation, or storage of carbon in the roots is treated as suggested by Wiegert and Wetzel (1979). During July and August, the plants store 75% of gross primary production in the roots. Storage rates are minimal during the remainder of the year.

Fixed carbon within the shoot stock was lost to grazing, mortality and respiration. Estimated losses to grazing were constant, representing 0.01% of the stock. The grazing rate was treated as density-dependent, feeding on shoots in relation to availability. Carbon is lost from the shoots following a

seasonal pattern to reflect an increase in damage and senescence beginning in July and peaking at 0.4% in September and October as reported by Houghton (1985). Mortality of shoots is the only input to the stock of shoot litter. The shoot litter pool was oxidized according to a temperature-dependent rate resulting in mineralization and ammonium release from dead plant material.

Respiration was represented as a loss of fixed carbon from the shoot stock. Respiration was derived from data reported by Mitsch and Gosselink (1993) and Blum et al. (1978). While variable, approximately 40% of photosynthesis was lost to respiration through a temperature-dependent relation.

#### Belowground Biomass

The non-photosynthetic root stock depends upon fixation of carbon and subsequent downward translocation (Table 5-4). The model begins with 250 g C m<sup>-2</sup> in the stock (Blum 1993). Assuming a 40% carbon to dry weight ratio and a four-fold difference between peak and minimum biomass, January values are assumed to be close to 250 g C m<sup>-2</sup>. Losses of carbon from the roots is similar to that in the shoots, including grazing, mortality and respiration. Upward translocation of carbon to the shoots in the spring represents an additional seasonal loss. Grazing pressure is estimated at ten times the rate of shoot grazing, supported by burrowing fauna. As in the shoot stock, grazers are opportunistic, selecting other food items as the stock was reduced. Root mortality is 25% of that used in the calculation of shoot mortality. Respiration is

temperature-dependent and results in the loss of fixed carbon from the roots and stored carbon as suggested by Blum et al. (1978).

## Dissolved Inorganic Nitrogen Sector

### Ammonium

Ammonium in the surface porewater is initialized at 250  $\mu\text{M}$   $\text{NH}_4$ , as observed in the low marsh of Jug Bay in the spring of 1997 (Chapter 3). Following unit conversion, integration to 5 cm and accounting for sediment within the spatial unit, 250  $\mu\text{M}$   $\text{NH}_4$  is equivalent to 0.13 g  $\text{NH}_4\text{-N m}^{-2}$ . Three flows into the ammonium pool are included:  $\text{NH}_4$  regenerated from litter decomposition, the reduction of nitrate, and atmospheric  $\text{NH}_4$  deposition (Table 5-5). Ammonium released by plant decomposition includes aerobic decomposition of shoots, anaerobic decomposition of root material and mineralization of organic material within the sediment that is not macrophyte material. All three processes are temperature-dependent. Plant decomposition on the sediment surface (aerobic shoot decomposition) contributes 30% of the  $\text{NH}_4$  directly released to the porewater pool. The balance is lost to overlying water and is lost from the system.

Dissimilatory nitrate reduction is a poorly-characterized rate process in the sediment nitrogen cycle. The transformation in the model, from  $\text{NO}_3$  to  $\text{NH}_4$ , approximates a Michaelis-Menten reaction, using a maximum rate of 2.0 g N

$\text{m}^{-2} \text{ d}^{-1}$ . The estimate reflects a measurement from surface sediment from a coastal marine environment reported by Sorensen (1978). The half-saturation coefficient is assumed to be similar to that of nitrification at  $0.10 \text{ g N m}^{-2}$ .

Atmospheric deposition is a significant source of ammonium as high rates of deposition are common in the region (Boynton et al. 1995), and were adapted from Correll and Ford (1982). Four measurements from a regional study (Correll and Ford 1982) were extrapolated to an annual cycle to provide seasonal estimates throughout the year.

Ammonium is lost from the sediment pool to macrophyte uptake, hydrologic loss by advection and by conversion to nitrate (nitrification). Plant uptake of ammonium is calculated based on stoichiometric requirements in support of predicted primary production (White and Howes 1994). A  $\text{NO}_3\text{-NH}_4$  preference function allows plants to draw from both inorganic nitrogen pools. Ammonium is lost to surface waters as a result of hydrologic forcing.

Ammonium-nitrogen flows to the nitrate stock via nitrification, a microbially-mediated conversion of  $\text{NH}_4$  to  $\text{NO}_3$ . Nitrification uses the maximum rate of  $4.6 \times 10^{-3} \text{ g N m}^{-2} \text{ d}^{-1}$  and half-saturation coefficient of  $0.105 \text{ g N m}^{-2}$  as presented by Kemp et al. (1990) and Jenkins and Kemp (1984), respectively. Thompson et al. (1995) found that temperature affects nitrification. A coefficient reflecting the oxygen-status of the sediment is included to allow nitrification only in the presence of sufficient oxygen.

## Nitrate

Nitrate in sediment porewater is initialized at 40  $\mu\text{M}$  as observed in the spring at Tivoli Bays tidal freshwater marsh. Three inflows and four outflows are modeled, including oxidative and reductive exchanges with the porewater ammonium stock (Table 5-6). Contributions to the nitrate pool originated from the atmosphere, groundwater and from nitrification of  $\text{NH}_4$ . Atmospheric deposition of nitrate was based on Correll and Ford (1982), a Chesapeake Bay region atmospheric deposition study.

Staver and Brinsfield (1996) clearly showed the large contributions of groundwater from agricultural systems on the Chesapeake Bay's eastern shore to coastal waters. Consequences of discharge of this large amount of nitrate through a fringing marsh system are unknown. Groundwater nitrate is included in the model to examine the possible relationships between denitrification and high nitrate loading from groundwater. Groundwater flow and nitrate concentration are from Staver and Brinsfield (1996), and modified using a tidal simulation coefficient (Table 5-7). Simulated tides allow groundwater flow to be slowed due to a shifting hydraulic head over the course of a tidal cycle. As the tide rises, groundwater flow slows, decreasing to minimum discharge rates at high tide.

Nitrate is supplied by nitrification, drawing from the  $\text{NH}_4$  stock following a relation based on Kemp et al. (1990), Jenkins and Kemp (1984) and Thompson et al. (1995). Details are included in the ammonium stock description.

Nitrate outflow from sediments occurs via  $\text{NO}_3$  reduction, macrophyte uptake, and denitrification. Nitrate is lost by hydrologic flushing which was consistent with that for ammonium described above. As with  $\text{NH}_4$ , macrophyte uptake of  $\text{NO}_3$  is based on net primary production and a  $\text{NO}_3$ -  $\text{NH}_4$  preference function.

Denitrification is modeled incorporating data from this dissertation (Chapters 3 and 4). The exchange of  $\text{N}_2$  gas is modeled as a reversible process and allows for nitrogen fixation. Denitrification rates are dependent upon nitrate concentration (Kana et al. 1998), temperature, oxygen concentration (Rysgaard et al. 1994) and organic material (Caffrey et al. 1993). Using experimental results from this dissertation,  $\text{N}_{2(\text{g})}$  exchange was modeled as a logarithmic relation to nitrate concentration.

## RESULTS AND CALIBRATION

### Macrophyte Production

Carbon modeling of dynamics of macrophyte standing stock and production are accurate, producing results consistent with several data sets (Figure 5-1). Aboveground biomass peaks in the late summer at  $150 \text{ g C m}^{-2}$ , similar to of by Morris and Haskin (1990) and Stribling (1994) who both report maximums of  $190 \text{ g C m}^{-2}$ . Multiple-year simulations produce an increase in aboveground biomass peak, to  $200 \text{ g C m}^{-2}$ . Although no calibration data is

available for seasonal root biomass, model results are realistic, reflecting a net gain over the course of a year. Beginning at 250 g C m<sup>-2</sup>, in December biomass accumulates to 350 g C m<sup>-2</sup>. Following a spring decline, an autumn increase reflects the storage of carbon for utilization over winter and spring.

Daily net primary production, following losses to respiration, grazing, mortality and translocation, was calculated by the model (Figure 5-2). The seasonal pattern of biomass shows positive net production occurring from mid-February through August. While the seasonality does not follow data presented by Smalley (1958), the model results peaks approximately 60 days later than the data, the magnitude of net primary production in the spring closely matches his data.

## Dissolved Inorganic Nitrogen

Modeling of sediment dissolved inorganic nitrogen pools was not as successful as plant carbon modeling. Much of the difficulty in calibration resulted from the lack of rate-specific data for nitrogen transformations in sediment. Multi-year simulations produced consistent results which suggests the model structure is stable.

Ammonium stocks in sediment porewater rapidly increase during the first days from an initial level of 0.13 g N m<sup>-2</sup> to 8.5 g N m<sup>-2</sup> (Figure 5-3). Nitrate reduction dominates the inflows to the ammonium stock at a steady rate of 2.5

$\text{g N m}^{-2} \text{ d}^{-1}$ . No seasonal variations are observed, due to the excessively high quantity of  $\text{NO}_3$  in the source stock. Ammonium is regenerated by macrophyte decomposition at a rate 1/250 that of the input from nitrate reduction.

Regeneration of  $\text{NH}_4$  slows from high early rates to remain relatively constant throughout the majority of the year at 0.01 to 0.02  $\text{g N m}^{-2} \text{ d}^{-1}$ . Atmospheric deposition is the smallest contributor to the  $\text{NH}_4$  stock, at 1/10 of the magnitude of regenerated  $\text{NH}_4$ . Data from Correll and Ford (1982) indicated a spring peak in  $\text{NH}_4$  deposition, with the lowest deposition rates occurring during the winter months.

Losses of ammonium are dominated by physical flushing of  $\text{NH}_4$  from sediment by the tidally-driven advective component representing groundwater flow (Figure 5-4). Tidal flushing removes  $\text{NH}_4$  according to a cyclical pattern, leading to a difference of as much as 2  $\text{g N m}^{-2}$  over a single tidal event. Maximum flushing rates occurs in the early months of the year, with a maximum rate of 9.0  $\text{g N m}^{-2} \text{ d}^{-1}$ . Losses of  $\text{NH}_4$  to both macrophyte uptake and nitrification are a small fraction of the tidally-driven losses. Ammonium incorporation by plants increases slowly early in the year, followed by a sharp increase in spring and summer, peaking at 0.30  $\text{g N m}^{-2} \text{ d}^{-1}$  in July. A rapid decline in uptake rate follows, ending in December uptake similar to that modeled in January. Nitrification is the smallest of the loss terms from the  $\text{NH}_4$  pool, exhibiting a seasonal pattern peaking in July at 0.004  $\text{g N m}^{-2} \text{ d}^{-1}$ .

Sediment porewater nitrate increases dramatically from 0.13  $\text{g N m}^{-2}$  to 1800  $\text{g N m}^{-2}$  early in the year (Figure 5-5). The stock fluctuates around these

values throughout the year and reaches peak mass during the summer at 2150 g N m<sup>-2</sup>. The quantities of nitrogen predicted by the model are clearly excessive, suggesting inflows and outflows of nitrate are not in proper balance. Groundwater additions reflecting loading from an agricultural system (Staver and Brinsfield 1996) were the largest source of NO<sub>3</sub> to the sediment porewater stock in the model. Low tide peak rates of groundwater nitrate loading were at 9000 g N m<sup>-2</sup> d<sup>-1</sup>. Groundwater supply drops to zero on each high tide due to a lack of hydraulic head between the groundwater source and tidal water. Spring supplies of groundwater nitrate are the largest of the year, while fall supplies are the lowest. The trend is largely the result of seasonal groundwater flow, with greater precipitation in the spring followed by lower precipitation and higher evapotranspiration in the summer. Relative to groundwater NO<sub>3</sub> supplies, inflows from atmospheric deposition and nitrification are insignificant, at maximum rates of 0.02 and 0.004 g N m<sup>-2</sup> d<sup>-1</sup>, respectively.

Nitrate is lost primarily through physical flushing by groundwater flows (Figure 5-6). Effectively much of the enormous groundwater nitrate load is flushed through the marsh sediment system unchanged. Loss rates follow the pattern exhibited by groundwater supply, with a spring peak of 9000 g N m<sup>-2</sup> d<sup>-1</sup>. Nitrate reduction to NH<sub>4</sub> is the second largest loss, at a constant 2.2 g N m<sup>-2</sup> d<sup>-1</sup>. Although this flow is modeled to vary with NO<sub>3</sub> availability, the large stock maintains the loss at its maximum rate throughout the year. Denitrification is of similar magnitude to macrophyte uptake of NO<sub>3</sub>, which peaks in the summer at 0.048 g N m<sup>-2</sup> d<sup>-1</sup>. Loss to denitrification increases with NO<sub>3</sub> stock early in the

year to remain constant at  $0.017 \text{ g N m}^{-2} \text{ d}^{-1}$ . This level was consistent with calibration data (Figure 5-7), and relies on a 10% reduction of the empirical data presented earlier in this dissertation (Chapters 3 and 4). Although nitrogen fixation is possible in the model, nitrate levels never falls below the threshold required to reverse the flow.

## Groundwater Scenarios

In the calibration runs, groundwater nitrate supply was the dominant nutrient flow. To determine how changes in groundwater flow affect marsh nutrient and carbon dynamics, sensitivity analysis was performed by varying groundwater nitrogen loads. When groundwater was removed from the model the resulting decline of the  $\text{NO}_3^-$  stock prevented the model from completing an annual cycle. Groundwater supplies at or above 1% of the data-supported load (Staver and Brinsfield 1996) provided sufficient  $\text{NO}_3^-$  for the model to run for an annual cycle. As  $\text{NO}_3^-$  supplies from groundwater were reduced from 100% of calibration values to 75%, 50% and 10%, maximum sediment porewater  $\text{NO}_3^-$  concentrations declined from  $1000 \text{ mM NO}_3^- \text{ L}^{-1}$ , to 750, 500, and  $120 \text{ mM NO}_3^- \text{ L}^{-1}$ , respectively. Coincident with the drop in  $\text{NO}_3^-$  concentrations, rates of denitrification declined. At 10% of the original groundwater supply rate denitrification occurred at a rate of  $750 \mu\text{M N m}^{-2} \text{ d}^{-1}$  and remained relatively constant throughout the year. As  $\text{NO}_3^-$  stocks increased, due to higher groundwater contributions, removal by denitrification became relatively

inefficient.

Annual denitrification at 100% groundwater supply of  $\text{NO}_3^-$  released 22 g  $\text{N m}^{-2} \text{y}^{-1}$  from the marsh surface to the atmosphere. Total N loss dropped to 18.5 g  $\text{N m}^{-2} \text{y}^{-1}$  when groundwater supplies were at 10% of the original rates. The majority of the  $\text{NO}_3^-$  supply, as much as 700 kg  $\text{N m}^{-2} \text{y}^{-1}$ , provided by the agriculturally-impacted groundwater was released to the estuary. While the marshes were capable of sustaining moderate to high rates of denitrification, supplies of  $\text{NO}_3^-$  are generally too large to be removed from the system.

## DISCUSSION AND SUMMARY

Shifts in organic matter C:N were hypothesized to be the driving force for the seasonal variability observed in Jug Bay experimental cores from the low and high marshes. The model was not sensitive to this shift, due to the large decrease in magnitude of the flow calculation necessary for the model to function. A lack of sensitivity to this variable should be expected until organic matter mineralization can be better estimated with field measurements of seasonal organic matter supply.

Nitrification and denitrification were not directly related during the model simulation. Coupled nitrification-denitrification has been suggested as the dominant pathway for total denitrification in aquatic sediments (Jenkins and Kemp 1984, Reddy et al. 1989, Risgaard-Petersen et al. 1994, Rysgaard et al.

1994). Nitrogen cycling in a tidal marsh is complicated by the shifting redox status of the surface sediment due to tidal flooding. Temporal deviations have not been examined in marsh sediments, and computer simulation models are an excellent approach to develop annual estimates of marsh denitrification in temporally-dynamic environments. The lack of relationship between nitrification and denitrification in the model is the result of the abundance of nitrate which never reaches limiting quantities in the sediment porewater. Additional data are necessary for further model development and calibration. It appears that long term estimates of a nitrogen sink via denitrification should be examined over shorter time intervals.

Table 5-1. Computer simulation model forcing functions. The model is constructed to use daily units and runs on a 0.25 day time step to include tidal dynamics.

Forcing Functions

	Model Abbreviation	Equation	Explanation
	Day	= MOD(time,364)	Daily step for generation of seasonal forcing functions.
Sediment porosity	porosity	= 0.72	Liebert 1996. Porosity of subtidal sediments used for marsh mesocosms at Horn Point Laboratory (HPL).
Photosynthetically Active Radiation	HPEL_PAR	= GRAPH(Day)	Fisher, pers. Comm. Data collected from HPL; E m <sup>-2</sup> d <sup>-1</sup> .
Temperature	Temp	= GRAPH(Day)	Swarth and Peters 1993. Surface temperature of Patuxent River at Jug Bay NERRS, 1991.
Deep Soil Temperature	soil_temp_deep	= GRAPH(Day)	Moderated water temperature.
Optimal Temperature for Decomposition	Decomp_°C_opt	= 15	Hypothesized optimal decomposition temperature for organic material in marsh sediment.
Tide Simulator	tide_simulator	= (SINWAVE (0.5,1.0)) + 0.5	Sine wave function representing tidal cycle.
Shoot N:C ratio	SA_shoot_N:C	= 0.02	White and Howes 1994. Molar N:C ratio for S. alterniflora litter.
River NH <sub>4</sub> Concentration	rvr_NH4	= GRAPH(Day)	Swarth & Peters 1993. High tide Jug Bay NH <sub>4</sub> concentration at south marsh site; μmol N L <sup>-1</sup> .
Atmospheric Deposition - NH <sub>4</sub>	NH4_atm_dep	= GRAPH(Day)	Correll and Ford 1982. Atmospheric NH <sub>4</sub> deposition measured in the Chesapeake Bay region. Data from 1980 for each of four seasons; mg NH <sub>4</sub> -N m <sup>-2</sup> d <sup>-1</sup> .
Atmospheric Deposition - NO <sub>3</sub>	NO3_atm_dep	= GRAPH(Day)	Correll and Ford 1982. Atmospheric NO <sub>3</sub> deposition measured in the Chesapeake Bay region. Data from 1980 for each of four seasons; mg NO <sub>3</sub> -N m <sup>-2</sup> d <sup>-1</sup> .

Table 5-2. (a) Live, aboveground *Spartina alterniflora* biomass stock and flows from the computer simulation model.  
 (b) Shoot litter decomposition variables are listed.

(a) *Spartina alterniflora* shoots (live aboveground biomass), Initial value = 33 g C m<sup>-2</sup>.

$$\text{SA\_SHOOT}(t) = \text{SA\_SHOOT}(t - dt) + (\text{SPART\_SHT\_PRO} + \text{SPART\_UP\_TRAN} - \text{SPART\_SHT\_GRZ} - \text{SPART\_SHOOT\_MRT} - \text{SPART\_SHOOT\_RESP} - \text{SPART\_DWN\_TRAN}) * dt$$

	Model Abbreviation	Equation	Explanation
<b>INFLOWS</b>			
Net Primary Production	SPART_SHT_PRO	= SA_productivity * SA_SHOOT * Density_lim * prod_mult	Net carbon fixed by <i>S. alterniflora</i> ; g C m <sup>-2</sup> d <sup>-1</sup> .
Carbon Translocation to Shoots	SPART_UP_TRAN	= if (day >90) then (if day <110 then SA_ROOT* 0.002 else 0) else 0	Release of carbon stored in roots to shoots to support spring growth; g C m <sup>-2</sup> d <sup>-1</sup> .
<b>OUTFLOWS</b>			
Shoot Grazing	SPART_SHT_GRZ	= SA_SHOOT * 0.0001	Mass of photosynthetic biomass consumed. Grazer is opportunistic, including relative abundance in feeding strategy; g C m <sup>-2</sup> d <sup>-1</sup> .
Shoot Mortality	SPART_SHOOT_MRT	= (SA_SHOOT * litter_season * Spart_mort_x )	Mortality of photosynthetic biomass as influenced by seasonal cues and mortality due to current (not historical) stress; g C m <sup>-2</sup> d <sup>-1</sup> .
Shoot Respiration	SPART_SHOOT_RESP	= (SA_SHOOT * 0.40) * 0.02 * EXP(Temp * 0.01)	Derived from Mitsch & Gosselink 1993 (p. 139) and Blum et al. 1978. 40% of photosynthesis lost in plant respiration, varies with temperature by Arrhenius equation; g C m <sup>-2</sup> d <sup>-1</sup> .
Belowground Carbon Storage	SPART_DWN_TRAN	= SA_seas_dwntrans * SPART_SHT_PRO * 0.75	Assumes 75% of gross primary production can be stored in roots following a seasonal cycle; g C m <sup>-2</sup> d <sup>-1</sup> .
<b>VARIABLES</b>			
Net Primary Production	SA_productivity	= SA_max_Prod_rate * SA_prod_limit	Net carbon fixed by <i>S. alterniflora</i> ; g C m <sup>-2</sup> d <sup>-1</sup> .
Maximum Productivity Rate	SA_max_Prod_rate	= 0.115	Wiegert & Wetzel 1979, Model version 3. <i>S. alterniflora</i> spring maximum gross primary production rate; d <sup>-1</sup> .

Productivity Limit	SA_prod_limit	= (SA_light_limit * N_limit) * SA_prod_temp_func	Primary feedback mechanism on <i>S. alterniflora</i> productivity -including limits from light, nitrogen and temperature; 0-1.
Density Limit	Density_lim	= 1 - (SA_SHOOT / (SA_SHOOT + 220) )	Dimensionless coefficient to limit production due to density constraints.
Productivity Coefficient	prod_mult	= 0.90	Dimensionless coefficient for application of sensitivity analysis.
Seasonal Senescence	litter_season	= GRAPH(Day)	Derived from Houghton 1985. Seasonal determination of peak senescence of leaves and mortality of photosynthetic biomass as litterfall. Reports 38% of damage/senescence in July and 62% in August for <i>S. alterniflora</i> . Dimensionless proportion multiplied by maximum specific rate of mortality.
Shoot Mortality Coefficient	Spart_mort_x	= 0.00415	Dimensionless coefficient for mortality of <i>S. alterniflora</i> shoots.

Table 5-2b. *S. alterniflora* shoot litter, Initial value = 8.0 g C m<sup>-2</sup>.

$$\text{SPART\_SHT\_LTR}(t) = \text{SPART\_SHT\_LTR}(t - dt) + (\text{SPART\_SHOOT\_MRT} - \text{Spart\_shoot\_aero}) * dt$$

	Model Abbreviation	Equation	Explanation
<b>INFLOW</b>			
Shoot Mortality	SPART_SHOOT_MRT	= (SA_SHOOT * litter_season * Spart_mort_x )	Mortality of photosynthetic biomass as influenced by seasonal cues and mortality due to current (not historical) stress; g C m <sup>-2</sup> d <sup>-1</sup> .
<b>OUTFLOW</b>			
Aerobic decomposition of shoots	Spart_shoot_aero	= SPART_SHT_LTR * SA_rc_aerob * SA_aerob_MM	Aerobic decomposition of <i>S. alterniflora</i> shoots; g C m <sup>-2</sup> d <sup>-1</sup> .
<b>VARIABLES</b>			
Shoot Decay Rate Constant	SA_rc_aerob	= 0.0036	Blum 1993. Decay rate measured in surface litterbag study at an interior marsh site; d <sup>-1</sup> .
Temperature-dependent Shoot Decomposition	SA_aerob_MM	= EXP (0.06 * (soil_temp_surf / soil_temp_surf + aerob_decomp_T))	Dimensionless Michaelis-Menten reaction of temperature dependent decay rates of shoot material.
Optimal Aerobic Decomposition Temperature	aerob_decomp_T	= 15	Optimal temperature for aerobic decomposition of <i>S. alterniflora</i> shoots; °C.

Table 5-3. *Spartina alterniflora* growth, determined by least limiting factor, nitrogen, light or temperature.

	Model Abbreviation	Equation	Explanation
Half-saturation Coefficient - NH <sub>4</sub>	SA_NH4_Ks	= 0.00855	Morris 1980; similar Bradley & Morris 1990. Results from N uptake culture experiments using <i>S. alterniflora</i> ; g NH <sub>4</sub> -N m <sup>-2</sup> .
NH <sub>4</sub> Limit to Growth	SA_NH4_limit	= (NH4 / (NH4 + SA_NH4_Ks))	Factor to reflect Michaelis-Menten relation of half-saturation coefficient and ambient concentration; 0-1.
Half-saturation Coefficient - NO <sub>3</sub>	SA_NO3_Ks	= 0.0171 * 0.005	Morris 1980. Results from N uptake culture experiments using <i>S. alterniflora</i> ; g NO <sub>3</sub> -N m <sup>-2</sup> .
NO <sub>3</sub> Limit to Growth	SA_NO3_limit	= NO3 / (SA_NO3_Ks + NO3)	Factor to reflect Michaelis-Menten relation of half-saturation coefficient and ambient concentration; 0-1.
Nitrogen Limit to Growth	N_limit	= MIN (SA_NH4_limit, SA_NO3_limit)	Dimensionless coefficient selects either NH <sub>4</sub> or NO <sub>3</sub> concentration as most N-limiting based on availability relative to need.
Light Limit to Growth	SA_light_limit	= HPL_PAR / SA_light_sat * exp(1- HPL_PAR / SA_light_sat)	Factor for light intensity feedback for photosynthesis of <i>S. alterniflora</i> . Inhibition occurs when light is above saturation; 0-1.
Light Saturation	SA_light_sat	= 120	Mitsch & Gosselink 1993. Light saturation intensity, based largely on work of Giurgevich & Dunn 1978, 1979; E m <sup>-2</sup> min <sup>-1</sup> .
Optimum Production Temperature	SA_opt_temp	= 25	Day et al. 1989 (page 216). Optimal temperature for maximum primary production, <i>S. alterniflora</i> 30-35°C; value adjusted following sensitivity analysis; °C.

Temperature Production Limit	SA_prod_temp_func	$= \exp(0.20 * (\text{Temp} - \text{SA\_opt\_temp})) * ((40 - \text{Temp}) / (40 - \text{SA\_opt\_temp}))^{0.20 * (40 - \text{SA\_opt\_temp})}$	Lassiter 1975- General Ecosystem Model. Temperature feedback mechanism including curvature parameter and maximum temperature for productivity; 0-1.
Productivity Limit	SA_prod_limit	$= (\text{SA\_light\_limit} * \text{N\_limit}) * \text{SA\_prod\_temp\_func}$	Primary feedback mechanism on <i>S. alterniflora</i> productivity -including limits from light, nitrogen and temperature; 0-1.

Table 5-4. (a) Belowground biomass state variable representing *Spartina alterniflora*. All inflows and outflows are listed. (b) Root litter and decomposition variables are listed.

(a) *Spartina alterniflora*, live belowground biomass, Initial value = 250 g C m<sup>-2</sup> (Houghton 1985)

$$\text{SA\_ROOT}(t) = \text{SA\_ROOT}(t - dt) + (\text{SPART\_DWN\_TRAN} - \text{SPART\_RT\_MRT} - \text{SPART\_RT\_GRZ} - \text{SPART\_RT\_RESP} - \text{SPART\_UP\_TRAN}) * dt$$

	Model Abbreviation	Equation	Explanation
<b>INFLOWS</b>			
Belowground Carbon Storage	SPART_DWN_TRAN	= SA_seas_dwntrans * SPART_SHT_PRO * 0.75	Assumes 75% of gross primary production can be stored in roots following a seasonal cycle; g C m <sup>-2</sup> d <sup>-1</sup> .
<b>OUTFLOWS</b>			
Root Mortality	SPART_RT_MRT	= SA_ROOT * spar_rt_mrt_x	Mortality of belowground biomass as a constant percentage of state variable; g C m <sup>-2</sup> d <sup>-1</sup> .
Root Grazing	SPART_RT_GRZ	= SA_root_graz_press * SA_ROOT	Mass of nonphotosynthetic biomass consumed. Grazer is opportunistic, including relative abundance in feeding strategy; g C m <sup>-2</sup> d <sup>-1</sup> .
Root Respiration	SPART_RT_RESP	= (SA_ROOT * 0.00015) + (0.07 * SPART_DWN_TRAN * EXP(Temp * 0.058))	Blum et al. 1978. Temperature limits growth by controlling efficiency, or losses to respiration, according to Arrhenius equation; g C m <sup>-2</sup> d <sup>-1</sup> .
Carbon Translocation to Shoots	SPART_UP_TRAN	= if (day > 90) then (if day < 110 then SA_ROOT * 0.002 else 0) else 0	Release of carbon stored in roots to shoots to support spring growth; g C m <sup>-2</sup> d <sup>-1</sup> .
<b>VARIABLES</b>			
Seasonal Carbon Translocation	SA_seas_dwntrans	= GRAPH(Day)	Wiegert & Wetzel 1979. Model #3 output for annual carbon translocation; dimensionless.
Net Primary Production	SPART_SHT_PRO	= SA_productivity * SA_SHOOT * Density_lim * prod_mult	Net carbon fixed by <i>S. alterniflora</i> ; g C m <sup>-2</sup> d <sup>-1</sup> .
Root Mortality Coefficient	spar_rt_mrt_x	= 0.0011	Dimensionless rate based on marsh plant mortality.
Root Grazing Coefficient	SA_root_graz_press	= 0.001	Constant grazing pressure; d <sup>-1</sup> .

Table 5-4b. *S. alterniflora* root litter, Initial value = 8.0 g C m<sup>-2</sup>

$$\text{SA\_ROOT\_LTR}(t) = \text{SA\_ROOT\_LTR}(t - dt) + (\text{SPART\_RT\_MRT} - \text{SA\_root\_anaerob}) * dt$$

	Model Abbreviation	Equation	Explanation
<b>INFLOWS</b>			
Root Mortality	SPART_RT_MRT	= SA_ROOT * spar_rt_mrt_x	Mortality of belowground biomass as a constant percentage of state variable; g C m <sup>-2</sup> d <sup>-1</sup> .
<b>OUTFLOWS</b>			
Anaerobic Root Decomposition	SA_root_anaerob	= SA_ROOT_LTR * EXP (soil_temp_deep / (Decomp_°C_opt + soil_temp_deep) * 0.069)	White & Howes 1994. Assumes 1 year turnover, max remineralization rate of 1 g C m <sup>-2</sup> d <sup>-1</sup> and 1 kg C m <sup>-2</sup> standing stock; g C m <sup>-2</sup> d <sup>-1</sup> .

Table 5-5. Ammonium flows and factors in the nitrogen sector of the marsh simulation model. Tables are presented by state variable, with all inflows and outflows listed for each. Flows between state variables are included in both source and destination tables. All flows between *Spartina alterniflora* state variables and nitrogen state variables undergo unit conversion from  $\text{g C m}^{-2} \text{ d}^{-1}$  to  $\text{g N m}^{-2} \text{ d}^{-1}$  as they enter or leave the nitrogen sector of the model.

$\text{NH}_4$  State Variable, Initial Value = 0.605 (Stribling 1994)

$$\text{NH4}(t) = \text{NH4}(t - dt) + (\text{SPART_REGEN_NH4} + \text{NO3_REDZN} + \text{ATM_DEP_NH4} - \text{SPART_NH4} - \text{NH4_FLUSH} - \text{NITRIFICATION}) * dt$$

	Model Abbreviation	Equation	Explanation
<b>INFLOWS</b>			
Regenerated $\text{NH}_4$ from <i>S. alterniflora</i> decomposition	SPART_REGEN_NH4	= (SA_shoot_aer_pw * SA_shoot_N:C) + ((SA_root_anaerob + Sed_OM_brkdn) * SA_shoot_N:C)	Regenerated N from decomposition of <i>S. alterniflora</i> leaves and roots; uses same N:C for shoots and roots; $\text{g N m}^{-2} \text{ d}^{-1}$ .
Nitrate Reduction	NO3_REDZN	= NO3_red_Vmax * (NO3 / NO3 + NO3_red_Km)	Guidance from Sorensen 1978, Dorge 1994. Units: $\text{g N m}^{-2} \text{ d}^{-1}$ .
Atmospheric Deposition	ATM_DEP_NH4	= NH4_atm_dep / 1000	Unit conversion from Correll and Ford 1982; $\text{g N m}^{-2} \text{ d}^{-1}$ .
<b>OUTFLOWS</b>			
<i>S. alterniflora</i> $\text{NH}_4$ uptake	SPART_NH4	= SPART_SHT_PRO * SA_shoot_N:C * (1 - SA_NO3:NH4_pref) * 4.0	$\text{NH}_4$ uptake by <i>S. alterniflora</i> as determined by productivity and relative preference of $\text{NH}_4$ relative to $\text{NO}_3$ ; $\text{g N m}^{-2} \text{ d}^{-1}$ .
$\text{NH}_4$ Flushed by Groundwater	NH4_FLUSH	= NH4 - (rvr_NH4 * 150 * 0.000014) * 24 * effective_hydraulic_head	$\text{NH}_4$ lost through groundwater flushing, relies on concentration gradient with ambient river water; $\text{g N m}^{-2} \text{ d}^{-1}$ .
Nitrification	NITRIFICATION	= Anox_effect * (Nitrif_Vmax * (NH4 / NH4 + Nitrif_Km)) * 0.15 * EXP(soil_temp_surf * 0.06)	Thompson et al. 1995. Average nitrification rate for natural marsh using modified acetylene block techniques; $\text{g N m}^{-2} \text{ d}^{-1}$ .
<b>VARIABLES</b>			
Mineralized N to porewater	SA_shoot_aer_pw	= Spart_shoot_aero * pw:sw_release	Dimensionless coefficient to retain a portion of N from shoot decomposition within porewater.
Aerobic decomposition of shoots	Spart_shoot_aero	= SPART_SHT_LTR * SA_rc_aerob * SA_aerob_MM	Aerobic decomposition of <i>S. alterniflora</i> shoots; $\text{g C m}^{-2} \text{ d}^{-1}$ .

Porewater : Surface water factor	pw:sw_release	= 0.30	Dimensionless relation to apportion mineralized N between surface water and sediment porewater.
Anaerobic Root Decomposition	SA_root_anaerob	= SA_ROOT_LTR * SO4_k * EXP (soil_temp_deep / (Decomp_°C_opt + soil_temp_deep) * 0.069)	White & Howes 1994. Assumes 1 year turnover, max remineralization rate of 1 g C m <sup>-2</sup> d <sup>-1</sup> and 1 kg C m <sup>-2</sup> standing stock; g C m <sup>-2</sup> d <sup>-1</sup> .
Decomposition of marsh organic matter	Sed_OM_brkdn	= 300 * 0.03 * 0.0027 * exp (0.069 * soil_temp_surf)	Belowground decay of organic matter not derived from <i>S. alterniflora</i> , includes benthic algae; g C m <sup>-2</sup> d <sup>-1</sup> .

Figure 5-6. Nitrate stock, flows and variables included in the marsh simulation model.

$\text{NO}_3$  State Variable, Initial Value =  $0.0007 \cdot \text{Porosity}$ ; units: g  $\text{NO}_3\text{-N m}^{-2}$  (Valiela et al. 1982).

$$\text{NO}_3(t) = \text{NO}_3(t - dt) + (\text{NO}_3_{\text{GRNDWTR}} + \text{ATM\_DEP\_NO}_3 + \text{NITRIFICATION} - \text{NO}_3_{\text{REDXN}} - \text{NO}_3_{\text{FLUSH}} - \text{SPART\_NO}_3 - \text{N}_2_{\text{EXCHG}}) \cdot dt$$

	Model Abbreviation	Equation	Explanation
<b>INFLOWS</b>			
Groundwater $\text{NO}_3$ supply	NO3_GRNDWTR	= gwtr_factor	Staver & Brinsfield 1996. Converted to g $\text{NO}_3\text{-N m}^{-2} \text{d}^{-1}$ .
Atmospheric Deposition	ATM_DEP_NO3	= NO3_atm_dep / 1000	Unit conversion from Correll and Ford 1982; g $\text{N m}^{-2} \text{d}^{-1}$ .
Nitrification	NITRIFICATION	= Anox_effect * (Nitrif_Vmax * (NH4 / NH4 + Nitrif_Km)) * 0.15 * EXP(soil_temp_surf * 0.06)	Thompson et al. 1995. Average nitrification rate for natural marsh using modified acetylene block techniques; g $\text{NO}_3\text{-N m}^{-2} \text{d}^{-1}$ .
<b>OUTFLOWS</b>			
Nitrate Reduction	NO3_REDZN	= NO3_red_Vmax * (NO3 / NO3 + NO3_red_Km)	Guidance from Sorensen 1978, Dorge 1994. Units: g $\text{NO}_3\text{-N m}^{-2} \text{d}^{-1}$ .
$\text{NO}_3$ Flushed by Groundwater	NO3_FLUSH	= NO3 * effective_hydraulic_head * 0.010	$\text{NO}_3$ lost through groundwater flushing; g $\text{NO}_3\text{-N m}^{-2} \text{d}^{-1}$ .
S. alterniflora $\text{NO}_3$ uptake	SPART_NO3	= SA_shoot_N:C * SPART_SHT_PRO * SA_NO3:NH4_pref	$\text{NO}_3$ uptake by S. alterniflora as determined by productivity and relative preference of $\text{NO}_3$ relative to $\text{NH}_4$ ; g $\text{NO}_3\text{-N m}^{-2} \text{d}^{-1}$ .
Denitrification / Nitrogen Fixation	N2_EXCHG	= (77 * LOGN(NO3 * (50 / 14)) - 193) * 24 * (14 / 1000000) * 0.10	Merrill 1999. Relation of denitrification and nitrogen fixation to nitrate concentration as determined by a series of $\text{N}_{2(g)}$ exchange experiments in two tidal freshwater marshes; g $\text{NO}_3\text{-N m}^{-2} \text{d}^{-1}$ .
<b>VARIABLES</b>			
Low Oxygen Factor	Anox_effect	= 1 - Anox_index	Dimensionless coefficient.
Low Oxygen Index	Anox_index	= SA_ROOT_LTR / 50	Constant relation to changing root litter state variable to allow for low oxygen concentrations resulting from decomposition; dimensionless.

Nitrification Maximum Rate	Nitrif_Vmax	= 0.0046	Kemp et al. 1990 (Table 3). Subtidal Chesapeake Bay sediments, maximum rate in November; g NO <sub>3</sub> -N m <sup>-2</sup> d <sup>-1</sup> .
Nitrification Half-saturation Coefficient	Nitrif_Km	= 0.105	Based on Jenkins & Kemp 1984. Converted to g N m <sup>-2</sup> .
NO <sub>3</sub> Reduction Maximum Rate	NO3_red_Vmax	= 2.0	Estimate based on Sorensen 1978. Data from top 3 cm of coastal marine sediment; g NO <sub>3</sub> -N m <sup>-2</sup> d <sup>-1</sup> .
NO <sub>3</sub> Reduction Half-saturation Coefficient	NO3_red_Km	= 0.10	Assumes similar relation to nitrification; g NO <sub>3</sub> -N m <sup>-2</sup> .
S. alterniflora NO <sub>3</sub> :NH <sub>4</sub> preference	SA_NO3:NH4_pref	= 0.40	Percent of S. alterniflora N uptake as NO <sub>3</sub> .

Table 5-7. Groundwater nitrate supplies included in the marsh nitrogen computer simulation model. Data from Staver and Brinsfield (1996) provided seasonal flows and nitrate concentrations from an agriculturally-dominated watershed on Maryland's eastern shore. Groundwater flows were modified by tidal forcing in the model. As tidal height increased groundwater was slowed, resuming to the measured flow as the tide ebbed.

#### Groundwater Nitrate

	Model Abbreviation	Equation	Explanation
Effective Hydraulic Head	effective液压_head	= gwtr_flow * (1-tide_simulator)	Groundwater flow hampered by flooding tide.
Groundwater Factor	gwtr_factor	= effective液压_head * gwtr_gN_m3	Groundwater NO <sub>3</sub> delivery; g N m <sup>-1</sup> streambank.
Unit-converted NO <sub>3</sub> Concentration	gwtr_gN_m3	= gwtr_conc * (14000/1000000)	Unit conversion for groundwater NO <sub>3</sub> delivery.
Seasonal Groundwater Flow	gwtr_flow	= GRAPH(Day)	Staver & Brinsfield 1996. Groundwater flows measured under a Chesapeake Bay agro-ecosystem using an array of piezometers.
Groundwater NO <sub>3</sub> Concentration	gwtr_conc	= GRAPH(Day)	Staver & Brinsfield 1996. Groundwater nitrate concentrations measured under a Chesapeake Bay agro-ecosystem. Data from piezometer rs-0-130; μmol N L <sup>-1</sup> .

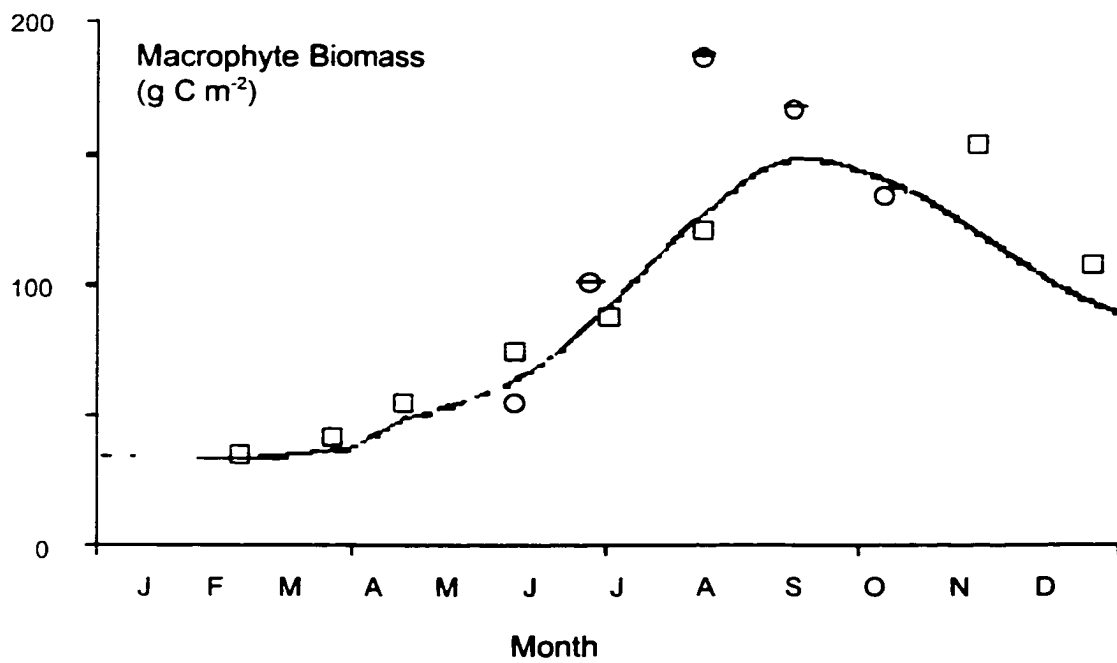


Figure 5-1. Macrophyte aboveground biomass presented with calibration data from Morris and Haskin □ (1990) and Stribling ○ (1994) for *Spartina alterniflora*.

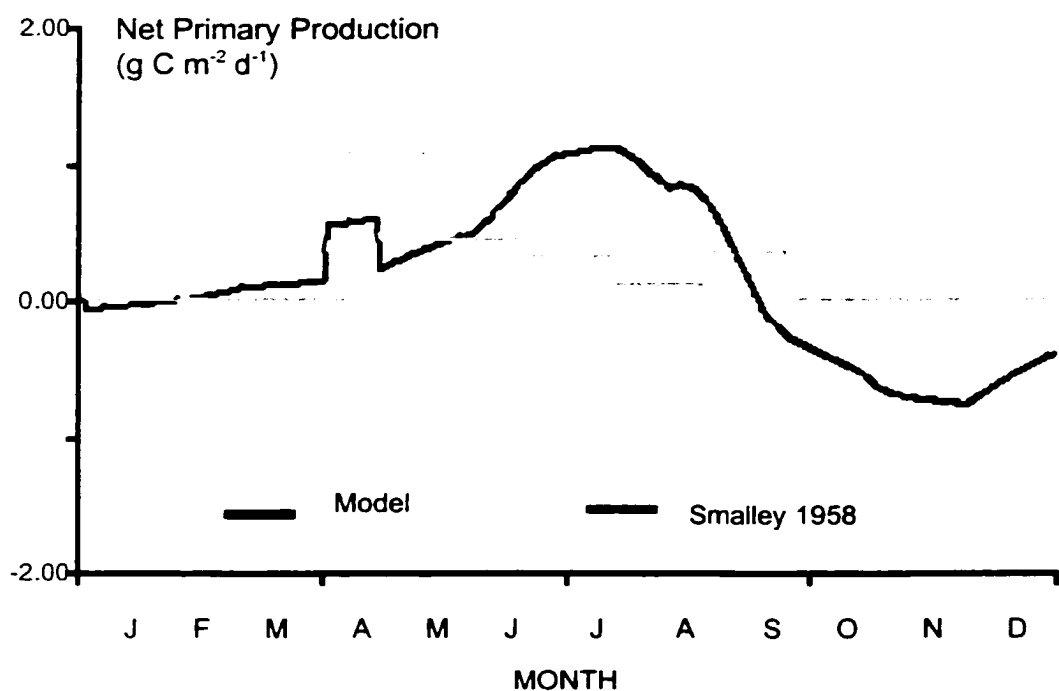
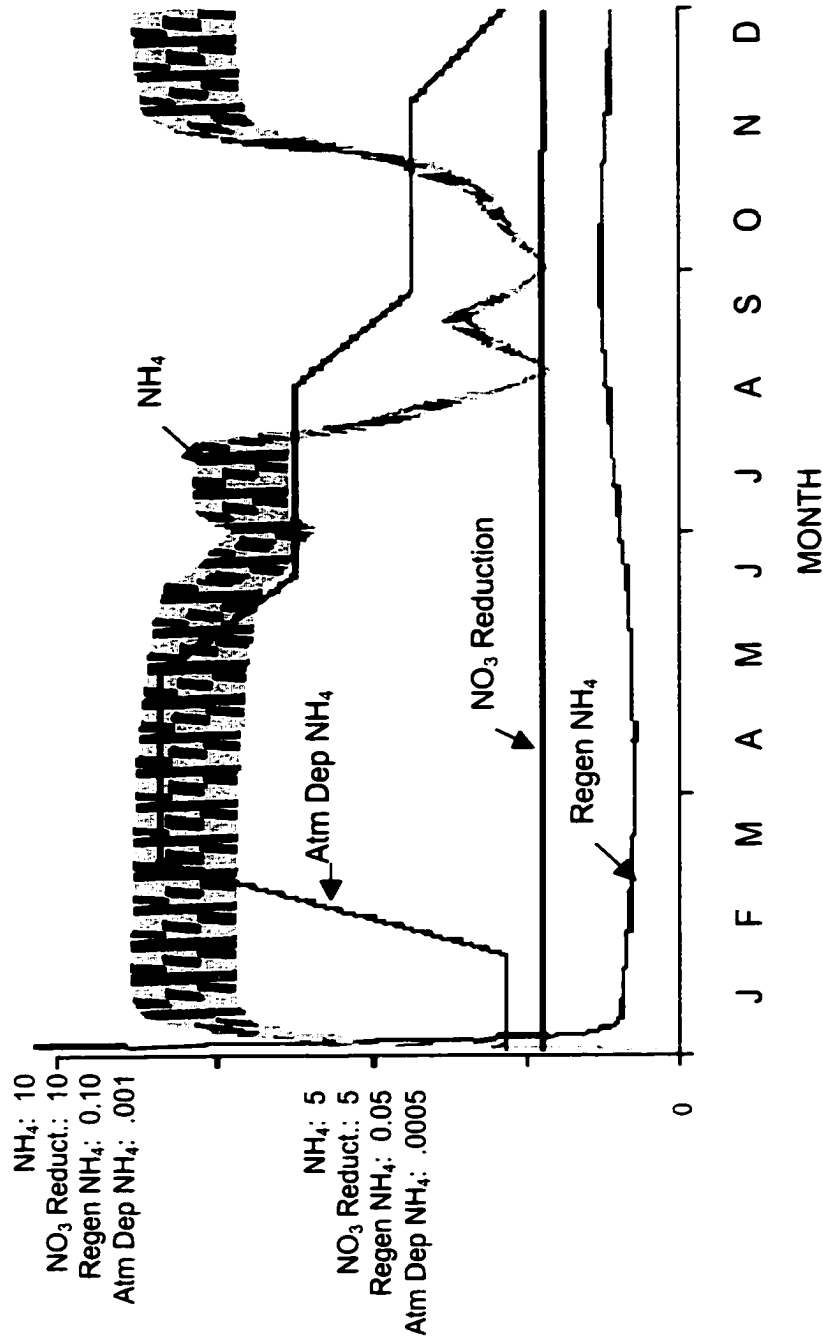
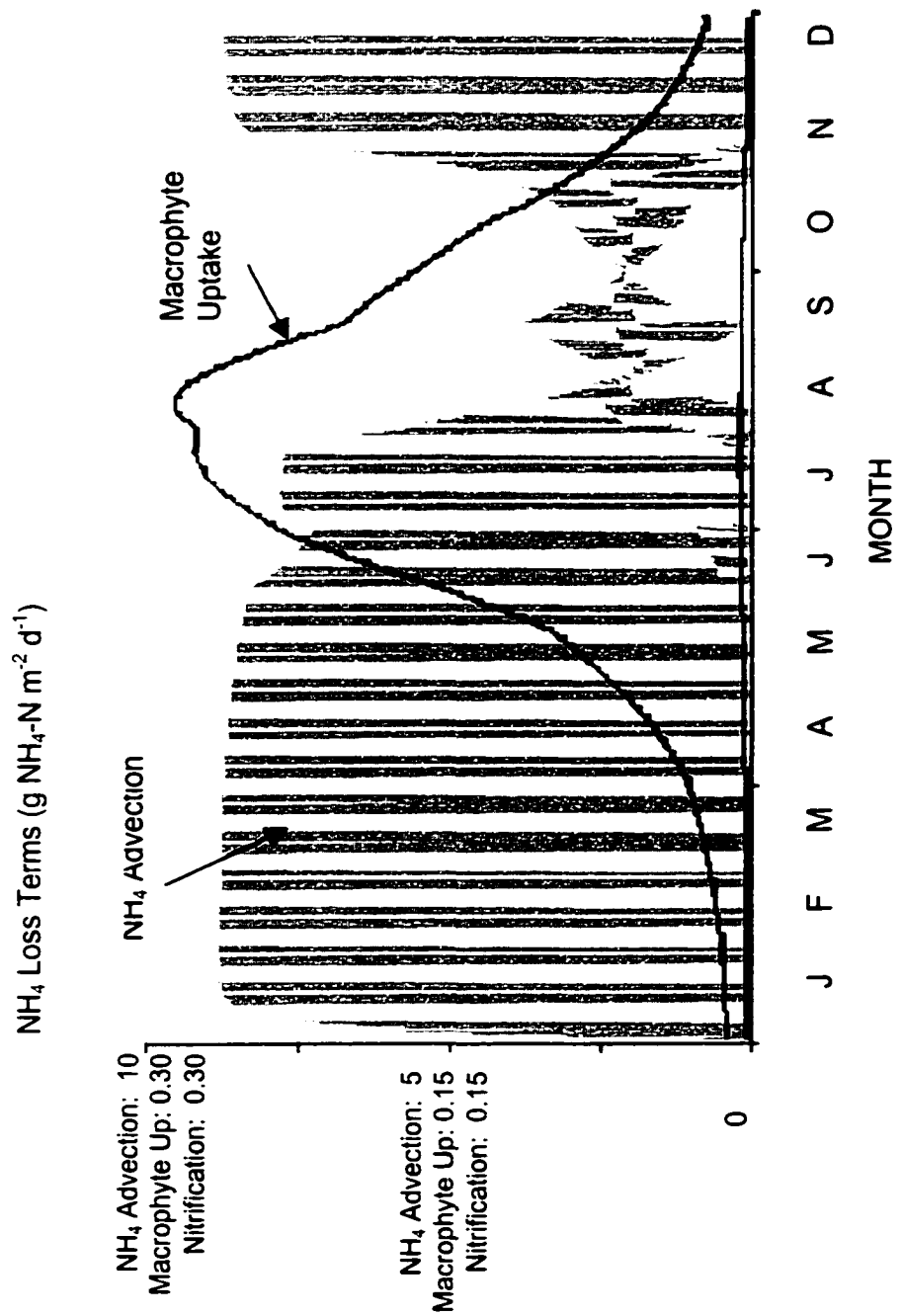


Figure 5-2. Net macrophyte primary production for one year following losses to respiration, grazing and mortality. Model output is shown with net production reported by Smalley (1958).

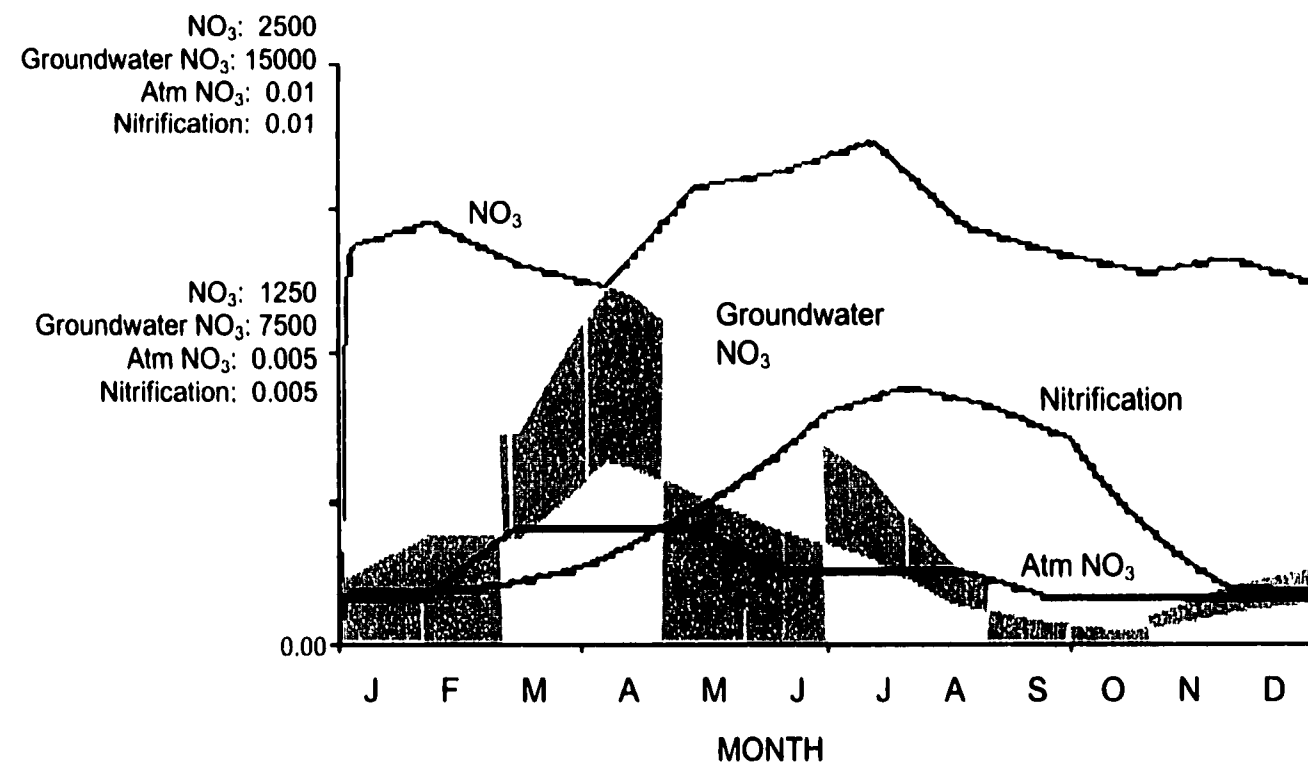
**Figure 5-3. Model ammonium porewater concentration ( $\text{g NH}_4\text{-N m}^{-2}$ ) and supply rates ( $\text{g NH}_4\text{-N m}^{-2} \text{d}^{-1}$ ). Nitrate reduction to ammonium, release of ammonium from macrophyte litter mineralization and atmospheric deposition were the sources of porewater ammonium. See Table 5-5 for a description of model calculations.**



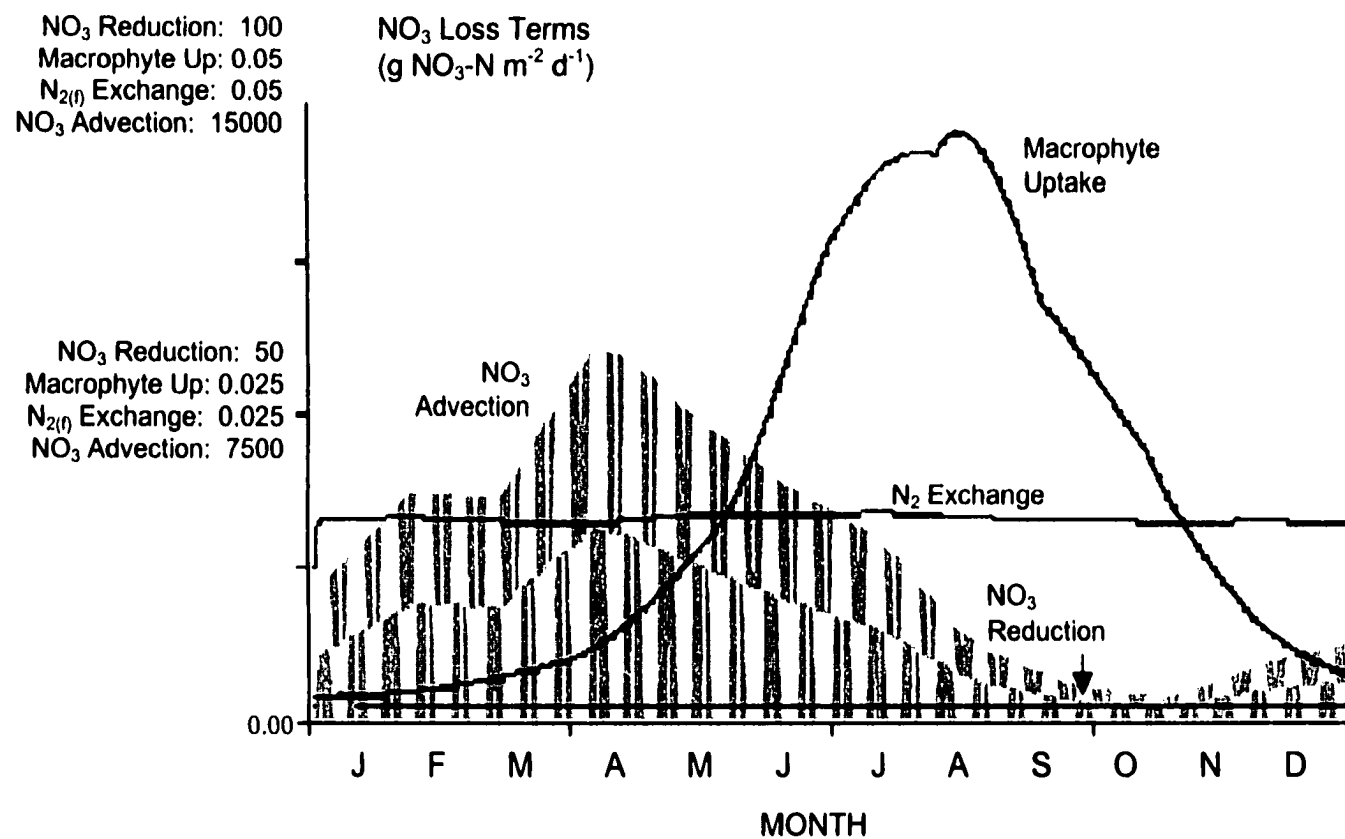
**Figure 5-4. Porewater ammonium losses in the marsh simulation model.** Advection of porewater from the sediments tracked the tidal cycle, peaking during low tide and declining to zero at high tide due to shifting hydraulic gradients. A description of model calculations can be found in Table 5-5.



**Figure 5-5. Nitrate pool ( $\text{g NO}_3\text{-N m}^{-2}$ ) and supply terms in the simulation model. Groundwater nitrate was supplied according to a hydraulic gradient caused by tidal forcing. Details of model calculations are shown in Table 5-6.**



**Figure 5-6.** Nitrate losses included in the simulation model. Gaseous nitrogen exchange was modeled as a bi-flow, but did not fall below zero which would indicate nitrogen fixation. Net denitrification was suggested throughout the year. Details of model calculations are given in Table 5-6.



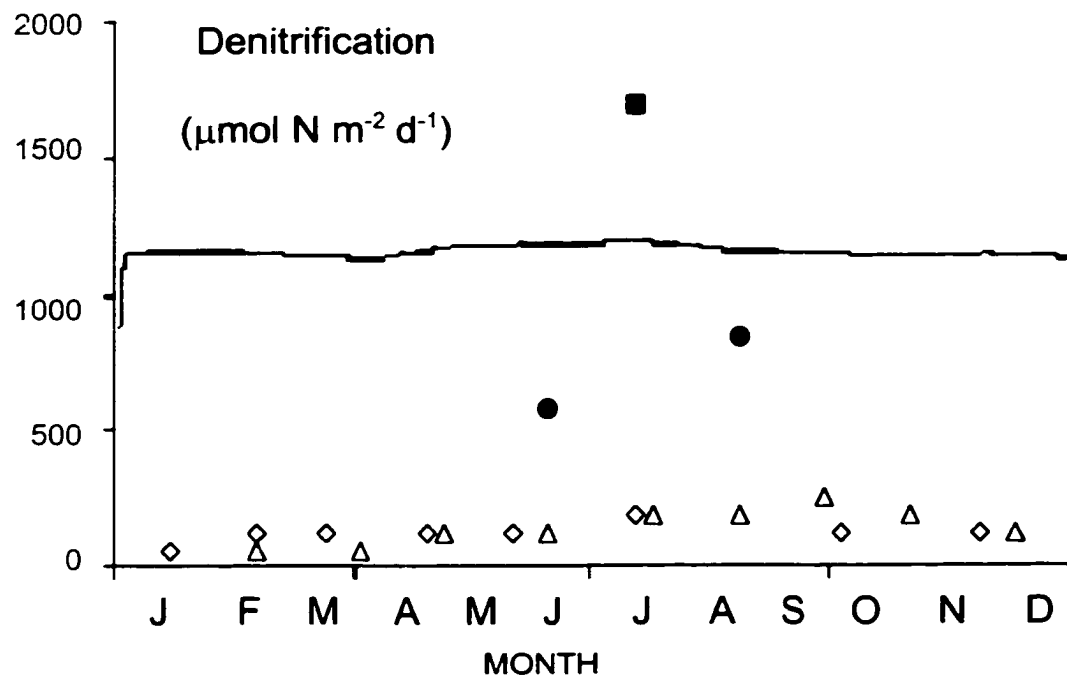


Figure 5-7. Denitrification rates from model output with calibration data. Filled symbols are empirical data from tidal freshwater systems included in this dissertation. Both Jug Bay, Patuxent River (○) and Tivoli Bays, Hudson River (■) denitrification rates were measured using membrane inlet mass spectrometry (MIMS). Data from two salt marshes, Great Sippewissett ( $\Delta$ , Kaplan et al. 1979) and a North Carolina site ( $\diamond$ , Thompson et al. 1995) is included for comparison.

## **APPENDIX A: THE EFFECT OF A BRACKISH CHESAPEAKE BAY MARSH ON THE NUTRIENT BUDGET OF A RURAL WATERSHED**

### **INTRODUCTION**

Understanding the role of tidal marshes in larger ecosystems remains a daunting challenge in wetland ecosystem science. Numerous ecological and water quality functions have been attributed to tidal marshes, ranging from particulate filtration to nursery habitat for juvenile fish. Declining water velocities over marsh surfaces leads to particulate settling and incorporation into the permanent marsh substrate, while dissolved nutrient uptake or transformation via autotrophic or heterotrophic processes can be another major flux term. Allochthonous particulate inputs, combined with autochthonous organic matter production, allows the surface of a marsh to maintain elevation despite rising sea level (Stevenson et al. 1985). Nutrient retention in marsh soils may be considered a long-term or permanent sink for

nutrients with potential water quality benefits in systems experiencing eutrophication from excess nutrients.

Although the eutrophic Chesapeake Bay is one of the most heavily studied estuaries in the world, the impact of tidal marshes on nutrient budgets of this ecosystem has not been examined in detail. Previous estimates of Chesapeake Bay marsh nutrient retention capacities have been derived from tidal exchange studies (Heinle and Flemer 1976; Stevenson et al. 1977), though such studies may be problematic for understanding net annual fluxes (e.g. Murray and Spencer 1997). The potential importance of tidal marsh sediment nutrient burial was identified previously (Nixon 1980) and measured for other systems such as the Louisiana Delta (DeLaune et al. 1983). Khan and Brush (1994) examined sedimentation using palynological dating techniques in the Patuxent River, but estimated nitrogen and phosphorus burial at only two sites. Work presented earlier in this dissertation describes in more detail the importance of tidal freshwater marshes to surrounding estuaries.

One of the critical factors which allows tidal freshwater marshes to play such an important role in estuarine water quality is their location in the watershed. Nutrient and sediment loads are generally high as a result of watershed activities such as land clearing and agriculture. The role of coastal, submerged upland marshes is not as clear. Marshes such as those surrounding Monie Bay, at the mouth of the Wicomico River, in Somerset County Maryland, do not receive the high mineral sediment loads associated

with tidal freshwater marshes. Stevenson et al. (1988) suggested this type of marsh as requires high rates of primary production and organic matter accretion to maintain surface elevation relative to the apparent rise in sea level.

Previous research has shown that marshes of the eastern shore of the Chesapeake Bay exhibit a sediment deficiency which is believed to be leading to their conversion to subtidal systems (Stevenson et al. 1985; 1986; Kearney and Ward 1986; Kearney et al. 1988; Kearney and Stevenson 1991). In Monie Bay marshes Kearney et al. (1994) reported accretion rates between 3 and 7 mm  $y^{-1}$ . These marshes apparently keep pace with rising sea level, incorporating large quantities of nitrogen and phosphorus into the marsh sediment. The goal of this study is to determine the quantity of nutrients permanently sequestered in the tidal marsh sediments of a brackish submerged upland marsh and to relate the burial to inputs to the system from an agriculturally-dominated watershed. Accretion rates and nutrient concentrations were measured to estimate the magnitude of N and P burial. Rates were examined relative to nutrient inputs estimated from land use coefficient-derived inputs to the aquatic ecosystem.

## MONIE BAY WATERSHED

Monie Bay is located on the eastern shore of Chesapeake Bay in Somerset County, Maryland (Figure A-1). Salinity within Monie Bay varies between 12 and 17 psu. Brackish marshes fringe Monie Bay and continue

along the three tributaries, Little Creek, Little Monie Creek and Monie Creek. A portion of the marshes are included in the Maryland National Estuarine Research Reserve System (NERRS) and have been examined by researchers previously (Ward et al. 1988, Cornwell et al. 1990, 1994, Stribling 1994).

Monie Creek is the largest tributary, while Little Monie Creek and Little Creek are much smaller share a mouth on Monie Bay. Hence, the three tributaries display a gradient of salinity, ranging from brackish at Monie Bay to freshwater where the tributaries form. Of particular interest are the contrasting basins of Little Monie Creek and Little Creek. The basin of Little Monie Creek is dominated by row agriculture and poultry farms, while the land surrounding Little Creek is almost entirely forested. *Spartina alterniflora* is the dominant plant species, with *S. patens*, *S. cynosuroides*, *Amaranthus cannabinus*, *Juncus roemerianus*, *Distichlis spicata* and *Phragmites australis* also present (Stribling 1994).

Monie Bay is surrounded by a rural watershed of approximately 76 km<sup>2</sup> (18,800 acres). Land use in the watershed is divided approximately into thirds between forested land, agricultural land including corn and soybean crops, and wetlands. Poultry farming, while not a dominant land use feature in terms of land coverage, enhances potential nutrient loads to Monie Bay through the use of poultry litter as an organic fertilizer on corn crops. Usual crop rotations in the region consist of 2 years of soybeans, which receive no poultry litter, followed by a year of corn. At any point in time then,

approximately 11% of the Monie Bay watershed is in corn production, and receiving poultry litter additions, commonly at a rate of 3 tons per acre annually. Collectively, the poultry farms within Monie Bay's watershed have the capacity to raise 500,000 chickens, generally 5.5 flocks can be raised per facility annually, which allows the Monie Bay poultry growers to supply 2,750,000 chickens per year. The USDA's Soil Conservation Service in Somerset County estimates approximately 65% of the poultry litter produced within the Monie Bay watershed is utilized and not exported to other watersheds.

The extensive marshes within the Monie Bay system have been categorized into three sub-environments by Kearney et al. (1994): channel-side, marsh interior, and shoreline. Sediments of the marshes vary with sub-environment and have been characterized for biogeochemistry parameters by Cornwell et al. (1990; 1994). Monie Bay shoreline marshes are on a sandy substrate, with tidal flushing from the Bay. Channel-side marshes maintain higher organic matter concentrations and are flushed by the tidal creeks on a regular basis, removing toxins (i.e. hydrogen sulfide and other reduced species) and supplying nutrients. Interior marsh areas are characterized by surface hummocks and have high organic matter concentrations that support high rates of sulfate reduction. Flushing rates are limited leading to a build up of porewater sulfides (Stribling 1994). All three marsh types were examined in this study. Kearney et al. (1994) reported sedimentation rates using  $^{210}\text{Pb}$  which are very near the rate of regional sea level rise. Observations by local

extension agents suggest the marshes are encroaching on uplands at a rapid pace- recently farmed croplands now resemble the older, well-established marshes.

## METHODS

### Sediment Accretion and Nutrient Burial

A McAuley corer was used to collect seven sediment cores (Bricker-Urso et al. 1989) during the summer of 1993. Sites were located in the three marsh types described by Kearney et al. (1994) and were collected from 10 to 40 m inland. Cores were immediately divided into 3 or 5 cm samples to a depth of 1 meter. Samples were placed on ice and returned to the laboratory. Bulk density was determined by weighing known volumes of sample. The sediment was then dried at 65°C and ground with a ceramic mortar and pestle.

Total phosphorus was determined by combusting sediments at 550°C and extracting phosphorus with 1 N HCl (Aspila et al. 1976). Inorganic phosphorus was measured in the same manner, using an unashed sample. Concentrations were determined using a colorimetric technique (Parsons et al. 1984). Organic phosphorus was assumed to be the difference between total and inorganic P. Nitrogen were measured using a Control Instruments CHN analyzer with a precision better than 5%.

Sediment accretion was determined using the  $^{210}\text{Pb}$  technique (Robbins 1978). Secular equilibrium was assumed between  $^{210}\text{Pb}$  and  $^{210}\text{Po}$ , which is extracted from the sediment samples using  $\text{HNO}_3$  and  $\text{HCl}$  following Sugai (1990). The constant input concentration model (Robbins 1978) was used to calculate the rate of sediment deposition. A linear regression of the natural log of unsupported  $^{210}\text{Po}$  activity with cumulative mass provides an estimate of sediment mass buried per area unit time. Regressions with  $r^2 < 0.85$  were not used for nutrient burial rate calculations.

In addition to the seven cores analyzed in this study, sites used in Ward et al. (1988)/Kearney et al. (1994) were sampled to determine nutrient concentrations. Sediment burial rates ( $\text{g m}^{-2} \text{ yr}^{-1}$ ) for the three Monie Bay sites were taken from Ward et al. (1988). Sites were sampled with duplicate cores and nutrient concentrations were measured at three depths: 0-3 cm, 12-15 cm, and 45-50 cm. Phosphorus, nitrogen, and carbon deposition rates were calculated using the 45-50 cm section average of both cores at each of the three sites. Deep samples represent refractory material below the zone of root activity, which is approximately 18 cm (Stribling 1994). The deep sediment section was used to represent the sediment final nutrient concentration following plant uptake and diagenesis. In all cases, nutrient burial was calculated as the product of the sediment deposition rate and nutrient concentration at 45 to 50 cm deep in the core (DeLaune et al. 1981; Johnston et al. 1984).

Nutrient inputs to Monie Bay from the immediate watershed were

estimated for comparison to the calculations of nutrient burial in the marsh sediments. Nutrient runoff and deposition coefficients were integrated over estimated land use to calculate potential nutrient loading rates to the Monie Bay system (Table A-1). Somerset County USDA Soil Conservation Service provided land use coverage estimates based on a recent land use map for the Monie Bay watershed. Covering 76.1 km<sup>2</sup>, the watershed is equally distributed. Forested land covers 26.6 km<sup>2</sup>, and wetlands cover 25.4 km<sup>2</sup>. Agriculture accounts for the remaining 24.1 km<sup>2</sup>, and is in a soybean-soybean-corn rotation as mentioned previously. Nutrient inputs to Monie Bay from the forested land in the watershed was approximated using runoff estimates from Reckow et al. (1980). The runoff coefficients for nitrogen and phosphorus represent the end product leaving forested land and therefore include the effects of atmospheric deposition. Deposition of nitrogen and phosphorus directly to the wetlands was included, taken from the National Atmospheric Deposition Program, 1991, and Correll et al. (1992), respectively. Phosphorus deposition data from Correll et al. (1992) was collected from a Chesapeake Bay subestuary and should provide a close estimate for the region.

Nutrient inputs as a result of poultry litter fertilization of corn crops is the focus of much scientific and legislative attention, and the estimate presented here represents only a cursory examination intended to provide a comparison with the potential of marsh retention capacity. Due to the variation in production and use of poultry litter between farms the actual

application rates of litter to corn crops is not known. Nitrogen and phosphorus additions to agricultural fields were approximated based on poultry production numbers for watershed poultry houses (Table A-2). With the capacity to raise 500,000 chickens simultaneously, assuming watershed poultry farms produce their maximum, the farms collectively produce approximately 56,340 kg N and 28,170 kg P annually. This assumes the birds produce 0.31 kg N per day and 0.15 kg P per day per 1000 birds (Agricultural Waste Management Field Handbook 1992). A portion of poultry litter produced within the Monie Bay watershed is exported to surrounding systems, while an estimated 65% remains within the watershed (USDA Soil Conservation Service), primarily to be used as fertilizer on corn crops. As a result, nitrogen and phosphorus applications of poultry litter were estimated at 36,600 kg nitrogen and 18,300 kg phosphorus throughout the watershed annually.

For comparison with surrounding watersheds, the application rates of nitrogen and phosphorus presented above, based on poultry production, were used to back-calculate potential average total litter application rates for the Monie Bay watershed. Assuming the nitrogen and phosphorus application rates are those presented above, total litter application rates are near 0.3 tons litter per acre corn. This back-calculation requires the use of a recognized standard 70-60-50 N-P-K (pounds nutrient per ton litter) for regional poultry litter. If this estimation is a reflection of the Monie Bay agricultural system, then application rates in this watershed are 10% of those common throughout

the lower eastern shore of Maryland. Neighboring Wicomico County Soil Conservation Service reports typical poultry litter application rates of 3 tons per acre corn per year. Since the application of poultry litter to corn crops is primarily a mechanism to dispose of the animal waste, and imports of litter to the Monie Bay watershed are not documented, the conservative estimate presented earlier based on poultry production was used to estimate litter applications.

By far the most difficult, and least well-understood step in estimating the contribution of agricultural land use to an ecosystem nutrient budget is the approximation of nutrient runoff. Release of nitrogen and phosphorus from poultry litter into a water system such as Monie Bay and its tributaries depends on a host of characteristics, all of which vary in time and space. Use of best management practices (BMPs) can reduce the amount of nutrients released to surrounding water bodies. Time of application, plowing litter under the soil, the use of buffer strips and cover crops during winter months are all techniques which can be employed by the farmer to reduce runoff. Other characteristics such as soil type and proximity to the water are beyond the control of the farmer and can affect nutrient runoff. A detailed budget for the agricultural contribution is beyond the scope of this study and so both a conservative and a high rough approximation of potential runoff were used for a comparison with marsh burial. Agricultural researchers currently investigation nutrient runoff suspect at least 5% of the litter nutrients added may enter a nearby body of water. Runoff equivalent to 15% of the litter

nutrients added is likely to be high. Estimates, both conservative at 5% and high, at 15% were used to approximate the agricultural contribution to the ecosystem nutrient budget (Table A-2). The reader must bear in mind these figures represent averages across a collection of farming practices, soil conditions and field locations.

Although groundwater inputs have been determined to be important nutrient sources draining agricultural lands on the eastern shore of the Chesapeake Bay (Staver and Brinsfield 1996), difficulty in approximating flows and concentrations prevented the inclusion of this mechanism of nutrient introduction.

## RESULTS

### Physical Properties of the Sediment

Monie Bay marsh sediments are highly organic with percent loss on ignition (%LOI) reaching as much as 75% (Figure A-2). Profiles of %LOI exhibited non-uniform variability through depth and were not distinguishable by sub-environment as defined by Ward et al. (1988). Bulk density was generally lower in this marsh than in other systems within the Chesapeake, an observation consistent with high percent loss on ignition (%LOI) values (Table A-3). Organic content was similar to that found within the marshes of Narragansett Bay (Bricker-Urso et al. 1989), where over 90% of vertical

accretion was attributed to organic matter deposition.

## Sediment Accretion

Lead-210 dating was successful in six of the seven cores collected from the Monie Bay marshes (Figure A-3). Sediment accretion rates in the Monie Bay marshes ranged from  $0.23$  to  $0.68 \text{ cm y}^{-1}$  (Table A-4). Rates were distributed by marsh environment. The highest rates were measured at the tributary bank sites. Sediment accretion rates found at the back marsh sites ( $0.23$  to  $0.26 \text{ cm y}^{-1}$ ) were lower than regional sea level rise. The site located on the shores of Monie Bay had a rate of  $0.44 \text{ cm y}^{-1}$ , near the median of the vertical sedimentation range for the entire system.

## Phosphorus Speciation

Phosphorus profiles showed a dominance of organic phosphorus preservation over inorganic phosphorus (Figure A-4). Variability with depth in the profiles was low, with the exception of sites 3 and 6. Site 3 is located the greatest distance from a distinct tidal channel and site 6 is located near Little Creek with the forested basin. The concentrations of inorganic P ranged from  $0.02$  to  $0.58 \text{ mg g}^{-1}$ . Sites 3 and 6 showed surface increases in inorganic P, possibly due to post-depositional mobility associated with diagenesis of sedimentary iron. Total P concentrations varied between  $0.10$  and  $2.03 \text{ mg g}^{-1}$ .

sediment<sup>-1</sup>. The cores did not exhibit any recent increases in total P concentrations, despite increases in P inputs for point and non-point sources (Boynton et al. 1995). There were no apparent patterns in phosphorus speciation with location in the Monie Bay system.

## Phosphorus and Nitrogen Retention

Phosphorus burial in Monie Bay marshes ranged from 0.25 to 1.35 grams TP m<sup>-2</sup> y<sup>-1</sup> (Table A-4) and averaged  $0.63 \pm 0.38$  g m<sup>-2</sup> y<sup>-1</sup> (n=9). Burial of total nitrogen ranged from 1.4 to 19.8 g TN m<sup>-2</sup> y<sup>-1</sup>, averaging 10.6 ( $\pm 6.08$ ) g TN m<sup>-2</sup> y<sup>-1</sup>. Site 4, located on Monie Bay proper, had one of the highest phosphorus burial rates found, while the nitrogen burial rate was much lower than any of the others. Within the creek marshes, phosphorus burial rates decreased and nitrogen burial rates increased due to the increased importance of organic matter to the sediment matrix. Inorganic P contributed less than 50% of the total P retained in almost all sites and depths.

## DISCUSSION

Tidal marshes are an important component of the Monie Bay subestuary. The sediment matrix of the marshes may retain a large portion of the nutrients delivered to the system from its watershed every year. Despite relatively low rates of sediment accretion, the marshes retain large quantities of nitrogen through the burial of organic matter. Rates in the system are comparable to that of other watersheds (Table A-5).

### Sediment Characteristics and Marsh Subsidence

Monie Bay has a range of wetland sedimentary environments and as a result may be a complex mixture of stable marshes and marshes which have the potential to be lost to rising sea levels. This study suggests that both the marshes which border Monie Bay directly and those found along the tributaries are stable, with accretion rates well above that of rising sea level. However, interior marsh areas with high organic matter content, high rates of sulfate reduction (Stribling 1994) and a hummocky surface are not accreting rapidly enough to escape inundation. At first glance, this suggests that narrow creek banks will survive with large tracts of area behind them converted from back marsh areas to open water. This is not the case in Monie Bay. Kearney et al. (1994) have described the seemingly random microtopography which appear to control the site specific sediment accretion rate. The authors suggest some areas of marsh may be degrading, but the

sites are limited and physical changes are much slower than in other areas of the Chesapeake. In addition, USDA agricultural agents have observed the encroachment of marsh systems into agricultural fields. These observations suggest the landward transgression of the marshes continues with sea level rise, resulting in an increase in marsh coverage within the watershed.

Marsh sediments may affect nitrogen and phosphorus concentrations to varying degrees, effectively shifting N:P which may have consequences on estuarine water quality (Fisher et al. 1992). Monie Bay is more effective at retaining nitrogen than phosphorus in the marsh sediment matrix, a reflection of the elemental composition of local vegetation. Stribling (1994) reports *Spartina alterniflora* shoot N:P between 16 and 50. Sediment values range between 4.6 and 140, with an overall average of approximately 30 across all depths and sites (Figure A-5). As remineralization occurs, the sediments are releasing more P relative to nitrogen, as seen in the increases in N:P through depth (Figure A-5) and declines in P concentrations (Figure A-4).

Phosphorus inputs to marsh systems tend to be in the particulate form, and with little particulate transport and deposition in the marsh system, this mechanism of supply to the sediments is restricted. High pore water and solid phase sulfides (Cornwell et al. 1990) make inorganic P retention more difficult because of the loss of P-retaining iron oxide minerals to pyrite and iron monosulfides (Krom and Berner 1981).

## Watershed Inputs

A comparison of the nutrient sources to the Monie Bay ecosystem reveals several interesting relationships (Tables A-1 and A-2). Atmospheric deposition of both nitrogen and phosphorus was twice the runoff coefficient used to represent contributions from forested lands. The relationship is consistent with research suggesting forests provide a substantial buffering effect from atmospheric, and other, nutrient sources (Correll et al. 1992). Because of the high rates of atmospheric deposition of both nitrogen and phosphorus in the region, as noted by Boynton et al. (1995), this source was dominant in the watershed when the most conservative estimates of agricultural N and P contributions were used (5% runoff). Exceptionally large tracts of marshes, covering one-third of the watershed area, also increased the relative magnitude of the atmospheric input. Under the conservative scenario agricultural contributions of phosphorus were double that from forested lands. High rates of agricultural runoff, 15%, increase the phosphorus load to double the atmospheric contributions. Nitrogen contributions remain a relatively small factor in the watershed. Clearly, if the agricultural system surrounding Monie Bay were to employ application rates similar to those practiced in the region (3 tons litter per acre per year) nitrogen and phosphorus contributions would increase ten-fold, leading nitrogen contributions and dominating the input of phosphorus.

A simple mass balance approach shows that the marshes of Monie

Bay are critical for maintaining water quality in this rural system. While the sedimentation rates are modest compared with other marshes, the sheer expanse of the marshes suggests that if they can accrete rapidly enough to survive rising sea level they are an enormous factor in the ecosystem nutrient budget (Table A-6). Despite the loosely-described potential nutrient contributions from local agriculture, the importance of the marshes in maintaining water quality are clear. In the absence of the marshes the nutrient budget of the estuary would be vastly different. Marsh systems must begin to be included in the analysis of ecosystem nutrient budgets.

The watersheds of Little Monie Creek and Little Creek represent two extremes of land use on the eastern shore of the Chesapeake Bay. Little Creek is surrounded by unbroken forests, while the watershed of Little Monie Creek is primarily cropland. Based on runoff coefficients for land use patterns of the watersheds, we expect nutrient inputs to be much greater to the marshes of Little Monie Creek. Agricultural fields are plowed multiple times over the year and particulate inputs to the estuary should be large. Sediment N and P incorporation rates in the two systems were equal, indicating that in the Monie Bay system, the wetland filtration capacity is not related to the inputs of total suspended solids. In addition, the nutrient concentrations are comparable between the two branches, suggesting that nutrient burial is not dependent on ambient tidal water nutrient concentration.

This first order budget for Monie Bay marsh-estuarine nutrient removal suggests that the marshes can be important sinks for nitrogen and

phosphorus in an estuarine environment. To reduce the error associated with the budget a good approximation of high and low marsh area is needed. This mass balance approach for determining N and P inputs to the wetland-estuary has large uncertainties and extrapolation to the spatially heterogeneous marsh-subestuary ecosystem is difficult. Despite the large potential pliability of the final numbers, this ecosystem approach to determining the relative importance of wetlands to their surrounding is of considerable value. Scaling up from individual to ecosystem level measurements remains a difficult task, and future efforts should be devoted to a better understanding of scale-related extrapolations. Future research must include estimates of groundwater nutrient inputs from these rural agricultural areas (Staver and Brinsfield 1996).

**Table A-1. Estimated total nitrogen and phosphorus contributions to the Monie Bay ecosystem from atmospheric deposition directly to wetlands and runoff from forested land.**

	Area km <sup>2</sup>	Nitrogen g m <sup>-2</sup> y <sup>-1</sup>	N Load kg y <sup>-1</sup>	Phosphorus g m <sup>-2</sup> y <sup>-1</sup>	P Load kg y <sup>-1</sup>
Atmospheric	25.4	0.54 <sup>1</sup>	13,700	0.051 <sup>2</sup>	1,300
Forested Land <sup>3</sup>	26.6	0.25	6,660	0.020	533

<sup>1</sup>National Atmospheric Deposition Program, 1991

<sup>2</sup>Correll et al. 1992

<sup>3</sup>Reckhow et al. 1980

Table A-2. Estimated agricultural inputs of nitrogen and phosphorus to Monie Bay using poultry production capacity of 500,000 birds within the watershed. These calculations represent a conservative estimate based on chicken production and the need for waste disposal. Overestimating litter export from the watershed or imported litter for field fertilization will cause these estimates to be low. Field application rates at this level are approximately 10% of that commonly found in the region (3 tons poultry litter per acre per year).

	Nitrogen	Phosphorus
Nutrient per chicken per day (g) <sup>1</sup>	0.31	0.15
Annual production from all watershed operations (kg)	56,300	28,200
Estimated annual watershed application (kg) <sup>2</sup>	36,600	18,300
Conservative runoff, 5% (kg y <sup>-1</sup> ) <sup>3</sup>	1,830	916
High-end runoff, 15% (kg y <sup>-1</sup> )	5,490	2,750

<sup>1</sup>Poultry litter characterization, Agricultural Waste Management Field Handbook, 1992

<sup>2</sup>Assumes 65% of litter produced in watershed is applied to agricultural fields within the watershed boundaries.

<sup>3</sup>Runoff estimates intended only for large-scale comparison of nutrient inputs. Nutrient runoff varies with time of application, crop cover, tillage practices, weather events, proximity to body of water and soil characteristics among others.

**Table A-3. Sediment physical characteristics of Monie Bay marsh sediments.**  
 Bulk density was measured using water volume displacement. Carbon and nitrogen were analyzed on a Control Instruments CHN analyzer. Percent sediment carbon and nitrogen ranges found in marsh cores are listed.

Site	Bulk Density g cm <sup>-3</sup>		% Carbon	% Nitrogen
	Avg. to 25 cm	Range		
1	0.214	0.116 - 0.302	8.32 - 13.4	0.62 - 0.88
2	0.285	0.107 - 1.38	6.41 - 14.3	0.49 - 0.98
3	0.161	0.116 - 1.14	2.04 - 10.8	0.70 - 2.0
4	0.303	0.163 - 0.383	0.51 - 14.4	0.11 - 1.58
5	0.317	0.106 - 0.378	8.92 - 18.8	0.77 - 1.15
6	0.305	0.159 - 0.411	1.02 - 8.70	0.66 - 1.29
7	0.307	0.199 - 0.359	6.41 - 14.3	0.49 - 0.77

Table A-4. Monie Bay sediment accretion rates and rates of total nitrogen and total phosphorus burial. Core 2 did not exhibit an exponential decrease in  $^{210}\text{Pb}$ . Cores with a W designation are taken from sites that were  $^{210}\text{Pb}$ -dated by Ward et al. (1988); nutrient analyses were conducted at these sites from samples collected in 1994. Nutrient burial rates are calculated as the product of sediment accumulation ( $\text{g cm}^{-2} \text{y}^{-1}$ ) and nitrogen or phosphorus concentration ( $\text{mg g sediment}^{-1}$ ) measured at 45-50 cm, below the estimated zone of plant mining.

Site	Marsh Type	$\text{cm y}^{-1}$	$\text{g cm}^{-2} \text{y}^{-1}$	$\text{g TN m}^{-2} \text{y}^{-1}$	$\text{g TP m}^{-2} \text{y}^{-1}$
1	Bank	0.68	0.18	14.4	1.06
2	Bank	-	-	-	-
3	Bank	0.63	0.09	18.5	0.29
4	Bay Shore	0.44	0.13	1.40	0.67
5	Back Marsh	0.26	0.07	8.28	0.40
6	Back Marsh	0.25	0.08	10.5	0.81
7	Back Marsh	0.22	0.06	5.16	0.36
W3		0.40	0.16	10.68	0.50
W5		0.72	0.40	19.75	1.35
W8		0.32	0.09	6.62	0.25
Average:				$10.6 \pm 4.67$	$0.63 \pm 0.302$

Table A-5. Nutrient burial rates in other estuarine systems.

	TN Burial g TN m <sup>-2</sup> y <sup>-1</sup>	TP Burial g TP m <sup>-2</sup> y <sup>-1</sup>	Method	Reference
Monie Bay	11.5	0.68	<sup>210</sup> Pb	this study
Louisiana marsh			<sup>137</sup> Cs	Hatton et al. 1982
Fresh	9-16	0.5-1.0		
Brackish	10-25	0.5-2.4		
Salt	11	1.1		
Louisiana salt marsh	13.4-21.0	0.8-3.2	<sup>137</sup> Cs	DeLaune et al. 1981
North Carolina salt marsh	1.32-10.3	-	<sup>137</sup> Cs	Craft and Richardson 1993
Chesapeake Bay Subtidal	3.46-10.9	0.68-2.56	<sup>210</sup> Pb	Boynton et al. 1995

**Table A-6. Calculation of Monie Bay marsh nutrient retention relative to estimated nitrogen and phosphorus inputs from the watershed. Burial rates reflect total N and P and were calculated by multiplying sedimentation rate as determined by  $^{210}\text{Pb}$  dating by sediment nutrient concentration. Burial rates were distributed over the total marsh surface area of 25.4 km $^2$ . Nutrient inputs were estimated using forest runoff coefficients, atmospheric deposition and an approximation of agricultural inputs as described in the text.**

	Nitrogen	Phosphorus
Marsh Burial Rate (g m $^{-2}$ y $^{-1}$ )	10.6 $\pm$ 4.7	0.63 $\pm$ 0.30
Marsh Nutrient Retention (kg y $^{-1}$ )	269,000	16,000
Estimated Nutrient Inputs (kg y $^{-1}$ )	22,200-25,900	2,750-4,580
Difference (kg y $^{-1}$ )	247,000-243,000	13,300-11,400

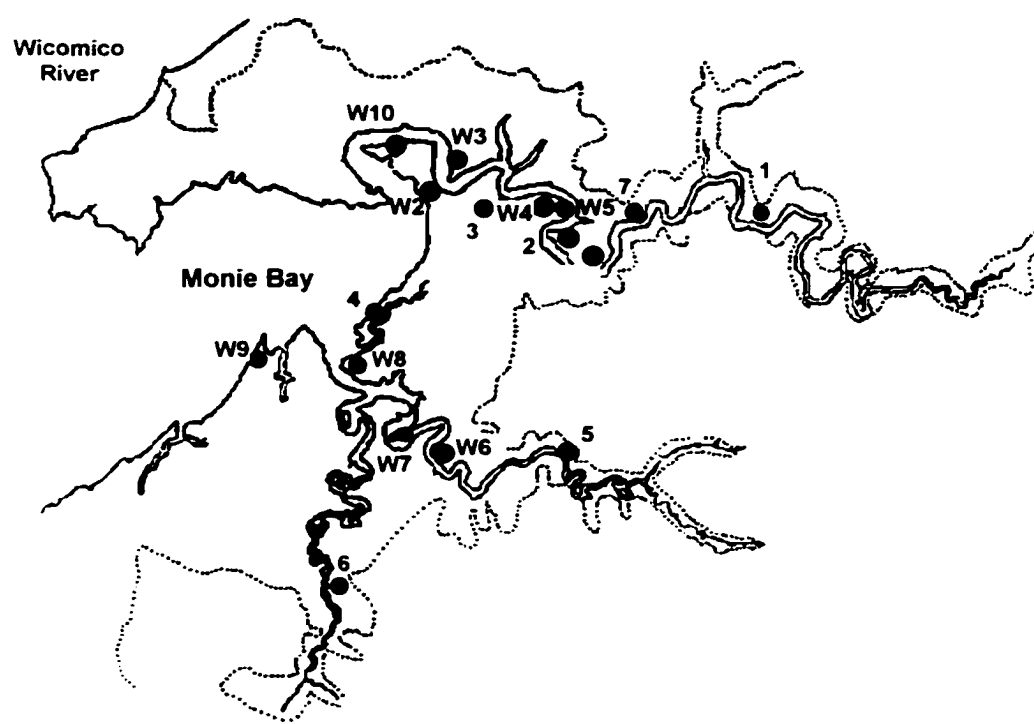
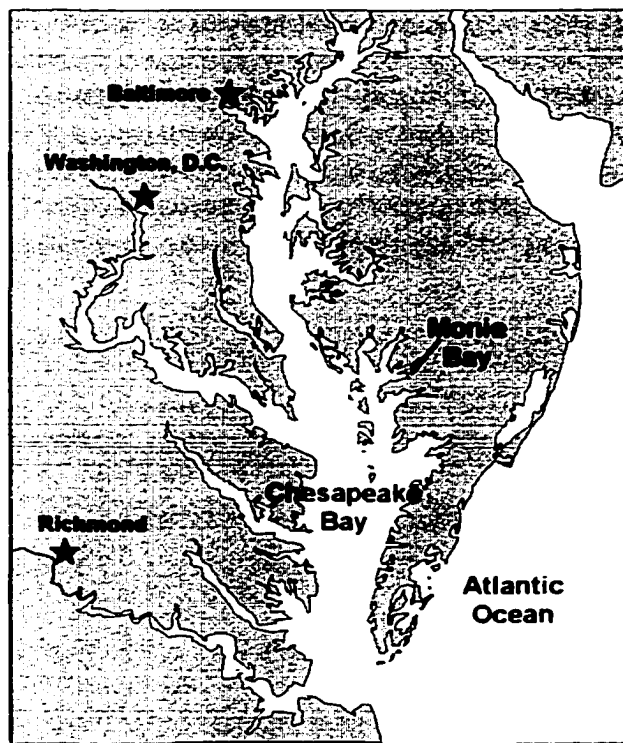


Figure A-1. Monie Bay sampling sites used in the nutrient burial study.  
Geochronological dating at 'W' sites originally completed by Ward et al. 1988.

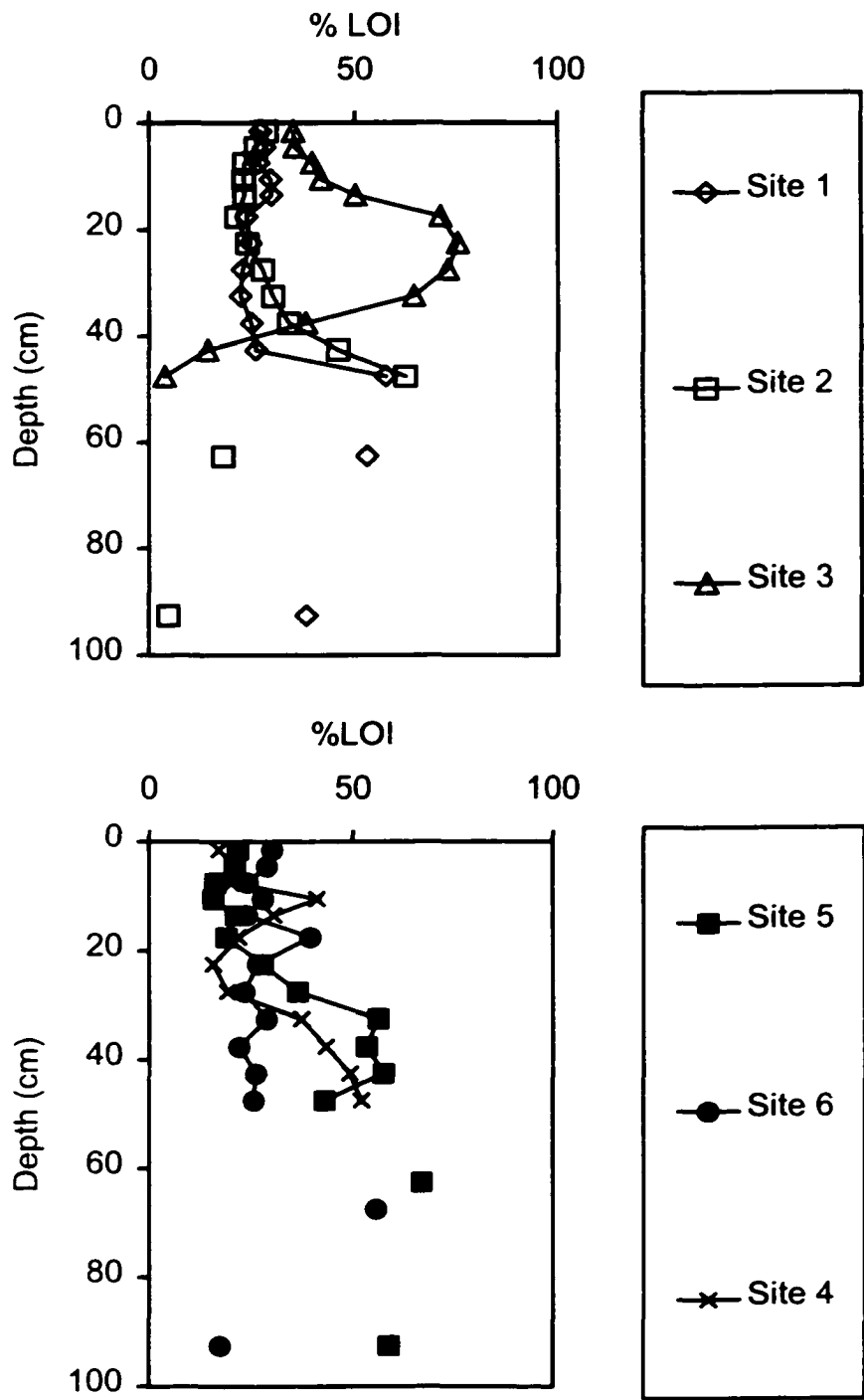
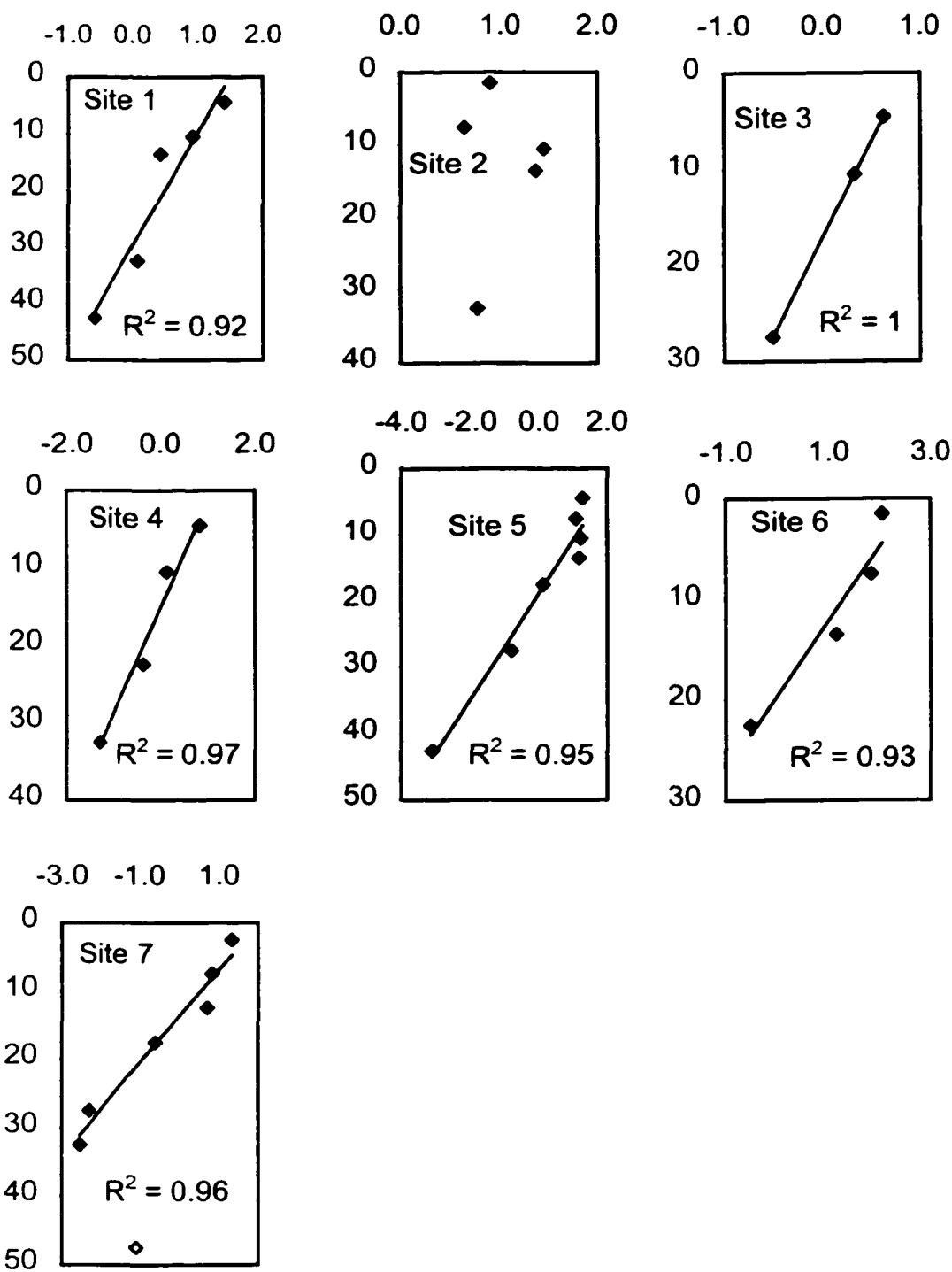
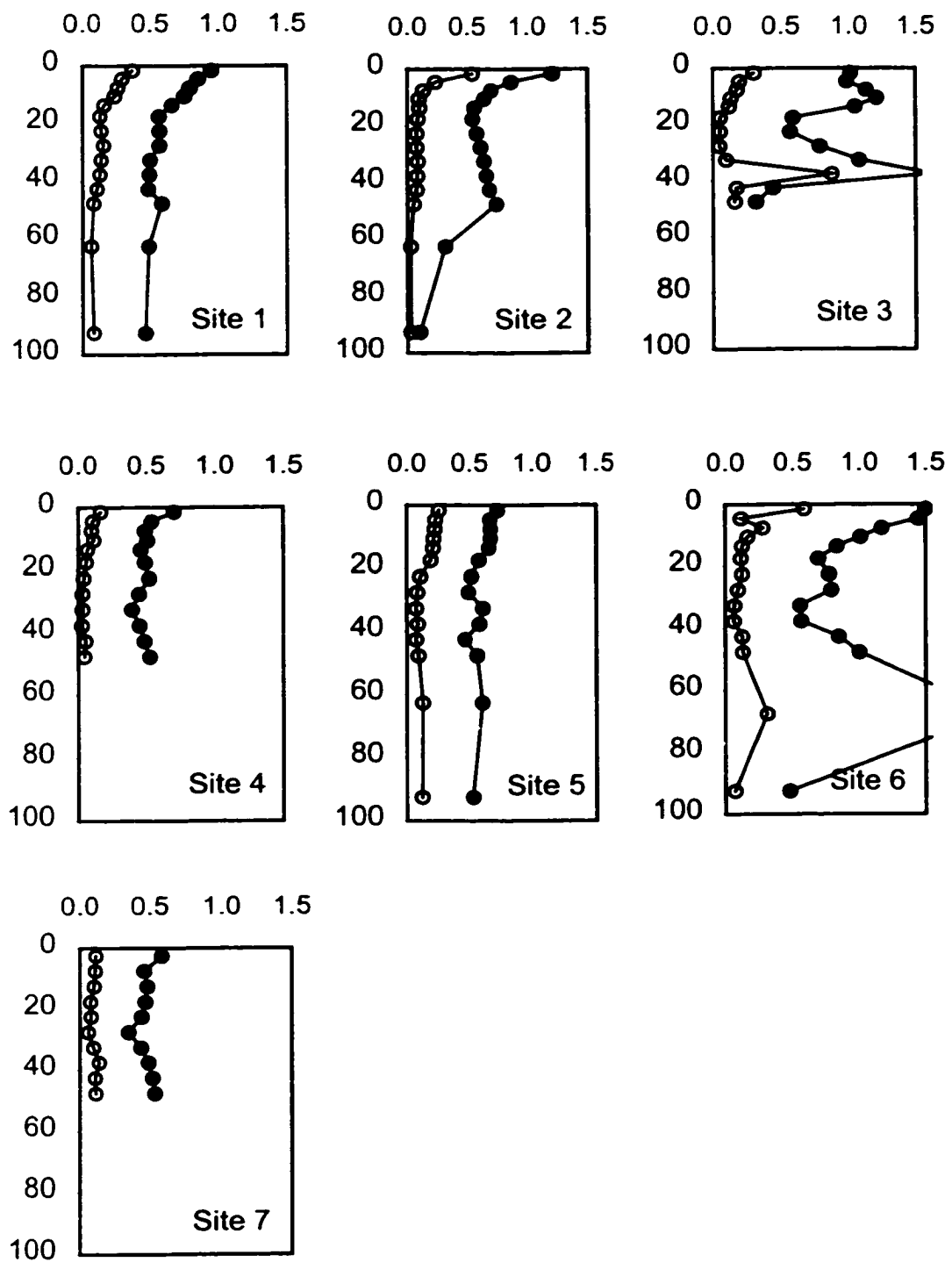


Figure A-2. Monie Bay marsh sediment profiles of percent weight loss on ignition (%LOI). The upper graph includes more rapidly accreting bank marsh sites. The lower graph shows back marsh sites. Note the less variable organic contribution in the bank marsh profiles.

Figure A-3. Monie Bay marsh sediment  $^{210}\text{Pb}$  profiles. Activity was natural log transformed and fit with a linear regression following the constant input concentration model (Robbins 1978). One open symbol represents a point left out of the regression.



**Figure A-4.** Total and inorganic phosphorus profiles of Monie Bay marsh sediments with depth (cm) on the vertical axis. Concentrations are given as mg P per gram sediment. Open symbols represent inorganic P and closed symbols represent total P. The difference was attributed to organic forms of phosphorus.



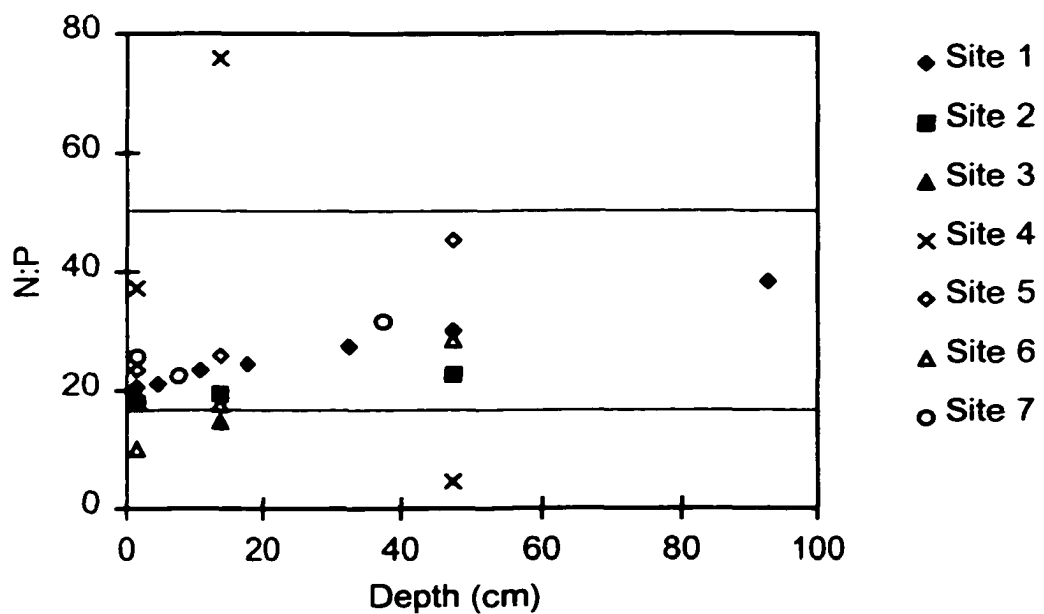


Figure A-5. Molar N:P ratios of the Monie Bay sediments. Stribling (1994) reported *Spartina alterniflora* shoot N:P values of 16 to 50 which are indicated on the graph with horizontal lines.

## **APPENDIX B: SEDIMENTATION IN UPPER ESTUARINE MARSHES OF THE CHESAPEAKE BAY AS DETERMINED BY $^{210}\text{PB}$ DATING**

### **INTRODUCTION**

Despite increasing attention to sediment deposition and vertical accretion mechanisms in coastal marshes (Reed 1989, Orson et al. 1990, Kahn and Brush 1994, Pasternack and Brush 1998), little is known about the impact of rapidly accreting marshes on estuarine sediment budgets. One of the most tangible functions of tidal marshes, particularly in oligohaline regions of estuaries, is the ability of the marshes to trap and retain particulate material from the estuarine water column during periods of submergence (Sharma et al. 1987, Orson et al. 1990, Kearney et al. 1994). As marsh surfaces are flooded by tidal waters, the marshes act as a filter for particulate matter. Water velocity decreases over the marsh surface and allows particulate material to settle on the marsh surface. Particle deposition to marsh sediments is responsible for a portion of the accretion necessary for marshes

to maintain themselves in the face of rising sea level (Bricker-Urso 1989).

Along the east coast of North America annual sea level rise ranges from 1 to 3 mm (Stevenson et al. 1986). In coastal marshes, mineral matter may be supplied by the watershed or by the flooding tides. Organic matter is supplied through deposition of water column particulates and *in situ* above and below-ground primary production. Without sufficiently rapid accretion, coastal marshes will be converted to open water systems (Stevenson et al. 1985, Kearney and Ward 1986).

Earlier studies suggest brackish, lower estuarine marshes retain between 15% (Nixon 1980) and 5-11% (Stevenson et al. 1988) of the total sediment load to the Chesapeake Bay. Both authors suggest that tidal freshwater marshes may be more important sediment traps than brackish marshes, but no large-scale studies have been published yet. The role of the Chesapeake's one million acres of tidal marshes (Field et al. 1991) remains a largely unknown variable in sediment budget calculations.

## MEASUREMENT OF SEDIMENTATION

Vertical accretion in tidal marshes has been estimated by a number of techniques. Tracking the depth of a particular layer of sediment over time through the use of a label has been a common approach. Natural markers such as pollen from opportunistic plant species in strata of cores is very time consuming and relies on historical information concerning land clearing

activities (Brush et al. 1982). Artificial markers such as brick dust can be used to estimate sediment accretion, but only over relatively short periods of time. Atmospheric nuclear testing in the 1950's and 1960's released <sup>137</sup>Cs which provides a marker horizon corresponding to the early 1960's. While <sup>137</sup>Cs can be a reliable tracer in saline systems (Hatton et al. 1983), signal dilution and post-depositional mobility are common in sediments of inland, freshwater aquatic ecosystems (Davis et al. 1984).

Radioisotopes have provided the most useful estimates of vertical accretion in marsh systems by allowing researchers to determine sediment age through the interpretation of decay by naturally occurring radioactive isotopes. Radiocarbon is used to date sediments and derive deposition rates when sediments are on the order of thousands of years old. Lead-210 ( $t_{1/2} = 22.3$  y) was chosen for this study because its decay rate is similar to the time scale of interest (approximately 100 years). In addition, steps within the decay process from <sup>226</sup>Ra to <sup>210</sup>Pb are unique and provide additional information which allows for the aging of sediment.

The decay of <sup>226</sup>Ra, an eventual daughter in the <sup>238</sup>U decay series, releases gaseous <sup>222</sup>Rn from the earth's crust to the atmosphere. While in the atmosphere, <sup>222</sup>Rn decays to <sup>210</sup>Pb. The particle-bound lead is flushed from the atmosphere largely during precipitation events. Deposited on the land and water surfaces, <sup>210</sup>Pb can be transported into water bodies and settle to the sediment-water interface. Lead-210 supplied to the sediment through this pathway is termed "unsupported <sup>210</sup>Pb activity" as opposed to

"supported activity" which is the result of decay within the earth's crust.

Supported activity is derived from  $^{222}\text{Ra}$  which did not escape the earth's crust, but continued to decay in place. Unsupported decay should exhibit an exponentially decreasing concentration through depth in the sediment since it is supplied to the sediment surface and undergoes radioactive decay. Total  $^{210}\text{Pb}$  activity is composed of activity derived directly from the decay of  $^{226}\text{Ra}$  within the sediment (supported) and the unsupported activity, supplied through atmospheric and ecosystem cycling. Unsupported activity is calculated by subtracting the supported activity from the total activity at a given depth.

Sediment accretion rates have been determined in three tidal marsh systems within the Chesapeake Bay. Lead-210 was used as an indicator of sedimentation at twelve individual sites and four transects of three to four cores for a total of twenty-seven cores from the marshes of the Patuxent River (Figure B-1). Other systems sampled include tidal freshwater marshes of the Eastern Shore's Choptank River and Otter Point Creek near the head of the Bay. For the sake of brevity the Monie Bay is included in this dissertation as Appendix A and will not be addressed in this Appendix.

## Site Descriptions

Brackish and tidal fresh marshes fringing the Patuxent River on the western shore of Chesapeake Bay were sampled (Figure B-1). Salinity was

generally about 1.0 ppt and tidal amplitudes in the area were approximately 0.8 m (Swarth and Peters 1993). Vegetation consisted of three species of *Spartina*, *Peltandra virginica*, *Nuphar advena*, *Arrow arum*, *Typha* spp., *Scirpus americanus*, *Hibiscus* spp., *Impatiens capensis*, and *Zizania aquatica*. Two general marsh elevations were sampled, low marshes dominated by *Nuphar advena* and *Peltandra virginica*, and higher marsh communities, dominated by *Scirpus americanus* and *Typha* species. Historical records indicate that in the 1600's ocean-going ships once navigated the Patuxent River through reaches which are now approximately one meter in depth at low tide (Kahn and Brush 1994) indicating extremely high rates of sedimentation, providing an enormous particulate supply to the marshes along the river banks.

Otter Point Creek is a tidal freshwater marsh located at the northern end of Chesapeake Bay, at the mouth of the Bush River (Figure B-1). Pasternack and Brush (1998) identified a linear shift with plant community with distance from open water, including pioneer mudflats, floating leaf, low marsh, middle marsh, high marsh and shrub marsh. Sediment loading at this site is high as a result of intense land clearing and the watershed is moderately developed (21% urban, Pasternack and Brush 1998).

Maryland's Choptank River was included as a representative of an agriculturally-dominated tidal freshwater marsh (Figure B-1). Total suspended solids and nutrient loads were high over a six year study period from 1986-1991 (Staver et al. 1996). An earlier sediment budget for the River

by Yarbro et al. (1983) found the largest sediment inputs were due to shore erosion, followed by upland runoff in the upper watershed due to agricultural activity. Marshes in the tidal freshwater region appeared to have a moderating effect on sediment loading from the watershed.

## METHODS

During the summers of 1993, 1994, and 1995, 1 m long cores were collected from the four subestuaries. A McAuley corer was used to minimize compaction (Bricker-Urso et al. 1989). Cores were immediately sectioned into 3, 5 and 10 cm subsamples, sealed, placed on ice, and returned to Horn Point Laboratory (HPL) for analysis. Volume was determined by the displacement of water. Wet bulk density was calculated for each sample by dividing the wet weight by the sample volume. Sediment was dried and weighed, and dry density was calculated by dividing the dry weight by the original sample volume. Sediment was ground with a mortar and pestle. Loss on ignition (LOI) was used as an indicator of organic matter content and was calculated as the percent of weight lost in a sample following the ignition of a subsample in a 550°C muffle furnace for 2.5 hours.

A known quantity of polonium tracer was added to 1 g of sample. Analysis of each core was carried out using either  $^{208}\text{Po}$  (activity) or  $^{209}\text{Po}$  (activity) for approximately half of the samples. Polonium-210 was extracted from the sediment using an acid digestion with concentrated  $\text{HNO}_3$  and  $\text{HCl}$  at

80-90°C (Sugai 1990). Centrifugation removed particles from the solution, which was repeatedly evaporated and diluted with 6 N HCl to replace nitrates which interfere with plating. A weak acid solution (0.10 N HCl) was used to increase the volume and create the plating solution. Iron interference was reduced by the addition of ascorbic acid. Both polonium isotopes were plated on silver and counted on an alpha counting system. Uncertainty associated with the counting system was always less than  $\pm 10\%$ . Measured  $^{208}\text{Po}$  or  $^{209}\text{Po}$  activity was used to calculate  $^{210}\text{Po}$  activity originating from the sediment sample by comparison of integrated peak values. Results from the two tracers were not significantly different (ANOVA F-test, alpha = 0.05).

Two models of  $^{210}\text{Pb}$  activity have been developed and are commonly used in sedimentation studies. The constant rate of supply (CRS) model relies on the assumption that  $^{210}\text{Pb}$  activity supplied to the sediment remains constant, but that the sedimentation rate may vary. The technique allows for increases (or decreases) in  $^{210}\text{Pb}$  activity with depth over short sections of the core due to concentration (or dilution) of the activity by varying amounts of deposited sediment. The constant initial concentration (CIC) model used on all data in the study is a linear regression model which assumes sedimentation rates have remained constant. Without the measurement of  $^{210}\text{Pb}$  activity of every section of each core, the CRS model is of limited value. Activities must be interpolated for the unknown sections since time and cost constrained the total number of samples which could be analyzed. Interpolating activities for these unmeasured sections results in sedimentation

estimates which are not different from the CIC model (Robbins 1978). In this study no significant difference was found using the different models ( $\alpha = 0.05$ ) which agrees with results presented by Bricker-Urso et al. (1989). A linear regression of the natural logarithm of unsupported activity with section depth generated the accretion rate at each site in depth per year. Using cumulative mass in the regressions generated sedimentation rates in terms of annual mass burial per unit area. Linear regressions of the data were accepted for calculation of sedimentation rate if the value of  $r^2$  was greater than 0.90.

## RESULTS

Twenty-two cores have been successfully dated on the Patuxent River, ranging from U.S. Route 4, south to King's Landing (Figure B-1). Lead-210 profiles clearly indicated exponential decay and were relatively uniform. Sedimentation rates vary from 1.1 to 25.4 mm  $y^{-1}$  (Table B-1).

Four transects of cores were collected in the Patuxent River system. The first was located in the Jug Bay NERR, on the northern shore of Jug Bay and consisted of three cores (Figure B-1). The first was located adjacent to the River, and consisted of very unconsolidated sediments, with a low organic matter content (%LOI=18) (Table B-1). Lead-210 dating at this site was successful, which is accreting at a rate of 2.2 cm  $y^{-1}$  (0.52 g  $cm^{-2} y^{-1}$ ,  $r^2 = 0.99$ ). The second site of this transect was located at mid-pier, but  $^{210}Pb$  data were

not explained adequately by the CIC model. No exponential decay in  $^{210}\text{Pb}$  activity was observed, most likely due to a combination of variable deposition, and bioturbation. Loss on ignition suggested a higher organic matter content (20%). The final site in the transect was taken from the edge of the upland vegetation. Organic matter content increased again, to 36% LOI. The sedimentation rate decreased to  $0.54 \text{ cm y}^{-1}$  ( $0.22 \text{ g cm}^{-2} \text{ y}^{-1}$ ,  $r^2 = 0.94$ ) (Table B-1).

Four cores composed Transect A, located south of Jug Bay (Figure B-1). The first core was taken 11 m from the River, and exhibited a constant profile of  $^{210}\text{Po}$ , preventing the determination of a sedimentation rate (Figure B-2). A second core was collected 30 inland, and exponential decay of  $^{210}\text{Pb}$  with depth was apparent. Sedimentation here is approximately  $1.1 \text{ cm y}^{-1}$  (Table B-1). Two cores were taken 50 m from the shoreline to determine small scale variability. Both were successfully dated and rates of 2.0 and  $1.8 \text{ cm y}^{-1}$  estimated. Background activities of  $^{210}\text{Pb}$  declined with distance from the River, with the interior cores reaching  $2.0 \text{ dpm g}^{-1}$  sediment  $^{226}\text{Ra}$  supported activity. Bulk density of the sediment also declined with distance from the River.

Transect B was collected from the western shore of the Patuxent River, north of Hall Creek (Figure B-1). Cores were collected 2, 11, 30, and 60 meters from the River. Exponential decay of  $^{210}\text{Pb}$  was found in all cores (Figure B-3). Rates of sedimentation were  $1.6$ ,  $0.31$ ,  $0.55$ , and  $0.41 \text{ cm y}^{-1}$  respectively and a constant decline in bulk density was found with distance

from the Patuxent River (Figure B-3). Radium-226 supported activities of  $^{210}\text{Pb}$  were all approximately 2.0 dpm g<sup>-1</sup> sediment.

Transect C was collected on the western shore of the River, just south of King's Landing (Figure B-1). Starting at the edge of the river, four cores were taken, each 30 m apart. The streamside site showed the highest rate of sedimentation, 0.62 cm y<sup>-1</sup> (0.31 g cm<sup>-2</sup> y<sup>-1</sup>,  $r^2=0.97$ ) (Table B-1). The sedimentation rate 30 m inland decreased to 0.11 cm y<sup>-1</sup> (0.01 g cm<sup>-2</sup> y<sup>-1</sup>,  $r^2=0.97$ ). At the two interior sites, 60 and 90 m inland, sedimentation rate remained constant at 0.20 and 0.21 cm y<sup>-1</sup> (0.03 g cm<sup>-2</sup> y<sup>-1</sup> for both cores,  $r^2=0.95, 0.99$ ). Supported  $^{210}\text{Po}$  activities at these sites ranged from 0.29 to 0.60 dpm g<sup>-1</sup> sediment (Figure B-4). The shallowest asymptotic value is in the core 30 m from the riverbank, in the 20-25 cm section. The remaining three cores reach their supported activity values below 70 cm. The riverbank core is the most variable of the four, indicating irregular sedimentation patterns at the River's edge. Organic matter increases steadily with distance from the River (Table B-1).

Cores collected from Otter Point Creek NERR had a higher bulk density and lower organic content than the other marshes studied (Table B-1). With a bulk density approaching that of sand (1.2 g cm<sup>-3</sup>) and low organic matter it appears that Otter Creek marshes are almost totally dependent upon external sources for mineral sediment supply to maintain surface elevation. Polonium-210 activity supported directly by the decay of  $^{226}\text{Ra}$  was approximately 0.7 dpm g<sup>-1</sup> sediment. Exponential decay was seen in the

three cores and rates of vertical accretion are between 0.21 and 1.02 cm y<sup>-1</sup> (Figure B-5).

Cores collected from the tidal fresh portion of the Choptank River showed exponential decay of <sup>210</sup>Po with depth, with minimal bioturbation (Figure B-6). Radium-226 supported activity was approximately 0.50 dpm g<sup>-1</sup> sediment. Sedimentation rates were high, ranging from 0.61 to 1.07 cm y<sup>-1</sup>, with the upstream site accreting more slowly than the two lower sites (Table B-1). Organic matter content and bulk density of the Choptank River marshes were in the middle of the range of values found within the Chesapeake Bay marshes.

## DISCUSSION

### <sup>210</sup>Pb Observations

Supported <sup>210</sup>Pb activities varied between marsh systems in the Chesapeake Bay. Patuxent River marsh sediment supported activities ranged from 0.5 to 2.0 dpm g<sup>-1</sup> sediment. Low values of 0.5 dpm g<sup>-1</sup> sediment were found in Transect C, the southern-most transect, while the highest supported values were found in Transect B (2.0 dpm g<sup>-1</sup> sediment). At other points along the Patuxent River the supported activity was approximately 1.0 dpm g<sup>-1</sup> sediment. All three cores from the Otter Point Creek marshes

maintained a supported activity of 0.4 dpm g<sup>-1</sup> sediment. Choptank River marshes had a slightly lower supported <sup>210</sup>Pb activity of 0.2 dpm g<sup>-1</sup> sediment.

While the examination of <sup>210</sup>Pb profiles is a proven method for the determination of sedimentation rates in marshes (i.e.: Armentano and Woodwell 1975, DeLaune et al. 1989), the absolute activities vary with many local effects. Because it originates in the atmosphere, the supply of <sup>210</sup>Pb to marsh sediments is linked to the wet and dryfall of the surroundings (Krishnaswami and Lal 1978). Increases in precipitation can increase the amount of <sup>210</sup>Pb ultimately supplied to the marsh sediments. In addition, the supply of <sup>210</sup>Pb activity to the atmosphere varies with location, and can depend upon local soil characteristics, and atmospheric pressure (Krishnaswami and Lal 1978). Prevailing wind patterns can transport this <sup>210</sup>Pb to different locations, impacting its regional distribution. These variables can account for the small differences in absolute values found at the study sites.

Noise in the <sup>210</sup>Pb profiles can be associated with bioturbation of the sediments, and variations in supply. Variability was seen in the level of <sup>226</sup>Ra supported <sup>210</sup>Pb activity across the surface of the Patuxent River marshes. At the Lyon's Creek transect higher supported activities were seen near the River. Maximum unsupported activities, the depth at which the supported value is located, and the associated activity are all dependent on atmospheric, physical and biological characteristics of the surrounding system. The depth at which unsupported activity drops to negligible is

dependent upon the sedimentation rate and organic matter in the sediments. With increasing sedimentation rates,  $^{210}\text{Pb}$  asymptotic values will be reached deeper in the cores. Lead-210 activity is diluted at sites with high burial rates, and in the marshes most of this dilution appeared to be the result of organic matter burial.

## Sedimentation Patterns

Apparent sea level rise in the Chesapeake has been estimated at 0.39 cm  $\text{y}^{-1}$  (Stevenson et al. 1985). With a few exceptions, the marshes sampled in this study were accreting at a faster pace than sea level rise, with many of the highest rates found in the Patuxent River. An average sedimentation rate of 0.95 cm  $\text{y}^{-1}$  ( $n = 22$ ,  $sd = 0.712$ ), and 0.36 g  $\text{cm}^{-2} \text{y}^{-1}$  ( $n = 22$ ,  $sd = 0.274$ ) was calculated including all Patuxent River sites. Spatial heterogeneity of the marshes is reflected in the high variability found in the standard deviation. No discernable pattern was found in sedimentation rates along the longitudinal axis of the River.

Marsh transects taken within the Patuxent River system show distinct patterns in the deposition rates and characteristics. All of the transects exhibit higher rates of sedimentation at the sites closest to the River, and drop as much as 80% at interior marsh sites. Similar results are reported for salt marshes (DeLaune et al. 1981, Craft et al. 1993) and freshwater marshes (Craft and Richardson 1993). Slower accretion results from decreased

supplies of suspended sediment, as seen in the increase in sediment organic content with distance from the River (Table B-1). Increased organic matter at interior sites supports the hypothesis that the marsh is sustained by the burial of organic matter (Stevenson et al. 1985, Bricker-Urso et al. 1989). This suggests that primary production by marsh plants may be a limiting factor in the accretion rates of interior marsh sites.

Calculated accretion rates in this study are comparable to those found by other researchers. Similarly high accretion rates are reported in Louisiana marshes (DeLaune 1981). Rates of  $13.5 \text{ mm y}^{-1}$  were found for a streamside marsh using  $^{137}\text{Cs}$  as a radioisotopic tracer. An earlier study (Armentano and Woodwell 1975) found accretion rates ranging from 4.7 to  $6.3 \text{ mm y}^{-1}$  in marshes on Long Island surrounding Flax Pond. A study by Sharma et al. (1987) reports accretion rates of  $1.4\text{-}4.5 \text{ mm y}^{-1}$  for a salt marsh in South Carolina using  $^{210}\text{Pb}$  as a tracer.

The marshes of the Patuxent River significantly reduce particulates in the water of the estuary. Roberts and Pierce (1976) report sediment loading of  $2.15 \times 10^8 \text{ kg y}^{-1}$ , measured in the region of the uppermost site in this study. Integrated over the surface area of the marsh, annual burial is approximately  $3.83 \times 10^7 \text{ kg}$ , suggesting the marshes can retain as much as 18% of the sediment delivered by the water of the upper Patuxent River Estuary.

These results highlight the need for studies of individual marshes within the Chesapeake Bay ecosystem. While marshes such as Blackwater

marsh, on the eastern shore of the Bay, have been determined to be rapidly subsiding (Stevenson et al. 1986) other riverine marshes are building sufficiently to prevent inundation (Kearney et al. 1994, Kahn and Brush 1994).

Accretion mechanisms and sources of sedimentary material will play a major role in the determination of the fate of individual marshes within the Chesapeake Bay region. The sites in this study are located within riparian tidal marsh systems. Delivery of mineral matter to these marshes via riparian transport may be what allows for the marsh accretion at the riverbanks and the development of levees.

Tidal freshwater marshes may be extremely important component of Chesapeake Bay sediment budgets, such as that presented by Hobbs et al. (1992) (Table B-2). Tidal freshwater marshes in this study retain  $0.345 \text{ g cm}^{-2} \text{ y}^{-1}$  ( $n=28$ ,  $sd = 0.250$ ), 28.6% of which is organic material. Therefore, the  $106 \text{ km}^2$  of Chesapeake Bay marshes may trap  $2.61 \times 10^8 \text{ kg y}^{-1}$  of mineral matter. Hobbs et al. (1992) report  $2.6 \times 10^6$  metric tons of mud are delivered over 100 years from the Susquehanna River to the Chesapeake Bay. If sedimentation rates are constant over this 100 year time-frame, the tidal freshwater marshes have retained the equivalent of 25% of the suspended sediment delivered by the Susquehanna River.

Clearly the upper estuarine tidal freshwater marshes play an important role in the sediment budget of Chesapeake Bay. More detailed mapping of the marshes, elevation and sediment characteristics, would allow for a more

**constrained estimate, but even with uncertainty presented by this approach  
the importance of upper estuarine marshes as sediment traps is apparent.**

Table B-1. Accretion rates and relative organic content of marsh sediment in three tidal freshwater marsh systems of the Chesapeake Bay. Locations correlate to Figure B-1. Linear regressions were performed on natural log transformed excess  $^{210}\text{Pb}$  activity with depth and cumulative mass to generate sedimentation rates. The number of data points (n) and  $r^2$  value are given, as is the percent mass loss on ignition (%LOI) of the sediment at 550°C.

	Site	$\text{cm y}^{-1}$	$\text{g cm}^{-2}\text{y}^{-1}$	$r^2$	n	% LOI
Otter Point Creek	1	1.02	0.53	0.92	6	13.7
	2	0.21	0.12	0.96	4	11.8
	3	0.27	0.24	0.97	4	10.7
Patuxent River	1	0.76	0.51	0.97	5	22.8
	2	0.23	0.14	0.91	5	19.1
	3	0.66	0.40	0.98	5	32.6
	4	--	--	--	-	18.5
	5	2.54	0.86	0.97	5	22.3
	6	1.34	0.42	0.97	5	33.9
	7	0.44	0.08	0.98	3	55.0
	8	1.28	0.69	0.91	7	21.3
	9	0.85	0.17	0.99	3	48.9
	10	--	--	--	-	14.6
	11	--	--	--	-	18.1
	12	0.79	0.33	0.98	5	21.8
Jug Bay, Patuxent	1	2.19	0.52	0.99	4	18.0
	2	--	--	--	-	20.0
	3	0.54	0.22	0.94	6	36.2
Patuxent Transect A	11 m	--	--	--	--	20.7
	30 m	1.70	0.60	0.97	7	21.6
	50 m	1.81	0.63	0.96	6	26.1
	50 m	1.89	0.54	0.90	5	26.2
Patuxent Transect B	2 m	1.59	0.93	0.94	6	17.8
	11 m	0.31	0.11	0.84	5	22.8
	30 m	0.55	0.20	0.90	7	31.1
	60 m	0.41	0.11	0.98	6	38.6
Patuxent Transect C	0 m	0.62	0.31	0.97	4	17.5
	30 m	0.11	0.01	0.97	5	50.1
	60 m	0.20	0.03	0.95	5	64.8
	90 m	0.21	0.03	0.99	4	66.2
Choptank River	1	0.61	0.24	0.91	5	26.9
	2	1.09	0.40	0.99	4	19.5
	3	1.07	0.28	0.93	4	31.3

**Table B-2. Chesapeake Bay sediment budget comparison to tidal freshwater marsh burial estimates.**

Tidal freshwater marsh area in Chesapeake Bay <sup>1</sup>	106 km <sup>2</sup>
Average deposition of 3 Tidal freshwater marsh systems	0.345 g cm <sup>-2</sup> y <sup>-1</sup>
Corrected for average %LOI	2.56 kg mineral material m <sup>-2</sup> y <sup>-1</sup>
Total Tidal Freshwater Marsh Mineral Deposition	2.71 x 10 <sup>8</sup> kg mineral matter y <sup>-1</sup>
Susquehanna Average Annual suspended sediment load <sup>2</sup>	10.7 x 10 <sup>8</sup> kg y <sup>-1</sup>
Average percent retained in Tidal Freshwater marsh sediment	25%

<sup>1</sup>Tidal freshwater marsh acreage from Field et al. 1991, NOAA 20<sup>th</sup> Anniversary.

<sup>2</sup>Loading rate from Hobbs et al. 1992.

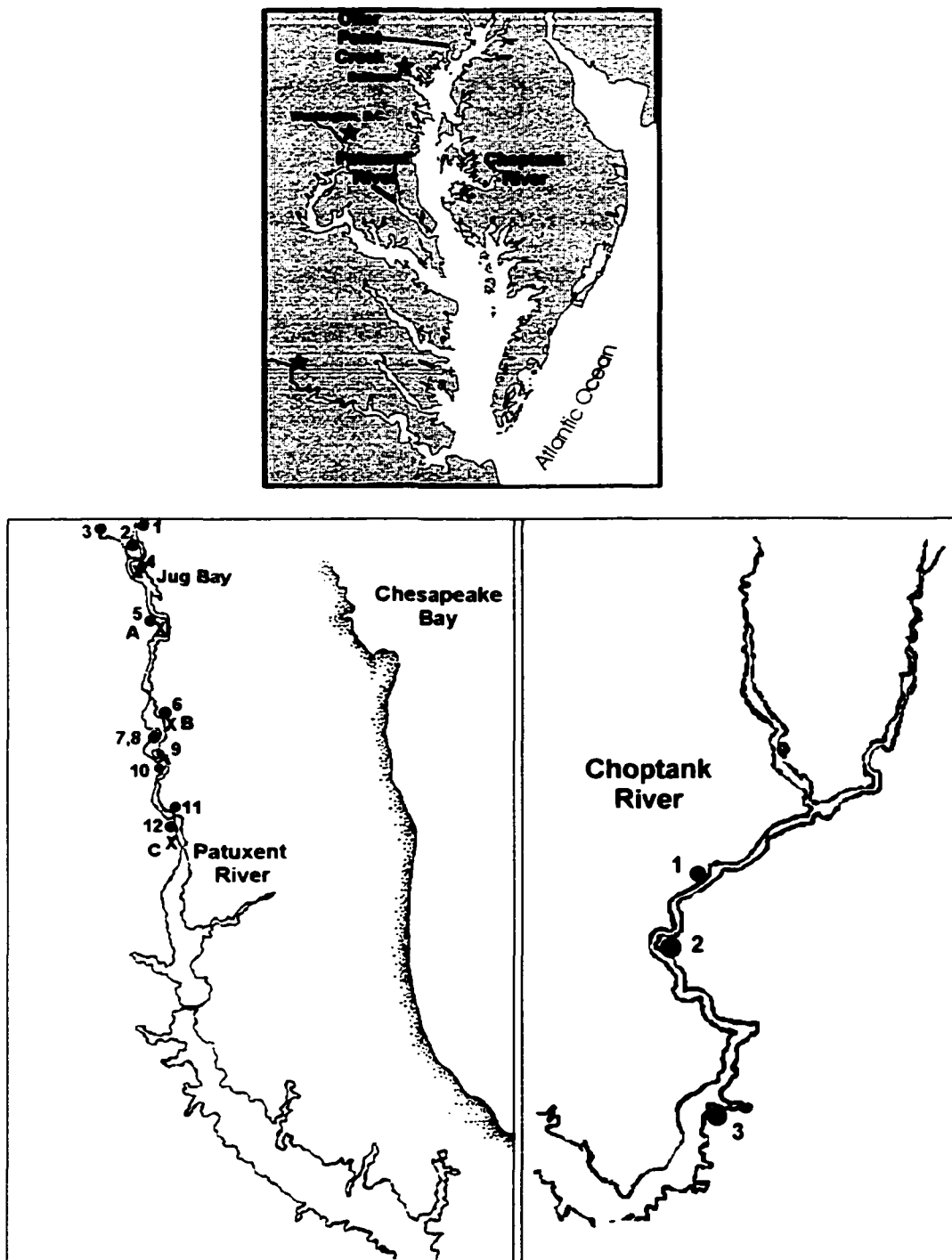


Figure B-1. Sedimentation study locations on the Chesapeake Bay. Marsh systems included the Patuxent River Estuary, Otter Point Creek, and the Choptank River.

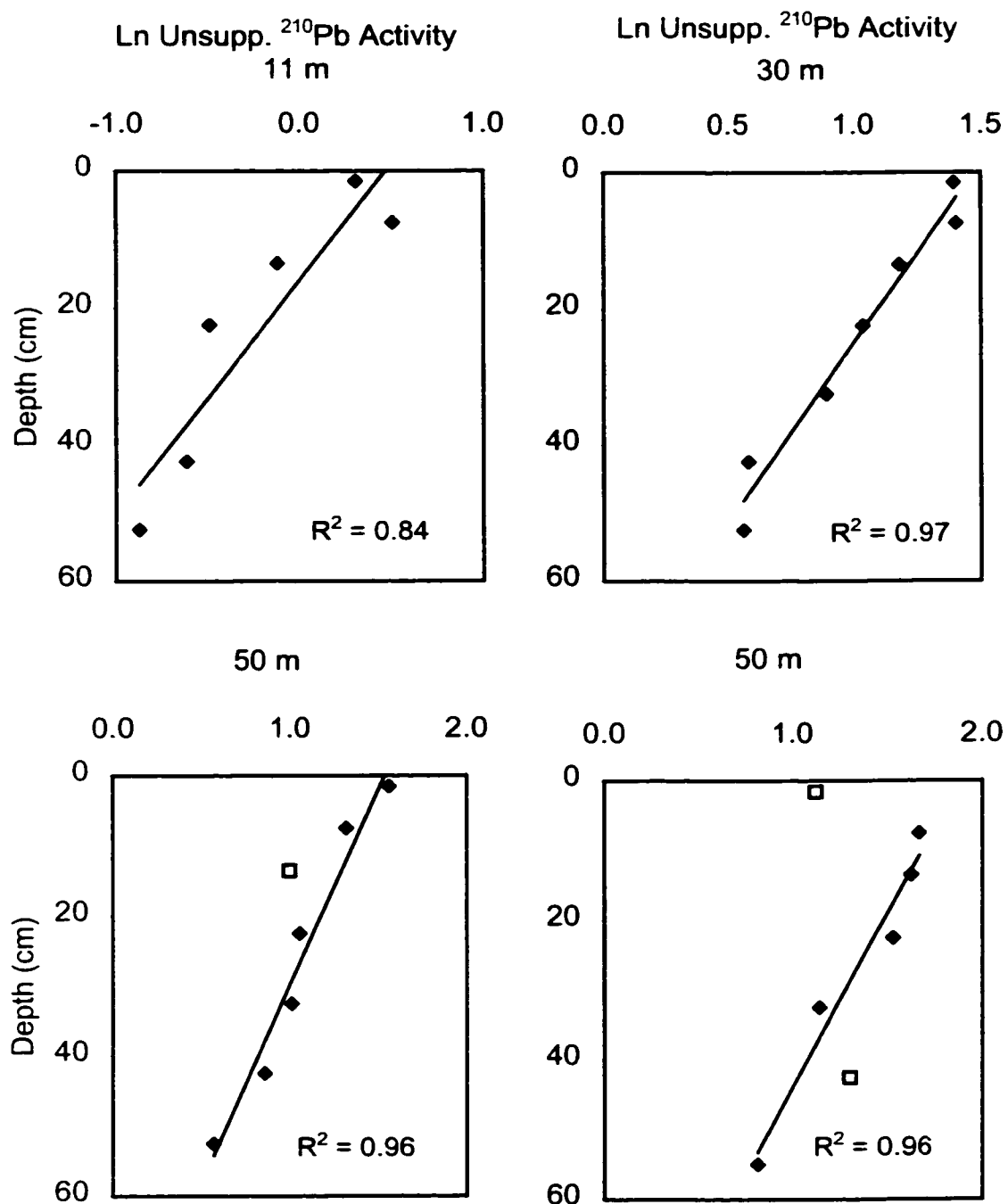


Figure B-2. Constant input concentration (CIC) models with  $^{210}\text{Pb}$  data from Transect A on the Patuxent River, distance from River is shown. Open symbols were data attributed to mixing and left out of regressions.

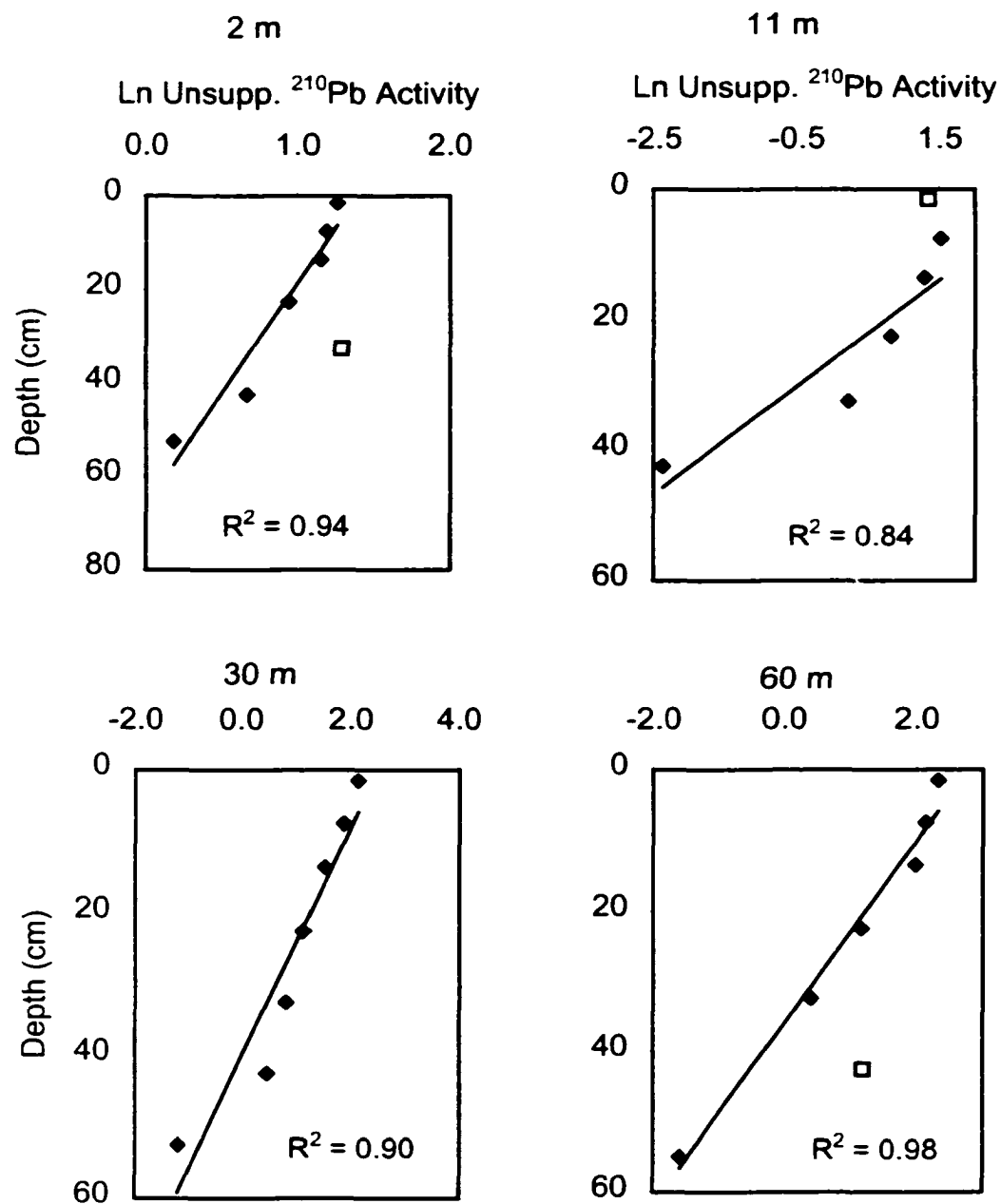


Figure B-3. Constant input concentration (CIC) models with  $^{210}\text{Pb}$  data from Transect B on the Patuxent River, distance from River is shown. Open symbols were data attributed to mixing and left out of regressions.

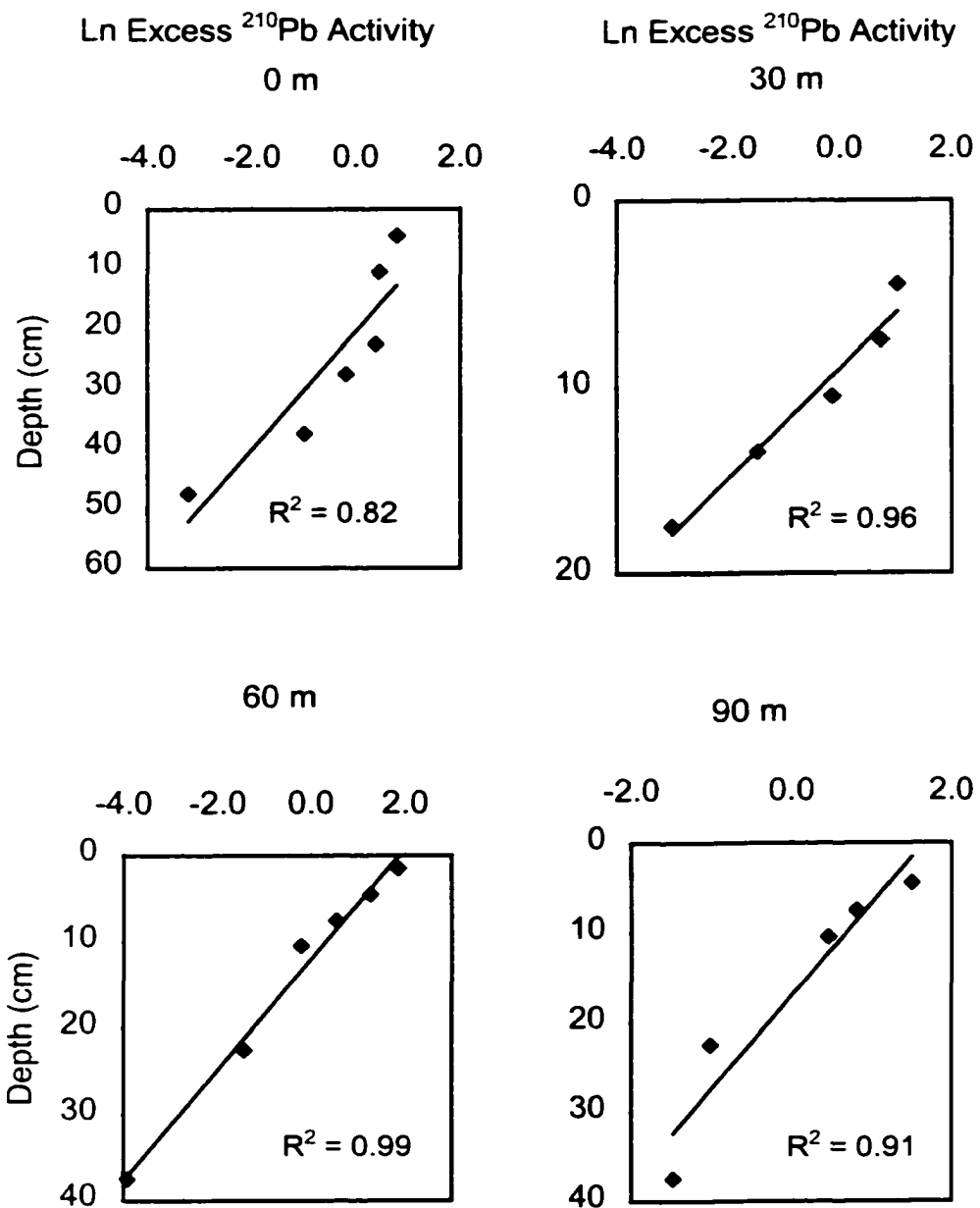


Figure B-4. Patuxent River Transect C natural log of excess  $^{210}\text{Pb}$  profiles (dpm per gram sediment). The line indicates CIC model prediction.

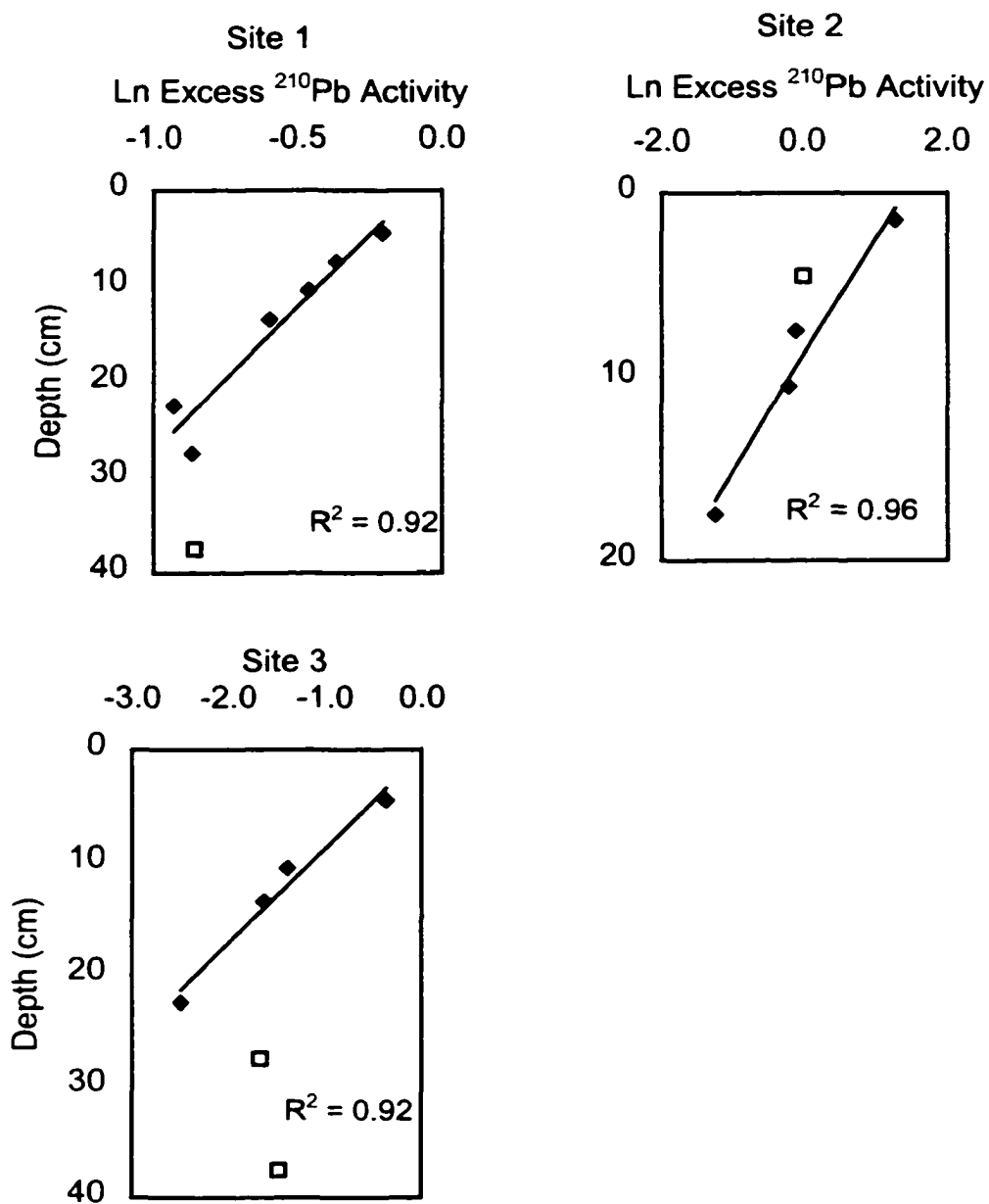


Figure B-5. Otter Point Creek profiles of the natural log of excess  $^{210}\text{Pb}$  activity ( $\text{dpm g}^{-1}$  sediment). CIC models are shown.

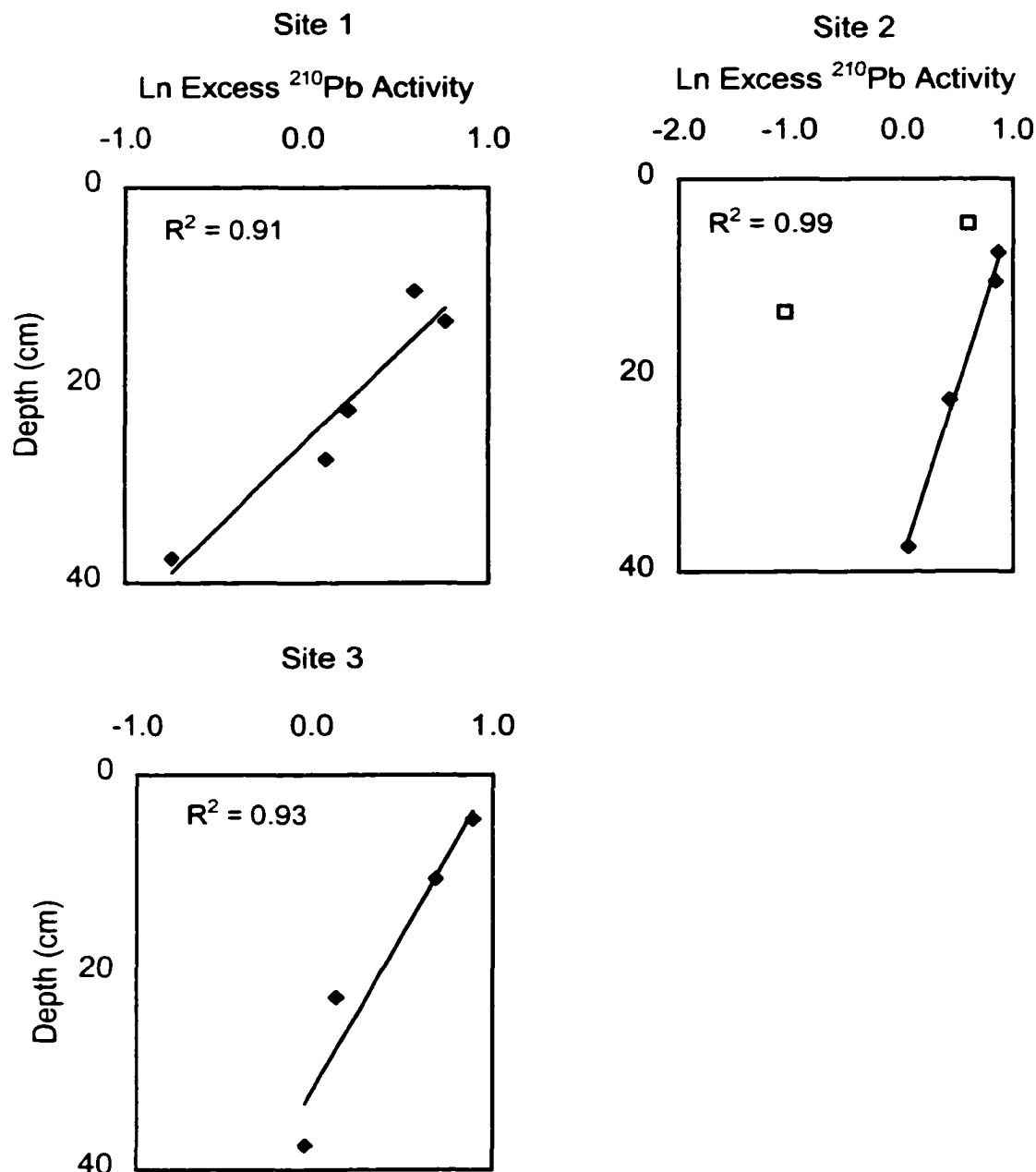


Figure B-6. Constant input concentration (CIC) models for the determination of sedimentation rates in Choptank River tidal freshwater marshes. The natural logarithm of excess  $^{210}\text{Pb}$  profiles is shown. Activity given as dpm per gram sediment. Open symbols were attributed to post-depositional mixing and were not included in the regressions.

## **Appendix C: Sediment Characteristics, Nutrients, Metals and $^{210}\text{Pb}$ in Five Coastal Wetlands**

Table C-1. Sediment characteristics in Patuxent River, Otter Point Creek, Choptank River, Monie Bay and Tivoli Bays, Hudson River tidal freshwater and oligohaline marshes. Date of collection is indicated in top left corner and locations are shown in Figure C-1. Cores were sectioned as indicated in columns two and three. Percent water was determined by weighing fresh sample, subtracting the weight of the oven-dried sample, dividing by the weight of the fresh sample and multiplying by 100. Wet and dry sample density were calculated using sample volume as determined by water volume displacement before drying the sample. Percent loss on ignition was the percent weight lost by combusting a subsample at 550°C for 2.5 hours. Site descriptions are given under each section of the table.

## PATUXENT RIVER

	Sample Depth		% Water	Wet Sample Density g cm <sup>-3</sup>	Dry Sample Density g cm <sup>-3</sup>	Average Dry Density to 25 cm g cm <sup>-3</sup>	% Weight Lost On Ignition % LOI	Average % LOI to 50 cm
	Top cm	Bottom cm						
Site 1	0	3	75.09	1.10	0.27	0.442	31.77	18.029
	3	6	73.70	1.14	0.30		28.91	
	6	9	68.98	1.19	0.37		22.65	
	9	12	61.99	1.27	0.48		18.98	
	12	15	59.31		0.51		17.94	
	15	20	59.82	1.35	0.54		19.64	
	20	25	61.11	1.30	0.50		22.11	
	25	30	55.14	1.38	0.62		21.27	
	30	35	47.69	1.54	0.80		10.81	
	35	40	47.59	1.55	0.81		11.86	
	40	45	47.76	1.57	0.82		12.19	
	45	50	46.59	1.60	0.86		10.27	
	50	60	68.82	1.26	0.39		16.54	
	70	80	46.49	1.53	0.82		9.12	
	90	100	39.51	1.62	0.98		9.77	
	100	110	50.45	1.42	0.70		12.19	
	120	130	55.41	1.32	0.59		16.10	
	140	150	51.08	1.39	0.68		15.13	

Site 1 was the upper boundary of sampling in the Patuxent River, located near the head of the tide just north of U.S. Route 4.

## PATUXENT RIVER

6/16/94	Sample Depth		% Water	Wet Sample Density g cm <sup>-3</sup>	Dry Sample Density g cm <sup>-3</sup>	Average Dry Density to 25 cm g cm <sup>-3</sup>	% Weight Lost On Ignition % LOI	Average % LOI to 50 cm
	Top cm	Bottom cm						
Site 2	0	3	77.95	1.11	0.24	0.477	28.28	14.930
	3	6	73.90	1.15	0.30		21.01	
	6	9	79.01	1.05	0.22		43.57	
	9	12	73.85	1.12	0.29		24.27	
	12	15	58.97	1.27	0.52		12.52	
	15	20	49.08	1.58	0.81		7.43	
	20	25	55.61	1.43	0.63		10.21	
	25	30	49.17	1.49	0.76		8.35	
	30	35	59.66	1.36	0.55		9.61	
	35	40	53.81	2.64	1.22		3.21	
	40	45	67.41	1.27	0.41		15.39	
	45	50	73.03	1.22	0.33		17.30	
	50	60	71.17	1.24	0.36		15.87	
	70	80	49.36	1.49	0.76		7.24	
	90	100	43.14	2.76	1.57		10.43	
	100	110	36.90	1.62	1.02		9.74	
	120	130	34.17	1.70	1.12		5.87	
	140	150	39.31	1.58	0.96			

Site 2 was located on the western bank of the Western Branch tributary.

## PATUXENT RIVER

	Sample Depth		% Water	Wet Sample Density g cm <sup>-3</sup>	Dry Sample Density g cm <sup>-3</sup>	Average Dry Density to 25 cm g cm <sup>-3</sup>	% Weight Lost On Ignition % LOI	Average % LOI to 50 cm
	Top cm	Bottom cm						
Site 3	0	3	79.58	1.02	0.21	0.397	42.14	24.233
	3	6	77.34	1.02	0.23		44.76	
	6	9	77.94	1.04	0.23		50.37	
	9	12	69.72	1.19	0.36		29.86	
	12	15	62.57	1.22	0.46		25.13	
	15	20	60.98	1.35	0.53		24.52	
	20	25	57.54	1.33	0.56		23.19	
	25	30	52.07	1.44	0.69		20.26	
	30	35	50.82	1.41	0.69		15.77	
	35	40	48.61	1.47	0.75		14.52	
	40	45	38.42	1.60	0.99		18.23	
	45	50	42.50	1.64	0.95		10.49	
	50	60	41.80	1.56	0.91		11.25	
	70	78	39.72	1.63	0.98		9.02	

Site 3 was located on the Western Branch tributary, upstream of site 2.

## PATUXENT RIVER

9/2/93	Sample Depth		% Water	Wet Sample Density g cm <sup>-3</sup>	Dry Sample Density g cm <sup>-3</sup>	Average Dry Density to 25 cm g cm <sup>-3</sup>	% Weight Lost On Ignition % LOI	Average % LOI to 50 cm
	Top cm	Bottom cm						
Site 4	0	3	79.51	0.96	0.20	0.375	25.92	16.206
	3	6	91.62	0.86	0.07		28.69	
	6	9	65.89	1.08	0.37		18.93	
	9	12	68.80	1.09	0.34		17.10	
	12	15	60.33	1.18	0.47		14.83	
	15	20	59.10	1.26	0.51		13.87	
	20	25	59.97	1.24	0.50		15.51	
	25	30	56.87	1.28	0.55		13.51	
	30	35	58.90	1.24	0.51		14.50	
	35	40	55.57	1.25	0.55		14.38	
	40	45	53.59	1.34	0.62		13.54	
	45	50	52.74	1.32	0.62		13.46	
	50	60	52.28	1.39	0.66		13.12	
	70	80	51.08	1.41	0.69		11.79	
	90	100	55.32	1.28	0.57		16.65	
	100	110	61.31	1.31	0.51		16.67	
	120	130	68.24	1.22	0.39		23.19	
	140	150	65.99	1.25	0.43		18.56	

Site 4 was located off the tip of the catwalk from the north side of the Jug Bay NERRS railroad bed. The site was dominated by *Zizania aquatica*.

PATUXENT RIVER

	6/16/94	Sample Depth		% Water	Wet Sample Density g cm <sup>-3</sup>	Dry Sample Density g cm <sup>-3</sup>	Average Dry Density to 25 cm g cm <sup>-3</sup>	% Weight Lost On Ignition	Average % LOI to 50 cm % LOI
		Top cm	Bottom cm						
<b>Site 5</b>									
	0	3	77.66	1.18	0.26	0.327	27.09	23.057	
	3	6	78.72	1.11	0.24		27.57		
	6	9	68.31	1.18	0.37		30.18		
	9	12	68.98	1.18	0.37		17.93		
	12	15	70.35	1.22	0.36		19.48		
	15	20	70.97	1.24	0.36		17.63		
	20	25	74.27	1.23	0.32		20.73		
	25	30	78.88	1.17	0.25		26.51		
	30	35	76.17	1.19	0.28		23.16		
	35	40	74.03	1.21	0.32		25.31		
	40	45	73.02	1.24	0.34		24.76		
	45	50	66.68	1.30	0.43		19.14		
	50	60	76.62	1.17	0.27		26.66		
	70	80	70.64	1.23	0.36		22.73		
	90	100	73.44	1.21	0.32		30.75		
	100	110	68.12	1.19	0.38		36.56		
	120	130	75.52	1.16	0.28		33.12		
	140	150	76.75	1.13	0.26		36.24		

PATUXENT RIVER

		Sample Depth	% Water	Wet Sample Density g cm <sup>-3</sup>	Dry Sample Density 9 cm <sup>-3</sup>	Average Dry Density to 25 cm g cm <sup>-3</sup>	% Weight Lost On Ignition	Average % LOI to 50 cm % LOI
		Top cm	Bottom cm					
<b>Site 6</b>	0	3	74.63	1.13	0.29	0.250	29.06	33.939
	3	6	78.22	1.03	0.22		36.79	
	6	9	76.47	1.16	0.27		30.00	
	9	12	73.45	1.20	0.32		25.52	
	12	15	--	--	0.26		28.84	
	15	20	80.74	1.02	0.20		39.18	
	20	25	77.57	1.05	0.24		39.93	
	25	30	77.45	1.13	0.25		38.79	
	30	35	76.59	1.10	0.26		35.97	
	35	40	77.32	1.09	0.25		36.30	
	40	45	77.76	1.09	0.24		31.40	
	45	50	74.05	1.16	0.30		27.70	
	50	60	67.93	1.20	0.38		23.88	
	70	80	66.95	1.20	0.40		27.49	
	90	100	69.56	1.17	0.35		29.53	
	100	110	72.86	1.13	0.31		33.87	
	120	130	75.45	1.16	0.28		57.36	
	140	150	65.50	1.27	0.44		20.92	

PATUXENT RIVER

		Sample Depth	% Water	Wet Sample Density g/cm <sup>3</sup>	Dry Sample Density g/cm <sup>3</sup>	Average Dry Density to 25 cm g/cm <sup>3</sup>	% Weight Lost On Ignition % LOI	Average % LOI to 50 cm
		Top cm	Bottom cm					
Site 7	0	3	85.32	0.97	0.14	0.163	63.81	39.126
	3	6	82.70	1.01	0.17		51.19	
	6	9	81.18	1.04	0.20		51.81	
	9	12	83.67	1.07	0.17		56.63	
	12	15	86.57	1.01	0.14		66.86	
	15	20	88.69	1.10	0.12		52.35	
	20	25	82.41	1.11	0.20		48.26	
	25	30	77.61	1.15	0.26		38.06	
	30	35	62.63	1.34	0.50		21.89	
	35	40	57.59	1.38	0.58		17.02	
	40	45	58.60	1.41	0.58		17.94	
	45	50	64.71	1.34	0.47		21.56	
	50	60	73.50	1.17	0.31		28.96	
	70	80	61.11	1.22	0.47		29.96	
	90	100	80.74	1.10	0.21		35.06	

PATUXENT RIVER

		Sample Depth Top cm	% Water Bottom cm	Wet Sample Density g cm <sup>-3</sup>	Dry Sample Density g cm <sup>-3</sup>	Average Dry Density to 25 cm g cm <sup>-3</sup>	% Weight Lost On Ignition % LOI	Average % LOI to 50 cm
<b>Site 8</b>	0	2	82.12	1.10	0.20	0.312	23.09	17.890
	2	4	79.41	1.13	0.23		22.83	
	4	6	78.80	1.13	0.24		22.78	
	6	8	73.52	1.14	0.30		21.70	
	8	10	71.03	1.19	0.34		21.87	
	10	12	69.55	1.24	0.38		24.18	
	14	16	64.66	1.17	0.41		23.07	
	16	18	65.08	1.19	0.42		25.71	
	18	20	58.74	1.30	0.54		21.06	
	20	25	54.78	1.40	0.63		15.55	
	25	30	52.87	1.43	0.67		14.41	
	30	35	53.40	1.44	0.67		14.12	
	35	40	—	1.49	0.64		13.38	
	40	45	56.70	1.41	0.61		15.37	
	45	50	57.24	1.39	0.59		14.11	
	50	60	55.11	1.35	0.61		16.44	
	70	80	56.34	1.33	0.58		17.80	
	90	100	54.65	1.37	0.62		17.49	

PATUXENT RIVER

	Sample Depth Top cm	% Water Bottom cm	Wet Sample Density g cm. <sup>-3</sup>	Dry Sample Density g cm. <sup>-3</sup>	Average Dry Density to 25 cm g cm. <sup>-3</sup>	% Weight Lost On Ignition % LOI	Average % LOI to 50 cm
<b>Site 9</b>	0	3	80.29	1.04	0.20	0.177	30.21
	3	6	79.86	1.10	0.22		32.41
	6	9	82.36	1.03	0.18		35.38
	9	12	81.78	1.07	0.20		30.36
	12	15	83.21	1.03	0.17		49.54
	15	20	82.79	1.01	0.17		62.60
	20	25	87.14	0.98	0.13		74.98
	25	30	88.92	0.95	0.10		69.13
	30	35	89.30	1.03	0.11		77.93
	35	40	91.18	1.01	0.09		81.07
	40	45	90.82	1.04	0.10		81.05
	45	50	90.84	1.00	0.09		77.87
	50	60	93.56	1.05	0.07		86.17
	60	70	92.86	1.04	0.07		88.02
	70	80	93.60	1.04	0.07		87.48
	80	100	90.61	1.01	0.09		79.30
	100	110	91.61	0.71	0.06		80.43
	110	120	86.26	0.73	0.10		59.20
	120	130					
	130	140					
	140	150					

PATUXENT RIVER

		Sample Depth	% Water	Wet Sample Density g cm <sup>-3</sup>	Dry Sample Density g cm <sup>-3</sup>	Average Dry Density to 25 cm g cm <sup>-3</sup>	% Weight Lost On Ignition	Average % LOI to 50 cm % LOI
		Top cm	Bottom cm					
Site 10	0	3	64.04	1.32	0.47	0.491	15.27	14.799
	3	6	62.79	1.24	0.46		14.16	
	6	9	62.89	1.24	0.46		14.29	
	9	12	69.43	1.21	0.37		18.66	
	12	15	59.98	1.31	0.52		13.35	
	15	20	60.65	1.34	0.53		13.88	
	20	25	59.80	1.37	0.55		13.69	
	25	30	60.39	1.38	0.55		14.09	
	30	35	59.39	1.32	0.54		13.71	
	35	40	59.96	1.34	0.53		15.72	
	40	45	59.85	1.35	0.54		15.73	
	45	50	61.53	1.37	0.53		15.74	
	50	60	61.78	1.31	0.50		16.39	
	70	80	58.57	1.34	0.56		14.71	
	90	100	54.98	1.40	0.63		14.26	
	100	110	63.32	1.26	0.46		17.83	
	120	130	56.73	1.32	0.57		15.07	
	140	150	54.74	1.36	0.62		12.13	

PATUXENT RIVER

		Sample Depth	% Water	Wet Sample Density g cm <sup>-3</sup>	Dry Sample Density 9 cm <sup>-3</sup>	Average Dry Density to 25 cm g cm <sup>-3</sup>	% Weight Lost On Ignition % LOI	Average % LOI to 50 cm
		Top cm	Bottom cm					
<b>Site 11</b>	0	3	66.99	1.16	0.38	0.417	24.07	18.370
	3	6	72.13	1.15	0.32			18.98
	6	9	69.68	1.17	0.35			18.90
	9	12	64.36	1.23	0.44			16.20
	12	15	68.09	1.21	0.39			18.21
	15	20	65.11	1.29	0.45			17.22
	20	25	61.97	1.32	0.50			15.24
	25	30	61.61	1.31	0.50			15.30
	30	35	68.28	1.23	0.39			23.88
	35	40	68.35	1.19	0.38			23.32
	40	45	59.37	1.36	0.55			15.17
	45	50	56.12	1.39	0.61			15.75
	50	60	57.10	1.37	0.59			15.17
	70	80	56.24	1.36	0.60			17.27
	90	100	57.55	1.39	0.59			12.96
	100	110	55.22	1.36	0.61			13.37
	120	130	48.49	1.43	0.74			11.54
	140	150	50.04	1.41	0.71			12.36

PATUXENT RIVER

	Sample Depth Top cm	Bottom cm	% Water	Wet Sample Density g cm <sup>-3</sup>	Dry Sample Density 9 cm <sup>-3</sup>	Average Dry Density to 25 cm g cm <sup>-3</sup>	% Weight Lost On Ignition % LOI	Average % LOI to 50 cm
<b>Site 12</b>	0	3	76.71	1.20	0.28	0.372	26.92	21.453
	3	6	73.32	0.31	0.34		22.00	
	6	9	71.09	1.16	0.34		22.90	
	9	12	70.96	1.17	0.34		22.91	
	12	15	67.91	1.19	0.38		24.78	
	15	20	67.57	1.27	0.41		19.03	
	20	25	65.27	1.32	0.46		18.00	
	25	30	66.83	1.30	0.43		19.12	
	30	35	..	..	0.41		21.22	
	35	40	69.12	1.27	0.39		23.03	
	40	45	68.31	1.28	0.40		20.57	
	45	50	68.25	1.28	0.41		21.84	
	50	60	63.64	1.31	0.48		18.25	
	70	80	72.71	1.16	0.32		32.25	
	90	100	65.65	1.28	0.44		20.23	
	100	110	80.04	1.09	0.22		42.80	
	120	130	69.14	1.18	0.36		29.43	
	140	150	69.60	1.19	0.36		23.94	

## PATUXENT RIVER

9/2/93	Sample Depth		% Water	Wet Sample Density g cm <sup>-3</sup>	Dry Sample Density g cm <sup>-3</sup>	Average Dry Density to 25 cm g cm <sup>-3</sup>	% Weight Lost On Ignition % LOI	Average % LOI to 50 cm
	Top cm	Bottom cm						
Jug Bay 1 High marsh	0	3	76.28	1.08	0.26	0.223	33.55	34.218
	3	6	75.99	1.02	0.25		33.01	
	6	9	75.98	1.07	0.26		32.07	
	9	12	78.94	1.02	0.21		34.13	
	12	15	79.26	1.04	0.22		38.66	
	15	20	80.20	1.06	0.21		40.18	
	20	25	81.44	1.04	0.19		37.70	
	25	30	76.38	1.06	0.25		31.22	
	30	35	77.69	1.10	0.24		33.72	
	35	40	78.01	1.10	0.24		32.80	
	40	45	75.24	1.11	0.27		28.65	
	45	50	79.87	1.01	0.20		35.06	
	50	60	78.39	1.08	0.23		39.54	
	70	80	78.26	1.11	0.24		52.59	
	90	100	80.25	1.06	0.21		43.26	
	100	110	79.12	1.08	0.23		44.92	
	120	130	74.97	1.13	0.28		36.50	
	140	150	71.62	1.20	0.34		30.31	

Jug Bay site1 was located at the upland border of the Jug Bay NERRS marsh boardwalk where *Typha* spp. and *Hibiscus* spp. were present.

## PATUXENT RIVER

9/2/93	Sample Depth		% Water	Wet Sample Density g cm <sup>-3</sup>	Dry Sample Density g cm <sup>-3</sup>	Average Dry Density to 25 cm g cm <sup>-3</sup>	% Weight Lost On Ignition % LOI	Average % LOI to 50 cm
	Top cm	Bottom cm						
Jug Bay 2	0	2	78.68	0.93	0.20	0.287	22.41	
	2	4	72.74	1.03	0.28		17.01	
	4	6	74.94	0.89	0.22		22.22	
	6	8	75.34	1.37	0.34		20.38	
	8	10	73.13	1.12	0.30		17.54	
	10	15	70.15	1.09	0.33		18.13	
	15	20	72.47	1.11	0.31		22.12	
	20	25	64.64	1.19	0.42		20.81	
	25	30	66.43	1.16	0.39		25.61	
	30	35	68.00	1.09	0.35		26.13	
	35	40	65.78	1.14	0.39		22.04	
	40	45	66.63	1.15	0.38		22.84	
	45	50	73.05	1.12	0.30		27.09	
	60	70	60.28	1.26	0.50		14.91	
	80	90	59.91	1.27	0.51		15.10	
	100	110	51.23	1.37	0.67		17.61	
	120	130	71.08	1.17	0.34		33.37	
	140	150	70.88	1.20	0.35		25.89	

The site was located approximately 5 meters from the Jug Bay NERRS boardwalk, 10 meters from the beginning of the boardwalk. The site was dominated by *Nuphar* spp. and *Peltandra virginica*.

## PATUXENT RIVER

9/2/93	Sample Depth		% Water	Wet Sample Density g cm <sup>-3</sup>	Dry Sample Density g cm <sup>-3</sup>	Average Dry Density to 25 cm g cm <sup>-3</sup>	% Weight Lost On Ignition % LOI	Average % LOI to 50 cm
	Top cm	Bottom cm						
Jug Bay 3	0	3	78.65	1.04	0.22	0.300	19.43	17.106
	3	6	75.35	1.10	0.27		20.81	
	6	9	73.21	1.10	0.29		18.16	
	9	12	73.55	1.06	0.28		17.59	
	12	15	73.72	1.14	0.30		17.84	
	15	20	73.22	1.18	0.31		17.14	
	20	25	67.52	1.12	0.36		16.51	
	25	30	60.06	1.22	0.49		16.91	
	30	35	65.04	1.13	0.40		15.74	
	35	40	63.88	1.18	0.43		16.38	
	40	45	63.18	1.21	0.44		15.49	
	45	50	62.24	1.25	0.47		16.60	
	50	60	62.33	1.26	0.47		15.68	
	70	80	56.41	1.33	0.58		13.49	
	90	100	54.49	1.35	0.61		12.52	
	100	110	53.19	1.35	0.63		17.70	
	120	130	64.57	1.25	0.44		24.07	
	140	150	65.07	1.23	0.43		25.41	

The site was dominated by *Nuphar advena* and located 20 m west of the observation blind at the end of the Jug Bay NERRS marsh boardwalk.

## PATUXENT RIVER

	8/8/96      Sample Depth		% Water	Wet Sample Density g cm <sup>-3</sup>	Dry Sample Density g cm <sup>-3</sup>	Average Dry Density to 25 cm g cm <sup>-3</sup>	% Weight Lost On Ignition % LOI	Average % LOI to 50 cm
	Top cm	Bottom cm						
TRANSECT A 11 m	0	3	79.38	1.11	0.23		20.43	20.658
	3	6	74.55	1.14	0.29		25.32	
	6	9	75.49	1.14	0.28		21.40	
	9	12	77.96	1.09	0.24		25.12	
	12	15	60.72	1.20	0.47		25.51	
	15	20	74.69	1.25	0.32		18.89	
	20	25	57.91	1.30	0.55		15.73	
	25	30	--	1.21	0.44		19.27	
	30	35	70.87	1.15	0.34		21.93	
	35	40	68.48	1.21	0.38		23.93	
	40	45	66.30	1.24	0.42		17.05	
	45	50	66.64	1.18	0.39		19.11	
	50	55	61.41	1.22	0.47		24.71	
	60	65	67.19	1.23	0.40		17.35	
	90	100	60.02	1.29	0.52		18.41	

Transect A was collected south of Jug Bay on the Patuxent River, from the western bank ( $38^{\circ}44'819''$  N by  $76^{\circ}41'882''$  W). The first core was collected 11 m from the river bank.

## PATUXENT RIVER

	Sample Depth		% Water	Wet Sample Density g cm <sup>-3</sup>	Dry Sample Density g cm <sup>-3</sup>	Average Dry Density to 25 cm g cm <sup>-3</sup>	% Weight Lost On Ignition % LOI	Average % LOI to 50 cm
	Top cm	Bottom cm						
TRANSECT A 30 m	0	3	79.17	1.16	0.24		23.62	21.620
	3	6	76.75	1.23	0.29		22.36	
	6	9	76.99	1.49	0.34		20.90	
	9	12	70.80	1.21	0.35		21.98	
	12	15	72.02	1.18	0.33		23.25	
	15	20	--	1.22	0.32		22.19	
	20	25	73.66	1.18	0.31		21.73	
	25	30	71.24	1.19	0.34			
	30	35	66.90	1.26	0.42		17.52	
	35	40	65.10	1.25	0.44			
	40	45	54.80	1.31	0.59		23.09	
	45	50	55.65	1.33	0.59			
	50	60	51.60	1.38	0.67			
	70	80	66.09	1.19	0.40		31.09	

The second core in Transect A was located 30 m from the river bank.

## PATUXENT RIVER

8/8/96

	Top cm	Bottom cm	% Water	Wet Sample Density g cm <sup>-3</sup>	Dry Sample Density g cm <sup>-3</sup>	Average Dry Density to 25 cm g cm <sup>-3</sup>	% Weight Lost On Ignition % LOI	Average % LOI to 50 cm
TRANSECT A	0	3	76.90	1.14	0.26		25.16	26.083
50 m	3	6	72.59	1.18	0.32		23.83	
	6	9	69.36	0.27	0.08		22.92	
	9	12	66.92	1.25	0.41		29.54	
	12	15	75.93	1.14	0.27		38.31	
	15	20	68.45	1.20	0.38		32.00	
	20	25	70.86	1.18	0.34		27.62	
	25	30	73.08	1.17	0.32			
	30	35	67.41	1.24	0.40		21.22	
	35	40	72.74	1.18	0.32			
	40	45	60.69	1.29	0.51		24.15	
	45	50	81.32	1.12	0.21		12.81	
	50	55	83.66	1.08	0.18		65.11	
TRANSECT A	0	3	78.39	1.13	0.24		25.89	26.196
50 m	3	6	74.86	1.15	0.29		24.21	
	6	9	72.60	1.16	0.32		24.63	
	9	12	73.28	1.16	0.31		22.79	
	12	15	75.72	1.15	0.28		28.48	
	15	20	72.37	1.15	0.32		27.64	
	20	25	69.56	1.17	0.36		23.53	
	25	30	74.79	1.17	0.29		27.70	
	30	35	77.38	1.14	0.26		28.22	
	35	40	78.43	1.13	0.24		29.25	
	40	45	76.79	1.14	0.26		25.85	
	45	50	77.15	1.15	0.26		24.17	
	50	55	78.05	1.12	0.25		33.62	
	60	65	80.45	1.10	0.22		50.04	

Two cores were collected 50 m from the river bank in Transect A.

## PATUXENT RIVER

	8/8/96		Sample Depth		% Water	Wet Sample Density g cm <sup>-3</sup>	Dry Sample Density g cm <sup>-3</sup>	Average Dry Density to 25 cm g cm <sup>-3</sup>	% Weight Lost On Ignition % LOI	Average % LOI to 50 cm
	Top cm	Bottom cm								
TRANSECT B 2 m	0	3	72.61	1.22	0.33				19.15	17.802
	3	6	69.80	1.14	0.34				18.77	
	6	9	69.61	1.22	0.37				20.68	
	9	12	69.74	1.19	0.36				20.12	
	12	15	66.08	1.25	0.42				20.20	
	15	20	62.48	1.27	0.48				19.55	
	20	25	57.76	1.33	0.56				16.92	
	25	30	55.37	1.33	0.59				16.30	
	30	35	57.87	1.31	0.55				16.29	
	35	40	54.87	1.37	0.62				15.83	
	40	45	56.71	1.31	0.57				16.89	
	45	50	52.96	1.40	0.66				16.89	
	50	60	55.95	1.33	0.59				18.62	
	70	80	65.31	1.24	0.43				20.08	
	90	100	62.26	1.28	0.48				18.54	

Transect B was located on the eastern bank of the Patuxent River just north of Lower Marlboro (38°42'260" N 76°41'843" W). The first core was collected 2 m from the river bank.

## PATUXENT RIVER

	Sample Depth		% Water	Wet Sample Density g cm <sup>-3</sup>	Dry Sample Density g cm <sup>-3</sup>	Average Dry Density to 25 cm g cm <sup>-3</sup>	% Weight Lost On Ignition % LOI	Average % LOI to 50 cm
	Top cm	Bottom cm						
TRANSECT B 10.5 m	0	3	78.09	1.15	0.25		21.47	22.837
	3	6	73.00	1.20	0.33		20.99	
	6	9	73.21	1.21	0.32		20.50	
	9	12	72.92	1.17	0.32		20.50	
	12	15	68.88	1.21	0.38		20.51	
	15	20	69.44	1.22	0.37		21.13	
	20	25	70.06	1.17	0.35		21.76	
	25	30	69.58	1.20	0.37			
	30	35	70.62	1.20	0.35		23.02	
	35	40	75.40	1.14	0.28			
	40	45	68.66	1.19	0.37		26.46	
	45	50	71.71	1.18	0.33			
	50	60	69.43	1.18	0.36		27.60	
	70	80	63.70	1.25	0.45			
	90	100	56.68	1.35	0.58		14.42	

The second core in Transect B was located 10.5 m from the river bank.

## PATUXENT RIVER

	Sample Depth		% Water	Wet Sample Density g cm <sup>-3</sup>	Dry Sample Density g cm <sup>-3</sup>	Average Dry Density to 25 cm g cm <sup>-3</sup>	% Weight Lost On Ignition % LOI	Average % LOI to 50 cm
	Top cm	Bottom cm						
TRANSECT B 30m	0	3	80.87	1.09	0.21		38.24	31.123
	3	6	75.70	1.13	0.27		38.50	
	6	9	76.64	1.13	0.26		38.75	
	9	12	74.64	1.12	0.28		35.74	
	12	15	74.66	1.13	0.29		32.72	
	15	20	71.05	1.18	0.34		29.49	
	20	25	67.44	1.21	0.39		26.26	
	25	30	68.47	1.21	0.38			
	30	35	68.30	1.21	0.38		25.98	
	35	40	66.78	1.17	0.39			
	40	45	74.32	1.15	0.29		31.46	
	45	50	74.02	1.16	0.30			
	50	60	75.95	1.14	0.27		31.90	
	70	80	72.46	1.17	0.32			
	90	100	57.60	1.36	0.57		18.73	

The third core in Transect B was 30 m from the river bank.

## PATUXENT RIVER

	8/8/96      Sample Depth		% Water	Wet Sample Density g cm <sup>-3</sup>	Dry Sample Density g cm <sup>-3</sup>	Average Dry Density to 25 cm g cm <sup>-3</sup>	% Weight Lost On Ignition % LOI	Average % LOI to 50 cm
	Top cm	Bottom cm						
TRANSECT B 60m	0	3	89.25	1.08	0.12		45.15	38.618
	3	6	88.46	1.06	0.12		44.17	
	6	9	73.98	1.08	0.28		46.59	
	9	12	--	1.11	0.27		41.29	
	12	15	77.53	1.14	0.26		37.94	
	15	20	74.79	1.14	0.29		36.58	
	20	25	74.50	1.13	0.29		36.99	
	25	30	75.26	1.12	0.28		40.09	
	30	35	76.46	1.11	0.26		37.90	
	35	40	81.08	1.12	0.21		35.98	
	40	45	80.67	1.12	0.22		34.80	
	45	50	77.37	1.14	0.26		34.76	
	50	60	81.70	1.10	0.20		50.68	
	70	80	78.80	1.13	0.24		37.47	
	90	100	60.59	1.31	0.52		19.85	

## PATUXENT RIVER

10/93	Sample Depth		% Water	Wet Sample Density g cm <sup>-3</sup>	Dry Sample Density g cm <sup>-3</sup>	Average Dry Density to 25 cm g cm <sup>-3</sup>	% Weight Lost On Ignition % LOI	Average % LOI to 50 cm
	Top cm	Bottom cm						
Transect C 0 m	0	3	69.87	1.31	0.39	0.523	15.98	25.652
	3	6	66.98	1.26	0.42		16.42	
	6	9	63.30	1.23	0.45		16.71	
	9	12	60.82	1.30	0.51		18.35	
	12	15	58.85	1.29	0.53		16.91	
	15	20	50.90	1.40	0.69		18.40	
	20	25	59.15	1.34	0.55		18.51	
	25	30	69.53	1.26	0.38		26.75	
	30	35	71.78	1.14	0.32		32.61	
	35	40	75.13	1.16	0.29		34.43	
	40	45	77.13	1.15	0.26		39.37	
	45	50	78.85	1.33	0.28		35.85	
	50	60	82.84	1.12	0.19		34.41	
	70	80	84.74	1.06	0.16		50.69	
	90	100	87.48	1.09	0.14		60.54	
	100	110	--	1.24	0.27		21.81	
	120	130	66.82	1.23	0.41		22.31	
	140	150	61.79	1.26	0.48		18.52	

Transect C designated the downstream border of sampled sites in this study. The transect was collected north of Chalk Point on the western bank of the Patuxent River. The first core was collected from the riverbank.

## PATUXENT RIVER

	7/7/94		Sample Depth		% Water	Wet Sample Density g cm <sup>-3</sup>	Dry Sample Density g cm <sup>-3</sup>	Average Dry Density to 25 cm g cm <sup>-3</sup>	% Weight Lost On Ignition % LOI	Average % LOI to 50 cm
	Top cm	Bottom cm								
Transect C 30 m	0	3	76.78	0.18	0.04	0.098	39.82	45.174		
	3	6	78.30	0.21	0.04		41.61			
	6	9	78.35	0.15	0.03		47.67			
	9	12	81.76	0.19	0.04		65.83			
	12	15	77.73	0.18	0.04		48.55			
	15	20	81.50	1.03	0.19		57.83			
	20	25	81.87	1.01	0.18		46.49			
	25	30	85.26	1.04	0.15		54.00			
	30	35	85.18	1.03	0.15		51.18			
	35	40	80.25	1.10	0.22		33.07			
	40	45	79.78	1.11	0.22		31.52			
	45	50	80.51	1.09	0.21		31.55			

This core was the second collected in Transect C, located 30 m from the river bank.

## PATUXENT RIVER

	Sample Depth		% Water	Wet Sample Density g cm <sup>-3</sup>	Dry Sample Density g cm <sup>-3</sup>	Average Dry Density to 25 cm g cm <sup>-3</sup>	% Weight Lost On Ignition % LOI	Average % LOI to 50 cm
	Top cm	Bottom cm						
Transect C	0	3	75.23	1.11	0.27	0.180	38.15	59.770
60 m	3	6	75.66	1.08	0.26		40.18	
	6	9	80.51	1.03	0.20		59.53	
	9	12	79.80	1.00	0.20		79.38	
	12	15	85.64	1.03	0.15		84.38	
	15	20	87.17	0.99	0.13		74.10	
	20	25	87.82	0.99	0.12		69.14	
	25	30	85.66	1.03	0.15		55.43	
	30	35	85.12	1.05	0.16		46.36	
	35	40	89.36	1.05	0.11		61.78	
	40	45	88.90	1.06	0.12		56.47	
	45	50	87.72	1.15	0.14		53.45	
	50	60	87.17	1.04	0.13		53.21	
	70	80	86.89	1.05	0.14		50.10	
	90	100	84.39	1.06	0.17		50.29	
	100	110	81.26	1.08	0.20		43.42	
	120	130	71.95	1.17	0.33		28.32	
	140	150	72.44	1.16	0.32		29.69	

The site was located 60 m from the river bank in Transect C and was dominated by *Scirpus* spp.

## PATUXENT RIVER

	7/7/94		Sample Depth		% Water	Wet Sample Density g cm <sup>-3</sup>	Dry Sample Density g cm <sup>-3</sup>	Average Dry Density to 25 cm g cm <sup>-3</sup>	% Weight Lost On Ignition % LOI	Average % LOI to 50 cm
	Top cm	Bottom cm								
Transect C 90 m	0	3	72.64	1.13	0.31	0.170	31.44	64.922		
	3	6	76.99	1.09	0.25		40.02			
	6	9	87.07	1.03	0.13		70.78			
	9	12	85.89	1.01	0.14		74.78			
	12	15	86.52	0.96	0.13		79.69			
	15	20	85.00	0.99	0.15		77.49			
	20	25	88.12	1.03	0.12		75.55			
	25	30	86.13	1.02	0.14		61.47			
	30	35	88.78	1.03	0.12		67.66			
	35	40	89.48	1.01	0.11		73.24			
	40	45	94.13	1.10	0.06		64.93			
	45	50	94.76	1.14	0.06		50.86			
	50	60	91.19	1.04	0.09		71.83			
	70	80	90.75	1.06	0.10		78.02			
	90	100	89.11	1.07	0.12		65.44			
	100	110	--	1.06	0.11		55.16			
	120	130	90.09	1.05	0.10		63.40			
	140	150	84.74	1.07	0.16		47.70			

The core was located in Transect C, 90 m from the river bank and vegetation was dominated by *Scirpus* spp.

**OTTER POINT CREEK**  
8/4/94

		Sample Depth	% Water	Wet Sample Density g cm <sup>-3</sup>	Dry Sample Density g cm <sup>-3</sup>	Average Dry Density to 25 cm g cm <sup>-3</sup>	% Weight Lost On Ignition % LOI	Average % LOI to 50 cm
<b>Site 1</b>	0	3	67.98	1.26	0.40	0.467	13.46	13.732
	3	6	66.19	1.22	0.41		12.70	
	6	9	64.23	1.28	0.46		12.61	
	9	12	62.48	1.23	0.46		13.56	
	12	15	61.71	1.27	0.49		14.82	
	15	20	61.57	1.26	0.48		14.47	
	20	25	32.49	0.77	0.52		13.90	
	25	30	61.58	1.28	0.49		14.52	
	30	35	57.75	1.31	0.55		13.33	
	35	40	50.65	1.38	0.68		11.68	
	40	45	51.43	1.44	0.70		12.54	
	45	50	51.21	1.51	0.74		11.38	
	50	60	49.48	1.46	0.74		11.19	
	70	80	38.93	1.61	0.99		8.83	
	90	100	35.68	0.86	0.55		5.69	
<b>Site 2</b>	0	3	65.45	1.24	0.43	0.597	13.85	11.841
	3	6	66.35	1.13	0.38		14.33	
	6	9	62.32	1.34	0.51		13.76	
	9	12	59.40	1.32	0.54		12.29	
	12	15	64.23	1.27	0.45		14.59	
	15	20	54.22	1.36	0.62		10.24	
	20	25	40.07	1.64	0.98		7.67	
	25	30	43.24	1.56	0.88		9.56	
	30	35	49.21	1.54	0.78		12.61	
	35	40	53.22	1.45	0.68		12.67	
	40	45	55.59	1.39	0.62		13.46	
	45	50	46.66	1.46	0.78		12.06	
	50	60	55.78	1.35	0.60		12.65	
	70	80	48.67	1.47	0.75		11.47	
	90	100	44.27	1.56	0.87		9.98	

## OTTER POINT CREEK

8/4/94	Sample Depth		% Water	Wet Sample Density g cm <sup>-3</sup>	Dry Sample Density g cm <sup>-3</sup>	Average Dry Density to 25 cm g cm <sup>-3</sup>	% Weight Lost On Ignition % LOI	Average % LOI to 50 cm
	Top cm	Bottom cm						
Site 3	0	3	69.64	1.22	0.37	0.745	13.39	10.702
	3	6	59.92	1.35	0.54		11.76	
	6	9	43.65	1.55	0.88		8.94	
	9	12	45.27	1.54	0.84		10.20	
	12	15	48.51	1.53	0.79		10.82	
	15	20	44.83	1.47	0.81		10.39	
	20	25	42.63	1.51	0.86		10.04	
	25	30	44.65	1.51	0.84		11.04	
	30	35	50.38	1.40	0.70		11.07	
	35	40	42.56	1.52	0.87		10.11	
	40	45	41.45	1.54	0.90		10.29	
	45	50	47.75	1.39	0.73		12.10	
	50	60	45.05	1.49	0.82		10.33	
	70	80	41.95	1.53	0.89		8.50	
	90	100	31.86	1.72	1.17		5.97	

**CHOPTANK RIVER**  
6/5/95

			Sample Depth	% Water	Wet Sample Density g cm <sup>-3</sup>	Dry Sample Density g cm <sup>-3</sup>	Average Dry Density to 25 cm g cm <sup>-3</sup>	% Weight Lost On Ignition % LOI	Average % LOI to 100 cm
<b>Site 1</b>	0	3	72.53	1.14	0.31	0.327	27.63	<b>28.885</b>	
	3	6	67.57	1.19	0.38			24.81	
	6	9	68.78	1.17	0.36			22.77	
	9	12	75.84	1.12	0.27			32.43	
	12	15	78.03	1.13	0.25			32.10	
	15	20	70.93	1.14	0.33			26.94	
	20	25	69.59	1.16	0.35			28.32	
	25	30	71.06	1.17	0.34			26.77	
	30	35	70.42	1.13	0.33			28.59	
	35	40	74.16	1.10	0.28			31.27	
	40	45	67.89	1.18	0.38			28.46	
	45	50	75.54	1.11	0.27			33.18	
	50	60	74.79	1.13	0.28			30.98	
	70	80	72.47	1.16	0.32			27.32	
	90	100	77.37	1.12	0.25			29.37	
<b>Site 2</b>	0	3	68.55	1.15	0.36	<b>0.416</b>	20.13	<b>26.788</b>	
	3	6	65.54	1.24	0.43			20.07	
	6	9	67.43	1.23	0.40			18.88	
	9	12	64.20	1.30	0.47			19.77	
	12	15	62.03	1.23	0.47			18.90	
	15	20	63.75	1.20	0.44			20.34	
	20	25	67.65	1.14	0.37			28.80	
	25	30	72.65	1.08	0.30			25.52	
	30	35	76.00	1.13	0.27			30.11	
	35	40	76.00	1.10	0.26			25.79	
	40	45	75.37	1.13	0.28			27.84	
	45	50	77.80	1.10	0.24			29.22	
	50	60	75.67	1.13	0.27			31.38	
	70	80	77.90	1.11	0.24			31.91	
	90	100	68.44	1.19	0.38			22.57	

**CHOPTANK RIVER**

	6/5/95	Sample Depth	% Water	Wet Sample Density g cm <sup>-3</sup>	Dry Sample Density g cm <sup>-3</sup>	Average Dry Density to 25 cm g cm <sup>-3</sup>	% Weight Lost On Ignition % LOI	Average % LOI to 100 cm % LOI
<b>Site 3</b>								
	0	3	77.49	1.07	0.24	0.230	36.04	27.100
	3	6	78.81	1.08	0.23		36.29	
	6	9	81.97	1.05	0.19		34.60	
	9	12	82.09	1.08	0.19		35.96	
	12	15	76.77	1.12	0.26		25.69	
	15	20	79.07	1.10	0.23		30.41	
	20	25	77.51	1.12	0.25		22.46	
	25	30	78.07	1.10	0.24		26.64	
	30	35	74.70	1.11	0.28		23.13	
	35	40	74.76	1.11	0.28		23.41	
	40	45	79.69	1.11	0.22		28.13	
	45	50	80.65	1.09	0.21		28.75	
	50	60	79.47	1.12	0.23		24.93	
	70	80	72.60	1.15	0.32		26.38	
	90	100	66.28	1.19	0.40		25.87	

**MONIE BAY**

	Sample Depth		% Water	Wet Sample Density g cm <sup>-3</sup>	Dry Sample Density g cm <sup>-3</sup>	Average Dry Density to 25 cm g cm <sup>-3</sup>	% Weight Lost On Ignition % LOI	Average % LOI to 50 cm
	Top cm	Bottom cm						
<b>Site 1</b>								
	0	3		0.19	0.214		27.22	28.689
	3	6		0.19			28.13	
	6	9		0.20			26.74	
	9	12		0.19			29.56	
	12	15		0.19			29.74	
	15	20		0.26			23.84	
	20	25		0.23			24.72	
	25	30		0.28			22.73	
	30	35		0.30			22.38	
	35	40		0.27			24.91	
	40	45		0.26			26.03	
	45	50		0.12			57.43	
	60	65		0.13			52.99	
	90	95		0.21			38.35	
<b>Site 2</b>								
	0	3		0.20	0.285		28.65	31.988
	3	6		0.24			26.06	
	6	9		0.30			23.31	
	9	12		0.30			23.13	
	12	15		0.32			23.31	
	15	20		0.32			21.34	
	20	25		0.27			23.94	
	25	30		0.23			27.72	
	30	35		0.22			30.19	
	35	40		0.18			34.00	
	40	45		0.15			45.88	
	45	50		0.11			62.14	
	60	65		0.35			18.04	
	90	95		1.39			4.67	

**MONIE BAY**

	Sample Depth		% Water	Wet Sample Density g cm <sup>-3</sup>	Dry Sample Density g cm <sup>-3</sup>	Average Dry Density to 25 cm g cm <sup>-3</sup>	% Weight Lost On Ignition	Average % LOI to 50 cm % LOI
	Top cm	Bottom cm						
<b>Site 3</b>								
0	3	3		0.20	0.161	35.24	46.029	
3	6	6		0.21		35.46		
6	9	9		0.19		39.67		
9	12	12		0.17		41.93		
12	15	15		0.16		50.20		
15	20	20		0.13		70.68		
20	25	25		0.12		74.93		
25	30	30		0.12		72.48		
30	35	35		0.18		64.22		
35	40	40		0.37		38.16		
40	45	45		0.80		14.35		
45	50	50		1.14		3.96		
<b>Site 4</b>								
0	3	3		0.35	0.303	17.32	31.845	
3	6	6		0.38		21.24		
6	9	9		0.35		20.40		
9	12	12		0.18		41.24		
12	15	15		0.22		30.68		
15	20	20		0.32		22.00		
20	25	25		0.30		15.92		
25	30	30		0.29		19.36		
30	35	35		0.21		37.44		
35	40	40		0.17		43.52		
40	45	45		0.17		49.40		
45	50	50		0.16		52.28		

**MONIE BAY**

		Sample Depth	% Water	Wet Sample Density g cm <sup>-3</sup>	Dry Sample Density g cm <sup>-3</sup>	Average Dry Density to 25 cm g cm <sup>-3</sup>	% Weight Lost On Ignition % LOI	Average % LOI to 50 cm
		Top cm	Bottom cm					
<b>Site 5</b>		0	3					
		3	6	0.25	0.317	22.04	35.170	
		6	9	0.29		21.20		
		9	12	0.34		16.32		
		12	15	0.31		15.80		
		15	20	0.28		21.40		
		20	25	0.32		19.04		
		25	30	0.38		27.92		
		30	35	0.26		36.56		
		35	40	0.16		56.20		
		40	45	0.14		53.32		
		45	50	0.14		57.44		
		60	65	0.16		43.20		
		90	95	0.11		66.84		
				0.14		58.92		
<b>Site 6</b>		0	3					
		3	6	0.26	0.305	30.37	27.450	
		6	9	0.29		29.03		
		9	12	0.31		24.32		
		12	15	0.32		28.04		
		15	20	0.34		24.09		
		20	25	0.30		39.65		
		25	30	0.31		26.70		
		30	35	0.32		23.46		
		35	40	0.30		29.00		
		40	45	0.29		22.08		
		45	50	0.31		26.35		
		65	70	0.30		25.70		
		90	95	0.16		55.73		
				0.41		17.45		

## MONIE BAY

	Sample Depth		% Water	Wet Sample Density g cm <sup>-3</sup>	Dry Sample Density g cm <sup>-3</sup>	Average Dry Density to 25 cm g cm <sup>-3</sup>	% Weight Lost On Ignition % LOI	Average % LOI to 50 cm
	Top cm	Bottom cm						
Site 7	0	5			0.28	0.307	23.17	28.359
	5	10			0.36		17.95	
	10	15			0.33		18.96	
	15	20			0.31		22.44	
	20	25			0.26		29.66	
	25	30			0.25		29.71	
	30	35			0.20		37.99	
	35	40			0.21		35.57	
	40	45			0.25		33.15	
	45	50			0.24		34.99	

## TIVOLI BAYS, HUDSON RIVER

	Sample Depth		% Water	Wet Sample Density g cm <sup>-3</sup>	Dry Sample Density g cm <sup>-3</sup>	Average Dry Density to 25 cm g cm <sup>-3</sup>	% Weight Lost On Ignition % LOI	Average % LOI to 50 cm
	Top cm	Bottom cm						
NORTH BAY	0	2	70.66	1.15	0.34		18.58	
Site 1	2	4	65.86	1.24	0.42		18.97	
	4	6	68.91	1.19	0.37		20.84	
	6	8	63.54	1.26	0.46		16.38	
	8	10	61.57	1.27	0.49		18.20	
	10	12	64.27	1.25	0.45		19.91	
	12	15	64.72	1.27	0.45		19.85	
	15	18	64.27	1.25	0.45		19.23	
	18	21	64.20	1.22	0.44		18.95	
	21	24	62.60	1.27	0.47		17.88	
	24	27	61.77	1.27	0.49		19.82	
	27	30	67.00	1.25	0.41		20.67	
	30	35	61.02	1.28	0.50		17.82	
	35	40	59.19	1.32	0.54		14.47	
	40	45	55.07	1.34	0.60		13.53	
	45	50	52.03	1.37	0.66		11.65	
	50	60	56.72	1.35	0.58		11.71	
	70	80	53.72	1.38	0.64		12.26	
	80	90	59.44	1.29	0.52		12.68	

## TIVOLI BAYS, HUDSON RIVER

	Sample Depth		% Water	Wet Sample Density g cm <sup>-3</sup>	Dry Sample Density g cm <sup>-3</sup>	Average Dry Density to 25 cm g cm <sup>-3</sup>	% Weight Lost On Ignition % LOI	Average % LOI to 50 cm
	Top cm	Bottom cm						
NORTH BAY Site 2	0	2	66.63	1.24	0.41		14.53	
	2	4	66.55	1.26	0.42			
	4	6	63.97	1.23	0.44		16.09	
	6	8	60.91	1.31	0.51			
	8	10	54.40	1.34	0.61		16.46	
	10	12	51.19	1.39	0.68			
	12	15	65.63	1.24	0.43		15.58	
	15	18	48.94	1.43	0.73			
	18	21	47.74	1.42	0.74		11.25	
	21	24	45.22	1.58	0.87			
	24	27	43.86	1.50	0.84		9.10	
	27	30	42.97	1.50	0.86			
	30	35	42.10	1.76	1.02		8.72	
	35	40	43.19	1.54	0.87			
	40	45	40.96	1.55	0.91		8.60	
	45	50	41.40	1.58	0.93			
	50	60	38.01	1.60	0.99			
	70	78	38.62	1.60	0.98			

## TIVOLI BAYS, HUDSON RIVER

	Sample Depth		% Water	Wet Sample Density g cm <sup>-3</sup>	Dry Sample Density g cm <sup>-3</sup>	Average Dry Density to 25 cm g cm <sup>-3</sup>	% Weight Lost On Ignition % LOI	Average % LOI to 50 cm
	Top cm	Bottom cm						
NORTH BAY	0	2	66.18	1.36	0.46		9.61	
Site 3	2	4	61.53	1.33	0.51		10.42	
	4	6	62.94	1.30	0.48		3.42	
	6	8	62.03	1.32	0.50		11.80	
	8	10	61.80	1.31	0.50		13.17	
	10	12	59.92	1.34	0.54		11.09	
	12	15	58.51	1.39	0.58		11.16	
	15	18	54.67	1.38	0.63		10.38	
	18	21	52.74	1.40	0.66		10.30	
	21	24	48.42	1.46	0.75		9.24	
	24	27	47.86	1.48	0.77		10.84	
	27	30	40.61	1.55	0.92		7.54	
	30	35	44.16	1.52	0.85		9.19	
	35	40	46.43	1.54	0.82		8.28	
	40	45	47.09	1.52	0.80		9.76	
	45	50	45.18	1.49	0.82		8.55	
	50	60	38.35	1.64	1.01		6.97	
	70	80	56.63	2.13	0.92		8.00	

## TIVOLI BAYS, HUDSON RIVER

	Sample Depth		% Water	Wet Sample Density g cm <sup>-3</sup>	Dry Sample Density g cm <sup>-3</sup>	Average Dry Density to 25 cm g cm <sup>-3</sup>	% Weight Lost On Ignition % LOI	Average % LOI to 50 cm
	Top cm	Bottom cm						
<b>NORTH BAY</b>	0	2	65.26	1.32	0.46		10.36	
Site 4	2	4	61.40	1.38	0.53			
Subtidal	4	6	60.68	1.36	0.53		9.85	
	6	8	61.65	1.33	0.51			
	8	10	59.24	1.38	0.56		9.69	
	10	12	55.04	1.43	0.65			
	12	15	50.33	1.46	0.73		10.97	
	15	18	47.74	1.48	0.77			
	18	21	53.39	1.48	0.69		11.51	
	21	24	55.15	1.39	0.62			
	24	27	56.90	1.40	0.60		12.22	
	27	30	51.57	1.47	0.71			
	30	35	48.85	1.54	0.79		8.77	
	35	40	45.40	1.57	0.86			
	40	45	48.40	1.51	0.78		8.79	
	45	50	44.98	1.53	0.84			
	50	60	37.91	1.61	1.00		7.10	
	70	80	31.19	1.79	1.23			

## TIVOLI BAYS, HUDSON RIVER

	Sample Depth		% Water	Wet Sample Density g cm <sup>-3</sup>	Dry Sample Density g cm <sup>-3</sup>	Average Dry Density to 25 cm g cm <sup>-3</sup>	% Weight Lost On Ignition % LOI	Average % LOI to 50 cm
	Top cm	Bottom cm						
SOUTH BAY	0	2	68.62	1.39	0.44		10.63	
Site 1	2	4	61.76	1.32	0.50			
Subtidal	4	6	63.70	1.31	0.48		9.68	
	6	8	63.70	1.31	0.47			
	8	10	62.23	1.33	0.50		10.02	
	10	12	61.15	1.36	0.53			
	12	15	58.18	1.37	0.57		9.74	
	15	18	57.83	1.39	0.59			
	18	21	59.25	1.33	0.54		12.89	
	21	24	53.37	1.40	0.65			
	24	27	54.71	1.45	0.66		11.19	
	27	30	51.75	1.47	0.71			
	30	35	45.97	1.51	0.82		8.56	
	35	40	46.03	1.59	0.86			
	40	45	47.92	1.51	0.79		8.39	
	45	50	43.82	1.55	0.85			
	50	60	42.41	1.58	0.91		7.34	
	70	75	40.53	1.62	0.96			

## TIVOLI BAYS, HUDSON RIVER

	Sample Depth		% Water	Wet Sample Density g cm <sup>-3</sup>	Dry Sample Density g cm <sup>-3</sup>	Average Dry Density to 25 cm g cm <sup>-3</sup>	% Weight Lost On Ignition % LOI	Average % LOI to 50 cm
	Top cm	Bottom cm						
SOUTH BAY	0	2	81.48	1.14	0.21		33.62	
Site 2	2	4	72.03	1.22	0.34		26.06	
Fringe Marsh	4	6	73.79	1.16	0.30		30.70	
	6	8	78.65	1.13	0.24			
	8	10	76.42	1.16	0.27		36.04	
	10	12	74.62	1.16	0.29		33.37	
	12	15	72.89	1.17	0.32		32.22	
	15	18	73.03	1.16	0.31		32.52	
	18	21	77.21	1.14	0.26		33.19	
	21	24	53.65	0.68	0.32		32.90	
	24	27	70.47	1.17	0.35		31.42	
	27	30	74.72	1.16	0.29		37.71	
	30	35	76.84	1.12	0.26		42.31	
	35	40	73.81	1.17	0.31		39.68	
	40	45	75.09	1.12	0.28		39.17	
	45	50	82.94	1.07	0.18		49.63	
	50	60	82.27	1.11	0.20		51.75	
	70	77	86.03	1.06	0.15			

**Table C-2.** Nutrient, carbon and metals data from all sediment cores collected in this study. Site locations correspond to Figure C-1. Total phosphorus was analyzed using a molybdenum-blue technique on a sample which was combusted at 550°C for 2.5 hours. Inorganic P was analyzed with the same technique using an unashed sample. Iron and manganese were analyzed on a Flame Atomic Absorption Spectrophotometer using a 1 N HCl extraction.

PATUXENT RIVER

	Depth cm	Total P mg g sediment <sup>-1</sup>	Inorganic P mg g sediment <sup>-1</sup>	%C	%N	[Fe] mg g sediment <sup>-1</sup>	[Mn] mg g sediment <sup>-1</sup>
Site 1	0-3	1.821	1.697	14.88	1.00	33.683	4.927
	3-6	2.586	2.217			46.897	3.152
	6-9	2.663	2.241	8.66	0.78	32.936	1.039
	9-12	2.078	2.043				
	12-15	1.800	1.549			13.958	0.598
	15-20	1.192	0.871				
	20-25	0.816	0.486	6.51	0.54	7.988	0.427
	25-30	0.717	0.449				
	30-35	0.632	0.414			3.649	0.296
	35-40	0.753	0.478				
	40-45	0.725	0.471				
	45-50	0.571	0.369	2.73	0.23	4.404	0.256
	50-60	1.030	0.724				
	70-80	0.497	0.339			4.915	0.224
	90-100	0.651	0.483	1.90	0.17		
Site 2	100-110	0.509	0.333				
	120-130	0.245	0.116			8.746	0.476
	0-3	1.831	1.714	10.72	0.85	27.326	6.364
	3-6	1.211	0.750			8.973	1.126
	6-9	0.972	0.420	15.79	1.17	7.429	0.957
	9-12	0.943	0.443				
	12-15	0.686	0.419			4.508	0.473
	15-20	0.472	0.315				
	20-25	0.705	0.529	2.90	0.21	4.188	0.353
	25-30	1.037	0.863				
	30-35	0.622	0.464			4.788	0.324
	35-40	0.469	0.399				
	40-45	2.167	1.938				
	45-50	1.410	1.032	6.47	0.46	9.673	0.579
Site 3	50-60	1.239	0.857				
	70-80	0.900	0.762			6.412	0.296
	90-100	0.886	0.685	1.70	0.13		
	100-110	0.981	0.791				
	120-130	0.814	0.582			9.826	0.249
	0-3	3.140	2.388	17.88	1.34	44.918	1.728
	3-6	2.363	2.146			42.381	0.942
	6-9	1.399	0.757	23.20	1.61	17.554	0.672
	9-12	1.453	1.071				
	12-15	2.158	1.872			20.624	0.596
	15-20	1.728	1.420				
	20-25	1.967	1.440	8.60	0.68	21.121	0.429
	25-30	2.013	1.900				
	30-35	1.711	1.726			49.669	1.497
	35-40	1.286	1.087				
	40-45	0.971	0.827				
	45-50	1.130	1.020	2.64	0.22	10.385	3.275
	50-60	1.073	0.878				
	70-78	0.827	0.706			8.237	0.329

**PATUXENT RIVER**

Sample Depth	Total P	Inorganic P	%C	%N	[Fe]	[Mn]
cm	mg P g sediment <sup>-1</sup>	mg IP g sediment <sup>-1</sup>			mg g sediment <sup>-1</sup>	mg g sediment <sup>-1</sup>
Site 4	0-3	2.547	2.084	10.14	0.79	15.665
	3-6	3.332	2.423			0.716
	6-9	2.082	1.696	5.54	0.55	26.167
	9-12	2.548	2.215			0.860
	12-15	2.549	2.358	3.64	0.36	12.279
	15-20	3.147	3.146			0.447
	20-25	2.241	2.125	3.30	0.32	13.892
	25-30	2.353	2.335			0.504
	30-35	1.780	1.530	3.95	0.36	13.778
	35-40	1.509	1.218			0.459
	40-45	1.253	0.930			0.468
	45-50	1.429	1.097	3.25	0.30	13.235
	50-60	1.284	0.946			0.355
	70-80	1.239	0.940			13.192
	90-100	1.265	0.938	3.65	0.32	0.359
Site 5	100-110	0.596	0.371			0.404
	120-130	0.462	0.229			
Site 6	0-3	1.924	1.744	10.07	0.80	21.583
	3-6	1.673	1.632			1.720
	6-9	1.501	1.422	7.62	0.68	21.435
	9-12	1.967	1.994			0.867
	12-15	1.748	1.658			21.824
	15-20	1.629	1.456			1.560
	20-25	0.939	0.605	7.88	0.63	8.476
	25-30	0.781	0.471			0.707
	30-35	1.694	1.559			13.685
	35-40	1.562	1.420			0.591
	40-45	1.053	0.676			
	45-50	0.966	0.664	6.93	0.54	7.083
	50-60	1.119	0.721			0.367
	70-80	0.823	0.470			6.181
	90-100	0.653	0.323	12.79	0.73	0.401
	120-130	0.486	0.147			9.869
						0.561

**PATUXENT RIVER**

	Sample Depth	Total P	Inorganic P	%C	%N	[Fe]	[Mn]
	cm	mg P g sediment <sup>-1</sup>	mg IP g sediment <sup>-1</sup>			mg g sediment <sup>-1</sup>	mg g sediment <sup>-1</sup>
Site 7	0-3	2.352	1.679	30.28	1.68	32.996	5.652
	3-6	2.627	1.794			34.438	6.131
	6-9	1.555	0.854	20.06	1.55	26.700	2.184
	9-12	2.138	1.526				
	12-15	0.921	0.398			9.398	0.660
	15-20	1.110	0.656				
	20-25	1.107	0.624	18.64	1.19	19.558	0.807
	25-30	1.943	1.498			20.346	1.107
	30-35	1.722	1.387				
	35-40	1.871	1.666				
	40-45	1.439	1.052				
	45-50	1.128	0.618	8.23	0.68	9.854	0.880
	50-60	1.134	0.553				
	70-80	0.774	0.381			10.726	0.445
	90-100	1.037	0.364	13.78	0.90		
Site 8	0-2	3.155	2.950	8.93	0.75	49.305	0.865
	2-4	3.039	2.851			37.756	0.629
	4-6	2.369	2.087			28.302	0.497
	6-8	1.391	1.082	8.27	0.71		
	8-10	1.066	0.767			13.472	0.221
	10-12	0.945	0.650				
	14-16	1.022	0.750	9.16	0.67	11.999	0.198
	16-18	0.940	0.673				
	18-20	0.949	0.716			12.402	0.175
	20-25	1.401	1.222				
	25-30	1.302	1.103	3.83	0.36		
	30-35	1.455	1.359			21.349	0.406
	35-40	1.117	0.948				
	40-45	1.398	1.202	4.70	0.42		
	45-50	1.700	1.449			14.818	0.303
	50-60	1.586	1.348				
	70-80	1.662	1.542				
	90-100	1.170	0.990				0.401
Site 9	0-3	1.121	0.503	11.78	0.97	15.659	0.914
	3-6	1.000	0.389			7.368	0.472
	6-9	0.990	0.342	12.78	1.07	5.382	0.447
	9-12	1.044	0.404				
	12-15	0.913	0.331	18.49	1.29	9.018	0.747
	15-20	0.681	0.114				
	20-25	0.682	0.106	34.23	1.98	9.478	0.622
	25-30	0.656	0.069		2.13		
	30-35	0.587	0.067	37.94	2.28	10.674	0.782
	35-40	0.538	0.052				
	40-45	0.559	0.062				
	45-50	0.593	0.096	40.09	2.49	9.117	0.882
	50-60	0.496	0.071				
	70-80	0.438	0.049			6.115	0.938
	90-100	0.454	0.074	47.00	2.24		
	120-130	0.567	0.034			3.804	0.699
	140-150	0.752	0.071				

PATUXENT RIVER

	Sample Depth cm	Total P mg P g sediment <sup>-1</sup>	Inorganic P mg IP g sediment <sup>-1</sup>	%C	%N	[Fe] mg g sediment <sup>-1</sup>	[Mn] mg g sediment <sup>-1</sup>
Site 10	0-3	2.032	1.749	4.86	0.44	27.278	2.935
	3-6	2.226	1.901			30.827	4.366
	6-9	2.095	1.813	4.44	0.40	31.213	3.625
	9-12	2.289	1.989				
	12-15	2.286	2.075			33.528	2.118
	15-20	2.407	2.610				
	20-25	1.990	1.680	3.93	0.36	33.049	2.115
	25-30	2.442	2.277				
	30-35	2.296	2.006			24.424	0.736
	35-40	2.304	2.050				
	40-45	2.628	2.108				
	45-50	2.952	2.909	4.64	0.43	19.900	0.523
	50-60	1.687	1.447				
	70-80	1.661	1.427			15.066	0.444
	90-100	1.554	1.272	3.60	0.35		
	120-130	1.422	1.256			16.222	0.380
Site 11	0-3	2.055	1.854	7.26	0.61	31.212	1.142
	3-6	2.356	2.117			43.107	0.964
	6-9	2.711	2.693	6.32	0.56	43.957	1.216
	9-12	2.843	2.781				
	12-15	2.289	2.174			24.802	0.518
	15-20	2.192	1.921				
	20-25	2.241	2.083	4.62	0.39	21.878	0.675
	25-30	2.304	2.028				
	30-35	1.381	1.191			27.548	1.330
	35-40	0.810	0.552				
	45-50	1.330	1.211	4.95	0.32	33.461	1.440
	50-60	1.245	1.089				
	70-80	1.517	1.304			26.270	1.291
	90-100	1.430	1.182	3.20	0.28		
	100-110	1.433	1.261				
	120-130	1.505	1.397			17.690	0.887
	140-150	1.418	1.360				
Site 12	0-3	1.460	1.104	7.84	0.68	22.077	1.639
	3-6	1.782	1.249			18.563	0.808
	6-9	0.877	0.536	7.33	0.61	11.355	0.509
	9-12	0.823	0.481				
	12-15	0.755	0.458			11.277	0.356
	15-20	0.748	0.427				
	20-25	0.736	0.426	5.66	0.46	8.232	0.319
	25-30	0.731	0.409				
	30-35	0.743	0.424			5.478	0.258
	35-40	0.731	0.431				
	40-45	0.762	0.451				
	45-50	0.773	0.452	7.44	0.51	4.585	0.228
	50-60	0.676	0.416				
	70-80	0.522	0.250			28.170	0.365
	90-100	0.401	0.215	6.22	0.42		
	120-130	0.414	0.153			10.598	0.346
	140-150	0.356	0.161				

**PATUXENT RIVER**

	Sample Depth	Total P	Inorganic P	%C	%N	[Fe]	[Mn]
	cm	mg P g sediment <sup>-1</sup>	mg IP g sediment <sup>-1</sup>			mg g sediment <sup>-1</sup>	mg g sediment <sup>-1</sup>
Jug Bay 1	0-3	1.873	1.596	13.62	1.08	38.462	14.377
	3-6	1.905	1.676			48.089	13.673
	6-9	1.936	1.652	13.49	1.07	45.949	13.961
	9-12	1.910	1.663				
	12-15	1.675	1.400	15.90	1.16	29.501	5.169
	15-20	1.030	0.508				
	20-25	0.903	0.400	14.72	1.14	10.930	1.029
	25-30	0.926	0.372				
	30-35	0.931	0.433	13.81	1.08	10.433	0.921
	35-40	0.838	0.344				
	40-45	0.826	0.347				
	45-50	0.861	0.343	14.28	1.06	9.707	0.818
	50-60	0.765	0.251				
	70-80	0.660	0.138			7.225	0.704
	90-100	0.777	0.167				
Jug Bay 2	120-130	0.482	0.090			6.731	0.571
	140-150	0.358	0.087				
	0-2	2.419	2.081	8.19	0.76	27.828	1.146
	2-4	2.286	2.022	5.41	0.60	24.042	1.110
	4-6	2.350	2.069	7.66	0.73	27.308	1.294
	6-8	1.919	1.706	7.25	0.67	--	--
	8-10	1.971	1.732	5.80	0.59	18.490	1.009
	10-15	2.306	2.090	5.43	0.59		
	15-20	2.105	1.847	8.25	0.73	18.248	0.674
	20-25	1.973	1.796	6.98	0.61		
	25-30	2.025	1.784	9.82	0.73	22.815	0.566
	30-35	1.416	1.016	10.68	0.72		
	35-40	1.250	0.937	7.83	0.58		
	40-45	1.253	0.909	8.06	0.60	17.378	0.464
Jug Bay 3	45-50	1.264	0.868				
	60-70	1.472	1.150	4.09	0.36	15.360	0.610
	80-90	1.063	0.807				
	120-130	0.422	0.171			9.203	0.601
	0-3	2.617	2.346	7.16	0.72	24.911	0.741
	3-6	2.620	2.633			24.829	0.641
	6-9	2.881	2.697	5.60	0.55	27.727	0.698
	9-12	2.899	2.731				
	12-15	2.847	2.726	5.30	0.52	29.023	0.704
	15-20	2.803	2.653				
	20-25	2.872	2.711	4.99	0.49	29.035	0.559
	25-30	2.856	2.675				
	30-35	2.842	2.715			30.691	0.639
	40-45	2.856	2.643				
	45-50	2.868	2.742	4.27	0.41	29.863	0.649
	50-60	2.860	2.652				
	70-80	1.805	1.521			25.694	0.686
	90-100	1.299	1.055	2.74	0.28		
	100-110	0.869	0.790				
	120-130	0.305	0.156			10.355	0.450
	140-150	0.302	0.133				

PATUXENT RIVER

	Sample Depth cm	Total P mg P g sediment <sup>-1</sup>		Sample Depth cm	Total P mg P g sediment <sup>-1</sup>
TRANSECT A 11 m	0-3	2.131	TRANSECT A 50 m	0-3	2.318
	3-6	1.959		6-9	1.224
	6-9	2.094		12-15	1.204
	9-12	2.036		20-25	1.064
	12-15	1.465		30-35	1.153
	15-20	1.762		40-45	1.188
	20-25	1.823		50-55	1.437
	25-30	1.603			
	30-35	1.112			
	35-40	1.422			
	40-45	1.574			
	45-50	1.689			
	50-55	1.451			
	60-65	1.268			
TRANSECT A 30 m	90-100	0.850			
	0-3	1.778	TRANSECT A 50 m	0-3	1.184
	6-9	1.887		3-6	1.859
	9-12			6-9	2.127
	12-15	2.126		9-12	1.836
	15-20			12-15	1.355
	20-25	1.438		15-20	1.718
	25-30			20-25	1.362
	30-35	1.466		25-30	1.292
	35-40			30-35	1.185
	40-45	1.507		35-40	2.247
	70-80	0.873		40-45	1.196
				45-50	1.177
				50-55	1.145
				60-65	0.890

PATUXENT RIVER

	Sample Depth cm	Total P mg P g sediment <sup>-1</sup>		Sample Depth cm	Total P mg P g sediment <sup>-1</sup>
TRANSECT B 2 m	0-3	1.744	TRANSECT B 30 m	0-3	1.756
	3-6	1.881		6-9	0.955
	6-9	1.815		12-15	1.064
	9-12	1.567		20-25	0.987
	12-15	1.650		30-35	1.178
	15-20	1.419		40-45	1.404
	20-25	1.961		50-60	1.397
	25-30	1.552			
	30-35	1.441			
	35-40	2.020			
	40-45	1.155			
	45-50	0.911			
TRANSECT B 10.5 m	50-60	0.850	TRANSECT B 60 m	12-15	1.061
	70-80	1.040		15-20	1.078
	90-100	0.529		20-25	1.325
				25-30	1.477
				30-35	1.390
	6-9	2.034		35-40	1.192
	12-15	1.441		40-45	1.310
	30-35	1.155		45-50	1.152
	40-45	1.220		50-60	0.913
	50-60	0.743		70-80	0.516
				90-100	0.240

PATUXENT RIVER

	Depth cm	Total P mg P g sediment <sup>-1</sup>	Inorganic P mg IP g sediment <sup>-1</sup>	%C	%N	[Fe] mg g sediment <sup>-1</sup>	[Mn] mg g sediment <sup>-1</sup>
TSECT							
C	0-3	1.983	1.669	4.73	0.46	28.723	4.832
0 m	3-6	2.140	1.750			33.789	4.775
	6-9	1.822	1.285	5.08	0.49	24.237	2.512
	9-12	2.038	1.598			32.053	3.171
	12-15	2.123	1.780	5.63	0.48	27.762	1.651
	15-20	1.487	1.071			21.731	1.284
	20-25	1.385	1.003	5.11	0.43	19.412	0.629
	25-30	1.080	0.628			10.180	0.504
	30-35	0.999	0.456	12.06	0.75	8.833	0.473
	35-40	0.896	0.394			6.624	0.319
	40-45	1.000	0.425			7.254	0.452
	45-50	0.814	0.362	14.15	0.68	9.543	0.474
	50-60	0.817	0.342			10.988	0.791
	70-80	1.500	0.968			10.484	0.677
	90-100	0.990	0.317	18.33	1.66	7.891	0.723
	100-110	0.544	0.337			8.307	0.490
	120-130	0.415	0.217			7.555	0.302
	140-150	0.385	0.230			6.370	0.284
TSECT	0-3	2.061	1.405	15.15	1.17	31.058	2.237
C	3-6	1.607	0.919			20.369	0.685
30 m	6-9	0.810	0.263	21.14	1.17	4.098	0.172
	9-12	0.857	0.267			3.864	0.186
	12-15	0.574	0.207			19.488	0.177
	15-20	0.766	0.258			7.316	0.179
	20-25	0.574	0.153	20.50	1.00	4.426	0.113
	25-30	0.669	0.161			4.022	0.102
	30-35	0.678	0.176			5.107	0.116
	35-40	0.861	0.455			6.678	0.164
	40-45	0.615	0.295			5.783	0.134
	45-50	0.467	0.171	13.71	0.77	7.631	0.159
TSECT	0-3	0.993	0.433	17.01	1.22	4.924	0.844
C	3-6	1.054	0.362			2.982	0.174
60 m	6-9	0.788	0.251	26.60	1.42	2.871	0.145
	9-12	0.510	0.126			7.682	0.115
	12-15	0.610	0.120			5.374	0.148
	15-20	1.044	0.359			2.169	0.181
	20-25	1.094	0.227	34.08	1.52	0.431	0.155
	25-30	0.788	0.192			0.000	0.196
	30-35	0.855	0.186			0.019	0.260
	35-40	0.937	0.227			1.290	0.352
	40-45	1.081	0.364			0.204	0.332
	45-50	0.871	0.273	22.96	1.34	0.377	0.287
	50-60	0.846	0.355			2.680	0.217
	70-80	1.104	0.453			1.775	0.092
	90-100	1.041	0.562	18.20	1.18	3.094	0.051
	100-110	0.640	0.250			0.647	0.096
	140-150	0.493	0.300			2.741	0.080

PATUXENT RIVER

	Depth cm	Total P mg P g sediment <sup>-1</sup>	Inorganic P mg IP g sediment <sup>-1</sup>	%C	%N	[Fe] mg g sediment <sup>-1</sup>	[Mn] mg g sediment <sup>-1</sup>
TSECT	0-3	0.936	0.373	12.30	0.93	5.023	0.201
C	3-6	1.031	0.346	17.40	1.19	4.238	0.145
90 m	6-9	0.835	0.201	32.02	1.81	1.983	0.207
	9-12	0.719	0.169	37.18	1.66	4.830	0.217
	12-15	0.647	0.120	37.84	1.86	7.509	0.287
	15-20	0.516	0.090	36.76	1.54	5.144	
	20-25	0.672	0.089	35.35	1.67	3.404	0.304
	25-30	0.645	0.122	28.93	1.48	9.013	0.273
	30-35	0.707	0.144	32.47	1.56	4.361	0.328
	35-40	0.750	0.141	35.79	1.77	3.605	0.305
	40-45	0.668	0.115	31.11	1.60	1.434	0.322
	45-50	0.586	0.121	23.11	1.27	1.906	0.247
	50-60	1.177	0.597	33.55	1.67	4.709	0.314
	70-80	0.808	0.146	35.45	2.06	3.419	0.240
	90-100	0.668	0.105	31.92	1.78	1.028	0.102
	100-110	0.631	0.148			1.054	0.079
	140-150	0.618	0.216			1.817	0.060

OTTER POINT CREEK

	Depth cm	Total P mg P g sediment <sup>-1</sup>	Inorganic P mg IP g sediment <sup>-1</sup>	%C	%N	[Fe] mg g sediment <sup>-1</sup>	[Mn] mg g sediment <sup>-1</sup>
Site 1	0-3	0.535	0.301	4.35	0.33	10.814	0.363
	3-6	0.559	0.286	3.91	0.32	10.782	0.300
	6-9	0.487	0.253	4.27	0.33	9.302	0.265
	9-12	0.508	0.233	4.39	0.32		
	12-15	0.550	0.251	4.77	0.35	7.704	0.183
	15-20	0.504	0.223	5.44	0.39		
	20-25	0.542	0.261	4.9	0.36	9.335	0.238
	25-30	0.540	0.297	4.66	0.33		
	30-35	0.595	0.274	4.07	0.32	9.034	0.222
	35-40	0.564	0.280	3.21	0.25		
	40-45	0.610	0.309	3.1	0.24		
	45-50	0.529	0.282	2.7	0.22	19.872	0.905
	50-60	0.524	0.269	2.62	0.21		
	70-80	0.392	0.207	1.66	0.12	14.773	0.918
	90-100	0.243	0.131	1.39	0.08		

**OTTER POINT CREEK**

	Depth cm	Total P mg P g sediment <sup>-1</sup>	Inorganic P mg IP g sediment <sup>-1</sup>	%C	%N	[Fe] mg g sediment <sup>-1</sup>	[Mn] mg g sediment <sup>-1</sup>
Site 2	0-3	0.564	0.301	4.08	0.29	9.310	0.673
	3-6	0.611	0.304		0.305	8.227	0.446
	6-9	0.602	0.290	4.95	0.32	7.096	0.311
	9-12	0.594	0.310		0.34		
	12-15	0.695	0.368	4.65	0.36	9.947	0.430
	15-20	0.368	0.168		0.26		
	20-25	0.312	0.134	2.18	0.16	3.267	0.124
	25-30	0.402	0.181		0.22		
	30-35	0.407	0.188	4	0.28	5.914	0.147
	35-40	0.449	0.189				
	40-45	0.505	0.221				
	45-50	0.518	0.215	3.19	0.25	8.456	0.182
	50-60	0.565	0.276				
	70-80	0.492	0.190			10.331	0.228
	90-100	0.434	0.178	2.39	0.18		
Site 3	0-3	0.518	0.275	4.07	0.31	10.530	0.386
	3-6	0.440	0.232			7.005	0.190
	6-9	0.412	0.211	2.56	0.2	5.481	0.129
	9-12	0.476	0.270				
	12-15	0.560	0.300	2.86	0.23	6.224	0.123
	15-20	0.475	0.251				
	20-25	0.424	0.209	2.84	0.23	7.992	0.164
	25-30	0.475	0.211				
	30-35	0.440	0.175	3.23	0.25	7.680	0.166
	35-40	0.461	0.196				
	40-45	0.473	0.211				
	45-50	0.521	0.230	3.16	0.22	9.093	0.181
	50-60	0.480	0.230				
	70-80	0.411	0.214			10.569	0.510
	90-100	0.264	0.149	1.19	0.08		

**CHOPTANK RIVER**

	Depth cm	Total P mg P g sediment <sup>-1</sup>	Inorganic P mg IP g sediment <sup>-1</sup>	%C	%N	[Fe] mg g sediment <sup>-1</sup>	[Mn] mg g sediment <sup>-1</sup>
Site 1	0-3	0.649	0.318	11.13	0.90	5.597	0.180
	3-6	0.681	0.215	9.18	0.78	4.895	0.161
	6-9			9.98	0.77	6.969	0.243
	9-12	0.749	0.210	12.99	0.93		
	12-15			14.16	1.00	6.549	0.292
	15-20			11.78	0.87		
	20-25	0.791	0.153	11.65	0.87	3.925	0.250
	25-30			11.10	0.84		
	30-35			13.02	0.93	3.874	0.311
	35-40			12.06	0.83		
	40-45	0.867	0.157	12.17	0.83		
	45-50			14.17	0.87	3.856	0.340
	50-60			12.67	0.74		
	70-80			13.24	0.72	5.985	0.357
	90-100			13.82	0.75		
Site 2	0-3	1.245	0.851	6.96	0.63	20.191	2.384
	3-6	1.277	0.835			20.630	2.508
	6-9			6.98	0.62	19.066	1.515
	9-12	0.970	0.602				
	12-15			7.38	0.62	8.763	0.458
	15-20						
	20-25	0.523	0.177	8.55	0.63	4.192	1.658
	25-30						
	30-35			11.25	0.74	6.978	1.809
	35-40						
	40-45	0.555	0.186				
	45-50			12.82	0.80	5.631	0.273
	50-60						
	70-80					2.785	0.211
	90-100			9.42	0.58		
Site 3	0-3	0.693	0.278	15.74	0.98	7.033	0.242
	3-6	0.575	0.181			7.493	0.213
	6-9			14.71	0.91	7.035	0.200
	9-12	0.593	0.163				
	12-15			10.60	0.75	6.037	0.178
	15-20						
	20-25	0.642	0.286	11.00	0.73	5.651	0.181
	25-30						
	30-35			9.42	0.68	4.672	0.150
	35-40						
	40-45	0.534	0.146				
	45-50			11.40	0.74	4.047	0.161
	50-60						
	70-80					5.722	0.127
	90-100			10.78	0.72		

## MONIE BAY

	Depth cm	Total P mg P g sediment <sup>-1</sup>	Inorganic P mg IP g sediment <sup>-1</sup>	%C	%N	[Fe] mg g sediment <sup>-1</sup>	[Mn] mg g sediment <sup>-1</sup>
Site 1	0-3	0.950	0.374	10.62	0.88	3.256	0.025
	3-6	0.852	0.296	10.54	0.81	2.960	0.031
	6-9	0.795	0.263			2.629	0.035
	9-12	0.757	0.240	11.6	0.8		
	12-15	0.663	0.161			2.620	0.056
	15-20	0.569	0.133	8.32	0.63		
	20-25	0.574	0.139			4.148	0.108
	25-30	0.574	0.159				
	30-35	0.500	0.142	8.88	0.62	2.675	0.072
	35-40	0.499	0.130				
	40-45	0.488	0.112				
	45-50	0.589	0.085	13.19	0.8	2.559	0.121
	60-65	0.493	0.067				
	90-95	0.468	0.082	13.44	0.81	8.542	0.114
Site 2	0-3	1.213	0.541	9.11	0.98	10.478	0.400
	3-6	0.872	0.227			3.150	0.244
	6-9	0.703	0.128			2.075	0.146
	9-12	0.644	0.092				
	12-15	0.556	0.099	6.41	0.49	5.962	0.121
	15-20	0.541	0.086				
	20-25	0.576	0.073			3.157	0.126
	25-30	0.613	0.073				
	30-35	0.640	0.083			2.321	0.196
	35-40	0.661	0.080				
	40-45	0.688	0.073				
	45-50	0.748	0.051	14.35	0.77	3.748	
	60-65	0.307	0.022				
	90-95	0.102	0.026			0.875	
Site 3	0-3	1.017	0.304	10.78	0.9		0.469
	3-6	0.985	0.198			7.715	0.098
	6-9	1.130	0.177			6.154	0.033
	9-12	1.213	0.133				
	12-15	1.047	0.122	8.47	0.7	2.389	0.009
	15-20	0.589	0.055				
	20-25	0.564	0.055				0.020
	25-30	0.785	0.048				
	30-35	1.076	0.097			5.427	0.016
	35-40	1.634	0.872				
	40-45	0.441	0.174				
	45-50	0.315	0.159	2.04	2.01	0.760	

**MONIE BAY**

	Depth cm	Total P mg P g <sup>-1</sup> sediment <sup>-1</sup>	Inorganic P mg IP g <sup>-1</sup> sediment <sup>-1</sup>	%C	%N	[Fe] mg g <sup>-1</sup> sediment <sup>-1</sup>	[Mn] mg g <sup>-1</sup> sediment <sup>-1</sup>
Site 4	0-3	0.707	0.166	14.37	1.19	5.790	0.027
	3-6	0.540	0.107			3.210	0.021
	6-9	0.492	0.097			2.530	0.008
	9-12	0.509	0.114				
	12-15	0.461	0.066		0.51	1.910	
	15-20	0.492	0.055		4.440	0.004	
	20-25	0.523	0.042				
	25-30	0.447	0.031		3.300	0.006	
	30-35	0.395	0.031				
	35-40	0.454	0.028				
Site 5	40-45	0.488	0.052	2.73	0.11	5.250	
	45-50	0.530	0.045				
	0-3	0.728	0.253	8.92	0.77	5.760	0.015
	3-6	0.669	0.222			3.850	0.001
	6-9	0.672	0.218			4.930	0.013
	9-12	0.672	0.211				
	12-15	0.658	0.204	13.77	0.77	4.800	0.024
	15-20	0.579	0.184			3.210	0.017
	20-25	0.513	0.104				
	25-30	0.492	0.083			4.110	0.084
Site 6	30-35	0.610	0.073				
	35-40	0.582	0.087	18.82	1.15	1.260	0.042
	40-45	0.464	0.073				
	45-50	0.561	0.090			7.330	
	60-65	0.606	0.125			12.974	
	90-95	0.530	0.118			2.905	
	0-3	1.500	0.587	8.7	0.68	7.089	0.219
	3-6	1.445	0.116			9.664	0.137
	6-9	1.169	0.280			6.100	0.091
	9-12	1.009	0.165				
	12-15	0.828	0.128			1.372	0.102
	15-20	0.688	0.118				
	20-25	0.770	0.128			0.477	0.044
	25-30	0.787	0.094				
	30-35	0.554	0.066				
	35-40	0.563	0.062				
	40-45	0.844	0.124				
	45-50	0.998	0.131	1.02	1.29	3.357	
	65-70	2.028	0.309				
	90-95	0.477	0.073				

## MONIE BAY

	Depth cm	Total P mg P g sediment <sup>-1</sup>	Inorganic P mg IP g sediment <sup>-1</sup>	%C	%N	[Fe] mg g sediment <sup>-1</sup>	[Mn] mg g sediment <sup>-1</sup>
Site 7	0-5	0.583	0.117	9.11	0.68		
	5-10	0.459	0.110				
	10-15	0.481	0.101	6.41	0.49		
	15-20	0.470	0.076				
	20-25	0.441	0.079				
	25-30	0.349	0.059				
	30-35	0.440	0.100				
	35-40	0.490	0.142				
	40-45	0.518	0.110				
	45-50	0.538	0.113	14.35	0.77		

## TIVOLI BAYS, HUDSON RIVER

	Depth cm	Total P mg P g sediment <sup>-1</sup>	Inorganic P mg IP g sediment <sup>-1</sup>	%C	%N
NORTH BAY Core 1	0-2	1.176	0.724	8.66	0.66
	2-4	1.147			
	4-6	1.096	0.574	10.56	0.76
	6-8	1.051			
	8-10	0.930	0.529	6.62	0.54
	10-12	0.974			
	12-15	1.021	0.541	8.48	0.64
	15-18	1.017			
	18-21	1.007	0.549	8.89	0.62
	21-24	0.963			
NORTH BAY Core 2	24-27	1.045	0.590	8.44	0.55
	27-30	0.996			
	30-35	0.901	0.502	7.83	0.51
	35-40	0.844			
	40-45	0.860	0.545	6.30	0.43
	45-50	0.878			
	50-60	0.856	0.556	4.79	0.35
	70-80	0.854			
	80-90	0.785		5.30	0.36
	0-2	1.053		6.51	0.47
Core 2	4-6	0.945		6.86	0.45
	8-10	0.808		7.37	0.43
	12-15	0.874		6.53	0.45
	18-21	0.949		4.63	0.34
	24-27	0.833		3.83	0.31
	30-35	0.824		3.42	0.28
	40-45	0.805		3.37	0.27
	50-60	0.708		2.52	0.23

TIVOLI BAYS, HUDSON RIVER

	Depth cm	Total P mg P g sediment <sup>-1</sup>	Inorganic P mg IP g sediment <sup>-1</sup>	%C	%N
NORTH BAY Core 3	0-2	1.200		4.04	0.35
	2-4	1.113			
	4-6	1.128		5.02	0.39
	6-8	1.057			
	8-10	0.997		5.11	0.40
	10-12	0.948			
	12-15	1.032		4.50	0.36
	15-18	0.894			
	18-21	1.081		3.90	0.32
	21-24	0.784			
	24-27	0.743		3.35	0.28
	27-30	0.769			
	30-35	0.722		3.25	0.27
	35-40	0.766			
NORTH BAY Core 4	40-45	0.774		5.83	0.34
	45-50	0.787			
	50-60	0.716		2.19	0.20
	70-80	0.736			
SOUTH BAY Core 1	0-2	1.166	0.911	4.09	0.34
	4-6	1.283	0.885	5.03	0.35
	8-10	1.125	0.950	5.04	0.33
	12-15	1.110	0.857	7.03	0.31
	18-21	0.868	0.675	7.99	0.35
	24-27	0.998	1.000	5.83	0.37
	30-35	0.821	0.609	3.47	0.28
	40-45	0.829	0.570	3.37	0.29
	50-60	0.657		2.43	0.24
	0-2	0.810	0.723	3.92	0.37
	4-6	0.582	0.695	4.05	0.38
	8-10	1.068	0.761	4.07	0.39
	12-15	0.905	0.727	4.08	0.34
	18-21	0.870	0.683	6.03	0.40
	24-27	0.759	0.517	4.52	0.37
	30-35	0.658	0.497	3.54	0.28
	40-45	0.683	0.513	3.18	0.28
	50-60	0.656	0.503	2.63	0.23

---

SOUTH	0-2	<b>0.882</b>	15.59	0.95
BAY	4-6	<b>0.620</b>	13.16	0.78
Core 2	8-10	<b>0.690</b>	15.53	1.04
Fringe	10-12	<b>0.753</b>		
Marsh	12-15	<b>0.697</b>	13.47	0.99
	15-18	<b>0.715</b>		
	18-21	<b>0.752</b>	14.08	0.96
	21-24	<b>0.729</b>		
	24-27	<b>0.832</b>	14.32	1.08
	27-30	<b>0.995</b>		
	30-35	<b>0.982</b>	17.10	1.34
	35-40	<b>0.946</b>		
	40-45	<b>0.971</b>	14.88	1.27
	45-50	<b>0.920</b>		
	50-60	<b>0.940</b>	17.44	1.62

---

Table C-3. Lead-210 data from all sites included in this study. Depth of the sediment section is given, as well as the mass of sediment to the bottom of that sediment section. The cumulative mass was used to generate accretion rates in sediment mass buried per unit time per unit area. Polonium-210 and  $^{209}\text{Po}$  disintegration numbers have been corrected for decay between sample processing and counting of the sample plates. Total  $^{210}\text{Po}$  activity is assumed to be in secular equilibrium with  $^{210}\text{Pb}$  as discussed in the text. The natural log of excess  $^{210}\text{Po}$  activity,  $^{210}\text{Po}$  activity above the asymptotic value for total activity, was used to calculate accretion rate. Overall efficiency reflects the efficiency of the extraction, plating and counting process. Data given below the horizontal line for a specific site were not included in the regression calculations.

PATUXENT RIVER

	Depth	Cumulative Mass	$^{210}\text{Po}$ Disint.	$^{209}\text{Po}$ Disint.	Total $^{210}\text{Po}$ Activity dpm gram $^{-1}$	$\ln( \frac{\text{Unsup.}}{^{210}\text{Po Activity}} )$	Standard Error	% Overall Efficiency	Accretion cm $\text{y}^{-1}$ g cm $^{-2}$ y $^{-1}$
	cm	g cm $^{-2}$			sediment	dpm g $^{-1}$			
<b>Site 1</b>	3-6	1.72	884	5281	2.640	0.604	0.099	41.1	0.76 0.51
	9-12	4.28	2354	14862	2.010	0.182	0.046	43.0	
	20-25	11.05	3612	15837	1.830	0.020	0.035	45.8	
	30-35	18.18	754	2096	1.330	-0.654	0.058	19.5	
	45-50	30.63	1995	13575	1.110	-1.204	0.028	39.3	
	90-100	67.63	596	2054	1.150	-1.079	0.055	19.1	
	140-150	100.18	1616	13743	0.810	--	0.022	39.8	
<b>Site 2</b>	3-6	1.63	1795	10384	2.280	0.285	0.060	43.1	0.23 0.14
	6-9	2.29	598	853	2.690	0.554	0.145	15.1	
	9-12	3.18	1607	9513	1.990	0.039	0.055	39.5	
	12-15	4.74	384	2372	1.270	-1.139	0.072	20.4	
	15-20	8.77	349	1346	0.780	--	0.048	19.9	
	20-25	11.93	766	5397	0.960	-4.605	0.038	42.0	
	30-35	18.46	683	2765	0.990	-3.219	0.044	25.8	
	45-50	28.27	1458	5805	1.800	-0.163	0.054	45.2	
	90-100	72.29	516	2189	0.950	--	0.048	20.4	
	140-150	124.36	575	5151	0.790	--	0.036	40.1	

PATUXENT RIVER

	Depth	Cumulative Mass	$^{210}\text{Po}$ Disint.	$^{209}\text{Po}$ Disint.	Total $^{210}\text{Po}$ Activity	$\ln(\frac{\text{Unsup.}}{\Sigma^{210}\text{Po}} \text{Activity})$	Standard Error	% Overall Efficiency	Accretion
	cm	g cm <sup>-2</sup>	dpm gram <sup>-1</sup>	dpm gram <sup>-1</sup>	dpm g <sup>-1</sup>	dpm g <sup>-1</sup>	cm y <sup>-1</sup>	cm y <sup>-1</sup>	g cm <sup>-2</sup> y <sup>-1</sup>
<b>Site 3</b>	3-6	1.32	1600	8150	3.120	0.438	0.087	46.1	0.66
	9-12	3.09	1569	8290	2.860	0.255	0.080	46.9	0.40
	12-15	4.46	496	727	2.780	0.191	0.164	12.9	
	20-25	9.92	2028	7702	2.100	-0.635	0.053	43.6	
	35-40	20.60	2133	10291	1.570	--	0.038	42.7	
	70-78	47.18	1751	12218	1.120	--	0.029	50.7	
<b>Site 4</b>	6-9	1.91	181	591	2.340	-0.236	0.199	12.2	0.16
	12-15	4.33	437	945	1.630	-2.526	0.094	20.1	
	20-25	9.38	432	835	1.780	-1.470	0.106	17.8	
	25-30	12.14	234	647	1.450	--	0.111	13.3	
	30-35	14.69	506	1166	1.730	-1.715	0.092	24.8	
	90-100	56.04	403	1022	1.550	--	0.091	14.3	
<b>Site 5</b>	3-6	1.50	396	2503	2.560	0.140	0.141	48.0	1.11
	9-12	3.72	395	2732	2.310	-0.105	0.127	52.3	
	20-25	8.18	643	2187	2.360	-0.051	0.108	41.9	
	45-50	16.24	398	1852	1.740	-1.109	0.098	35.5	
	90-100	32.35	629	1825	1.410	--	0.067	10.6	
	140-150	47.61	828	7531	--	--	--	--	--
<b>Site 6</b>	0-3	0.86	5392	754	2.355	0.542	0.921	5.4	
	3-6	1.54	3117	454	1.547	-0.093	0.784	4.9	
	9-12	3.31	5348	457	2.427	0.583	1.191	4.9	
	20-25	6.24	2721	297	1.895	0.230	1.168	3.2	
	45-50	12.75	1848	274	1.416	-0.249	0.925	2.9	
	70-80	24.49	780	332	0.964	-1.115	0.644	3.7	
	90-100	31.80	1075	582	0.636	--	0.331	4.1	

PATUXENT RIVER

	Depth	Cumulative Mass	$^{210}\text{Po}$ Disint.	$^{209}\text{Po}$ Disint.	Total $^{210}\text{Po}$ Activity dpm gram <sup>-1</sup> sediment	$\ln(\text{Unsupp. } ^{210}\text{Po Activity})$	Standard Error	% Overall Efficiency	Accretion $\text{cm y}^{-1}$ $\text{g cm}^{-2} \text{y}^{-1}$
	cm	g cm <sup>2</sup>			dpm g <sup>-1</sup>		dpm g <sup>-1</sup>		
<b>Site 7</b>	3-6	0.95	3695	278	2.739	0.382	1.717	3.1	0.78 0.37
	6-9	1.54	393	823	3.910	0.970	0.243	16.7	
	9-12	2.07	2103	364	2.420	0.137	1.390	4.1	
	12-15	2.47	214	745	2.490	0.196	0.196	15.1	
	20-25	4.07	3141	388	1.705	-0.841	0.926	4.3	
	35-40	10.77	2282	518	1.731	-0.780	0.852	5.8	
	45-50	16.06	3232	315	2.162	-0.118	1.289	3.5	
	70-80	27.84	2929	873	1.274	-6.950	0.497	5.5	
	90-100	33.39	1697	455	1.273	--	0.682	5.0	
<b>Site 8</b>	0-2	0.39	4649	607	2.886	0.671	1.271	3.5	1.28 0.69
	2-4	0.86	2403	473	2.042	0.106	1.052	3.2	
	4-6	1.34	4767	682	2.725	0.584	1.132	4.0	
	6-8	1.94	2091	336	2.509	0.456	1.506	2.3	
	10-12	3.38	1989	426	1.902	-0.029	1.041	2.9	
	40-45	23.04	1121	346	1.199	-1.316	0.762	2.9	
	70-80	37.88	2165	828	0.931	--	0.385	6.6	
<b>Site 9</b>	0-3	0.61	3428	330	3.584	1.151	2.091	2.3	0.24 0.04
	3-6	1.28	36662	318	2.387	0.674	1.408	3.6	
	9-12	2.41	7114	542	2.727	0.834	1.227	3.8	
	12-15	2.93	2457	388	2.459	0.711	1.356	4.3	
	15-20	3.79	681	417	0.637	-1.544	0.403	4.6	
	20-25	4.42	607	292	0.432	-4.788	0.315	2.0	
	35-40	5.94	343	249	0.462	-3.278	0.396	1.7	
	45-50	6.87	564	270	0.424	--	0.321	1.3	

PATUXENT RIVER		$^{210}\text{Po}$		$^{208}\text{Po}$	Total $^{210}\text{Po}$	$\ln(\text{Unsup. } ^{210}\text{Po Activity})$	Standard Error	% Overall Efficiency	Accretion
Depth	Cumulative Mass	Disint.	Disint.	dpm gram <sup>-1</sup> sediment	dpm g <sup>-1</sup>		dpm g <sup>-1</sup>	cm y <sup>-1</sup>	g cm <sup>-2</sup> y <sup>-1</sup>
cm	g cm <sup>-2</sup>								
<b>Site 10</b>									
3-6	2.81	6515	507	2.502	-0.015	1.166	3.5	--	--
6-9	4.18	606	990	2.380	-0.147	0.124	20.1		
9-12	5.29	5807	500	2.427	-0.095	1.143	3.5		
12-15	6.86	479	720	2.480	-0.038	0.148	14.6		
15-20	9.51	2415	507	1.731	-1.541	0.855	5.6		
20-25	12.27	2477	274	1.819	-1.198	1.173	4.4		
35-40	20.35	3667	587	2.375	-0.153	1.071	4.0		
45-50	25.69	2122	241	1.796	-1.275	1.239	3.8		
70-80	41.55	2371	523	1.517	--	0.743	4.3		
90-100	53.78	2173	316	2.323	0.843	1.419	2.2		
<b>Site 11</b>									
3-6	2.12	2105	315	2.198	-0.403	1.344	3.5	0.78	0.37
6-9	3.18	495	702	2.740	0.191	0.163	14.3		
9-12	4.49	3080	589	1.892	-1.017	0.865	4.1		
12-15	5.65	614	976	2.350	-0.199	0.123	17.3		
15-20	7.90	2950	595	1.973	-0.814	0.898	4.9		
20-25	10.41	2583	517	1.935	-0.903	0.948	3.6		
45-50	22.57	2125	580	1.488	--	0.711	4.0		
70-80	40.33	2035	449	1.571	-3.203	0.830	3.7		
90-100	52.17	1724	369	1.530	--	0.892	2.5		
<b>Site 12</b>									
3-6	1.76	1028	193	2.030	0.268	1.618	1.3	0.77	0.32
6-9	2.77	527	802	2.560	0.609	0.146	14.2		
9-12	3.79	2420	507	1.928	0.188	0.958	3.5		
15-20	7.00	389	747	1.830	0.103	0.116	13.2		
20-25	9.29	1978	507	1.530	-0.213	0.779	3.3		
35-40	15.47	1152	389	1.098	-0.976	0.655	3.2		
45-50	19.53	1113	437	0.981	-1.351	0.569	2.8		
70-80	31.41	545	262	0.722	--	0.553	2.2		
90-100	39.58	1028	520	0.740	--	0.413	3.0		

## JUG BAY, PATUXENT RIVER

Depth	Cumulative Mass	$^{210}\text{Po}$ Disint.	$^{208}\text{Po}$ Disint.	Total $^{210}\text{Po}$ Activity dpm gram <sup>-1</sup>	Ln (Unsup. $^{210}\text{Po}$ Activity)	Standard Error	% Overall Efficiency	Accretion cm $\text{y}^{-1}$	$\text{g cm}^{-2} \text{y}^{-1}$
cm	g cm <sup>-2</sup>	sediment	dpm g <sup>-1</sup>						
High Marsh	0-3	0.67	2834	430	2.547	0.141	1.327	5.2	0.54
	3-6	1.48	3030	313	2.017	-0.475	1.201	3.6	
	6-9	2.36	2560	559	1.862	-0.761	0.879	4.5	
	9-12	3.21	2510	465	2.107	-0.340	1.075	3.7	
	9-12	--	2098	179	2.435	0.039	1.903	2.0	
	20-25	7.50	2038	259	1.632	-1.439	1.084	4.0	
30-35	11.91	3795	644	2.235	-0.174	0.960	4.0		
	18.62	1716	246	1.461	-2.716	1.003	3.8		
	45-50	46.57	1395	398	1.395	--	0.797	4.7	
	90-100								
Mid Marsh	2-4	0.96	5852	516	2.357	-0.096	1.084	3.5	--
	4-6	1.40	189	544	2.850	0.337	0.242	12.4	
	6-8	2.07	159	672	2.600	0.140	0.231	15.3	
	8-10	2.67	3435	387	1.859	-0.893	1.001	4.4	
	20-25	7.94	1939	381	1.886	-0.829	1.068	3.1	
	40-45	15.50	3294	375	1.825	-0.980	0.998	4.3	
50-60	21.02	2412	351	2.664	0.194	1.527	4.2		
	60-70	26.04	858	1794	1.640	-1.657	0.069	14.2	
	90-100	42.07	1382	384	1.449	--	0.841	4.6	
River's Edge	3-6	1.50	4341	398	2.286	0.270	1.199	2.7	--
	9-12	2.91	5596	537	2.190	0.195	0.991	3.6	
	20-25	5.58	3460	370	1.933	-0.043	1.059	2.5	
	45-50	11.66	2567	321	1.690	-0.335	1.003	2.2	
	90-100	23.11	1290	527	0.975	--	0.506	3.6	

## PATUXENT RIVER, TRANSECT A

	Depth	Cumulative Mass	$^{210}\text{Po}$ Disint.	$^{209}\text{Po}$ Disint.	Total $^{210}\text{Po}$ Activity dpm gram $^{-1}$ sediment	Ln (Unsupp. $^{210}\text{Po}$ Activity)	Standard Error	% Overall Efficiency	Accretion
	cm	g cm $^{-2}$				dpm g $^{-1}$			cm y $^{-1}$ g cm $^{-2}$ y $^{-1}$
11 m	0-3	0.69	2712	18440	5.175	0.309	0.106	23.6	1.26
	6-9	2.40	4537	16818	5.477	0.509	0.092	21.5	0.51
	12-15	4.53	2658	10227	4.699	-0.121	0.102	13.1	
	20-25	8.85	2909	11969	4.422	-0.496	0.091	15.3	
	40-45	16.74	1379	6050	4.352	-0.619	0.130	20.4	
	50-55	21.06	1162	5040	4.229	-0.877	0.138	17.0	
30 m	0-3	0.73	1351	4222	7.094	1.393	0.222	18.6	1.70
	6-9	2.61	1304	3864	7.138	1.404	0.229	17.0	0.85
	12-15	4.67	1142	3470	6.314	1.178	0.215	15.3	
	20-25	7.82	1369	4355	5.889	1.038	0.182	18.3	
	30-35	11.60	1597	4724	5.505	0.891	0.159	19.9	
	40-45	16.74	994	3686	4.851	0.579	0.173	15.5	
	50-55	26.37	748	2992	4.818	0.560	0.197	12.6	
50 m	0-3	0.79	2654	9748	6.402	1.563	0.140	16.0	1.81
	6-9	2.01	2512	8861	5.366	1.318	0.121	14.6	0.63
	20-25	7.68	948	3887	4.509	1.058	0.163	19.7	
	30-35	11.27	830	2917	4.377	1.011	0.172	14.8	
	40-45	15.42	764	3017	3.983	0.856	0.161	15.3	
	50-55	17.35	1141	6394	3.387	0.565	0.109	27.0	
50 m	6-9	2.56	2482	6890	7.114	1.663	0.167	24.7	1.63
	12-15	4.32	2727	6159	6.905	1.623	0.159	22.1	0.49
	20-25	7.69	1626	4775	6.445	1.528	0.185	17.1	
	30-35	10.45	1337	4257	4.975	1.144	0.156	16.6	
	50-60	16.69	728	2224	4.100	0.817	0.175	8.7	

## PATUXENT RIVER, TRANSECT B

	Depth	Cumulative Mass	$^{210}\text{Po}$ Disint.	$^{209}\text{Po}$ Disint.	Total $^{210}\text{Po}$ Activity dpm gram $^{-1}$ sediment	Ln (Unsupp. $^{210}\text{Po}$ Activity)	Standard Error	% Overall Efficiency	Accretion
	cm	g cm $^{-2}$				dpm g $^{-1}$			cm y $^{-1}$ g cm $^{-2}$ y $^{-1}$
0 m	0-3	1.00	419	4457	6.092	1.261	0.311	16.3	1.59 0.93
	6-9	3.15	276	2879	5.851	1.190	0.369	10.5	
	12-15	5.50	716	4955	5.724	1.151	0.229	19.3	
	20-25	10.68	888	4680	5.140	0.947	0.188	18.2	
	40-45	22.35	497	3234	4.533	0.678	0.218	12.6	
	50-55	31.52	282	3218	3.766	0.186	0.234	16.8	
30 m	6-9	2.70	664	4273	6.743	1.518	0.281	13.9	0.31 0.11
	12-15	4.78	696	4992	5.816	1.291	0.235	16.2	
	20-25	8.40	387	4208	4.465	0.827	0.237	13.6	
	30-35	12.00	419	3109	3.442	0.234	0.179	10.1	
	40-45	15.26	179	4367	2.271	-2.373	0.173	15.7	
60 m	0-3	0.63	581	3861	10.917	2.125	0.486	15.6	0.55 0.20
	6-9	2.24	625	4794	9.024	1.869	0.384	19.4	
	12-15	3.91	379	3351	7.114	1.520	0.386	13.6	
	20-25	7.63	363	3034	5.588	1.114	0.310	12.3	
	30-35	11.45	831	7988	4.786	0.809	0.174	15.9	
	40-45	14.87	520	8898	4.134	0.466	0.187	17.7	
	50-55	19.12	437	6443	2.845	-1.188	0.141	12.8	
90 m	0-3	0.35	837	4772	11.759	2.316	0.441	17.5	0.41 0.11
	6-9	1.56	649	3595	10.038	2.130	0.428	13.2	
	12-15	3.13	719	3451	8.896	1.984	0.365	17.6	
	20-25	6.02	1864	15272	4.815	1.161	0.118	19.9	
	30-35	8.72	1031	12142	3.106	0.396	0.101	15.8	
	50-60	14.17	575	13719	1.824	-1.592	0.078	14.3	

PATUXENT RIVER, TRANSECT C

Depth	Cumulative		$^{210}\text{Po}$ Disint.	Total $^{210}\text{Po}$ Activity dpm gram $^{-1}$ sediment	$\ln(\text{Unsupp.}$ $^{210}\text{Po Activity})$	Standard Error	% Overall Efficiency	Accretion $\text{cm y}^{-1}$ g cm $^{-2}$ y $^{-1}$
	cm	g cm $^{-2}$						
0 m	3-6	2.43	3040	434	2.714	0.774	1.417	2.8
	9-12	5.31	3467	642	2.110	0.448	0.925	4.2
	20-25	13.07	2083	429	2.001	0.375	1.083	2.8
	25-30	14.99	2478	714	1.382	-0.179	0.599	4.1
	35-40	18.04	2148	871	0.919	-0.987	0.378	5.1
	45-50	20.76	510	350	0.586	-3.219	0.424	2.3
	90-100	28.91	467	335	0.546	--	0.398	2.7
30 m	3-6	0.26	1021	4511	3.410	1.019	0.122	33.3
	6-9	0.35	512	823	2.730	0.737	0.156	12.2
	9-12	0.46	490	5779	1.510	-0.139	0.074	42.6
	12-15	0.58	178	834	0.870	-1.470	0.074	12.3
	15-20	1.53	393	4604	0.690	-2.996	0.038	19.1
	20-25	2.44	390	4617	0.600	--	0.033	34.0
	30-35	3.97	620	3892	0.640	--	0.029	16.2
	45-50	7.24	435	4711	0.720	--	0.037	34.7
60 m	0-3	0.82	1112	707	6.740	1.844	0.328	13.7
	3-6	1.61	2418	8349	3.950	1.261	0.097	39.7
	6-9	2.21	253	627	2.150	0.548	0.163	12.2
	9-12	2.82	702	8730	1.230	-0.211	0.052	41.5
	20-25	4.50	328	7670	0.660	-1.427	0.040	17.1
	35-40	6.58	437	7650	0.440	-3.912	0.023	17.0
	70-80	11.94	264	2578	0.420	--	0.028	8.6
	140-150	29.45	487	3225	0.610	-1.661	0.031	13.4
90 m	3-6	1.68	3141	10085	4.650	1.472	0.100	41.1
	6-9	2.08	362	1207	2.440	0.765	0.149	17.9
	9-12	2.50	866	7482	1.780	0.399	0.068	30.5
	20-25	4.25	555	8271	0.560	-1.309	0.026	31.4
	35-40	6.07	500	8515	0.420	-2.040	0.021	32.3
	70-80	9.54	341	13291	0.190	--	0.011	29.6
	140-150	17.95	650	16368	0.290	--	0.012	36.4

### OTTER POINT CREEK

	Depth	Cumulative Mass	$^{210}\text{Po}$ Disint.	$^{209}\text{Po}$ Disint.	Total $^{210}\text{Po}$ Activity dpm gram $^{-1}$ sediment	$\ln(\text{Unsupp. } ^{210}\text{Po Activity})$	Standard Error	% Overall Efficiency	Accretion cm $\text{y}^{-1}$ g $\text{cm}^{-2} \text{y}^{-1}$
<b>Site 1</b>	3-6	2.45	357	2100	1.376	-0.203	0.084	18.2	1.02 0.53
	6-9	3.83	708	2311	1.254	-0.365	0.055	19.8	
	9-12	5.21	327	2203	1.190	-0.462	0.076	19.1	
	12-15	6.67	398	1457	1.111	-0.595	0.064	12.5	
	20-25	11.69	513	2189	0.955	-0.928	0.050	19.0	
	25-30	14.14	456	1897	0.981	-0.864	0.052	15.4	
	70-80	53.35	510	3635	0.560	--	0.029	15.0	
	35-40	20.32	356	1481	0.984	--	0.062	12.8	
<b>Site 2</b>	3-6	1.28	1092	1923	4.071	1.261	0.155	15.0	0.21 0.12
	6-9	3.94	762	1974	1.454	-0.091	0.063	16.0	
	9-12	5.55	929	5292	1.360	-0.199	0.052	21.8	
	15-20	10.03	279	1297	0.829	-1.243	0.056	22.0	
	20-25	14.93	492	3675	0.541	--	0.028	15.2	
	3-6	2.42	887	4589	1.550	--	0.061	18.9	
<b>Site 3</b>	3-6	2.74	401	2504	1.314	-0.362	0.077	22.5	0.27 0.24
	9-12	7.89	334	2930	0.868	-1.386	0.055	24.7	
	12-15	10.25	241	1193	0.815	-1.624	0.059	20.2	
	20-25	18.62	365	1996	0.701	-2.491	0.043	16.8	
	70-80	64.46	194	1211	0.618	--	0.050	2.8	
	25-30	22.80	315	1570	0.806	--	0.051	23.9	
	35-40	30.63	393	1879	0.846	--	0.051	15.8	

### CHOPTANK RIVER

Depth cm	Cumulative Mass g cm <sup>-2</sup>	<sup>210</sup> Po Disint.	<sup>209</sup> Po Disint.	Total <sup>210</sup> Po Activity dpm gram <sup>-1</sup> sediment	$\ln(\frac{\text{Unsup.}}{\text{sup.}} \cdot \text{Activity})$		% Overall Efficiency	Accretion $\text{cm y}^{-1}$	$\text{g cm}^{-2} \text{y}^{-1}$
					Standard Error	dpm g <sup>-1</sup>			
<b>Site 1</b>									
9-12	4.00	349	1121	2.238	0.601	0.144	3.8	0.61	0.21
12-15	4.74	689	1201	2.572	0.769	0.125	18.3		
20-25	8.16	372	866	1.684	0.239	0.109	2.9		
25-30	9.86	392	987	1.550	0.128	0.095	15.0		
35-40	12.95	245	1071	0.895	-0.730	0.067	3.6		
70-80	25.27	132	1285	0.413	--	0.040	3.2		
3-6	2.10	360	1231	2.200	0.580	0.139	4.2		
<b>Site 2</b>									
6-9	3.56	1597	2334	2.740	0.867	0.089	18.3	1.09	0.41
9-12	4.96	157	474	2.694	0.847	0.267	3.8		
20-25	10.40	171	359	1.881	0.419	0.187	2.9		
35-40	14.55	170	487	1.410	0.048	0.135	2.9		
70-80	24.96	139	1505	0.360	--	0.035	8.2		
3-6	1.08	275	1009	2.161	0.588	0.155	3.4		
12-15	6.37	407	2210	0.714	-1.040	0.039	17.3		
<b>Site 3</b>									
3-6	1.40	209	589	2.603	0.893	0.226	3.2	1.07	0.28
9-12	2.56	293	1117	2.143	0.685	0.152	10.0		
20-25	5.74	122	371	1.308	0.138	0.147	2.1		
35-40	9.75	178	638	1.126	-0.035	0.104	5.5		
70-80	20.11	13	296	0.163	--	0.052	2.6		

### MONIE BAY

	Depth cm	Cumulative Mass g cm <sup>-2</sup>	<sup>210</sup> Po Disint.	<sup>209</sup> Po Disint.	Total <sup>210</sup> Po Activity dpm gram <sup>-1</sup> sediment	Ln ( <sup>Unsup.</sup> <sup>210</sup> Po Activity) dpm g <sup>-1</sup>	Standard Error	% Overall Efficiency	Accretion cm y <sup>-1</sup> g cm <sup>-2</sup> y <sup>-1</sup>
<b>Site 1</b>	3-6	1.14	2282	303	4.381	1.405	0.270	24.1	0.68 0.18
	9-12	2.31	3501	436	2.835	0.928	0.176	29.0	
	12-15	2.89	2253	432	1.839	0.428	0.129	28.0	
	30-35	8.30	1294	370	1.393	0.084	0.084	32.3	
	40-45	10.97	859	371	0.852	-0.603	0.075	24.7	
	60-65	13.45	281	357	0.305	--	0.025	31.1	
<b>Site 2</b>	0-3	0.61	8080	37108	3.438	0.900	0.043	45.3	-- --
	6-9	2.25	6786	34233	2.883	0.642	0.039	41.8	
	9-12	3.16	327	995	5.251	1.452	0.336	7.0	
	12-15	4.12	116	199	4.907	1.369	0.575	6.0	
	30-35	9.33	595	1509	3.135	0.770	0.153	6.5	
	40-45	10.95	3036	24097	0.978	--	0.019	29.4	
	60-65	15.49	151	3727	0.262	--	0.022	8.2	
<b>Site 3</b>	3-6	1.23	1436	238	2.479	0.628	0.178	19.7	
	9-12	2.30	1431	265	1.996	0.330	0.137	22.0	
	25-30	4.65	1106	378	1.205	-0.511	0.075	16.4	
	40-45	11.39	648	423	0.605	--	0.040	18.4	

**MONIE BAY**

Depth cm	Cumulative Mass g cm <sup>-2</sup>	<sup>210</sup> Po Disint.	<sup>209</sup> Po Disint.	Total <sup>210</sup> Po Activity dpm gram <sup>-1</sup> sediment	$\ln(\frac{\text{Unsupp.}}{\text{supp.}} \cdot \text{Po}_0)$		Standard Error	% Overall Efficiency	Accretion cm yr <sup>-1</sup> g cm <sup>-2</sup> y <sup>-1</sup>
					ln (Unsupp. <sup>210</sup> Po Activity)	dpm g <sup>-1</sup>			
<b>Site 4</b>									
3-6	2.19	3973	604	2.468	0.843	0.109	35.0	0.44	0.13
9-12	3.78	1668	398	1.287	0.134	0.073	23.1		
20-25	7.57	1654	757	0.847	-0.351	0.038	37.4		
30-35	10.05	297	239	0.417	-1.297	0.038	18.1		
45-50	12.54	209	567	0.144	--	0.013	27.6		
<b>Site 5</b>									
3-6	1.62	306	622	3.955	1.293	0.277	5.7	0.26	0.07
6-9	2.63	169	416	3.313	1.099	0.304	3.8		
9-12	3.57	441	971	3.758	1.237	0.216	9.8		
12-15	4.42	975	2157	3.602	1.191	0.140	8.4		
15-20	--	5814	32188	1.452	0.131	0.021	39.3		
25-30	9.25	469	476	0.359	-0.822	0.024	23.6		
40-45	11.45	112	2522	0.358	-3.100	0.035	4.2		
60-65	14.08	120	3354	0.313	--	0.029	4.7		
<b>Site 6</b>									
0-3	0.78	391	647	8.406	2.042	0.542	6.5	0.25	0.08
6-9	2.58	497	637	6.893	1.824	0.414	6.4		
12-15	4.56	441	971	3.869	1.154	0.223	9.8		
20-25	7.62	1530	9576	1.288	-0.527	0.036	44.1		
65-70	19.43	129	1443	0.698	--	0.065	3.0		
40-45	13.69	719	9673	0.593	--	0.023	44.6		

MONIE BAY

Depth cm	Cumulative Mass g cm <sup>-2</sup>	<sup>210</sup> Po Disint.	<sup>208</sup> Po Disint.	Total <sup>210</sup> Po Activity dpm gram <sup>-1</sup> sediment	Ln (Unsup. <sup>210</sup> Po Activity)	Accretion	
						Standard Error dpm g <sup>-1</sup>	% Overall Efficiency cm y <sup>-1</sup> g cm <sup>-2</sup> y <sup>-1</sup>
site 7							
0-5	1.39	378	751	3.874	1.316	0.246	6.3 0.22 0.06
5-10	3.18	245	804	2.426	0.824	0.178	6.8
10-15	4.84	293	1032	2.154	0.697	0.143	11.0
30-35	9.92	466	832	0.222	-2.566	0.014	1.2
45-50	13.43	507	1298	0.146	--	0.008	1.9
15-20	6.38	810	8936	0.696	-0.598	0.026	41.2
25-30	8.93	267	8515	0.243	-2.325	0.015	39.2
45-50	13.43	196	3266	0.485	-1.082	0.036	6.8

## TIVOLI BAYS, HUDSON RIVER

	Sample Depth	Cumulative Mass	$^{210}\text{Po}$ Disint.	$^{209}\text{Po}$ Disint.	Total $^{210}\text{Po}$ Activity dpm gram $^{-1}$ sediment	Ln (Unsupp. $^{210}\text{Po}$ Activity)	Standard Error	% Overall Efficiency	Accretion	
	cm	g cm $^{-2}$				dpm g $^{-1}$			cm y $^{-1}$ g cm $^{-2}$ y $^{-1}$	
<b>NORTH</b>										
BAY	0-2	0.67	1448	6588	4.485	1.151	0.131	20.2	0.46	0.23
Site 1	2-4	1.52	1821	6515	5.860	1.513	0.156	20.0		
	4-6	2.26	804	4743	6.332	1.611	0.243	6.7		
	6-8	3.18	1048	4994	4.252	1.075	0.145	15.3		
	8-10	4.16	894	4235	4.383	1.119	0.162	5.9		
	10-12	5.05	1061	4873	3.726	0.877	0.127	15.0		
	12-15	6.39	494	3273	3.161	0.609	0.153	4.6		
	21-24	10.46	984	8282	1.867	-0.606	0.064	7.9		
	27-30	13.15	1059	8972	2.127	-0.216	0.070	12.2		
	35-40	18.34	974	7672	2.037	-0.336	0.070			
	45-50	24.64	1053	8461	1.494	-1.759	0.049			
	70-80	36.85	728	7419	1.322	--	0.052			
	80-90	42.08	947	8980	1.555	-1.456	0.054			
	15-18	7.73	952	5563	1.702	-0.967	0.060			

## TIVOLI BAYS, HUDSON RIVER

	Sample Depth	Cumulative Mass	$^{210}\text{Po}$ Disint.	$^{209}\text{Po}$ Disint.	Total $^{210}\text{Po}$ Activity	Ln (Unsupp. $^{210}\text{Po}$ Activity)	Standard Error	% Overall Efficiency	Accretion
	cm	$\text{g cm}^{-2}$			dpm gram $^{-1}$ sediment		dpm g $^{-1}$		cm y $^{-1}$ g cm $^{-2}$ y $^{-1}$
NORTH BAY Core 3	0-2	0.92	1027	7547	3.220	0.949	0.109	15.9	0.69 0.50
	2-4	1.94	1700	9261	2.882	0.809	0.078	11.7	
	6-8	2.91	2494	11957	3.974	1.205	0.089	15.1	
	10-12	4.91	1662	6402	3.675	1.111	0.103	11.8	
	15-18	7.71	1244	5012	3.028	0.872	0.098	6.3	
	21-24	11.58	5603	34353	1.884	0.221	0.028	14.2	
	27-30	16.15	3808	49985	1.375	-0.303	0.024	20.6	
	35-40	23.15	3322	39895	1.284	-0.435	0.024	16.5	
	45-50	31.29	2652	31942	1.353	-0.333	0.028	14.7	
	70-80	45.51	579	12031	0.637	--	0.029	15.4	
	80-90	54.75	657	13260	0.693	--	0.029	17.0	
NORTH BAY Core 2	0-2	0.83	372	3805	2.537	0.309	0.138	14.7	0.37 0.30
	4-6	2.55	532	4879	1.939	-0.268	0.089	17.7	
	8-10	4.80	442	5307	1.496	-1.135	0.075	19.3	
	12-15	7.43	431	4752	1.714	-0.618	0.087	17.2	
	18-21	11.85	339	4589	1.299	-2.088	0.073	16.6	
	24-27	16.97	1036	9878	1.362	-1.675	0.045	19.6	
	30-35	24.65	843	10004	1.286	-2.193	0.047	19.8	
	40-45	33.59	723	8678	1.200	-3.674	0.047	17.2	
	50-60	48.16	583	8104	1.175	--	0.051	16.0	
	24-27	426	5533	1.393	-0.279	0.071	21.1		

## TIVOLI BAYS, HUDSON RIVER

	Sample Depth	Cumulative Mass	$^{210}\text{Po}$ Disint.	$^{209}\text{Po}$ Disint.	Total $^{210}\text{Po}$ Activity	Ln (Unsupp. $^{210}\text{Po}$ Activity)	Standard Error	% Overall Efficiency	Accretion
	cm	$\text{g cm}^{-2}$			dpm gram $^{-1}$ sediment		dpm g $^{-1}$		$\text{cm y}^{-1}$ $\text{g cm}^{-2} \text{y}^{-1}$
NORTH	0-2	0.92	784	5183	3.737	0.919	0.145	19.7	0.13 0.09
BAY	4-6	3.05	760	4460	3.666	0.889	0.146	17.0	
Core 4	8-10	5.20	766	4594	3.278	0.716	0.129	17.5	
	12-15	8.66	388	5439	1.356	-2.090	0.072	20.7	
	18-21	13.05	314	4267	1.284	-2.954	0.076	16.3	
	24-27	16.73	319	3886	1.401	-1.779	0.083	14.8	
	30-32	22.81	373	4140	1.314	-2.497	0.072	15.8	
	40-45	31.00	461	4987	1.516	-1.257	0.075	19.0	
	50-60	383	5494		1.232	--	0.066	20.9	
SOUTH	0-2	0.42	507	4643	3.165	0.573	0.151	18.0	0.37 0.12
BAY	4-6	1.72	649	4175	3.253	0.621	0.140	16.2	
Core 2	8-10	2.74	1282	6323	3.098	0.534	0.097	21.0	
	12-15	4.29	874	5433	2.604	0.192	0.097	18.0	
	18-21	6.01	542	4605	1.890	-0.697	0.088	15.3	
	24-27	7.99	415	4491	1.661	-1.313	0.087	14.9	
	30-35	10.16	440	5043	1.392	--	0.071	18.5	
	40-45	13.10	436	5062	1.455	-2.762	0.074	18.6	
SOUTH	0-2	0.87	1811	12948	3.026	0.701	0.080	16.6	0.33 0.19
BAY	2-4	1.88	1636	10292	2.851	0.610	0.080	13.2	
Core 1	18-21	10.94	728	10116	1.237	-1.483	0.050	12.2	
subtidal	24-27	14.87	951	13468	1.292	-1.265	0.046	16.2	
	30-35	21.07	705	11261	1.010	--	0.042	13.5	
	40-45	29.30	1004	12779	1.244	-1.454	0.043	15.3	

## BIBLIOGRAPHY

- Arheimer, B., and H. B. Wittgren. 1994. Modeling the effects of wetlands on regional nitrogen transport. *Ambio*. 23(6):378-386.
- Armentano, T. V., and G. M. Woodwell. 1975. Sedimentation rates in a Long Island marsh determined by  $^{210}\text{Pb}$  dating. *Limnology and Oceanography*. 20:452-456.
- Aspila, K. I., H. Agemian, and A. S. Y. Chau. 1976. A semi-automated method for the determination of inorganic, organic and total phosphate in sediments. *Analyst*. 101:187-197.
- Barnes, R. O., K. K. Bertine, and E. D. Goldberg. 1975.  $\text{N}_2\text{:Ar}$ , nitrification and denitrification in southern California borderland basin sediments. *Limnology and Oceanography*. 20(6):962-970.
- Baumann, R. H., J. W. Day, Jr., and C. A. Miller. 1984. Mississippi deltaic wetland survival: sedimentation versus coastal submergence. *Science*. 224:1093-1094.
- Beulac, M. N., and K. H. Reckhow. 1982. An examination of land use-nutrient export relationships. *Water Resources Bulletin*. 18(6):1013-1024.
- Bianchi, T. S., S. Findlay, and R. Dawson. 1993. Organic matter sources in the water column and sediments of the Hudson River Estuary: the use of plant pigments as tracers. *Estuarine and Coastal Shelf Science*. 36:359-376.
- Blackburn, T. H. 1979. Method for measuring rates of  $\text{NH}_4^+$  turnover in anoxic marine sediments, using a  $^{15}\text{N}-\text{NH}_4^+$  dilution technique. *Applied and Environmental Microbiology*. 37:760-765.
- Blackburn, T. H., N. D. Blackburn, K. Jensen, and N. Risgaard-Petersen. 1994. Simulation model of the coupling between nitrification and denitrification in a freshwater sediment. *Appl. Environ. Microbiol.* 60:3089-3095.
- Bopp, R., H. J. Simpson, C. R. Olsen, R. M. Trier, and N. Kostyk. 1982. Chlorinated hydrocarbons and radionuclide chronologies in sediments of the Hudson River and estuary, New York. *Environmental Science and Technology*. 16:666-676.
- Bowden, W. B. 1986. Nitrification, nitrate reduction, and nitrogen immobilization in a tidal freshwater sediment. *Ecology*. 67(1):88-99.

- Bowden, W. B. 1987. The biogeochemistry of nitrogen in freshwater wetlands. *Biogeochemistry*. 4:313-348.
- Bowden, W. B., C. J. Vorosmarty, J. T. Morris, B. J. Peterson, J. E. Hobbie, P. A. Steudler, and B. Moore III. 1991. Transport and processing of nitrogen in a tidal freshwater wetland. *Water Resources Research*. 27:389-408.
- Boynton, W. R. and W. M. Kemp. 1985. Nutrient regeneration and oxygen consumption by sediments along an estuarine salinity gradient. *Marine Ecology Progress Series*. 23:45-55.
- Boynton, W. R., J. H. Garber, R. Summers, and W. M. Kemp. 1995. Inputs, transformations and transport of nitrogen and phosphorus in Chesapeake Bay and selected tributaries. *Estuaries*. 18(1B):285-314.
- Brady, N. C. 1990. *The Nature and Property of Soils*, 10<sup>th</sup> ed. Macmillan.
- Bricker, S. B., and J. C. Stevenson. 1996. Nutrients in coastal waters: a chronology and synopsis of research. *Estuaries*. 19(2B):337-341.
- Bricker-Urso, S., S. W. Nixon, J. K. Cochran, D. J. Hirschberg, and C. Hunt. 1989. Accretion rates and sediment accumulation in Rhode Island salt marshes. *Estuaries*. 12:300-317.
- Brush, G. S., E. A. Martin, R. S. DeFries, and C. A. Rice. 1982. Comparisons of <sup>210</sup>Pb and pollen methods for determining rates of estuarine sediment accumulation. *Quaternary Research*. 18:196-217.
- Caffrey, J. M., and W. M. Kemp. 1992. Influence of the submersed plant, *Potamogeton perfoliatus*, on nitrogen cycling in estuarine sediments. *Limnology and Oceanography*. 37:1483-1495.
- Caffrey, J. M., N. P. Sloth, H. F. Kaspar, and T. H. Blackburn. 1993. Effect of organic loading on nitrification and denitrification in a marine sediment microcosm. *FEMS Microbial Ecology*. 12:159-167.
- Cahoon, D. R., and J. C. Stevenson. 1986. Production, predation, and decomposition in a low-salinity *Hibiscus* marsh. *Ecology*. 67(5):1341-1350.
- Carpenter, R., J. T. Bennett, and M. L. Peterson. 1981. <sup>210</sup>Pb activities in and fluxes to sediments of the Washington continental slope and shelf. *Geochimica et Cosmochimica Acta*. 45:1155-1172.

- Chambers, R. M., and W. E. Odum. 1990. Pore water oxidation, dissolved phosphate and the iron curtain. *Biogeochemistry* 10:37-52.
- Chambers, R. M., J. W. Harvey, and W. E. Odum. 1992. Ammonium and phosphate dynamics in a Virginia salt marsh. *Estuaries*. 15:349-359.
- Childers, D. L., and J. W. J. Day. 1990. Marsh-water column interactions in two Louisiana estuaries. 1. Sediment dynamics. *Estuaries*. 13(4):393-403.
- Childers, D. L., S. Cofer-Shabica, and L. Nakashima. 1993. Spatial and temporal variability in marsh-water column interactions in a southeastern USA salt marsh estuary. *Marine Ecological Progress Series*. 95:25-38.
- Christensen, P. B., L. P. Nielsen, J. Sorensen, and N. P. Revsbech. 1990. Denitrification in nitrate-rich streams: diurnal and seasonal variation related to benthic oxygen metabolism. *Limnology and Oceanography*. 35(3):640-651.
- Cole, J. J., N. F. Caraco, and B. L. Peierls. 1992. Can phytoplankton maintain a positive carbon balance in a turbid, freshwater, tidal estuary? *Limnology and Oceanography*. 37(8):1608-1617.
- Cornwell, J. C. C., D. J. Conley, M. Owens, and J. C. Stevenson. 1996. A sediment chronology of the eutrophication of Chesapeake Bay. *Estuaries*. 19(2B):488-499.
- Cornwell, J. C., J. M. Stribling, and J. C. Stevenson. 1990. Biogeochemical studies at the Monie Bay National Estuarine Research Reserve. Final Report, National Oceanic and Atmospheric Administration National Estuarine Research Reserve System. Report No. NA89AA/D C2 130.
- Cornwell, J. C., J. Stribling, and J. C. Stevenson. 1994. Biogeochemical studies at the Monie Bay National Estuarine Research Reserve, p. 645-655. *In Proceedings of the 13<sup>th</sup> International Conference of the Coastal Society*. The Coastal Society, Gloucester, Massachusetts.
- Correll, D. L., T. E. Jordan, and D. E. Weller. 1992. Nutrient flux in a landscape: effects of coastal land use and terrestrial community mosaic on nutrient transport to coastal waters. *Estuaries*. 15:431-442.
- Costanza, R., E. B. DeBellevue, T. Maxwell, and M. Jacobsen. 1993. Development of the Patuxent Landscape Model (PLM). Report to Maryland DNR, CBL Ref. No. 190.

- Craft, C. B. and C. J. Richardson. 1993. Peat accretion and N, P, and organic C accumulation in nutrient-enriched and unenriched Everglades peatlands. *Ecological Applications*. 3(3):446-458.
- Craft, C. B., and C. J. Richardson. 1993. Peat accretion and phosphorus accumulation along a eutrophication gradient in the northern Everglades. *Biogeochemistry*. 22:133-156.
- Craft, C. B., E. D. Seneca, and S. W. Broome. 1993. Vertical accretion in microtidal regularly and irregularly flooded estuarine marshes. *Estuarine Coastal and Shelf Science*. 37:371-386.
- Cronin, W. B., and D. W. Pritchard. 1975. Additional Statistics on the Dimensions of the Chesapeake Bay and its Tributaries: Cross-section widths and segment volumes per meter depth. Special Report 42. Chesapeake Bay Institute, the Johns Hopkins University. Reference 75-3.
- Curran, C. A., and H. W. Paerl. 1998a. Environmental and physiological controls on diel patterns of N<sub>2</sub> fixation in epiphytic cyanobacterial communities. *Microbial Ecology*. 35(1):34-45.
- Curran, C. A., and H. W. Paerl. 1998b. Epiphytic nitrogen fixation associated with standing dead shoots of smooth cordgrass, *Spartina alterniflora*. *Estuaries*. 21(1):108-117.
- Dame, R. F., J. D. Spurrier, T. M. Williams, B. Kjerfve, R. G. Zingmark, T. G. Wolaver, T. H. Chrzanowski, and H. N. McKellar. 1991. Annual material processing by a salt marsh estuarine basin in South Carolina, USA. *Marine Ecology Progress Series*. 72:153-166.
- Dame, R., T. Chrzanowski, K. Bildstein, B. Kjerfve, H. McKellar, D. Nelson, J. Spurrier, S. Stancyk, H. Stevenson, J. Vernberg, and R. Zingmark. 1986. The outwelling hypothesis and North Inlet, South Carolina. *Marine Ecological Progress Series*. 33:217-229.
- Davis, R. B., C. T. Hess, S. A. Norton, D. W. Hanson, K. D. Hoagland, and D. S. Anderson. 1984. <sup>137</sup>Cs and <sup>210</sup>Pb dating of sediments from soft-water lakes in New England (USA) and Scandinavia, a failure of <sup>137</sup>Cs dating. *Chemical Geology*. 44:151-185.
- DeLaune, R. D., C. J. Smith, and W. H. Patrick, Jr. 1983. Nitrogen losses from a Louisiana Gulf Coast Salt Marsh. *Estuarine, Coastal and Shelf Science*. 17:133-141.

- DeLaune, R. D., C. N. Reddy, and W. H. Patrick Jr. 1981. Accumulation of plant nutrients and heavy metals through sedimentation processes and accretion in a Louisiana salt marsh. *Estuaries*. 4:328-334.
- DeLaune, R. D., J. H. Whitcomb, W. H. Patrick Jr., J. H. Pardue, and S. R. Pezeshki. 1989. Accretion and canal impacts in a rapidly subsiding wetland.  $^{137}\text{Cs}$  and  $^{210}\text{Pb}$  techniques. *Estuaries*. 12:247-259.
- DeLaune, R. D., T. C. Feijtel, and W. H. Patrick Jr. 1989. Nitrogen flows in Louisiana Gulf Coast salt marsh: spatial considerations. *Biogeochemistry*. 8:25-37.
- Devol, A. H. 1991. Direct measurement of nitrogen gas fluxes from continental shelf sediments. *Nature*. 349:319-321.
- DeVries, C., and C. B. DeWitt. 1987. Freshwater tidal wetlands community description and relation of plant distribution to elevation and substrate, IX p. 1-43. *In* Final Report to Tibor T. Polgar Fellowship Program. Hudson River Foundation.
- Duff, J. H., F. J. Triska, and R. S. Oremland. 1984. Denitrification associated with stream periphyton: Chamber estimates from undisrupted communities. *Journal of Environmental Quality*. 13:514-518.
- Field, D. W., A. J. Reyer, P. V. Genovese, and B. D. Shearer. 1991. Coastal Wetlands of the United States: An accounting of a valuable natural resource. NOAA 20<sup>th</sup> Anniversary Report.
- Findlay, S., K. Howe, and H. K. Austin. 1990. Comparison of detritus dynamics in two tidal freshwater wetlands. *Ecology*. 71(1):288-295.
- Findlay, S., M. L. Pace, D. Lints, J. J. Cole, N. F. Caraco, and B. Peierls. 1991. Weak coupling of bacterial and algal production in a heterotrophic ecosystem: The Hudson River Estuary. *Limnology and Oceanography*. 36(2):268-278.
- Finkelstein, K., and C. S. Hardaway. 1988. Late Holocene sedimentation and erosion of estuarine fringing marshes, York River, Virginia. *Journal of Coastal Research*. 4(3):447-456.
- Fisher, T. R., E. R. Peele, J. W. Ammerman, and L. W. Harding Jr. 1992. Nutrient limitation of phytoplankton in Chesapeake Bay. *Marine Ecological Progress Series*. 82:51-63.

- Flemer, D. A., D. H. Hamilton, C. W. Keefe, and J. A. Mihursky. 1970. Final Report to Office of Water Resources Research on the Effects of Thermal Loading and Water Quality on Estuarine Primary Production. Chesapeake Biological Laboratory, Natural Resources Institute, University of Maryland.
- Frey, R. W., and P. B. Basan. 1985. Coastal salt marshes, p. 225-301. In R. A. Davis Jr. [eds.], *Coastal Sedimentary Environments*. Springer-Verlag.
- Gardner, W. S., T. F. Nalepa, and J. M. Malczyk. 1987. Nitrogen mineralization and denitrification in Lake Michigan sediments. *Limnology and Oceanography* 32:1226-1238.
- Gehrels, J., and G. Mulamoottil. 1989. The transformation and export of phosphorus from wetlands. *Hydrological Processes*. 3:365-370.
- Gosselink, J., and R. Baumann. 1980. Wetland inventories: wetland loss along the United States coast. *Z. Geomorph. N.F. Supplemental-Bd.*, 34:173-187.
- Groffman, P. M. 1994. Denitrification in freshwater wetlands. *Current Topics in Wetland Biogeochemistry*. 1:15-35.
- Harding, L. W., Jr., B. W. Meeson, and T. R. Fisher Jr. 1986. Phytoplankton production in two east coast estuaries: Photosynthesis-light functions and patterns of carbon assimilation in Chesapeake and Delaware Bays. *Estuarine and Coastal Shelf Science*. 23:773-806.
- Harrison, E. Z., and A. L. Bloom. 1974. The response of Connecticut salt marshes to the recent rise in sea level. *Geological Society of America. Abstracts with Programs* 6:35-36.
- Hatton, R. S., R. D. DeLaune, and W. H. J. Patrick. 1983. Sedimentation, accretion, and subsidence in marshes of Barataria Basin, Louisiana. *Limnology and Oceanography*. 28(3):494-502.
- Hatton, R. S., W. H. Patrick Jr., and R. D. DeLaune. 1982. Sedimentation, nutrient accumulation, and early diagenesis in Louisiana Barataria Basin coastal marshes, p. 255-267. In V. S. Kennedy [ed.], *Estuarine Comparisons*. Academic Press.
- Heinle, D. R. and D. A. Flemer. 1976. Flows of materials between poorly flooded tidal marshes and an estuary. *Marine Biology*. 35:359-373.

- Hobbs, C. H., III, J. P. Halka, R. T. Kerhin, and M. J. Carron. 1992. Chesapeake Bay sediment budget. *Journal of Coastal Research*. 8:292-300.
- Howarth, R. W., and A. Giblin. 1983. Sulfate reduction in the salt marshes at Sapelo Island, Georgia. *Limnology and Oceanography*. 28:70-82.
- Howarth, R. W., G. Billen, D. Swaney, A. Townsend, N. Jaworski, K. Lajtha, J. A. Downing, R. Elmgren, N. Caraco, T. Jordan, F. Berendse, J. Freney, V. Kudeyarov, P. Murdoch, and Z. Zhao-Liang. 1996a. Regional nitrogen budgets and riverine N & P fluxes for the drainages to the North Atlantic Ocean: Natural and human influences. *Biogeochemistry*. 35:75-139.
- Howarth, R. W., J. R. Fruci, and D. Sherman. 1991. Inputs of sediment and carbon to an estuarine ecosystem: influence of land use. *Ecological Applications*. 1:27-39.
- Howarth, R. W., R. Marino, R. Garrett, and D. Sherman. 1992. Ecosystem respiration and organic carbon processing in a large, tidally influenced river: the Hudson River. *Biogeochemistry*. 16:83-102.
- Howarth, R. W., R. Schneider, and D. Swaney. 1996b. Metabolism and organic carbon fluxes in the tidal freshwater Hudson River. *Estuaries*. 19(4):848-865.
- Howes, B. L., J. W. H. Dacey, and D. D. Goehringer. 1986. Factors controlling the growth form of *Spartina alterniflora*: feedbacks between above-ground production, sediment oxidation, nitrogen and salinity. *Journal of Ecology*. 74:881-898.
- Howes, B. L., J. W. H. Dacey, and J. M. Teal. 1985. Annual carbon mineralization and belowground production of *Spartina alterniflora* in a New England salt marsh. *Ecology*. 66:595-605.
- Jahnke, R. A., S. R. Emerson, and J. W. Murray. 1982. A model of oxygen reduction, denitrification, and organic matter mineralization in marine sediments. *Estuaries*. 27(4):610-623.
- Jaworski, N. A., P. M. Groffman, A. A. Keller, and J. C. Prager. 1992. A watershed nitrogen and phosphorus balance: the upper Potomac River basin. *Estuaries*. 15(1):83-95.
- Jenkins, M. C., and W. M. Kemp. 1984. The coupling of nitrification and denitrification in two estuarine sediments. *Limnology and Oceanography*. 29:609-619.

- Johnston, C. A. 1991. Sediment and nutrient retention by freshwater wetlands: effects on surface water quality. *Critical Reviews in Environmental Control*. 21:491-565.
- Johnston, C. A., G. D. Bubenzer, G. B. Lee, F. W. Madison, and J. R. McHenry. 1984. Nutrient trapping by sediment deposition in a seasonally flooded lakeside wetland. *Journal of Environmental Quality*. 13(2):283-290.
- Jordan, T. E., D. L. Correll, and D. F. Whigham. 1983. Nutrient flux in the Rhode River: tidal exchange of nutrients by brackish marshes. *Estuarine and Coastal Shelf Science*. 17:651-667.
- Jordan, T. E., J. W. Pierce, and D. L. Correll. 1986. flux of particulate matter in the tidal marshes and subtidal shallows of the Rhode River estuary. *Estuaries*. 9:310-319.
- Jorgensen, K. S. 1989. Annual pattern of denitrification and nitrate ammonification in estuarine sediment. *Applied Environmental Microbiology*. 55(7):1841-1847.
- Joye, S. B., and J. T. Hollibaugh. 1995. Influence of sulfide inhibition on nitrification on nitrogen regeneration in sediments. *Science*. 270:623-625.
- Kahn, H., and G. S. Brush. 1994. Nutrient and metal accumulation in a freshwater tidal marsh. *Estuaries*. 17(2):345-360.
- Kana, T. M., C. Darkangelo, D. M. Hunt, J. B. Oldham, G. E. Bennett, and J. C. Cornwell. 1994. Membrane inlet mass spectrometer for rapid high-precision determination of N<sub>2</sub>, O<sub>2</sub>, and Ar in environmental water samples. *Analytical Chemistry*. 66(23):4166-4170.
- Kana, T. M., M. B. Sullivan, J. C. Cornwell, and K. M. Groszkowski. 1998. Denitrification in estuarine sediments determined by membrane inlet mass spectrometry. *Limnology and Oceanography*. 43(2):334-339.
- Kaplan, W., I. Valiela, and J. M. Teal. 1979. Denitrification in a salt marsh ecosystem. *Limnology and Oceanography*. 24(4):726-734.
- Kearney, M. S. and J. C. Stevenson. 1991. Island land loss and marsh vertical accretion rate evidence for historical sea-level changes in Chesapeake Bay. *Journal of Coastal Research*. 7(2):403-415.

- Kearney, M. S. and L. G. Ward. 1986. Accretion rates in brackish marshes of a Chesapeake Bay estuarine tributary. *Geo-Marine Letters*. 6:41-49.
- Kearney, M. S., J. C. Stevenson, and L. G. Ward. 1994. Spatial and temporal changes in marsh vertical accretion rates at Monie Bay: Implications for sea-level rise. *Journal of Coastal Research*. 10:1010-1020.
- Kearney, M. S., R. E. Grace and J. C. Stevenson. 1988. Marsh loss in Nanticoke Estuary, Chesapeake Bay. *Geographical Review*. 78(2):205-220.
- Kemp, W. M., and W. R. Boynton. 1984. Spatial and temporal coupling of nutrient inputs to estuarine primary production: the role of particulate transport and decomposition. *Bulletin of Marine Science*. 35(3):522-535.
- Kemp, W. M., P. Sampou, J. Caffrey, M. Mayer, K. Henriksen, and W. R. Boynton. 1990. Ammonium recycling versus denitrification in Chesapeake Bay sediments. *Limnology and Oceanography*. 35:1545-1563.
- Khan, H., and G. S. Brush. 1994. Nutrient and metal accumulation in a freshwater tidal marsh. *Estuaries*. 17:345-360.
- Knowles, R. 1990. Acetylene inhibition technique: Development, advantages, and potential problems, p. 151-166. *In* N. P. Revsbech and J. Sorensen [eds.], *Denitrification in Soil and Sediment*. Plenum Press.
- Krishnaswami, S., and D. Lal. 1978. Radionuclide limnochronology. p. 153-177. *In*: A. Lerman [ed.], *Lakes: Chemistry, Geology, Physics*. Springer Verlag.
- Krishnaswamy, S., D. Lal, J. M. Martin, and M. Meybeck. 1971. Geochronology of lake sediments. *Earth and Planetary Science Letters*. 11:407-414.
- Krom, M. D., and R. A. Berner. 1981. The diagenesis of phosphorus in a nearshore marine sediment. *Geochimica et Cosmochimica Acta*. 45:207-216.
- Lickus, M. and P. Barten. 1991. Hydrology of a tidal freshwater marsh in the Hudson River Estuary, I p. 1-45. *In* E. A. Blair and J. R. Waldman [eds.], *Final Reports of the Tibor T. Polgar Fellowship Program, 1990*. Hudson River Foundation.

- Limburg, K. E., M. A. Moran, and W. McDowell [eds.]. 1986. The Hudson River Ecosystem. Springer-Verlag.
- Lipschultz, F. 1978. Nitrogen fixation in Horn Point marsh on the upper Chesapeake Bay. M. S. Thesis, University of Maryland, College Park, Maryland.
- Lipschultz, F., S. C. Wofsy, and L. E. Fox. 1986. Nitrogen metabolism of the eutrophic Delaware River ecosystem. Limnology and Oceanography. 31(4):701-716.
- Lohse, L., H. T. Kloosterhuis, W. van Raaphorst, and w Helder. 1996. Denitrification rates as measured by the isotope pairing method and by the acetylene inhibition technique in continental shelf sediments of the North Sea. Marine Ecology Progress Series. 132:169-179.
- Lomax, K., and J. C. Stevenson. 1982. Diffuse-source loadings in a flat coastal plain watershed: Water movements and nutrient budgets. Maryland Department of Natural Resources, Annapolis, Maryland.
- Lyles, S. D., L. E. Hickman, Jr., and H. A. Debaugh, Jr. 1988. Sea Level Variations for the United States, 1855-1986. National Oceanic and Atmospheric Administration, Rockville, Maryland.
- Magnien, R. E., R. M. Summers, and K. G. Sellner. 1992. External nutrient sources, internal nutrient pools, and phytoplankton production in Chesapeake Bay. Estuaries. 15:497-516.
- Malone, T. C. 1992. Effects of water column processes on dissolved oxygen, nutrients, phytoplankton and zooplankton, p. 61-112. In D. E. Smith, M. Leffler, and G. Mackiernan [eds.], Oxygen Dynamics in the Chesapeake Bay. Maryland Sea Grant, College Park, Maryland.
- Marchesi, C. and P. Barten. 1992. Development of tidal discharge and sediment flux discharge functions in Tivoli Bays, I p. 1-42. In J. R. Waldman and E. A. Blair [eds.], Final Reports of the Tibor T. Polgar Fellowship Program, 1991. Hudson River Foundation.
- Marchetti, R., and N. Verna. 1992. Quantification of the phosphorus and nitrogen loads in the minor rivers of the Emilia-Romagna coast (Italy). A methodological study on the use of theoretical coefficients in calculating the loads. Science of the Total Environment. Supplement:315-336.

McCormick, J., and H. A. Somes Jr. [eds.]. 1982. The Coastal Wetlands of Maryland. Maryland Department of Natural Resources, Annapolis, Maryland.

Messer, J. and P. L. Brezonik. 1983. Comparison of denitrification rate estimation techniques in a large, shallow lake. *Water Resources*. 17:631-640.

Middelburg, J. J., K. Soetaert, and P. M. J. Herman. 1996. Evaluation of the nitrogen isotope-pairing method for measuring benthic denitrification: a simulation analysis. *Limnology and Oceanography*. 41(8):1839-1844.

Mitsch, W. J., and B. C. Reeder. 1991. Modeling nutrient retention of a freshwater coastal wetland: estimating the roles of primary productivity, sedimentation, resuspension and hydrology. *Ecological Modeling*. 54:151-187.

Mitsch, W. J., and J. G. Gosselink. 1993. *Wetlands*, 2nd ed. Van Norstrand Reinhold.

Morris, J. T. 1980. The nitrogen uptake kinetics of *Spartina alterniflora* in culture. *Ecology*. 61(5):1114-1121.

Morris, J. T., and W. B. Bowden. 1986. A mechanistic, numerical model of sedimentation, mineralization, and decomposition for marsh sediments. *Journal of the Soil Science Society of America*. 50:96-105.

Morris, J.T., and B. Haskin. 1990. A 5-yr record of aerial primary production and stand characteristics of *Spartina alterniflora*. *Ecology*. 71(6):2209-2217.

Murray, A. L., and T. Spencer. 1997. On the wisdom of calculating annual material budgets in tidal wetlands. *Marine Ecological Progress Series*. 150:207-216.

Nedwell, D. B., and S. Azni bin Abdul Aziz. 1980. Heterotrophic nitrogen fixation in an intertidal saltmarsh sediment. *Estuarine and Coastal Marine Science*. 10:699-702.

Nishio, T., I. Koike, and A. Hattori. 1982. Denitrification, nitrate reduction, and oxygen consumption in coastal and estuarine sediments. *Applied and Environmental Microbiology*. 43(3):648-653.

Nixon, S. W. 1980. Between coastal marshes and coastal waters -- a review

- of twenty years of speculation in the role of salt marshes in estuarine productivity and water chemistry, p. 437-525. In P. Hamilton and K. Macdonald [eds.], Estuarine and Wetland Processes. Plenum Press.
- Nixon, S. W., and V. Lee. 1986. Wetlands and Water Quality. United States Army Corps of Engineers, Washington, D.C.
- Nyman, J. A., and R. D. DeLaune. 1991. CO<sub>2</sub> emissions and soil E<sub>h</sub> responses to different hydrological conditions in fresh, brackish, and saline marsh soils. Limnology and Oceanography. 36:1406-1414.
- Nyman, J. A., R. D. DeLaune, H. H. Roberts, and W. H. J. Patrick. 1993. Relationship between vegetation and soil formation in a rapidly submerging coastal marsh. Marine Ecological Progress Series. 96:269-279.
- Odum, W. E. 1988. Comparative ecology of tidal freshwater and salt marshes. Annual Review of Ecological Systematics. 19:147-176.
- Odum, W. E., T. J. Smith, J. K. Hoover, and C. McIvor. 1984. The ecology of tidal freshwater marshes of the United States east coast: a community profile. United States Fish and Wildlife Service FWS/OBS-83/17.
- Ogilvie, B., D. B. Nedwell, R. M. Harrison, A. Robinson, and A. Sage. 1997. High nitrate, muddy estuaries as nitrogen sinks: the nitrogen budget of the River Colne estuary (United Kingdom). Marine Ecology Progress Series. 150:217-228.
- Orson, R. A., R. L. Simpson, and R. E. Good. 1990. Rates of sediment accumulation in a tidal freshwater marsh. Journal of Sedimentary Petrology. 60:859-869.
- Parsons, T. R., Y. Maita, and C. M. Lalli. 1984. A Manual of Chemical and Biological Methods for Seawater Analysis. Pergamon Press.
- Pasternack, G. B. and G. S. Brush. 1998. Sedimentation cycles in a river-mouth tidal freshwater marsh. Estuaries. 21(3):407-415.
- Peller, P. and R. Bopp. 1986. Recent sediment and pollutant accumulation in the Hudson River National Estuarine Sanctuary, VII p. 1-29. In J.C. Cooper [ed.], Polgar Fellowship Reports of the Hudson River National Estuarine Sanctuary Program, 1985. Hudson River Foundation.
- Peterjohn, W. T., and D. L. Correll. 1984. Nutrient dynamics in an agricultural watershed: observations on the role of a riparian forest. Ecology. 65:1466-1475.

- Phillips, P. J., J. M. Denver, R. J. Shedlock, and P. A. Hamilton. 1993. Effect of forested wetlands on nitrate concentrations in ground water and surface water on the Delmarva peninsula. *Wetlands*. 13:75-83.
- Reckhow, K. H., M. N. Beaulac and J. T. Simpson. 1980. Modeling phosphorus loading and lake response under uncertainty: A manual and compilation of export coefficients. Clean Lakes Section of U. S. E. P. A., Washington, D. C., EPA 440/5-80-011.
- Reddy, K. R., R. D. DeLaune, W. F. DeBusk, and M. S. Koch. 1993. Long-term nutrient accumulation rates in the Everglades. *Journal of the Soil Science Society of America*. 57:1147-1155.
- Reddy, K. R., W. H. J. Patrick, and C. W. Lindau. 1989. Nitrification-denitrification at the plant root-sediment interface in wetlands. *Limnology and Oceanography*. 34(6):1004-1013.
- Reed, D. J. 1989. Patterns of sediment deposition in subsiding coastal salt marshes, Terrebonne Bay, Louisiana: The role of winter storms. *Estuaries*. 12(4):222-227.
- Rice, D. L.. 1982. The detritus nitrogen problem: new observations and perspectives from organic chemistry. *Marine Ecology Progress Series*. 9:153-162.
- Richard, G. A. 1978. Seasonal and environmental variations in sediment accretion in a Long Island salt marsh. *Estuaries*. 1(1):29-35.
- Risgaard-Petersen, N., S. Rysgaard, L. P. Nielsen, and N. P. Revsbech. 1994. Diurnal variation of denitrification and nitrification in sediments colonized by benthic microphytes. *Limnology and Oceanography*. 39(3):573-579.
- Robbins, J. A. 1978. Geochemical and geophysical applications of radioactive lead, p. 285-405. In J. O. Nraigu [ed.], *The Biogeochemistry of Lead in the Environment*. Elsevier.
- Roberts, W. P., and J. W. Pierce. 1976. Deposition in upper Patuxent estuary, Maryland, 1968-1969. *Estuarine and Coastal Marine Science*. 4:267-280.
- Rysgaard, S., N. Risgaard-Petersen, L. P. Nielsen, and N. P. Revsbech. 1993. Nitrification and denitrification in lake and estuarine sediments measured by the  $^{15}\text{N}$  dilution technique and isotope pairing. *Applied Environmental Microbiology*. 59:2093-2098.

- Rysgaard, S., N. Risgaard-Petersen, N. P. Sloth, K. Jensen, and L. P. Nielsen. 1994. Oxygen regulation of nitrification and denitrification in sediments. *Limnology and Oceanography*. 39(7):1643-1652.
- Rysgaard, S., P. B. Christensen, and L. P. Nielsen. 1995. Seasonal variation in nitrification and denitrification in estuarine sediment colonized by benthic microalgae and bioturbating infauna. *Marine Ecology Progress Series*. 126:111-121.
- Santschi, P., P. Hoehner, G. Benoit, and M. B. Brink. 1990. Chemical processes at the sediment-water interface. *Marine Chemistry*. 30:269-315.
- Schubauer, J. P., and C. S. Hopkinson. 1984. Above- and belowground emergent macrophyte production and turnover in a coastal marsh ecosystem. *Limnology and Oceanography*. 29:1052-1065.
- Seitzinger, S. P. 1987. Nitrogen biogeochemistry in an unpolluted estuary: the importance of benthic denitrification. *Marine Ecology Progress Series*. 37:65-73.
- Seitzinger, S. P. 1988. Denitrification in freshwater and coastal marine ecosystems: ecological and geochemical significance. *Limnology and Oceanography*. 33:702-724.
- Seitzinger, S. P. 1994. Linkages between organic matter mineralization and denitrification in eight riparian wetlands. *Biogeochemistry*. 25:19-39.
- Seitzinger, S. P., L. P. Nielsen, J. Caffrey, and P. B. Christensen. 1993. Denitrification measurements in aquatic sediments: A comparison of three methods. *Biogeochemistry*. 23:147-167.
- Seitzinger, S. P., S. W. Nixon, and M. E. Q. Pilson. 1984. Denitrification and nitrous oxide production in a coastal marine sediment. *Limnology and Oceanography* 29(1):73-83.
- Seitzinger, S. P., W. S. Gardner, and A. K. Spratt. 1991. The effect of salinity on ammonium sorption in aquatic sediments: Implications for benthic nutrient recycling. *Estuaries*. 14(2):167-174.
- Sharma, P., L. R. Gardner, W. S. Moore, and M. S. Bollinger. 1987. Sedimentation and bioturbation in a salt marsh as revealed by  $^{210}\text{Pb}$ ,  $^{137}\text{Cs}$  and  $^7\text{Be}$  studies. *Limnology and Oceanography*. 32:313-326.
- Simpson, R. L., R. E. Good, M. A. Leck, and D. F. Whigham. 1983. The ecology of freshwater tidal wetlands. *BioScience*. 33:255-259.

- Simpson, R. L., R. E. Good, R. Walker, and B. R. Frasco. 1983. The role of Delaware River freshwater tidal wetlands in the retention of nutrients and heavy metals. *Journal of Environmental Quality*. 12:41-48.
- Sloth, N. P., L. P. Nielsen, and T. H. Blackburn. 1992. Nitrification in sediment cores measured with acetylene inhibition. *Limnology and Oceanography*. 37(5):1108-1112.
- Smart, R. M., and J. W. Barko. 1980. Nitrogen nutrition and salinity tolerance of *Distichlis spicata* and *Spartina alterniflora*. *Ecology*. 61:630-638.
- Smith, D. E., M. Leffler, and G. Mackiernan [eds.]. 1992. *Oxygen Dynamics in the Chesapeake Bay*. Maryland Sea Grant, College Park, Maryland.
- Sorensen, J. 1978. Capacity for denitrification and reduction of nitrate to ammonia in a coastal marine sediment. *Applied and Environmental Microbiology*. 35(2):301-305.
- Staver, K. and R. Brinsfield. 1996. Seepage of groundwater nitrate from a riparian agroecosystem into the Wye River Estuary. *Estuaries*. 19(2B): 359-370.
- Staver, L. W., K. W. Staver, and J. C. Stevenson. 1996. Nutrient inputs to the Choptank River Estuary: Implications for watershed management. *Estuaries*. 19(2B):342-358.
- Stevenson, J. C., D. R. Heinle, D. A. Flemer, R. J. Small, R. A. Rowland, and J. F. Ustach. 1977. Nutrient exchanges between brackish water marshes and the estuary, p. 219-240. *In* M. Wiley [ed.], *Estuarine Processes*. Academic Press.
- Stevenson, J. C., L. G. Ward and M. S. Kearney. 1986. Vertical accretion in marshes with varying rates of sea level rise, p. 241-259. *In* D. A. Wolfe [ed.], *Estuarine Variability*. Academic Press.
- Stevenson, J. C., L. G. Ward, and M. S. Kearney. 1988. Sediment transport and trapping in marsh systems: Implications of tidal flux studies. *Marine Geology*. 80:37-59.
- Stribling, J. M. 1994. Sulfur and nutrient chemistry of *Spartina alterniflora* Loisel. in a low salinity marsh. Ph.D. Dissertation, University of Maryland, College Park, Maryland.
- Sugai, S. 1990. Transport and sediment accumulation of  $^{210}\text{Pb}$  and  $^{137}\text{Cs}$  in two southeast Alaskan fjords. *Estuaries*. 13(4):380-392.

- Sullivan, M. J., and C. A. Moncreiff. 1990. Edaphic algae are an important component of salt marsh food-webs: evidence from multiple stable isotope analyses. *Marine Ecology Progress Series*. 62:149-159.
- Sundback, K., V. Enoksson, W. Graneli, and K. Pettersson. 1991. Influence of sublittoral microphytobenthos on the oxygen and nutrient flux between sediment and water: a laboratory continuous-flow study. *Marine Ecological Progress Series*. 74:263-279.
- Swarth, C., and D. Peters. 1993. Water Quality and Nutrient Dynamics of Jug Bay on the Patuxent River. Jug Bay Wetlands Sanctuary Technical Report, Anne Arundel County Department of Recreation and Parks, Jug Bay Wetlands Sanctuary, Lothian, Maryland.
- Thompson, S. P., H. W. Paerl, and M. C. Go. 1995. Seasonal patterns of nitrification and denitrification in a natural and a restored salt marsh. *Estuaries*. 18(2):399-408.
- Valiela, I., K. Foreman, M. LaMontagne, J. Costa, P. Peckol, B. DeMeo-Andreson, C. D'Avanzo, M. Babione, C. H. Sham, J. Brawley, and K. Lajtha. 1992. Couplings of watersheds and coastal waters: sources and consequences of nutrient enrichment in Waquoit Bay, Massachusetts. *Estuaries*. 15:443-457.
- Vitousek, P. M., J. D. Aber, R. W. Howarth, G. E. Likens, P. A. Matson, D. W. Schindler, W. H. Schlesinger, and D. Tilman. 1997. Human alteration of the global nitrogen cycle: Sources and consequences. *Ecological Applications*. 7(3):737-750.
- Wang, X., and G. Benoit. 1992. A Chronological variations in concentrations of heavy metals in sediments of the Tivoli South Bay: A study using  $^{210}\text{Pb}$  dating methodology. In J. R. Waldman and E. A. Blair [eds.], Final Report to the Hudson River Foundation, Tibor T. Polgar Fellowship Program. Hudson River Foundation.
- Ward, L. G., M. S. Kearney, and J. C. Stevenson. 1988. Assessment of marsh stability at the estuarine sanctuary site at Monie Bay, implications for management. Report, Estuarine Sanctuary Program, NOAA, Washington, D.C.
- Water Resources Administration. 1980. Non-tidal wetlands study of the Patuxent River watershed. submitted to Maryland Legislature, Senate Joint Resolution No. 18, 1979.
- Whiting, G. J., H. N. McKellar, Jr., J. D. Spurrier, and T. G. Wolaver. 1989. Nitrogen exchange between a portion of vegetated salt marsh and the adjoining creek. *Limnology and Oceanography*. 34(2):463-473.

- Whiting, G. J., and D. L. Childers. 1989. Subtidal advective water flux as a potentially important nutrient input to southeastern U.S.A. saltmarsh estuaries. *Estuarine and Coastal Shelf Science*. 28:417-431.
- Wolaver, T. G., J. C. Zieman, R. Wetzel, and K. L. Webb. 1983. Tidal exchange of nitrogen and phosphorus between a mesohaline vegetated marsh and the surrounding estuary in the lower Chesapeake Bay. *Estuarine and Coastal Shelf Science*. 16:321-332.
- Woodwell, G. M., C. A. S. Hall, D. E. Whitney, and R. A. Houghton. 1979. The Flax Pond ecosystem study: Exchanges of inorganic nitrogen between an estuarine marsh and Long Island Sound. *Ecology*. 60(4):695-702.
- Yarbro, L. A., P. R. Carlson, T. R. Fisher, J. P. Chanton, and W. M. Kemp. 1983. A sediment budget for the Choptank River estuary in Maryland, U.S.A. *Estuarine and Coastal Shelf Science*. 17:555-570.